frontiers | Research Topics

The global threat of carbapenem-resistant gram-negative bacteria

volume II

Edited by
Ziad Daoud and Milena Dropa

Published in
Frontiers in Cellular and Infection Microbiology

ISSN 1664-8714
ISBN 978-2-8325-2394-0
DOI 10.3389/978-2-8325-2394-0

About Frontiers

Frontiers is more than just an open access publisher of scholarly articles: it is a pioneering approach to the world of academia, radically improving the way scholarly research is managed. The grand vision of Frontiers is a world where all people have an equal opportunity to seek, share and generate knowledge. Frontiers provides immediate and permanent online open access to all its publications, but this alone is not enough to realize our grand goals.

Frontiers journal series

The Frontiers journal series is a multi-tier and interdisciplinary set of open-access, online journals, promising a paradigm shift from the current review, selection and dissemination processes in academic publishing. All Frontiers journals are driven by researchers for researchers; therefore, they constitute a service to the scholarly community. At the same time, the *Frontiers journal series* operates on a revolutionary invention, the tiered publishing system, initially addressing specific communities of scholars, and gradually climbing up to broader public understanding, thus serving the interests of the lay society, too.

Dedication to quality

Each Frontiers article is a landmark of the highest quality, thanks to genuinely collaborative interactions between authors and review editors, who include some of the world's best academicians. Research must be certified by peers before entering a stream of knowledge that may eventually reach the public - and shape society; therefore, Frontiers only applies the most rigorous and unbiased reviews. Frontiers revolutionizes research publishing by freely delivering the most outstanding research, evaluated with no bias from both the academic and social point of view. By applying the most advanced information technologies, Frontiers is catapulting scholarly publishing into a new generation.

What are Frontiers Research Topics?

Frontiers Research Topics are very popular trademarks of the *Frontiers journals series*: they are collections of at least ten articles, all centered on a particular subject. With their unique mix of varied contributions from Original Research to Review Articles, Frontiers Research Topics unify the most influential researchers, the latest key findings and historical advances in a hot research area.

Find out more on how to host your own Frontiers Research Topic or contribute to one as an author by contacting the Frontiers editorial office: frontiersin.org/about/contact

The global threat of carbapenem-resistant gram-negative bacteria volume II

Topic editors

Ziad Daoud — Central Michigan University, United States

Milena Dropa — University of São Paulo, Brazil

Citation

Daoud, Z., Dropa, M., eds. (2023). *The global threat of carbapenem-resistant gram-negative bacteria volume II*. Lausanne: Frontiers Media SA.

doi: 10.3389/978-2-8325-2394-0

Table of contents

frontiers | Frontiers in Cellular and Infection Microbiology

TYPE Editorial
PUBLISHED 26 April 2023
DOI 10.3389/fcimb.2023.1196488

OPEN ACCESS

EDITED AND REVIEWED BY
Nahed Ismail,
University of Illinois at Chicago,
United States

*CORRESPONDENCE
Ziad Daoud
daoud1z@cmich.edu

RECEIVED 29 March 2023
ACCEPTED 04 April 2023
PUBLISHED 26 April 2023

CITATION
Daoud Z and Dropa M (2023) Editorial: The global threat of carbapenem-resistant gram-negative bacteria, volume II.
Front. Cell. Infect. Microbiol. 13:1196488.
doi: 10.3389/fcimb.2023.1196488

Editorial: The global threat of carbapenem-resistant gram-negative bacteria, volume II

Ziad Daoud[1]* and Milena Dropa[2]

[1]College of Medicine, Central Michigan University, Mount Pleasant, MI, United States, [2]Faculty of Public Health, University of São Paulo, São Paulo, Brazil

KEYWORDS

carbapenems resistance, gram-negative (G -) bacteria, mechanisms of resistance, KPC carbapenemase, Escerichia coli, Klebsiella pneumoniae

Editorial on the Research Topic
The global threat of carbapenem-resistant gram-negative bacteria, volume II

Multidrug-resistant bacteria pose a significant threat to global public health (World Health Organization, 2017; Centers for Disease Control and Prevention, 2020). In this context, many gram-negative bacteria have developed resistance to carbapenem antibiotics, which are often considered the last resort for treating severe infections caused by these organisms (Magiorakos et al., 2012; Tacconelli et al., 2017; Van Duin and Doi, 2017). Infections caused by carbapenem-resistant bacteria are associated with higher mortality rates and longer hospital stays, leading to increased healthcare costs. The emergence and spread of carbapenem-resistant bacteria are driven by several factors, including the overuse and misuse of antibiotics, inadequate infection control measures, and the global movement of people and goods. Addressing the threat of carbapenem-resistant gram-negative bacteria requires a multifaceted approach that includes increased surveillance, prudent antibiotic use, improved infection control measures, and the development of new antibiotics and alternative therapies.

The 11 manuscripts in this research issue revolve around the topic of resistance to carbapenems. Various studies and outbreaks are discussed, highlighting the importance of monitoring and controlling the spread of carbapenem-resistant gram-negative bacteria and other multidrug-resistant organisms in hospital settings. Some studies have developed predictive models and nomograms to identify high-risk patients and personalize risk prediction. Whole-genome sequencing and plasmid characterization techniques have been utilized to analyze the genetic mechanisms of antibiotic resistance and the dissemination of carbapenemases in various bacteria. Increased surveillance and strict infection control measures have been emphasized to contain outbreaks and prevent the further spread of resistance. Overall, the articles demonstrate the urgent need for effective treatment strategies and control measures to combat the growing threat of carbapenem resistance.

The study *"Carbapenem-Resistant Gram-Negative Bacterial Infection in Intensive Care Unit Patients: Antibiotic Resistance Analysis and Predictive Model Development"* analyzed antibiotic resistance in carbapenem-resistant gram-negative bacteria (CR-GNB) in ICU patients and developed a predictive model (Liao et al.). A total of 309 patients with GNB infection were recruited and divided into CR and carbapenem-susceptible (CS) groups.

Themost prevalent CR-GNB were carbapenem-resistant Klebsiella pneumoniae, carbapenem-resistant Acinetobacter baumannii, and carbapenem-resistant Pseudomonas aeruginosa. A history of combination antibiotic treatments, hospital-acquired infection, and mechanical ventilation ≥ 7 days were independent risk factors for CR-GNB infection. These factors were used to construct a nomogram-based predictive model. The model demonstrated good performance, with an area under the ROC curve (AUC) of 0.753 and 0.718 for the experimental and validation cohort, respectively. The model could be used to guide preventive and treatment measures in identifying patients at high risk of developing CR-GNB infection in the ICU. Another outbreak of multidrug resistant Klebsiella pneumoniae was discussed in the article *"Outbreak of colistin resistant, carbapenemase (blaNDM, blaOXA-232) producing Klebsiella pneumoniae causing blood stream infection among neonates at a tertiary care hospital in India"*, which involved 5 out of 7 neonates (Pathak et al.). The isolates were multidrug resistant, including carbapenems and colistin, and belonged to three different sequence types. The isolates harbored carbapenemase genes and extended-spectrum β-lactamases, but colistin resistance genes could not be detected. K. pneumoniae ST101 was isolated from filtered incubator water and harbored blaNDM-5, blaOXA-232 and ESBL genes, but it was negative for mcr genes. Strict infection control measures were applied, and the outbreak was contained, emphasizing the importance of early detection, surveillance, and proper infection control practices. The study *"Detection of IMP-4 and SFO-1 co-producing ST51 Enterobacter hormaechei clinical isolates"* investigated the genetic characteristics of Enterobacter hormaechei YQ13422hy and YQ13530hy, two multidrug-resistant clinical isolates co-producing the antibiotic resistance genes blaIMP-4 and blaSFO-1 (Qiao et al.). Whole-genome sequencing and plasmid characterization techniques were used to identify and analyze the genes and their genetic context. The study highlights the dissemination of blaIMP-4 in E. hormaechei and the transferable IncN-type plasmid carrying the blaIMP-4 resistance gene in this bacterium. It also emphasizes the importance of understanding the genetic mechanisms of antibiotic resistance for developing effective treatment strategies.

On the other hand, the study *"Development and Validation of Nomograms for Predicting the Risk Probability of Carbapenem Resistance and 28-day All-cause Mortality in Gram-negative Bacteremia among Patients with Hematological Diseases"* aimed to develop two nomograms to predict mortality and carbapenem resistance in hospitalized hematological patients with gram-negative bacteria bloodstream infections (Jian et al.). The study included 244 patients, and 31.6% of them were resistant to carbapenems. The nomograms were constructed using LASSO regression analysis and multivariate logistic regression analysis, and the models were internally validated. The carbapenem resistance nomogram had a modified C-index of 0.788, while the prognosis nomogram had a modified C-index of 0.873. The decision curve analysis demonstrated that the nomograms were clinically practical for predicting high-risk patients. The study suggests that the nomogram models can be an effective tool for personalized risk prediction in clinical practice. Moreover, a carbapenem-resistant Acinetobacter pittii strain, co-producing chromosomal NDM-1 and OXA-820 carbapenemases, was characterized from a bloodstream infection in the manuscript *"Emergence of uncommon KL38-OCL6-ST220 carbapenem resistant Acinetobacter pittii strain, co-producing chromosomal NDM-1 and OXA-820 carbapenemases"* (Tian et al.). The strain was resistant to imipenem, meropenem, and ciprofloxacin but susceptible to amikacin, colistin, and tigecycline. Whole-genome sequencing revealed the strain contained one circular chromosome and four plasmids, with blaNDM-1 and blaOXA-820 genes located in the chromosome. The strain also contained many virulence factors and 12 prophage regions. Phylogenetic analysis showed that the strain was closely related to an A. pittii strain from Anhui, China. Increased surveillance of this species in hospital and community settings is urgently needed due to the challenge presented by the co-existence of these carbapenemases. In this same context of resistance to carbapenems, the study *"Emergence of a Salmonella Rissen ST469 clinical isolate carrying blaNDM-13 in China"* describes a variant of the New Delhi metallo-β-lactamase that confers resistance to carbapenems, which was identified in a patient with fever and diarrhea (Huang et al.). SR33 was found to be multidrug-resistant and carried many virulence genes. The blaNDM-13 was located in a transmissible IncI1 plasmid and had a conserved genetic context and hybrid promoter. This is the first report of blaNDM-13 in Salmonella, highlighting the need for the monitoring and control of its dissemination. IS1294 may be involved in the movement of blaNDM-13.

In terms of transmission, the study *"Genomic transmission analysis of multidrug-resistant Gram-negative bacteria within a newborn unit of a Kenyan Tertiary hospital: a four-month prospective colonization study"* conducted in a Kenyan tertiary hospital investigated the prevalence of multidrug-resistant organisms (MDRO) and carbapenem-resistant organisms (CRO) in a newborn unit using routine microbiology, whole-genome sequencing (WGS), and hospital surveillance data (Villinger et al.). The study included 300 mother–baby pairs and detected MDRO in 16% of neonates at admission, increasing to 44% until discharge, with K. pneumoniae harboring blaNDM-1 and blaNDM-5 being the most frequent CRO. WGS analysis revealed 20 transmission clusters, indicating independent transmission events rather than a large outbreak scenario. The high CRO rate attributed to the spread of NDM-type carbapenemases is a cause for concern.

The prevalence and encoding plasmids in hypervirulent resistant organisms was addressed in two studies: "Prevalence of carbapenem-resistant hypervirulent Klebsiella pneumoniae and hypervirulent carbapenem-resistant Klebsiella pneumoniae in China determined via mouse lethality tests" (Hu et al.) and *"Hybrid plasmids encoding antimicrobial resistance and virulence traits among hypervirulent Klebsiella pneumoniae ST2096 in India"* (Shankar et al.). The first study investigated the epidemiology of carbapenem-resistant hypervirulent Klebsiella pneumoniae (CR-HvKP) and hypervirulent carbapenem-resistant Klebsiella pneumoniae (Hv-CRKP) in mainland China. The study analyzed 436 Klebsiella pneumoniae strains collected from seven hospitals between 2017 and 2018, using various tests such as sequencing, serotyping, and mouse lethality tests. The study found that the exact

prevalence of CR-HvKP is less than 1%, while that of Hv-CRKP is much lower. The authors recommend using mouse lethality tests to accurately determine the prevalence of CR-HvKP and Hv-CRKP.

The second study genetically characterized a collection of multidrug-resistant hypervirulent Klebsiella pneumoniae (MDR-HvKp) ST2096 isolates carrying both antimicrobial resistance (AMR) and virulence genes on a large hybrid plasmid. The hybrid plasmid carried a CRISPR-cas system, which harbored spacer regions against IncF plasmids, preventing their acquisition. This convergence of virulence and AMR in K. pneumoniae is clinically concerning and highlights the continued emergence of such genotypes globally across the species.

Biofilm formation and mortality has been investigated in *"Biofilm formation is not an independent risk factor for mortality in patients with Acinetobacter baumannii bacteremia"* (Chiang et al.). This retrospective study conducted in Taiwan analyzed 711 patients with Acinetobacter baumannii bacteremia, comparing the clinical features of those infected with biofilm-forming and non-biofilm-forming isolates. Multivariate analysis revealed that shock status, higher APACHE II score, lack of appropriate antimicrobial therapy, and carbapenem resistance were independent risk factors for 28-day mortality, but there was no significant difference between the biofilm-forming ability and survival. Patients infected with biofilm-forming isolates had a lower in-hospital mortality rate, and those with congestive heart failure, hematological malignancy, or who received chemotherapy were more likely to be infected with biofilm-forming isolates. Biofilm-forming ability did not influence carbapenem susceptibility.

In Argentina, where Klebsiella pneumoniae and the Enterobacter cloacae complex (ECC) are the two main CRE species, the study *"Novel insights related to the rise of KPC-producing Enterobacter cloacae Complex strains within the nosocomial niche"* shows that the increase in carbapenem-resistant Enterobacterales has led to the urgent need for new antibiotics (Knecht et al.). This study analyzed a patient colonized with both K. pneumoniae and ECC strains and *in vitro* competition assays between high-risk clones of KPC-producing ECC and K. pneumoniae. The results show that these high-risk clones can coexist in the same hospital environment, including the same patient. The findings suggest that the ability of some pandemic clones to compete and occupy a certain niche may explain the worldwide rise of KPC-ECC strains.

Author contributions

All authors listed have made a substantial, direct, and intellectual contribution to the work and approved it for publication.

Conflict of interest

The authors declare that the research was conducted in the absence of any commercial or financial relationships that could be construed as a potential conflict of interest.

Publisher's note

References

Centers for Disease Control and Prevention (2020) *Antibiotic resistance threats in the United States. retrieved.* Available at: https://www.cdc.gov/drugresistance/pdf/threats-report/2019-ar-threats-report-508.pdf.

Magiorakos, A. P., Srinivasan, A., Carey, R. B., Carmeli, Y., Falagas, M. E., Giske, C. G., et al. (2012). Multidrug-resistant, extensively drug-resistant and pandrug-resistant bacteria: an international expert proposal for interim standard definitions for acquired resistance. *Clin. Microbiol. Infection* 18 (3), 268–281. doi: 10.1111/j.1469-0691.2011.03570.x

Tacconelli, E., Magrini, N., and Kahlmeter, G. (2017) *Global priority list of antibiotic-resistant bacteria to guide research, discovery, and development of new antibiotics.* Available at: https://www.thelancet.com/pdfs/journals/laninf/PIIS1473-3099(17)30753-3.pdf.

Van Duin, D., and Doi, Y. (2017). The global epidemiology of carbapenemase-producing enterobacteriaceae. *Virulence* 8 (4), 460–469. doi: 10.1080/21505594.2016.1222343

World Health Organization (2017) *Global priority list of antibiotic-resistant bacteria to guide research, discovery, and development of new antibiotics.* Available at: https://www.who.int/publications/i/item/9789241514768.

frontiers | Frontiers in Cellular and Infection Microbiology

ORIGINAL RESEARCH
published: 27 April 2022
doi: 10.3389/fcimb.2022.875116

Hybrid Plasmids Encoding Antimicrobial Resistance and Virulence Traits Among Hypervirulent *Klebsiella pneumoniae* ST2096 in India

Chaitra Shankar[1†], Karthick Vasudevan[1†], Jobin John Jacob[1†], Stephen Baker[2], Barney J. Isaac[3], Ayyan Raj Neeravi[1], Dhiviya Prabaa Muthuirulandi Sethuvel[1], Biju George[4] and Balaji Veeraraghavan[1]*

[1] Department of Clinical Microbiology, Christian Medical College and Hospital, Vellore, India, [2] Cambridge Institute of Therapeutic Immunology & Infectious Disease (CITIID), Department of Medicine, University of Cambridge, Cambridge, United Kingdom, [3] Department of Pulmonary Medicine, Christian Medical College and Hospital, Vellore, India, [4] Department of Haematology, Christian Medical College and Hospital, Vellore, India

OPEN ACCESS

Edited by:
Milena Dropa,
University of São Paulo, Brazil

Reviewed by:
João Pedro Rueda Furlan,
University of São Paulo, Brazil
Costas C. Papagiannitsis,
University of Thessaly, Greece

***Correspondence:**
Balaji Veeraraghavan
vbalaji@cmcvellore.ac.in

[†]These authors have contributed equally to this work

Specialty section:
This article was submitted to Clinical Microbiology, a section of the journal Frontiers in Cellular and Infection Microbiology

Received: 13 February 2022
Accepted: 21 March 2022
Published: 27 April 2022

Citation:
Shankar C, Vasudevan K, Jacob JJ, Baker S, Isaac BJ, Neeravi AR, Sethuvel DPM, George B and Veeraraghavan B (2022) Hybrid Plasmids Encoding Antimicrobial Resistance and Virulence Traits Among Hypervirulent Klebsiella pneumoniae ST2096 in India. Front. Cell. Infect. Microbiol. 12:875116. doi: 10.3389/fcimb.2022.875116

Background: Hypervirulent variants of *Klebsiella pneumoniae* (HvKp) were typically associated with a broadly antimicrobial susceptible clone of sequence type (ST) 23 at the time of its emergence. Concerningly, HvKp is now also emerging within multidrug-resistant (MDR) clones, including ST11, ST15, and ST147. MDR-HvKp either carry both the virulence and resistance plasmids or carry a large hybrid plasmid coding for both virulence and resistance determinants. Here, we aimed to genetically characterize a collection of MDR-HvKp ST2096 isolates haboring hybrid plasmids carrying both antimicrobial resistance (AMR) and virulence genes.

Methods: Nine *K. pneumoniae* ST2096 isolated over 1 year from the blood sample of hospitalized patients in southern India that were MDR and suspected to be HvKp were selected. All nine isolates were subjected to short-read whole-genome sequencing; a subset (n = 4) was additionally subjected to long-read sequencing to obtain complete genomes for characterization. Mucoviscosity assay was also performed for phenotypic assessment.

Results: Among the nine isolates, seven were carbapenem-resistant, two of which carried $bla_{\text{NDM-5}}$ on an IncFII plasmid and five carried $bla_{\text{OXA-232}}$ on a ColKP3 plasmid. The organisms were confirmed as HvKp, with characteristic virulence genes (*rmpA2*, *iutA*, and *iucABCD*) carried on a large (~320 kbp) IncFIB–IncHI1B co-integrate. This hybrid plasmid also carried the *aadA2*, *armA*, $bla_{\text{OXA-1}}$, *msrE*, *mphE*, *sul1*, and *dfrA14* AMR genes in addition to the heavy-metal resistance genes. The hybrid plasmid showed about 60% similarity to the IncHI1B virulence plasmid of *K. pneumoniae* SGH10 and ~70% sequence identity with the first identified IncHI1B pNDM-MAR plasmid. Notably, the hybrid plasmid carried its type IV-A3 CRISPR-Cas system which harbored spacer regions against *traL* of IncF plasmids, thereby preventing their acquisition.

Conclusion: The convergence of virulence and AMR is clinically concerning in *K. pneumoniae*. Our data highlight the role of hybrid plasmids carrying both AMR and virulence genes in *K. pneumoniae* ST2096, suggesting that MDR-HvKp is not confined to selected clones; we highlight the continued emergence of such genotypes across the species. The convergence is occurring globally amidst several clones and is of great concern to public health.

Keywords: hypervirulent, *K. pneumoniae*, ST2096, hybrid plasmid, CRISPR-Cas, multidrug resistance

INTRODUCTION

Klebsiella pneumoniae (Kp) is a common cause of hospital-acquired infection (Marr and Russo, 2019). Some forms of *K. pneumoniae* can cause invasive diseases, affecting the liver and other internal organs, and are considered to be hypervirulent (HvKp) (Shon et al., 2013; Marr and Russo, 2019). While HvKp does not have a precise definition, it refers to isolates that carry the virulence plasmid (GenBank accession numbers CP025081, AY378100) coding for *rmpA/rmpA2*, *iucA*, *iutA*, and/or *iroB* (Marr and Russo, 2019). Although HvKp was confined to community-acquired infections, recent reports suggest that HvKp is an emerging nosocomial pathogen with the potential to cause devastating hospital outbreaks thereby establishing itself in both niches (Gu et al., 2018; Liu et al., 2020). HvKp infections are becoming prevalent globally and associated with increased mortality, and a recent study reports the gut colonization of MDR-HvKp in pregnant women (Shon et al., 2013; Marr and Russo, 2019; Huynh et al., 2020). Earlier, HvKp isolates were susceptible to the majority of clinically relevant antimicrobials as they were rarely associated with multidrug resistance plasmids (Shon et al., 2013). However, in the last decade, the organism has undergone several genomic changes and expanded its genome by acquiring multiple resistance plasmids (Lee et al., 2017; Gu et al., 2018; Liu et al., 2020).

It has been found that in the population structure of HvKp, when determined by multi-locus sequence typing (MLST) and whole-genome sequencing (WGS), most HvKp isolates belong to the clonal groups (CG) 23, 65, 86, 375, and 380 (Bialek-Davenet et al., 2014). Conversely, carbapenem-resistant *K. pneumoniae* (CRKp) is associated with a clonal expansion of CG258 in Europe and endemic dissemination of ST11, ST14, ST147, and ST231 clones in Asia and Europe (Qi et al., 2011; Lee et al., 2016; Navon-Venezia et al., 2017; Wyres et al., 2020). However, there have been recent reports on the the emergence of HvKp with multidrug resistance (MDR, resistant to one or more agents in ≥3 antimicrobial classes) phenotypes in divergent CGs (Lee et al., 2017; Turton et al., 2018; Lam et al., 2019), creating new strains with the ability to cause serious infection with limited treatment options (Bialek-Davenet et al., 2014; Yao et al., 2018; Yang et al., 2020). The convergence of MDR and virulence pathotypes in a single isolate occurs either by the uptake of a virulence plasmid by MDR isolate or by the uptake of plasmids carrying antimicrobial resistance genes (ARGs) by the virulent isolates (Tang et al., 2020). CRKp ST11 acquiring the pLVPK-like virulence plasmid and ST23 HvKp acquiring multiple resistance plasmids are some instances where both pathotypes have converged (Liu et al., 2020; Shankar et al., 2020).

Specifically, carbapenem-resistant hypervirulent *K. pneumoniae* (CR-HvKp) has arisen by the formation of mosaic plasmids and hybrid plasmids (Tang et al., 2020; Yang et al., 2021). These mosaic plasmids are typically composed of two or more different plasmid backbones and create a scenario where AMR and virulence determinants are encoded on a single large plasmid with a mosaic (medley) arrangement of resistance and virulence genes whereas the hybrid plasmids are co-integrates with two plasmid backbones (Lam et al., 2019; Turton et al., 2019). Mosaic plasmids with fragments of virulence plasmid and $IncFII_K$ coding for resistance and virulence have been described among ST15 *K. pneumoniae* from Europe (Lam et al., 2019). In contrast, the hybrid plasmids with a range of replicons (IncFIB–IncHI1B, IncFIBK–IncHI1B, IncFIB–IncR) have been described in China and Europe (Lam et al., 2019; Turton et al., 2019; Li et al., 2020; Xie et al., 2020; Yang et al., 2020) and are being increasingly reported among regional MDR clones. Our understanding of these CR-HvKp hybrid plasmids is limited due to an insufficient number of complete plasmid sequences. Here, we aimed to characterize a set of MDR-HvKp belonging to ST2096, possessing hybrid plasmids that simultaneously carry both AMR and virulence genes. The complete genome sequences of four of these isolates were further generated by long-read sequencing to elucidate the detailed structure of the hybrid plasmid *via* comparative genomics.

Abbreviations: ST, sequence type; MLST, multi-locus sequence typing; MDR, multidrug-resistant; AMR, antimicrobial resistance; HvKp, hypervirulent *Klebsiella pneumoniae*; CRKP, carbapenem-resistant *Klebsiella pneumoniae*; CR-HvKp, carbapenem-resistant hypervirulent *Klebsiella pneumoniae*; CG, clonal group; ARG, antimicrobial resistance genes; pLVPK, large virulence plasmid of *Klebsiella pneumoniae*; CRISPR, clustered regularly interspaced short palindromic repeats; XDR, extensively drug-resistant; SNP, single-nucleotide polymorphism; AST, antimicrobial susceptibility testing; OD, optical density.

MATERIALS AND METHODS

Bacterial Isolates

The *K. pneumoniae* were isolated from patients with bacteremia admitted to the Christian Medical College, Vellore, India, in 2019. The isolates were identified using standard microbiological methods and further confirmed by VITEK MS [Database v2.0, bioMerieux, Marcy-l'Étoile, France] (Versalovic et al., 2011).

The isolates were screened for hypermucoviscous phenotype using the string test (Shon et al., 2013). In addition, the mucoid phenotype-associated genes *rmpA* and *rmpA2* were detected by PCR (Turton et al., 2010; Compain et al., 2014). The demographic and clinical details of the nine patients from whom the organisms were isolated were accessed from electronic medical records. The study was approved by the Institutional Review Board of Christian Medical College, Vellore, with minute number 9616 (01/09/2015).

Antimicrobial Susceptibility Testing

Antimicrobial susceptibility testing (AST) was performed using the Kirby-Bauer disk diffusion method according to the CLSI 2019 guidelines (Clinical and Laboratory Standards Institute, 2019). The tested antimicrobials were cefotaxime (30 μg), ceftazidime (30 μg), piperacillin/tazobactam (100/10 μg), cefoperazone/sulbactam (75/30 μg), imipenem (10 μg), meropenem (10 μg), ciprofloxacin (5 μg), levofloxacin (5 μg), gentamicin (10 μg), amikacin (30 μg), and minocycline (30 μg). The minimum inhibitory concentration (MIC) of meropenem was determined by the broth microdilution (BMD) method. *Escherichia coli* ATCC® 25922, *Enterococcus faecium* ATCC® 29212, and *Pseudomonas aeruginosa* ATCC® 27853 were used as controls. Data were interpreted according to the 2019 CLSI guidelines (CLSI 2019).

Mucoviscosity Assay

Overnight culture of the HvKp isolates was inoculated in Luria Bertani (LB) broth (Oxoid, Hampshire, United Kingdom) and centrifuged at 1,000 rpm for 15 min as previously described (Mike et al., 2021). Briefly, the optical density (OD) of the supernatant was measured at 600-nm wavelength in the UV spectrophotometer (1st OD). 1 ml of PBS (phosphate-buffered saline) was added, and OD_{600} was adjusted to 1.00. This was centrifuged again at 1,000 rpm for 5 min, and the OD_{600} of the supernatant (3rd OD) was measured. Non-virulent isolate K. quasipneumoniae ATCC® 700603 was used as a control for mucoviscosity assay. This assay is based on the principle that hypermucoviscous isolates do not sediment easily and hence the OD_{600} after centrifugation will be higher than the counterparts of control and non-hypermucoviscous isolates. Hence, hypermucoviscous isolates will have a higher SAC ratio than the rest.

Sedimentation Assay Calculation (SAC) = Reading of 3rd OD_{600}/Reading of 1st OD_{600}.

DNA Extraction and Genome Sequencing

The isolates studied were revived from the archive of the Department of Clinical Microbiology, and a single colony was inoculated in LB broth at 37°C. Total genomic DNA was extracted from pelleted cells using the Wizard DNA Purification Kit (Promega, Madison, WI, USA). Extracted DNA was quantified using NanoDrop One spectrophotometry (Thermo Fisher Scientific, Waltham, MA, USA) and Qubit 3.0 fluorometry (Life Technologies, Carlsbad, CA, USA) and stored at -20°C until further use.

A sequencing library was prepared using the Nextera DNA Flex Library Preparation Kit (Illumina, San Diego, CA, USA). Subsequently, the paired-end library was subjected to sequencing on a HiSeq 2500 platform (Illumina, USA) generating 2 × 150-bp reads. Sequencing reads with a PHRED quality score below 20 were discarded, and adapters were trimmed using cutadapt v1.8.1 and assessed with FastQC v0.11.4 (Andrews, 2010; Martin, 2011). For a subset of four isolates, long-read sequencing was performed using an Oxford Nanopore MinION FLO-MIN106 R9 flow cell (Oxford Nanopore Technologies, UK). The long-read DNA library was prepared using the SQK-LSK108 ligation sequencing kit (v.R9) along with the ONT EXP-NBD103 Native Barcode Expansion kit (Oxford Nanopore Technologies, Oxford, UK). The library was loaded onto flow cells, run for 48 h using the standard MinKNOW software (Guppy version 3.6).

Genome Assembly and Evaluation

Draft genome sequence data generated using Illumina were assembled using SPAdes (v.3.13.0) (Bankevich et al., 2012). A hybrid *de novo* assembly was generated for a subset of four isolates (Vasudevan et al., 2020). The nanopore long reads were error-corrected with the standalone Canu error correction tool (v.1.7) and assembled using the Unicycler hybrid assembly pipeline (v 0.4.6) with the default settings (Koren et al., 2017; Wick et al., 2017). The genome sequences were polished using high-quality Illumina reads, as described previously using Pilon (Walker et al., 2014). The assembled genomes were subjected to quality assessment using CheckM v1.0.5 (Parks et al., 2015) and Quast v4.5 (Gurevich et al., 2013). *K. pneumoniae* NTUH-K2044 (GenBank accession number AP006725) was used as the reference genome since it is a well-characterized type of strain of ST23 hypervirulent *K. pneumoniae*.

Genome Analysis

Genome assemblies were submitted to NCBI GenBank and annotated using the NCBI Prokaryotic Genome Annotation Pipeline [PGAP v.4.1] (Tatusova et al., 2016).

The genomes described in the study are publicly available under the Bioproject ID PRJNA613369 in GenBank with accession numbers CP053765–CP053770, CP053771–CP053780, CP058798–CP058806, JAARNO010000001.1–JAARNO010000005.1, JAAQSG000000000, JAARNJ000000000, JAARMH000000000, and JAAQTC000000000. The antimicrobial resistance profile of the assembled genome sequences was identified using ResFinder v.4.1 available from CGE server (Bortolaia et al., 2020). Similarly, the presence of plasmids in the genomes was identified and characterized using PlasmidFinder (v.1.3) available at the CGE server (Carattoli et al., 2014). MLST and virulence loci (yersiniabactin, aerobactin, and other siderophore production systems) were identified using Kleborate (v.2.0.0) (Lam et al., 2021). The presence of virulence factors was confirmed using the virulence database at Pasteur Institute for *K. pneumoniae* (Jolley and Maiden, 2010). YbST and AbST, typing schemes based on yersiniabactin and aerobactin loci, were deduced from the database at Pasteur Institute for *K. pneumoniae* (https://bigsdb.pasteur.fr/cgi-bin/bigsdb/bigsdb.pl?db=pubmlst_klebsiella_seqdef&page=profiles). The K and O antigen loci were identified using Kaptive available at Kleborate (Wyres et al., 2016; Wick et al., 2018).

The final assembled circular chromosomes and plasmids were visualized using CGView server v.1.0 (Grant and Stothard, 2008) and Easyfig (Sullivan et al., 2011). CRISPR regions in the genomes were identified with the CRISPRCasTyper web server (Russel et al., 2020). The genetic distance between isolates was calculated using average nucleotide identity (ANI) available at OrthoANI (Lee et al., 2016). Pairwise distance between the nine isolates was determined with BA10835 as reference using SNP-dists v 0.6.3 (Wysocka et al., 2020) from the raw reads by aligning the short reads of each isolate against the reference. An SNP-based phylogenetic tree of the complete hybrid plasmids with IncHI1B–IncFIB (pNDM-MAR) replicon types which are mentioned in **Table S1** was constructed using CSI phylogeny (https://cge.cbs.dtu.dk/services/CSIPhylogeny/).

RESULTS

Clinical Manifestations and Microbiological Characteristics of the Isolates

During the routine surveillance of HvKp, we identified isolates that were negative for the string test, positive for *rmpA2* as determined by PCR, and carbapenem-resistant as determined by AST. These isolates were chosen for whole genome sequencing, and we identified nine ST2096 (a single-locus variant of ST14) *K. pneumoniae* associated with bacteremia in our hospital (**Table 1**). These nine *K. pneumoniae* ST2096 were resistant to all tested antimicrobials by disk diffusion assay and were initially considered to be extensively drug-resistant (XDR, non-susceptible to at least one agent in all but ≤2 classes of antimicrobials). However, upon MIC testing, two isolates were found to be susceptible to meropenem (MIC ≤0.5 μg/ml). The results of the mucoviscosity assay are mentioned in **Figure S1**. The isolates showed significantly higher OD_{600} when compared to the control strain indicating the lack of sedimentation by the hypervirulent isolates.

From the resulting nine genome sequences, the surface capsule (K) loci were predicted to be K64 whereas the O-antigen encoding loci was determined to be O1v1 in all isolates (**Tables 2** and **3**). The pairwise average nucleotide identity (ANI) among the nine draft genomes was >99.8% (**Figure S2A**). The pairwise SNP difference among the nine isolates segregated them into two clusters, with BA10835 and BA27935 being >260 SNPs from the remaining seven sequences (**Figure S2B**). Within the major cluster (7 isolates), BA10334 and BA1602 were highly

TABLE 1 | The demographic and clinical details of the patients with bacteremia caused by hypervirulent *K. pneumoniae* ST2096.

Micro no.	Month of isolation	Unit	Clinical manifestation	Risk factors	Prior hospitalization	Therapy administered and duration of therapy		Outcome
BA1602	January 2019	Surgery	Carcinoma ascending colon	Anastomotic leak with fecal peritonitis, MODS, fever, Cough	Yes	Polymyxin B, meropenem, teicoplanin, tigecycline	16 days	Succumbed to death
BP3636	March 2019	Hematology	Fever and giddiness	Congenital sideroblastic anemia, Stem cell transplant—day 28	Yes	Meropenem, tigecycline, fosfomycin, colistin	2 days	Succumbed to death
BA10334	April 2019	Gastroenterology	Persistent rise of temperature, recurrent vomiting, loss of weight	Disseminated tuberculosis, sepsis, pleural effusion	Yes, treated elsewhere for 10 days	Cefoperazone-sulbactam, meropenem, colistin, vancomycin	10 days	Succumbed to death
BA10835	April 2019	Hepatology	Acute febrile illness with Jaundice	Acute on chronic liver failure, portal hypertension, Wilson disease	No	Tigecycline	1 month	Recovered
BA25425	August 2019	Neurosurgery	Road traffic accident—head injury	Right subdural hematoma Temporal hemorrhagic contusion	Yes	Linezolid, piperacillin-tazobactam, cefoperazone-sulbactam, gentamicin	1 month	Succumbed to death
BA27935	September 2019	Casualty	Acute febrile illness with altered sensorium	Hypertension, intracranial bleed Hemiplegia	Yes, treated elsewhere for 10 days	Meropenem	1 day	Discharged against medical advice
BA28118	September 2019	Hematology	Acute promyelocytic leukemia Acute kidney injury	Fever, multiple episodes of bleeding from gums/per rectum	No	Meropenem, tigecycline, polymyxin B, amikacin	1 month	Recovered
BA32040	October 2019	Hematology	Acute febrile illness	Beta thalassemia post-allogenic stem cell transplant—day 280 Skin GVHD	Yes	Colistin, meropenem	15 days	Recovered
BA39100	December 2019	Hematology	Extramedullary granulocytic sarcoma	Invasive mucormycosis	Yes	Meropenem, tigecycline Teicoplanin polymyxin B	3 days	Recovered

GVHD, graft versus host disease; MODS, multiple-organ dysfunction syndrome.

TABLE 2 | Phenotypic and genotypic characteristics obtained using hybrid genome assembly of four Indian MDR hypervirulent *K. pneumoniae* ST2096.

Isolate ID	BA10835	BA27935	BP3636	BA32040
Accession numbers	CP053765–CP053770	CP058798–CP058806	CP053771–CP053780	JAARNO010000001.1 to JAARNO010000005.1
Meropenem MIC	128 µg/ml	4 µg/ml	64 µg/ml	≤0.5µg/ml
Chromosomal AMR genes	*aac(6')-Ib-cr*, *bla*$_{SHV}$, *bla*$_{OXA-1}$, *fosA*, *dfrA1*	*aac(6')-Ib-cr*, *bla*$_{SHV}$, *bla*$_{OXA-1}$, *fosA*, *dfrA1*	*bla*$_{SHV}$, *fosA*, *dfrA1*	*aac(6')-Ib-cr*, *bla*$_{SHV}$, *bla*$_{OXA-1}$, *fosA*, *dfrA1*
Chromosomal virulence genes	*fyuA*, *irp1*, *kfuABC*, *mrkACFJ*, *ybtAEPQSTUX*	*fyuA*, *irp1*, *kfuABC*, *mrkACFJ*, *ybtAEPQSTUX*	*fyuA*, *irp1*, *irp2*, *kfuABC*, *mrkABCDFHIJ*, *ybtAEPQSTUX*	*fyuA*, *irp1*, *kfuABC*, *mrkABCDFHIJ*, *ybtAEPQSTUX*
No. of plasmids	5	4	4	4
IncHI1B/IncFIB (pNDM-MAR)	*aadA2*, *armA*, *bla*$_{TEM-1B}$, *bla*$_{CTX-M-15}$, *mphE*, *msrE*, *sul1*, *tetD*, *dfrA12*	*aadA2*, *armA*, *bla*$_{TEM-1B}$, *bla*$_{CTX-M-15}$, *mphE*, *msrE*, *sul1*, *tetD*, *dfrA12*	*aadA2*, *armA*, *aac(6')-Ib-cr*, *bla*$_{TEM-1A}$, *bla*$_{CTX-M-15}$, *bla*$_{OXA-1}$, *mphE*, *msrE*, *sul1*, *tetD*, *dfrA12*, *dfrA14*	*bla*$_{TEM-1A}$, *bla*$_{CTX-M-15}$, *tetD*, *dfrA14*
Virulence plasmid	*iucABCD*, *iutA*, *rmpA2**	*iucABCD*, *iutA*, *rmpA2**	*iucABCD*, *iutA*, *rmpA2**	*iucABCD*, *iutA*, *rmpA2**
IncFIBK-IncFIIK	*catA1*	absent	No AMR gene	No AMR gene
ColKP3	absent	absent	*bla*$_{OXA-232}$	absent
IncFII	*aadA2*, *rmtB*, *bla*$_{NDM-5}$, *ermB*, *mphA*, *sul1*, *dfrA12*	*aadA2*, *rmtB*, *bla*$_{NDM-5}$, *bla*$_{TEM-1B}$, *ermB*, *mphA*, *sul1*, *dfrA12*	Absent	*rmtB*, *bla*$_{TEM-1B}$, *ermB*, *mphA*
Other plasmids	ColRNAI	Col(BS512), ColRNAI	ColRNAI	ColRNAI

rmpA2, rmpA2 allele number 8 was observed which is frameshifted; MIC, minimum inhibitory concentration determined by broth microdilution; AMR, antimicrobial resistance.*

TABLE 3 | Genotypic characteristics of multidrug-resistant hypervirulent *K. pneumoniae* belonging to ST2096 obtained from short read assembly.

Accession number and isolate ID	*rmpA* and/or *rmpA2*	Capsule type	O antigen	Ybt, ICEKp	Resistance genes	Plasmids	Virulence genes
JAARMH000000000 BA1602	*rmpA2**	K64	O1v1	*ybt14*; ICEKp5	*aac(6)-Ib-cr*, *aadA2*, *armA*, *bla*$_{SHV-106}$, *bla*$_{CTX-M-15}$, *bla*$_{OXA-1}$, *bla*$_{TEM-150}$, *fosA6*, *mphE*, *msrE*, *sul1*, *tetD*, *dfrA1*, *dfrA12*, *dfrA14*	ColKP3, IncFIBK, incFIB (pNDM-MAR), IncHI1B (pNDM-MAR)	*fyuA*, *irp1*, *irp2*, *kfuAB*, aerobactin, *mrkABCDFHIJ*
JAAQTC000000000 BA25425	*rmpA2**	K64	O1v1	*ybt14*; ICEKp5	*aadA2*, *armA*, *sat-2A*, *bla*$_{SHV-28}$, *bla*$_{CTX-M-15}$,*bla*$_{OXA-1}$, *bla*$_{TEM-1D}$, *bla*$_{OXA-232}$, *mphE*, *msrE*, *sul1*, *tetD*, *dfrA1*, *dfrA12*, *dfrA14*	ColKP3, ColRNAI, IncFIBK, IncFIB (pNDM-Mar), IncHI1B (pNDM-MAR)	*fyuA*, *irp1*, *irp2*, *kfuABC*, *mrkABCDFHIJ*
JAAQSG000000000 BA28118	*rmpA2**	K64	O1v1	*ybt14*; ICEKp5	*aadA2*, *armA*, *bla*$_{SHV-28}$, *bla*$_{CTX-M-15}$, *bla*$_{OXA-1}$, *bla*$_{TEM-1D}$, *bla*$_{OXA-232}$,*mphE*, *msrE*, *sul1*, *tetD*, *dfrA12*, *dfrA14*	IncFIBK, IncFIB(pNDM-Mar), ColKP3, ColBS512, IncHI1B (pNDM-MAR)	*fyuA*, *irp1*, *irp2*, aerobactin, *kfuABC*, *mrkABCDFHIJ*
JAARNJ000000000 BA39100	*rmpA2*	K64	O1v1	*ybt14*; ICEKp5	*aac(6)-Ib-cr*, *aadA2*, *armA*, *sat2A*, *bla*$_{SHV-106}$, *bla*$_{CTX-M-15}$, *bla*$_{OXA-1}$, *bla*$_{TEM-1B}$, *bla*$_{OXA-232}$, *catB*, *fosA6*, *mphE*, *msrE*, *sul1*, *tetD*, *dfrA1*, *dfrA12*, *dfrA14*,	ColKP3, IncFIBK, IncFIB (pNDM-Mar), IncHI1B (pNDM-MAR)	*fyuA*, *irp1*, *irp2*, *kfuA*, *kfuC*, aerobactin, *mrkABCDFHIJ*
JAAQSS00000000 BA10334	*rmpA2**	K64	O1v1	*ybt14*; ICEKp5	*aac(6)-Ib-cr*, *aadA2*, *armA*, *bla*$_{SHV}$, *bla*$_{CTX-M-15}$, *bla*$_{OXA-1}$, *bla*$_{TEM-1A}$, *bla*$_{OXA-232}$, *fosA*, *msrE*, *mphE*, *sul1*, *tetD*, *dfrA1*, *dfrA12*, *dfrA14*	ColKP3, IncHI1B (pNDM-MAR), IncFIB (pNDM_MAR), IncFIBK	*fyuA*, *irp1*, *irp2*,*iutA*, aerobactin, *kfuABC*, *mrkABCDFHIJ*

rmpA2, frameshift mutation.*

related (2 SNPs), and similarly, BA25425 and BP3636 (6SNPs) were related. Since this is a retrospective study, other specimen sources were not investigated to determine if there was an outbreak of ST2096 in the hospital and hence the dissemination of the plasmid cannot be explained.

Characterization of the HvKp ST2096 Chromosomes

Typically, *K. pneumoniae* chromosomes are characterized by the presence of *bla*$_{SHV}$ and *fosA*. In addition to these resistance genes, surprisingly, we found that three of the four MDR-HvKp isolates with complete genomes had the *aac(6')-Ib-cr*, *bla*$_{OXA-1}$ and *dfrA1* genes integrated into chromosome on mobile genetic elements. Specifically, *aac(6')-Ib-cr* and *bla*$_{OXA-1}$ were inserted by IS*26* in the central region of the chromosome at ~2.3 Mbp with a 7-bp flanking region (AGTCCGT) (**Figure 1A**). The *dfrA1* gene was associated with IS*Kpn26* and a class 1 integron, *intI1*, at position ~5.3 Mbp. From the nine draft genome sequences, we identified a type I-E CRISPR located on the chromosome, characterized by 7–12 spacers of 32 bp and an adjacent IS*Kpn26* (**Figure 1B**).

The key virulence determinant carried by the chromosome of *K. pneumoniae* is the *ybt* locus, which is mobilized by ICEKp. *ybt14* was carried on ICEKp5 and integrated into the chromosome

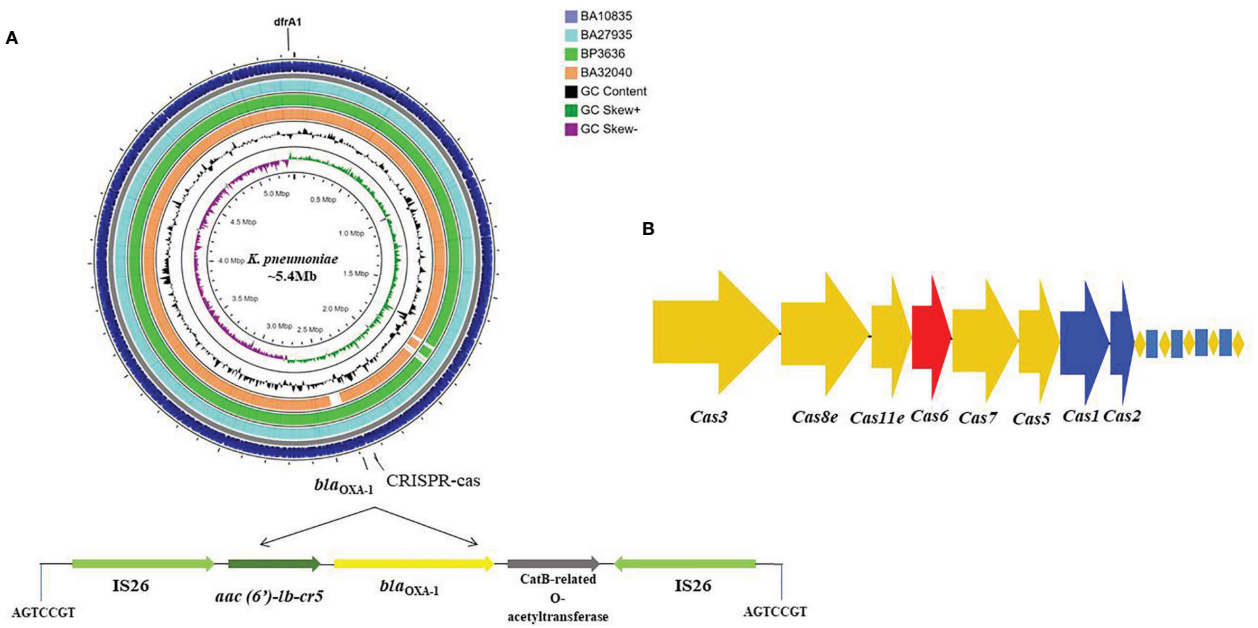

FIGURE 1 | Circular genome map of four MDR hypervirulent *K. pneumoniae* ST2096 chromosomes. **(A)** Circles from the outside to the inside show the CDS region of BA10835 (blue), BA27935 (cyan), BP3636 (green), BA32040 (yellow), GC skew (dark green and purple), and GC content (black). Linear view of the IS*26* mediated trans locatable units carrying *aac(6')-Ib-cr* (fluoroquinolones and aminoglycosides), bla_{OXA-1} (ampicillin), and *catB3* (chloramphenicol) inserted to the chromosome. A repeat region of 7 bases read as AGTCCGT was present on either ends where the insertion was observed. Map generated using CGView server (Grant and Stothard, 2008). **(B)** Type I-E CRISPR-Cas system identified in the chromosomes with repeat region of 28 bases.

in all nine sequenced isolates. The *fyuA* and *irp1* yersiniabactin receptors were also present on the chromosome, along with a *kfu* gene cluster encoding for iron uptake and the *mrk* gene cluster, which facilities biofilm formation. YbST, typing based on yersiniabactin loci, classified all the isolates as belonging to YbST140.

The genomes of BP3636 (5,352,701 bp) and BA32040 (5,298,155 bp) were smaller than the genomes of BA10835 (5,355,460 bp) and BA27935 (5,356,693 bp) and lacked some of the iron transporters and metal transporter-encoding genes on the chromosomes. In addition, BA32040 lacked some of the genes coding for ABC transporter, MFS transporter, and LysE and LysR family transcriptional regulators when compared to the other three complete genomes (data not shown).

Characterization of the Plasmids Among HvKp ST2096

The nine HvKp isolates were found to possess an array of AMR genes associated with 4–5 plasmids per genome, including the virulence plasmid (**Tables 2** and **3**). Notably, bla_{NDM-5} was carried on the IncFII plasmid (~97 kbp) along with *aadA2*, *rmtB*, *ermB*, *mphA*, *sul1*, *dfrA12*, and bla_{TEM-1B} (**Figure 2**). We also found a 293-bp segment of an IS30 family transposase, with similarity to the IS*Aba125*, adjacent to bla_{NDM-5}. The closest matching plasmid from the global database was from *K. pneumoniae* JUNP055 (GenBank accession no. LC506718), which also harbored bla_{NDM-5} but lacked a few IS elements (IS*Ec23* and IS6 family) when compared to IncFII of the ST2096 isolates (**Figure 2**). These pJUNP055 and IncFII plasmids from the present study shared ~80% sequence identity to those of *E. coli* M105 from Myanmar (GenBank accession no. AP018136), which lacked bla_{NDM-5}. As predicted, the $bla_{OXA-232}$ carbapenemase was encoded by a small 6Kb ColKP3 plasmid and was adjacent to a truncated IS*Ecp1* (207 bp). Notably, the two isolates (BA32040 and BA1602) that were susceptible to meropenem lacked a carbapenemase-encoding gene. Additionally, a large (~307-kbp) plasmid was present in all four of the assembled genomes and was found to be a fusion of IncFIB and IncHI1B plasmid backbones, carrying both AMR genes and virulence genes which will be referred to as p2096_hyb (**Table 2**). The isolates also harbored several small plasmids (<8 kbp), such as ColRNAI and Col(BS512), which did not encode either AMR or virulence genes.

Hybrid Plasmid Coding for Virulence and Antimicrobial Resistance

A large hybrid virulence plasmid, p2096_hyb, of ~307 kbp was the hallmark of all ST2096 isolates, and they carried a frameshifted *rmpA2* and the aerobactin siderophore, encoded by *iucABCD*. The hybrid plasmid in the four isolates BA10835, BA27935, BP3636, and BA32040 will be referred to as p10835_hyb, p27935_hyb, p3636_hyb, and p32040_hyb, respectively. This plasmid carried both IncHI1B and IncFIB replicons on the pNDM-MAR backbone and hence was called a hybrid plasmid. This plasmid-encoded several AMR genes as listed in **Table 2**. The backbone of the plasmid consisted of genes

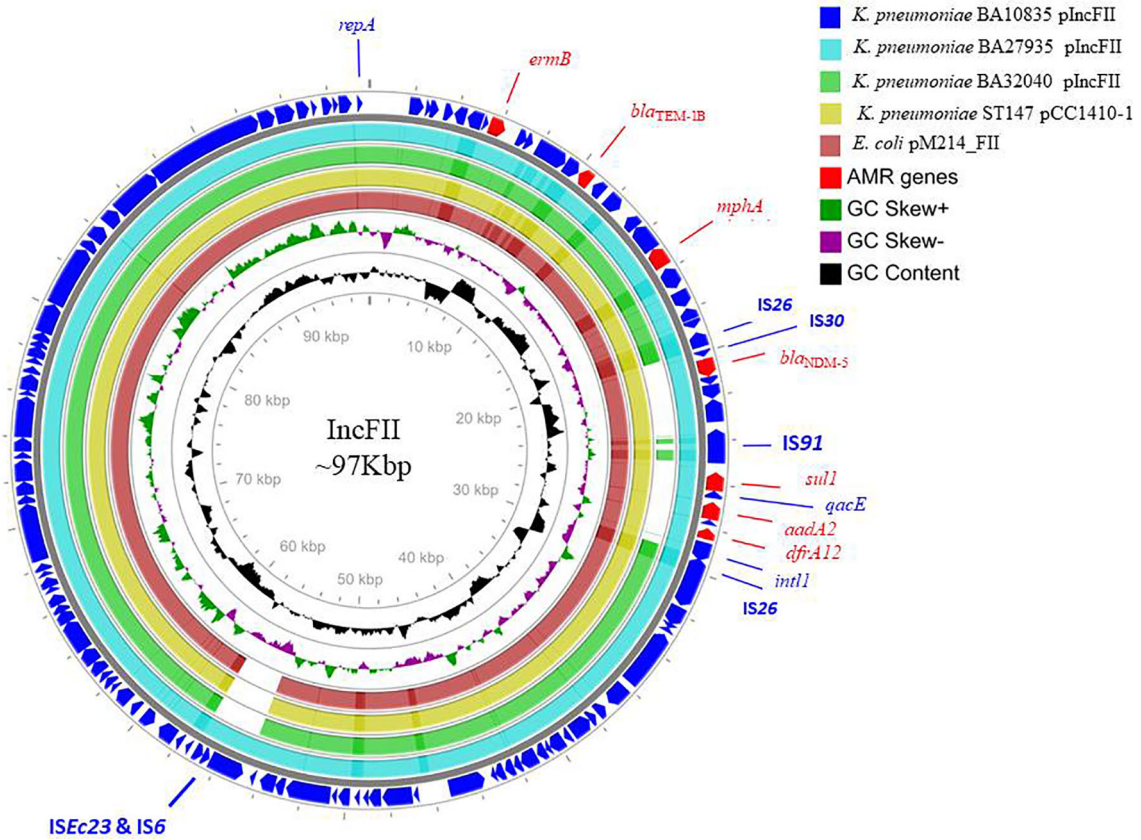

FIGURE 2 | Alignment of IncFII plasmids of three MDR hypervirulent *K. pneumoniae* belonging to ST2096. Circles from the outside to the inside show the CDS region of BA10835 (blue), BA27935 (cyan), BA32040 (green), and nearest matching reference plasmids that belong to *K. pneumoniae* pCC1410-1 (yellow; KT725788) and *E. coli* pM214 (red; AP018144). GC skew (dark green and magenta) and GC content (black) of the plasmid are represented in the inner circles. Maps were generated using the CGView server.

related to replication, toxin–antitoxin system, conjugative transfer, DDE transposase, transcriptional regulators, and tyrosine-specific recombinases. Notably, *dfrA12*, *aadA2*, and *sul1* genes were inserted into the virulence plasmid through a class 1 integron, *intI1*. The insertion of $bla_{\text{OXA-1}}$, *catB*, and *aac (6′)-lb-cr5* on the hybrid plasmid was through IS*26*, comparable to the arrangement observed in the chromosome (**Figures 1A, B**). A Tn*3* transposon contained several AMR genes including *msrE*, *mphE*, *sul1* and β-lactamases, such as $bla_{\text{OXA-1}}$, $bla_{\text{CTX-M-15}}$, and $bla_{\text{TEM-1}}$. In addition to Tn*3*, $bla_{\text{CTX-M-15}}$ and $bla_{\text{TEM-1}}$ were associated with IS*Ec9*, a resolvase, and IS*91* insertion sequence. The hybrid plasmid in BA32040 was shorter (272 kbp) and lacked *aadA2*, *armA*, $bla_{\text{OXA-1}}$, *msrE*, *mphE*, *sul*, *dfrA14* and the CRISPR array in comparison to plasmids found in the other three genomes.

Besides the virulence genes, p2096_hyb also carried genes encoding heavy metal tolerance such as *merARCTP* (mercury) and *terBEDWXZ* (tellurium) that were possibly inserted through the Tn*3* transposon, as shown in **Figure 3A**. Notably, a frameshift mutation was observed in *rmpA2* among all the isolates, which we presumed to be associated with the negative string test results as has been previously described (Yu et al., 2015; Shankar et al., 2021b). The frameshift occurred due to the deletion of an adenine base at the 346th base in *rmpA2*. Non-functional *rmpA2* and the absence of *rmpA* in these isolates contribute to the loss of a hypermucoid phenotype resulting from the decreased extracellular polysaccharide production. Aerobactin typing (AbST), a typing method using aerobactin alleles (*iucA*, *iucB*, *iucC*, *iucD*, and *iutA*), revealed all the study isolates that belonged to AbST-1. A type IV-A3 CRISPR-Cas system located on the hybrid plasmid of three isolates (BA10835, BA27935, BP3636) was characterized by the presence of 5–12 spacers and a 29-bp repeat region. One spacer each from the hybrid plasmid of the three isolates was comparable to *traL* of IncF plasmids that were found in *K. pneumoniae*, which may act as a potential obstacle in acquiring IncF plasmids and thereby limit the number of plasmids carried by these isolates.

Figures 3A, B show the BLAST comparison of the hybrid plasmids from the present study to another hybrid plasmid, MK649825, from ST2096 isolated from the same center earlier in 2017 (Wyres et al., 2020). The plasmid, MK649825, was much smaller (273 kbp) than the plasmids isolated during 2019 and

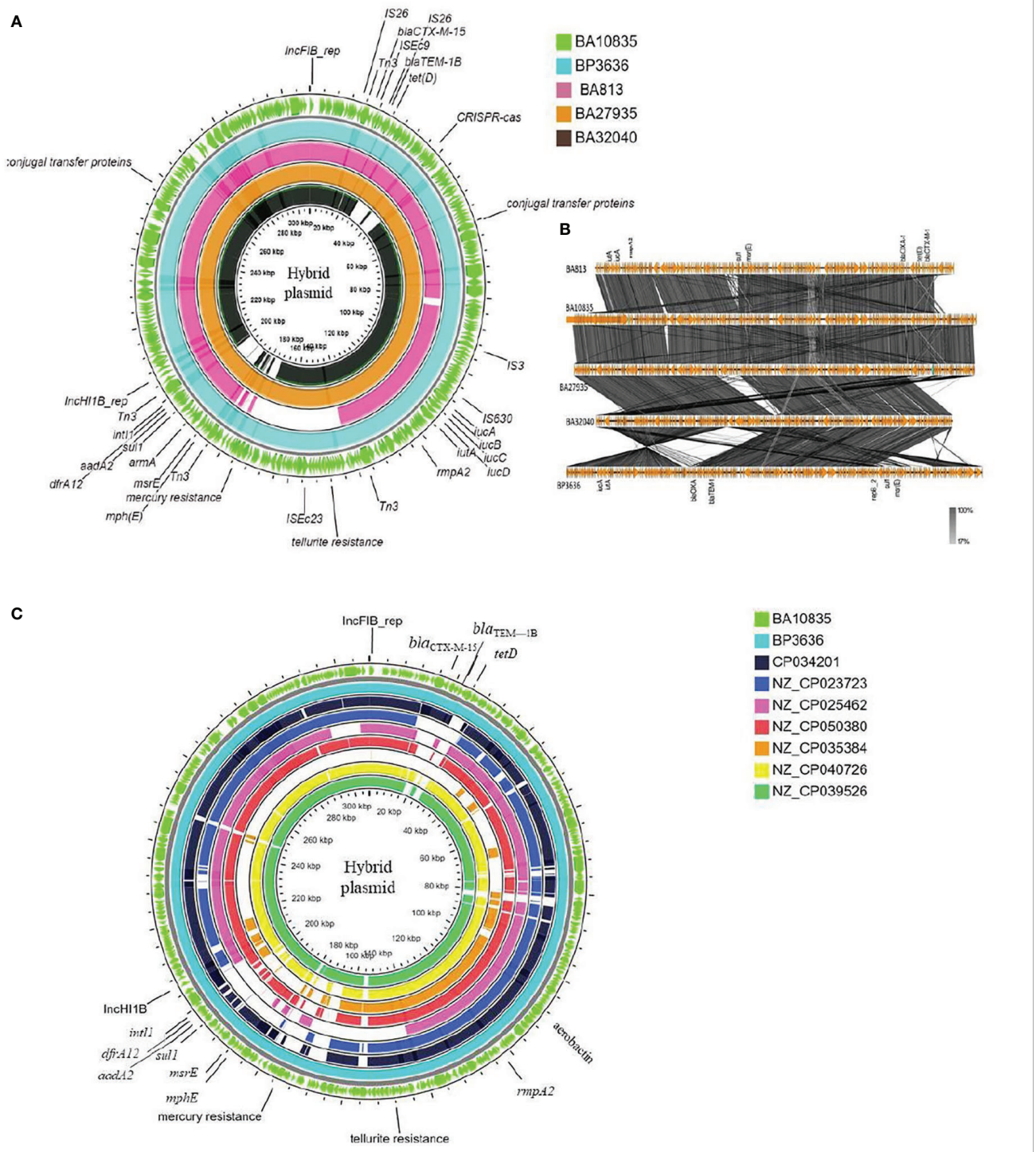

FIGURE 3 | Maps of ST2096 mosaic plasmids in comparison to previously reported IncHI1B-IncFIB virulence plasmids. **(A)** Circular genome comparison map of IncFIB–IncHIB mosaic plasmids from outer to inner rings-BA10835 (light green), BP3636 (teal), BA813 (red), BA27935 (orange), and BA32040 (black). All the isolates belong to ST2096 and mosaic plasmid from BA813 (MK649825) was isolated during 2017 from the same study center. It lacks the heavy metal resistance encoding region when compared to other plasmids that were isolated during 2019. **(B)** Linear alignment of the mosaic plasmids obtained *K. pneumoniae* ST2096 using Easyfig. **(C)** Circular genome comparison map of IncHI1B–IncFIB mosaic plasmids from outer to inner rings-BA10835 (light green), BP3636 (teal), CP034201 (navy blue), NZ_CP023723 (indigo), NZ_CP025462 (pink), NZ_CP050380 (red), NZ_CP035384 (orange), NZ_CP040726 (yellow), and NZ_CP039526 (dark green). NZ_CP035384 shows the least similarity to the plasmids from the present study. Details of resistance and virulence genes carried by these plasmids are detailed in **Supplementary Table 1**.

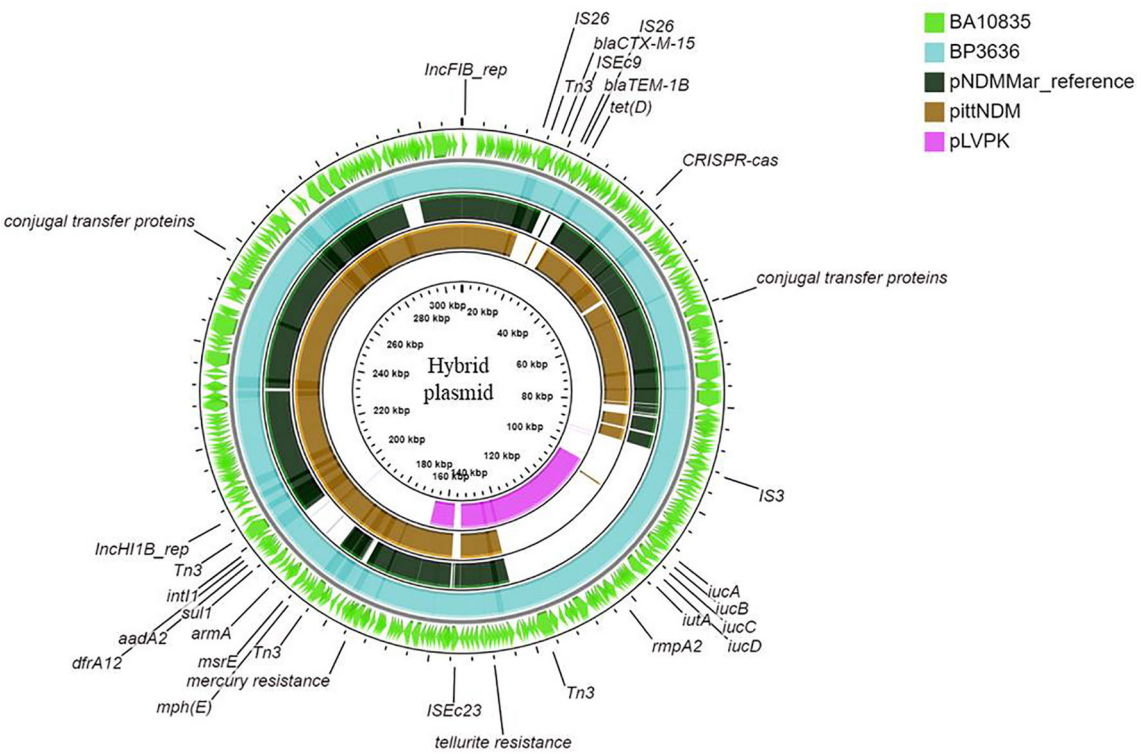

FIGURE 4 | Maps of ST2096 mosaic plasmids in comparison to previously reported reference plasmids. Circular comparison map of plasmids from outer to inner rings—BA10836, BP3636, IncHI1B (pNDM-MAR, JN420336.1), PittNDM (NZ_CP006799.1), and pLVPK (AY378100.1) plasmids.

lacked the genes encoding mercury and tellurite tolerance. p2096_hyb of ~307 kbp showed ≤50% sequence identity with the pLVPK (Chen et al., 2004) reference virulence plasmid having in common with the region coding for virulence genes (**Figure S3**). p2096_hyb showed about 60% similarity to the IncHI1B virulence plasmid of *K. pneumoniae* SGH10 (Lam et al., 2018) and ~70% sequence identity with the first identified IncHI1B pNDM-MAR plasmid, a 267-kbp plasmid (GenBank accession no. JN420336.1) from a *K. pneumoniae* ST15 (Villa et al., 2012) carrying $bla_{\text{NDM-1}}$ (**Figure S3**; **Figure 4**). While the p2096_hyb among HvKp ST2096 retained the regions coding for mercury, tellurite, β-lactam ($bla_{\text{OXA-1}}$ and $bla_{\text{CTX-M-15}}$), chloramphenicol, and aminoglycoside resistance, it had lost the segment carrying $bla_{\text{NDM-1}}$ when compared to the pNDM-MAR plasmid. The insertion of the virulence-encoding region into the pNDM-MAR plasmid is possibly through the insertion mediated by IS*3* and IS*66* family proteins (IS*Ec23*) (**Figure 3A**). **Figure 4** shows the circular comparison of two-hybrid plasmids of ST2096 to pLVPK (GenBank accession no. AY378100.1), IncHI1B (pNDM-MAR) [GenBank accession no. JN420336.1], and pittNDM (GenBank accession no NZ_CP006799.1) plasmids. The latter two plasmids lack the virulence genes but encode antimicrobial resistance genes with IncHI1B backbone.

Figure 3C shows the BLAST comparison between the hybrid plasmid from the present study and the previously reported *K. pneumoniae* hybrid plasmids comprising IncHI1B (pNDM-MAR)–IncFIB (pNDM-MAR) replicon types. The complete sequences of these plasmids have been reported from 2015 till date among diverse clones of *K. pneumoniae* such as ST11, ST383, ST15, ST147, and ST23 and vary in size ranging from 261 to 396 kbp. The particulars of antimicrobial resistance and virulence genes carried by these plasmids are mentioned in **Table S1**. Interestingly, apart from the hybrid plasmid in the present study, another plasmid obtained in China, p44-1, from ST11 carried frameshifted *rmpA2*. Hybrid plasmids of HvKp ST2096, p10835_hyb (307 kbp), and p3636_hyb (317 kbp) showed high similarity to pKpvST383L (372 kbp) and pHB25-1-vir (396 kbp) which were isolated in England and China, respectively.

An SNP-based phylogenetic tree of the complete hybrid plasmids is shown in **Figure S4**. The tree was rooted at pAP855 since it was distant from the others and belonged to an ST23 isolate, lacking *rmpA2* (Tian et al., 2021). All the other plasmids belonged to MDR clones such as ST11, ST15, ST147, ST383, and ST2096. The plasmids from the present study formed a separate cluster coding for mercury and tellurite tolerance, truncated *rmpA2*, and lacking carbapenemase. This group is closely related to two plasmids from China isolated during 2015 and 2016, one of which also carries a truncated *rmpA2* (**Table S1**). The plasmids from England and Prague formed a separate group, and these carried *rmpA* and functional *rmpA2* and also encoded tellurite resistance determinants (**Table S1**).

DISCUSSION

MDR-Kp or CR-Kp isolates are clinically challenging, and specific carbapenemases are associated with regional/endemic clones in various regions (Lee et al., 2016; Shankar et al., 2021a). Recent reports describing the independent emergence of convergent HvKp isolates with hybrid and mosaic plasmids in multiple geographical locations make these organisms a major concern (Lam et al., 2019; Turton et al., 2019). Studies have described the acquisition of MDR plasmids by HvKp clones (ST23) and the acquisition of the pLVPK-like virulence plasmid by classical *K. pneumoniae* (cKp) causing invasive infections (Cejas et al., 2014; Chen and Kreiswirth, 2017; Xu et al., 2019; Shankar et al., 2020). This bidirectional convergence has resulted in the emergence of MDR-HvKp/CR-HvKp isolates within the nosocomial clones. Consequently, the circulation of nosocomial clones carrying a virulence plasmid is a matter of major public health concern (Zhan et al., 2017; Gu et al., 2018; Zhao et al., 2019; Liu et al., 2020). We report the acquisition of virulence factors among MDR clones, ST2096, crafting CR-HvKp in India.

In the present study, the ~307-kb hybrid plasmid was comparable to previously reported fusion plasmids including pKpvST147L [GenBank accession no. CM007852], pKpvST383L [GenBank accession no. CP034201], pKpvST147B [GenBank accession no. CP040726], and pBA813_1 GenBank accession no. [MK649825] (Turton et al., 2019; Wyres et al., 2020). Remarkably, these reference plasmids are associated with a diverse collection of clones, which were found to harbor bla_{NDM} and bla_{OXA-48} carbapenemase genes. Moreover, the insertion of resistance cassettes carrying *aadA2*, *armA*, bla_{TEM-1B}, $bla_{CTX-M-15}$, *mphE*, *msrE*, *sul1*, and *dfrA12* into hybrid plasmids of independent origin may accelerate the spread of MDR-HvKp. To date, the reports of hybrid plasmids are from clinical isolates indicating that the antimicrobial pressure present in this niche not only selects such plasmids but also aids in their persistence and dissemination. Here, the hybrid plasmids were a merger of IncFIB/IncHI1B (pNDM-MAR) backbones leading to convergence of AMR and virulence on a single plasmid. In India, bla_{NDM} is endemic and widespread among several bacteria especially *E. coli* and *K. pneumoniae* and this gene is often carried on the pNDM-MAR plasmid. Under pressure and for persistence, CR-HvKp can integrate segments of virulence plasmid into the endemic plasmid types to obtain the two-fold advantage of coding antimicrobial resistance and virulence. Similar plasmids, which were the result of the fusion between IncFIB/IncHI1B and $IncFII_K$/$IncFIB_K$ backbones, have been reported from other regions (Lam et al., 2019; Turton et al., 2019), highlighting the susceptibility of IncF and IncH plasmids to undergo recombination to form co-integrates in *K. pneumoniae*. Among these HvKp with mosaic plasmids, the mosaic structures were likely formed by the integration of the virulence region from the virulence plasmid into IncFIB and $IncFII_K$ resistance plasmids (Lam et al., 2019; Tang et al., 2020).

Furthermore, we found that the MDR-HvKp clones carrying a hybrid virulence plasmid possessed a frameshift variant of *rmpA2* without *rmpA*. Mutations in *rmpA* and *rmpA2* led to a lack of hypermucoviscous phenotypes (Yu et al., 2015; Shankar et al., 2021b). The effect of inactivation of *rmpA2* and its stability on the hybrid plasmids carried by nosocomial clones of *K. pneumoniae* needs further investigation. In contrast, the hybrid plasmid in ST15 reported by Lam and colleagues carried only *rmpA* (Lam et al., 2019). The virulence plasmids described here also carried genes encoding heavy metal tolerance, such as tellurium and mercury. Similar hybrid plasmids, reported by Turton and colleagues, lacked the genes encoding for mercury tolerance (Turton et al., 2019). Given the community origin of HvKp, the co-occurrence of heavy-metal tolerance may provide an additional survival mechanism in harsh ecological niches found in the community and hospitals (Furlan et al., 2020).

The presence of CRISPR-Cas systems in MDR plasmids in *K. pneumoniae* has not been extensively studied. Recent reports of the type IV CRISPR-Cas system in *K. pneumoniae* mega plasmids/co-integrate plasmids suggest that these systems aid competition between plasmids (Kamruzzaman and Iredell, 2020; Newire et al., 2020). In the present study, the CRISPR-Cas system in the large co-integrate plasmid has acquired a spacer sequence identical to IncF-*traL*, which implies specific targeting for further gene invasion of plasmids (Kamruzzaman and Iredell, 2020). This might probably play a role in homologous recombination and integration of AMR and virulence determinants onto a single plasmid by preventing the entry of other plasmids such as IncF. The attainment of specific plasmid CRISPR spacers targeting different conjugative plasmids appears to be advantageous in *K. pneumoniae* to mitigate the fitness cost associated with carrying multiple AMR plasmids. Notably, the majority of the plasmids that carry plasmid-targeting spacers are co-integrate plasmids carrying IncFIB and IncHI1B replicons (Kamruzzaman and Iredell, 2020; Newire et al., 2020). This observation suggests that the plasmid-mediated CRISPR spacers not only target other plasmids but also may aid the formation of co-integrate/mega plasmids for improved stability and compatibility.

Globally, the prevalence of MDR-HvKp or CR-HvKp appears to be increasing (Siu et al., 2014; Gu et al., 2018; Liu et al., 2020). Given the large burden of MDR-HvKp and CR-HvKp infections in China, India, and Southeast Asia, these regions represent the most likely hotspot of MDR-virulence intersection and subsequent spread. Similarly, the spontaneous emergence of hybrid plasmids in these regions and their potential for clonal spread in healthcare settings represent a major focus of nosocomial outbreaks and their containment. If the incidence of the convergent clones with fusion plasmid continues, these pathotypes may replace the currently circulating CRKp clones (Liu et al., 2020). Continuous genome surveillance of MDR-HvKp would help in determining this niche shift from community to hospital. In China, ST11 was known to carry complete pLVPK with capsule-type K64 (clade1) while ST11 with K47 carried a shorter virulence plasmid with only *rmpA2* and aerobactin (clade3) (Dong et al., 2018; Liu et al., 2020; Zhang et al., 2020). These MDR-HvKp infections were predominantly associated with nosocomial infections, and the sub-lineages among ST11 with different capsule types were identified only through genomic studies. Although MDR-HvKp belonged to ST11 in the study described by Dong and colleagues, there are several differences

concerning the virulence profile of the two clades which comprised MDR-HvKp which can only be identified through genome surveillance (Dong et al., 2018). There can also be a selection of one of the clades of MDR-HvKp ST11 over time which has a better fitness, thereby eliminating the other two clades.

CONCLUSION

India has exceptionally high rates of AMR infections as stated by the annual report of the Antimicrobial Resistance Research and Surveillance Network during the year 2020 by the Indian Council of Medical Research (https://main.icmr.nic.in/sites/default/files/guidelines/AMRSN_annual_report_2020.pdf; accessed on November 15, 2021). The further generation of HvKp carrying carbapenemases on a virulence plasmid would be a potential catastrophe. The acquisition of AMR genes on the chromosome creates the further possibility of increased baseline resistance among the *K. pneumoniae* isolates. It is apparent that MDR-HvKp is no longer confined to selected clones and the containment of such isolates with the mosaic plasmid is very challenging. The presence of AMR and virulence among diverse *Klebsiella* clones present a global threat to the rapid spread of these emerging superbugs.

DATA AVAILABILITY STATEMENT

The datasets presented in this study can be found in GenBank under Bioproject ID PRJNA613369. The accession numbers of the genomes are mentioned in **Tables 2** and **3**.

ETHICS STATEMENT

The study was approved by the Institutional Review Board of Christian Medical College, Vellore, India, with minute number 9616 (01/09/2015).

AUTHOR CONTRIBUTIONS

CS: conceptualization, analysis, manuscript writing, and revising. KV: methodology, bioinformatics, manuscript writing. JJ: analysis, manuscript writing and revising. SB: manuscript correction and supervision. BI: resource. AN: methodology, data curation. DS: methodology. BG: resource. BV: conceptualization, manuscript revision. and supervision. All authors contributed to the article and approved the submitted version.

FUNDING

The study has been funded by the Indian Council of Medical Research, New Delhi, India (ref. no: AMR/Adoc/232/2020-ECD-II).

SUPPLEMENTARY MATERIAL

The Supplementary Material for this article can be found online at: https://www.frontiersin.org/articles/10.3389/fcimb.2022.875116/full#supplementary-material

REFERENCES

Andrews, S. (2010). *FastQC: A Quality Control Tool for High Throughput Sequence Data*. Available at: http://www.bioinformatics.babraham.ac.uk/projects/fastqc/.

Bankevich, A., Nurk, S., Antipov, D., Gurevich, A. A., Dvorkin, M., Kulikov, A. S., et al. (2012). SPAdes: A New Genome Assembly Algorithm and Its Applications to Single-Cell Sequencing. *J. Comput. Biol.* 19 (5), pp.455–pp.477. doi: 10.1089/cmb.2012.0021

Bialek-Davenet, S., Criscuolo, A., Ailloud, F., Passet, V., Jones, L., Delannoy-Vieillard, A. S., et al. (2014). Genomic Definition of Hypervirulent and Multidrug-Resistant *Klebsiella pneumoniae* Clonal Groups. *Emerg Infect. Dis.* 20 (11), 1812. doi: 10.3201/eid2011.140206

Bortolaia, V., Kaas, R. S., Ruppe, E., Roberts, M. C., Schwarz, S., Cattoir, V., et al. (2020). ResFinder 4.0 for Predictions of Phenotypes From Genotypes. *J. Antimicrob. Chemother.* 75 (12), 3491–3500. doi: 10.1093/jac/dkaa345

Carattoli, A., Zankari, E., García-Fernández, A., Voldby Larsen, M., Lund, O., Villa, L., et al. (2014). *In Silico* Detection and Typing of Plasmids Using PlasmidFinder and Plasmid Multilocus Sequence Typing. *Antimicrob. Agents Chemother* 58 (7), 3895–3903. doi: 10.1128/AAC.02412-14

Cejas, D., Fernández Canigia, L., Rincón Cruz, G., Elena, A. X., Maldonado, I., Gutkind, G. O., et al. (2014). First Isolate of KPC-2-producing *Klebsiella pneumoniae* Sequence Type 23 From the Americas. *J. Clin. Microbiol.* 52 (9), 3483–3485. doi: 10.1128/JCM.00726-14

Chen, Y. T., Chang, H. Y., Lai, Y. C., Pan, C. C., Tsai, S. F., and Peng, H. L. (2004). Sequencing and Analysis of the Large Virulence Plasmid pLVPK of Klebsiella pneumoniae CG43*Gene 337*, 189–198.

Chen, L., and Kreiswirth, B.N. (2017) Convergence of Carbapenem-Resistance and Hypervirulence in *Klebsiella pneumoniae*. *Lancet Infect. Dis.*, 18 (1), 2–3. doi: 10.1016/S1473-3099(17)30517-0

Clinical and Laboratory Standards Institute. (2019). *Performance Standards for Antimicrobial Susceptibility Testing; 29th Informational Supplement. M100-S29* (Wayne, PA: Clinical and Laboratory Standards Institute).

Compain, F., Babosan, A., Brisse, S., Genel, N., Audo, J., Ailloud, F., et al. (2014). Multiplex PCR for Detection of Seven Virulence Factors and K1/K2 Capsular Serotypes of *Klebsiella pneumoniae*. *J. Clin. Microbiol.* 52 (12), 4377–4380. doi: 10.1128/JCM.02316-14

Dong, N., Zhang, R., Liu, L., Li, R., Lin, D., Chan, E. W. C., et al. (2018). Genome Analysis of Clinical Multilocus Sequence Type 11 *Klebsiella pneumoniae* From China. *Microbial. Genomics* 4 (2), e000149. doi: 10.1099/mgen.0.000149

Furlan, J. P. R., Savazzi, E. A., and Stehling, E. G. (2020). Genomic Insights Into Multidrug-Resistant and Hypervirulent *Klebsiella pneumoniae* Co-Harboring Metal Resistance Genes in Aquatic Environments. *Ecotoxicol. Environ. Saf.* 201, 110782. doi: 10.1016/j.ecoenv.2020.110782

Grant, J. R., and Stothard, P. (2008). The CGView Server: A Comparative Genomics Tool for Circular Genomes. *Nucleic Acids Res.* 36 (suppl_2), W181–W184. doi: 10.1093/nar/gkn179

Gu, D., Dong, N., Zheng, Z., Lin, D., Huang, M., Wang, L., et al. (2018). A Fatal Outbreak of ST11 Carbapenem-Resistant Hypervirulent *Klebsiella pneumoniae* in a Chinese Hospital: A Molecular Epidemiological Study. *Lancet Infect. Dis.* 18 (1), 37–46. doi: 10.1016/S1473-3099(17)30489-9

Gurevich, A., Saveliev, V., Vyahhi, N., and Tesler, G. (2013). QUAST: Quality Assessment Tool for Genome Assemblies. *Bioinformatics* 29 (8), 1072–1075. doi: 10.1093/bioinformatics/btt086

Huynh, B. T., Passet, V., Rakotondrasoa, A., Diallo, T., Kerleguer, A., Hennart, M., et al. (2020). *Klebsiella pneumoniae* Carriage in Low-Income Countries: Antimicrobial Resistance, Genomic Diversity and Risk Factors. *Gut Microbes* 11 (5), 1287–1299. doi: 10.1080/19490976.2020.1748257

Jolley, K. A., and Maiden, M. C. (2010). BIGSdb: Scalable Analysis of Bacterial Genome Variation at the Population Level. *BMC Bioinf.* 11 (1), 1–11. doi: 10.1186/1471-2105-11-595

Kamruzzaman, M., and Iredell, J. R. (2020). CRISPR-Cas System in Antibiotic Resistance Plasmids in *Klebsiella pneumoniae*. *Front. Microbiol.* 10, 2934. doi: 10.3389/fmicb.2019.02934

Koren, S., Walenz, B. P., Berlin, K., Miller, J. R., Bergman, N. H., and Phillippy, A. M. (2017). Canu: Scalable and Accurate Long-Read Assembly *Via* Adaptive K-Mer Weighting and Repeat Separation. *Genome Res.* 27 (5), 722–736. doi: 10.1101/gr.215087.116

Lam, M., Wick, R. R., Watts, S. C., Cerdeira, L. T., Wyres, K. L., and Holt, K. E. (2021). A Genomic Surveillance Framework and Genotyping Tool for *Klebsiella pneumoniae* and Its Related Species Complex. *Nat. Commun.* 12 (1), 1–16. doi: 10.1038/s41467-021-24448-3

Lam, M. M., Wyres, K. L., Wick, R. R., Judd, L. M., Fostervold, A., Holt, K. E., et al. (2019). Convergence of Virulence and MDR in a Single Plasmid Vector in MDR *Klebsiella pneumoniae* ST15. *J. Antimicrob. Chemother.* 74 (5), 1218–1222. doi: 10.1093/jac/dkz028

Lee, I., Kim, Y. O., Park, S. C., and Chun, J. (2016). OrthoANI: An Improved Algorithm and Software for Calculating Average Nucleotide Identity. *Int. J. Syst. Evol. Microbiol.* 66 (2), 1100–1103. doi: 10.1099/ijsem.0.000760

Lee, C. R., Lee, J. H., Park, K. S., Jeon, J. H., Kim, Y. B., Cha, C. J., et al. (2017). Antimicrobial Resistance of Hypervirulent *Klebsiella pneumoniae*: Epidemiology, Hypervirulence-Associated Determinants, and Resistance Mechanisms. *Front. Cell. Infect Microbiol.* 7, 483. doi: 10.3389/fcimb.2017.00483

Lee, C. R., Lee, J. H., Park, K. S., Kim, Y. B., Jeong, B. C., and Lee, S. H. (2016). Global Dissemination of Carbapenemase-Producing *Klebsiella pneumoniae*: Epidemiology, Genetic Context, Treatment Options, and Detection Methods. *Front. Microbiol.* 7, 895. doi: 10.3389/fmicb.2016.00895

Li, R., Cheng, J., Dong, H., Li, L., Liu, W., Zhang, C., et al. (2020). Emergence of a Novel Conjugative Hybrid Virulence Multidrug-Resistant Plasmid in Extensively Drug-Resistant *Klebsiella pneumoniae* ST15. *Int. J. Antimicrob. Agents* 55 (6), 105952. doi: 10.1016/j.ijantimicag.2020.105952

Liu, C., Du, P., Xiao, N., Ji, F., Russo, T. A., and Guo, J. (2020). Hypervirulent *Klebsiella pneumoniae* Is Emerging as an Increasingly Prevalent *K.Pneumoniae* Pathotype Responsible for Nosocomial and Healthcare-Associated Infections in Beijing, China. *Virulence* 11 (1), 1215–1224. doi: 10.1080/21505594.2020.1809322

Marr, C. M., and Russo, T. A. (2019). Hypervirulent *Klebsiella pneumoniae*: A New Public Health Threat. *Expert Rev. Anti-Infect. Ther.* 17 (2), 71–73. doi: 10.1080/14787210.2019.1555470

Martin, M. (2011). Cutadapt Removes Adapter Sequences From High-Throughput Sequencing Reads. *EMBnet J.* 17 (1), 10–12. doi: 10.14806/ej.17.1.200

Mike, L. A., Stark, A. J., Forsyth, V. S., Vornhagen, J., Smith, S. N., Bachman, M. A., et al. (2021). A Systematic Analysis of Hypermucoviscosity and Capsule Reveals Distinct and Overlapping Genes That Impact *Klebsiella pneumoniae* Fitness. *PloS Pathog.* 17 (3), e1009376. doi: 10.1371/journal.ppat.1009376

Navon-Venezia, S., Kondratyeva, K., and Carattoli, A. (2017). *Klebsiella pneumoniae*: A Major Worldwide Source and Shuttle for Antibiotic Resistance. *FEMS Microbiol. Rev.* 41 (3), 252–275. doi: 10.1093/femsre/fux013

Newire, E., Aydin, A., Juma, S., Enne, V. I., and Roberts, A. P. (2020). Identification of a Type Iv-a CRISPR-Cas System Located Exclusively on IncHI1B/IncFIB Plasmids in Enterobacteriaceae. *Front. Microbiol.* 11, 1937. doi: 10.3389/fmicb.2020.01937

Parks, D. H., Imelfort, M., Skennerton, C. T., Hugenholtz, P., and Tyson, G. W. (2015). CheckM: Assessing the Quality of Microbial Genomes Recovered From Isolates, Single Cells, and Metagenomes. *Genome Res.* 25 (7), 1043–1055. doi: 10.1101/gr.186072.114

Qi, Y., Wei, Z., Ji, S., Du, X., Shen, P., and Yu, Y. (2011). ST11, the Dominant Clone of KPC-producing *Klebsiella pneumoniae* in China. *J. Antimicrob. Chemother.* 66 (2), 307–312. doi: 10.1093/jac/dkq431

Russel, J., Pinilla-Redondo, R., Mayo-Muñoz, D., Shah, S. A., and Sørensen, S. J. (2020). CRISPRCasTyper: Automated Identification, Annotation, and Classification of CRISPR-Cas Loci. *CRISPR J.* 3 (6), 462–469. doi: 10.1089/crispr.2020.0059

Shankar, C., Basu, S., Lal, B., Shanmugam, S., Vasudevan, K., Mathur, P., et al. (2021b). Aerobactin Seems to Be a Promising Marker Compared With Unstable RmpA2 for the Identification of Hypervirulent Carbapenem-Resistant *Klebsiella Pneumoniae: In Silico* and *In Vitro* Evidence. *Front. Cell. Infect. Microbiol.* 11, 709681. doi: 10.3389/fcimb.2021.709681

Shankar, C., Jacob, J. J., Sugumar, S. G., Natarajan, L., Rodrigues, C., Mathur, P., et al. (2021a). Distinctive Mobile Genetic Elements Observed in the Clonal Expansion of Carbapenem-Resistant *Klebsiella pneumoniae* in India. *Microbial. Drug Resist.* 27 (8), 1096–1104. doi: 10.1089/mdr.2020.0316

Shankar, C., Jacob, J. J., Vasudevan, K., Biswas, R., Manesh, A., Sethuvel, D. P. M., et al. (2020). Emergence of Multidrug Resistant Hypervirulent ST23 *Klebsiella pneumoniae*: Multidrug Resistant Plasmid Acquisition Drives Evolution. *Front. Cell. Infect. Microbiol.* 10, 575289. doi: 10.3389/fcimb.2020.575289

Shon, A. S., Bajwa, R. P., and Russo, T. A. (2013). Hypervirulent (Hypermucoviscous) *Klebsiella pneumoniae*: A New and Dangerous Breed. *Virulence* 4 (2), 107–118. doi: 10.4161/viru.22718

Siu, L. K. K., Huang, D. B., and Chiang, T. (2014). Plasmid Transferability of KPC Into a Virulent K2 Serotype *Klebsiella pneumoniae*. *BMC Infect. Dis.* 14 (1), 1–6. doi: 10.1186/1471-2334-14-176

Sullivan, M. J., Petty, N. K., and Beatson, S. A. (2011). Easyfig: A Genome Comparison Visualizer. *Bioinformatics* 27 (7), 1009–1010. doi: 10.1093/bioinformatics/btr039

Tang, M., Kong, X., Hao, J., and Liu, J. (2020). Epidemiological Characteristics and Formation Mechanisms of Multidrug-Resistant Hypervirulent *Klebsiella pneumoniae*. *Front. Microbiol.* 11, 2774. doi: 10.3389/fmicb.2020.581543

Tatusova, T., DiCuccio, M., Badretdin, A., Chetvernin, V., Nawrocki, E. P., Zaslavsky, L., et al. (2016). NCBI Prokaryotic Genome Annotation Pipeline. *Nucleic Acids Res.* 44 (14), 6614–6624. doi: 10.1093/nar/gkw569

Tian, D., Wang, M., Zhou, Y., Hu, D., Ou, H. Y., and Jiang, X. (2021). Genetic Diversity and Evolution of the Virulence Plasmids Encoding Aerobactin and Salmochelin in Klebsiella pneumoniae. *Virulence* 12 (1), 1323–1333. doi: 10.1080/21505594.2021.1924019

Turton, J., Davies, F., Turton, J., Perry, C., Payne, Z., and Pike, R. (2019). Hybrid Resistance and Virulence Plasmids in "High-Risk"Clones of *Klebsiella pneumoniae*, Including Those Carrying Blandm-5. *Microorganisms* 7 (9), 326. doi: 10.3390/microorganisms7090326

Turton, J. F., Payne, Z., Coward, A., Hopkins, K. L., Turton, J. A., Doumith, M., et al. (2018). Virulence Genes in Isolates of *Klebsiella pneumoniae* From the UK During 2016, Including Among Carbapenemase Gene-Positive Hypervirulent K1-ST23 and 'Non-Hypervirulent'types ST147, ST15 and ST383. *J. Med. Microbiol.* 67 (1), 118–128. doi: 10.1099/jmm.0.000653

Turton, J. F., Perry, C., Elgohari, S., and Hampton, C. V. (2010). PCR Characterization and Typing of *Klebsiella pneumoniae* Using Capsular Type-Specific, Variable Number Tandem Repeat and Virulence Gene Targets. *J. Med. Microbiol.* 59 (5), 541–547. doi: 10.1099/jmm.0.015198-0

Vasudevan, K., Ragupathi, N. K. D., Jacob, J. J., and Veeraraghavan, B. (2020). Highly Accurate-Single Chromosomal Complete Genomes Using IonTorrent and MinION Sequencing of Clinical Pathogens. *Genomics* 112 (1), 545–551. doi: 10.1016/j.ygeno.2019.04.006

Versalovic, J., Carroll, K. C., Funke, G., Jorgensen, J. H., Landry, M. L., and Warnock, D. W. (2011). *Manual of Clinical Microbiology* (Washington, DC: ASM Press).

Villa, L., Poirel, L., Nordmann, P., Carta, C., and Carattoli, A. (2012). Complete Sequencing of an IncH Plasmid Carrying the bla_{NDM-1}, $bla_{CTX-M-15}$ and *qnrB1* Genes. *J. Antimicrob. Chemother.* 67 (7), 1645–1650. doi: 10.1093/jac/dks114

Walker, B. J., Abeel, T., Shea, T., Priest, M., Abouelliel, A., Sakthikumar, S., et al. (2014). Pilon: An Integrated Tool for Comprehensive Microbial Variant Detection and Genome Assembly Improvement. *PloS One* 9 (11), e112963. doi: 10.1371/journal.pone.0112963

Wick, R. R., Heinz, E., Holt, K. E., and Wyres, K. L. (2018). Kaptive Web: User-Friendly Capsule and Lipopolysaccharide Serotype Prediction for *Klebsiella* Genomes. *J. Clin. Microbiol.* 56 (6), e00197–e00118. doi: 10.1128/JCM.00197-18

Wick, R. R., Judd, L. M., Gorrie, C. L., and Holt, K. E. (2017). Unicycler: Resolving Bacterial Genome Assemblies From Short and Long Sequencing Reads. *PloS Comput. Biol.* 13 (6), e1005595. doi: 10.1371/journal.pcbi.1005595

Wyres, K. L., Nguyen, T. N., Lam, M., Judd, L. M., van Vinh Chau, N., Dance, D. A., et al. (2020). Genomic Surveillance for Hypervirulence and Multidrug

Resistance in Invasive *Klebsiella pneumoniae* From South and Southeast Asia. *Genome Med.* 12 (1), 1–16. doi: 10.1186/s13073-019-0706-y

Wyres, K. L., Wick, R. R., Gorrie, C., Jenney, A., Follador, R., Thomson, N. R., et al. (2016). Identification of *Klebsiella* Capsule Synthesis Loci From Whole Genome Data. *Microbial. Genomics* 2 (12), e000102. doi: 10.1099/mgen.0.000102

Wysocka, M., Zamudio, R., Oggioni, M. R., Gołębiewska, J., Dudziak, A., and Krawczyk, B. (2020). The New *Klebsiella pneumoniae* ST152 Variants With Hypermucoviscous Phenotype Isolated From Renal Transplant Recipients With Asymptomatic Bacteriuria—Genetic Characteristics by WGS. *Genes* 11 (10), 1189. doi: 10.3390/genes11101189

Xie, M., Chen, K., Ye, L., Yang, X., Xu, Q., Yang, C., et al. (2020). Conjugation of Virulence Plasmid in Clinical *Klebsiella pneumoniae* Strains Through Formation of a Fusion Plasmid. *Adv. Biosyst.* 4 (4), 1900239. doi: 10.1002/adbi.201900239

Xu, M., Fu, Y., Fang, Y., Xu, H., Kong, H., Liu, Y., et al. (2019). High Prevalence of KPC-2-producing Hypervirulent *Klebsiella pneumoniae* Causing Meningitis in Eastern China. *Infect. Drug Resist.* 12, 641. doi: 10.2147/IDR.S191892

Yang, Q, Jia, X., Zhou, M., Zhang, H., Yang, W., Kudinha, T., and Xu, Y.. (2020). Emergence of ST11-K47 and ST11-K64 Hypervirulent Carbapenem-Resistant *Klebsiella pneumoniae* in Bacterial Liver Abscesses from China: A Molecular, Biological and Epidemiological Study. *Emerg. Microbes Infect.* 9 (1), 320–331. doi: 10.1080/22221751.2020.1721334

Yang, X., Dong, N., Chan, E. W. C., Zhang, R., and Chen, S. (2021). Carbapenem Resistance-Encoding and Virulence-Encoding Conjugative Plasmids in *Klebsiella pneumoniae*. *Trends Microbiol.* 29 (1), 65–83. doi: 10.1016/j.tim.2020.04.012

Yao, H., Qin, S., Chen, S., Shen, J., and Du, X. D. (2018). Emergence of Carbapenem-Resistant Hypervirulent *Klebsiella pneumoniae*. *Lancet Infect. Dis.* 18 (1), 25. doi: 10.1016/S1473-3099(17)30628-X

Yu, W. L., Lee, M. F., Tang, H. J., Chang, M. C., and Chuang, Y. C. (2015). Low Prevalence of *Rmpa* and High Tendency of *Rmpa* Mutation Correspond to Low Virulence of Extended Spectrum β-Lactamase-Producing *Klebsiella pneumoniae* Isolates. *Virulence* 6 (2), 162–172. doi: 10.1080/21505594.2015.1016703

Zhang, Y., Jin, L., Ouyang, P., Wang, Q., Wang, R., Wang, J., et al. (2020). Evolution of Hypervirulence in Carbapenem-Resistant *Klebsiella pneumoniae* in China: A Multicentre, Molecular Epidemiological Analysis. *J. Antimicrob. Chemother.* 75 (2), 327–336. doi: 10.1093/jac/dkz446

Zhan, L., Wang, S., Guo, Y., Jin, Y., Duan, J., Hao, Z., et al. (2017). Outbreak by Hypermucoviscous *Klebsiella pneumoniae* ST11 Isolates With Carbapenem Resistance in a Tertiary Hospital in China. *Front. Cell. Infect. Microbiol.* 7, 182. doi: 10.3389/fcimb.2017.00182

Zhao, Y., Zhang, X., Torres, V. V. L., Liu, H., Rocker, A., Zhang, Y., et al. (2019). An Outbreak of Carbapenem-Resistant and Hypervirulent *Klebsiella pneumoniae* in an Intensive Care Unit of a Major Teaching Hospital in Wenzhou, China. *Front. Public Health* 7, 229. doi: 10.3389/fpubh.2019.00229

Conflict of Interest: The authors declare that the research was conducted in the absence of any commercial or financial relationships that could be construed as a potential conflict of interest.

Publisher's Note: All claims expressed in this article are solely those of the authors and do not necessarily represent those of their affiliated organizations, or those of the publisher, the editors and the reviewers. Any product that may be evaluated in this article, or claim that may be made by its manufacturer, is not guaranteed or endorsed by the publisher.

frontiers | Frontiers in Cellular and Infection Microbiology

ORIGINAL RESEARCH
published: 01 June 2022
doi: 10.3389/fcimb.2022.882210

Prevalence of Carbapenem-Resistant Hypervirulent *Klebsiella pneumoniae* and Hypervirulent Carbapenem-Resistant *Klebsiella pneumoniae* in China Determined *via* Mouse Lethality Tests

Dakang Hu[1†], Wenjie Chen[2†], Qi Zhang[3†], Meng Li[4], Zehua Yang[5], Yong Wang[6], Yunkun Huang[7], Gang Li[8], Dongxing Tian[1], Pan Fu[1,9], Weiwen Wang[1], Ping Ren[10], Qing Mu[11], Lianhua Yu[12] and Xiaofei Jiang[1*]*

[1] Department of Laboratory Medicine, Huashan Hospital, Fudan University, Shanghai, China, [2] Department of Infectious Diseases, Huashan Hospital, Fudan University, Shanghai, China, [3] Department of Laboratory Medicine, Henan Provincial People's Hospital & the People's Hospital of Zhengzhou University, Zhengzhou, China, [4] Department of Clinical Laboratory, The First Affiliated Hospital of Guangxi Medical University, Nanning, China, [5] Department of Laboratory Medicine, Sixth Hospital of Shanxi Medical University, Taiyuan, China, [6] Department of Clinical Laboratory, Shandong Provincial Hospital Affiliated to Shandong University, Jinan, China, [7] Department of Laboratory Medicine, Kunming Yan'an Hospital, Kunming, China, [8] Department of Laboratory Medicine, Jinshan Hospital of Fudan University, Shanghai, China, [9] Microbiology Department. Children's Hospital of Fudan University, Shanghai, China, [10] Zhejiang Provincial Demonstration Centre of Laboratory Medicine Experimental Teaching, Wenzhou Medical University, Wenzhou, China, [11] School of Pharmacy, Fudan University, Shanghai, China, [12] Department of Laboratory Medicine, Taizhou Municipal Hospital, Taizhou, China

Objective: To investigate the epidemiology of carbapenem-resistant hypervirulent *Klebsiella pneumoniae* (CR-HvKP) and hypervirulent carbapenem-resistant *Klebsiella pneumoniae* (Hv-CRKP).

Methods: Totally 436 *K. pneumoniae* strains were collected from 7 hospitals in mainland China between 2017.01 and 2018.02. Sequence types, serotypes, antimicrobial-resistance and virulence genes were analyzed. Additionally, string test, capsule stain, Periodic Acid Schiff stain, fitness analysis, quantitative real-time PCR and mouse lethality test were also performed. Molecular combinations were used to screen putative bla_{KPC}(+)-HvKP and Hv-bla_{KPC}(+)-KP, followed by the confirmation of mouse lethality test.

Results: Diverse detection rates were found for the virulence genes, ranging from *c-rmpA* (0.0%) to *entB* (100.0%). According to the molecular criteria, 127, 186, 9 and 26 strains were putatively denoted as HvKP, bla_{KPC}(+)-KP, bla_{KPC}(+)-HvKP and Hv-bla_{KPC}(+)-KP. Mouse lethality test confirmed 2 bla_{KPC}(+)-HvKP strains (JS184 and TZ20) and no Hv-bla_{KPC}(+)-KP. JS184 showed K2 serotype, thin capsule, positive exopolysaccharid and string test. TZ20 presented K20 serotype, thin capsule, negative exopolysaccharide and string test. Compared with the positive control NTUH-K2044, equal *galF* expression and growth curves were confirmed for JS184 and TZ20.

OPEN ACCESS

Edited by:
Milena Dropa, University of São Paulo, Brazil

Reviewed by:
Theodoros Karampatakis, Papanikolaou General Hospital of Thessaloniki, Greece
Yonghong Xiao, Zhejiang University, China

***Correspondence:**
Xiaofei Jiang
jiangxi2154@sina.com
Lianhua Yu
yulianhua64@126.com

†These authors have contributed equally to this work and share first authorship

Specialty section:
This article was submitted to Clinical Microbiology, a section of the journal Frontiers in Cellular and Infection Microbiology

Received: *23 February 2022*
Accepted: *20 April 2022*
Published: *01 June 2022*

Citation:
Hu D, Chen W, Zhang Q, Li M, Yang Z, Wang Y, Huang Y, Li G, Tian D, Fu P, Wang W, Ren P, Mu Q, Yu L and Jiang X (2022) Prevalence of Carbapenem-Resistant Hypervirulent Klebsiella pneumoniae and Hypervirulent Carbapenem-Resistant Klebsiella pneumoniae in China Determined via Mouse Lethality Tests. Front. Cell. Infect. Microbiol. 12:882210. doi: 10.3389/fcimb.2022.882210

Conclusions: Molecular determination of CR-HvKP and Hv-CRKP brings remarkable bias compared with mouse lethality test. The exact prevalence of CR-HvKP is less than 1.0%, which of Hv-CRKP is much lower.

Keywords: carbapenem-resistant hypervirulent *Klebsiella pneumoniae*, hypervirulent carbapenem-resistant *Klebsiella pneumoniae*, epidemiology, mouse lethality test, hypervirulence, carbapenemase

INTRODUCTION

Klebsiella pneumoniae is a gram-negative and rod-shaped bacterium that belongs to the *Enterobacteriaceae* family (Adeolu et al., 2016), and was first described by Carl Friedlander in 1882. *K. pneumoniae* is considered a prominent nosocomial pathogen worldwide, and is a member of the "ESKAPE" (*Enterococcus faecium*, *Staphylococcus aureus, K. pneumoniae*, *Acinetobacter baumannii*, *Pseudomonas aeruginosa*, and *Enterobacter* species) pathogens (Pendleton et al., 2013). General nosocomial infections caused by *K. pneumoniae* include pneumonia, bacteraemia, and urinary tract infections (UTIs) (Paczosa and Mecsas, 2016). The frequent use of antimicrobials has resulted in the development of carbapenem-resistant *K. pneumoniae* (CRKP) strains which first emerged in 1996 (Yigit et al., 2001). CRKP strains generally contain mobile genetic elements harbouring a variety of antimicrobial resistance genes, including beta-lactamase *K. pneumoniae* carbapenemase gene (bla_{KPC}), New Delhi metallo-β-lactamase gene (bla_{NDM}), and oxacillinase-48 gene (bla_{OXA-48}) (Lee et al., 2016; Zhang et al., 2015), among which bla_{KPC} has been found to be shared in approximately 78.6% (44/56) (Lin et al., 2020) and 89.5% (34/38) of isolates in two studies (Lin et al., 2018). CRKP strains account for over 30.0% of *K. pneumoniae* strains and present great challenges in clinical practice (Effah et al., 2020). CRKP is associated with mortality rates of 34.7% (17/49) for pneumonia, 37.8% (34/90) for bacteraemia, and 7.4% (9/121) for UTI (Hauck et al., 2016). Furthermore, CRKP treatment is associated with a higher medical cost than that of carbapenem-susceptible *K. pneumoniae* (Huang et al., 2018). CRKP constitutes a major public health issue, especially in endemic countries (Karampatakis et al., 2016). Therefore, CRKP control is considered a priority by the World Health Organization (World Health Organization, 2017). CRKP is usually denoted as classical *K. pneumoniae* (cKP) regarding its virulence (Russo and Marr, 2019; Zhang et al., 2020).

Hypervirulence in *K. pneumoniae* represents another major concern. Hypervirulent *K. pneumoniae* (HvKP) was first reported to cause pyogenic liver abscess (PLA) and septic endophthalmitis in seven healthy individuals (Liu et al., 1986). HvKP, which has a considerably lower median lethal dose (LD_{50}) than that of cKP in mouse model, generally produces various virulence factors such as hypercapsules, excessive siderophores, exopolysaccharides, and fimbriae (Paczosa and Mecsas, 2016; Russo and Marr, 2019). Apart from PLA, HvKP can also cause multiple invasive infectious diseases such as endogenous endophthalmitis, necrotising fasciitis, and meningitis, and the infection can undergo metastatic spread. PLA is endemic to East Asia and associated with a morbidity rate of 15.45 per 100,000 person-years in 2011 and a mortality rate of 8.2% (Chen et al., 2016; Siu et al., 2012). It has been estimated that 60% of endogenous endophthalmitis cases are associated with PLA caused by *K. pneumoniae* (Wong et al., 2000). Even with intravenous and intravitreal antimicrobial treatment, 89% of endophthalmitis cases show visual acuity of light perception or worse, and over 40% of affected eyes require evisceration or enucleation (Yang et al., 2007).

Recently, a combination of hypervirulence and extreme drug resistance has been reported in *K. pneumoniae*, thereby exacerbating the scarcity of effective treatments and resulting in high mortality (Zhang et al., 2015; Gu et al., 2018). The prevalence of infections caused by carbapenem-resistant hypervirulent *K. pneumoniae* (CR-HvKP) and hypervirulent carbapenem-resistant *K. pneumoniae* (Hv-CRKP) presents a global concern and a great challenge in clinical practice. However, the epidemiology of CR-HvKP and Hv-CRKP has not been extensively studied. The estimated prevalence of CR-HvKP/Hv-CRKP strains ranges among 5.0–15.0% among CRKP strains in mainland China, based on molecular determination or the *Galleria mellonella* (greater wax moth) lethality test (Zhang et al., 2020; Zhan et al., 2017). The gold standard method for evaluating the virulence of *K. pneumoniae* involves the use of mouse models, rather than the *G. mellonella* lethality test (Russo and MacDonald, 2020). Here, we analysed 436 clinical *K. pneumoniae* strains using molecular techniques and mouse lethality tests to elucidate the prevalence of CR-HvKP and Hv-CRKP strains.

MATERIALS AND METHODS

K. pneumoniae Strains

In this study, 436 non-duplicate and consecutive *K. pneumoniae* isolates were collected from seven hospitals across six provinces in China (Huashan Hospital, 180 strains; Jinshan Hospital, 28 strains; Taizhou Municipal Hospital, 84 strains; The First Affiliated Hospital of Guangxi Medical University, 20 strains; Kunming Yan'an Hospital, 34 strains; Sixth Hospital of Shanxi Medical University, 60 strains; Shandong Provincial Hospital Affiliated to Shandong University, 30 strains) from January 2017 to February 2018. The 436 isolates were collected from diverse sources: 255 isolates (58.5%) were obtained from sputum samples, 98 isolates (22.5%) from urine samples, 29 isolates (6.7%) from blood samples, and 54 isolates (12.4%) were obtained from other sources. All the isolates were cultured on sheep blood agar plates and kept at -80°C prior to use.

Identification of *K. pneumoniae* was performed using a matrix-assisted laser desorption/ionization time-of-flight mass spectrometry system (Bruker Daltonics Inc., Fremont, CA, USA) using the standard strains *P. aeruginosa* ATCC 27853, *K. pneumoniae* ATCC 700603, and *E. coli* ATCC 25922 as controls.

K. pneumoniae NTUH-K2044 (Accession number: **AP006725.1**) obtained from the Department of Internal Medicine, National Taiwan University Hospital, Taipei, Taiwan, is a typical hypervirulent *K. pneumoniae* serotype K1 strain (Fang et al., 2004). *K. pneumoniae* HS11286 (Accession number: **CP003200.1**) isolated from the Department of Laboratory Medicine, Huashan Hospital, Fudan University, Shanghai, China, is a *K. pneumoniae* serotype K47 strain containing bla_{KPC} and low virulence (Liu et al., 2012).

All the *K. pneumoniae* strains were investigated as the flow chart in **Figure 1**.

Multilocus Sequence Typing

DNA was extracted from the 436 *K. pneumoniae* strains using the QIAamp DNA mini kit (QIAGEN, Düsseldorf, Germany) according to the manufacturer's protocol. Seven housekeeping genes (*gapA*, *infB*, *mdh*, *pgi*, *phoE*, *rpoB*, and *tonB*) were amplified *via* polymerase chain reaction (PCR) (Diancourt et al., 2005) and then sequenced using an ABI 3730XL DNA Analyser (Applied Biosystems, San Ramon, CA, USA), and then compared with sequences available on the *K. pneumoniae* MLST database (http://www.pasteur.fr/recherche/genopole/PF8/mlst/Kpneumoniae.html). The primers used are shown in **Table S1**.

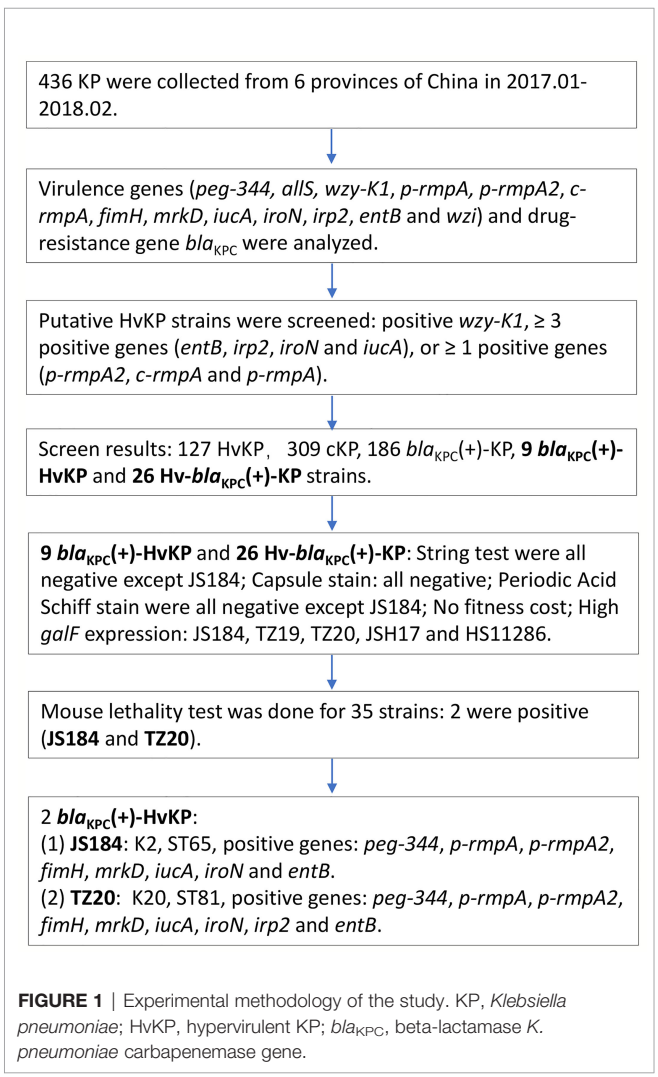

FIGURE 1 | Experimental methodology of the study. KP, *Klebsiella pneumoniae*; HvKP, hypervirulent KP; bla_{KPC}, beta-lactamase *K. pneumoniae* carbapenemase gene.

Determination of Serotypes, Antimicrobial-Resistance, and Virulence Genes

The capsule type was determined *via* PCR amplification and sequencing of the *wzi* loci (Brisse et al., 2013), followed by comparison with sequences on the database of Institute Pasteur (https://bigsdb.pasteur.fr/klebsiella/klebsiella.html).

The antimicrobial resistance gene (bla_{KPC}) and virulence genes (*wzy-K1*, *allS*, *entB*, *irp2*, *iroN*, *iucA*, *fimH*, *mrkD*, *p-rmpA2*, *c-rmpA*, *p-rmpA*, *peg-344*, and *wzi*) (Compain et al., 2014; Gu et al., 2018; Russo et al., 2018) were analysed *via* PCR amplification, using an Applied Biosystems Veriti PCR system (Applied Biosystems). The primers used are shown in **Table S1**.

Determination of Putative HvKP, cKP, Hv-bla_{KPC}(+)-KP, and bla_{KPC}(+)-HvKP Strains

On the basis of molecular characteristics, HvKP and cKP were putatively defined as a reference (Hu et al., 2021) (**Figure 1**). Hv-bla_{KPC}(+)-KP was defined as bla_{KPC}-positive cKP which acquired key virulence genes that conferred hypervirulence. bla_{KPC}(+)-HvKP (K1, K2, K5, K10, K20, K25, K27, and K57) (Chen et al., 2016; Siu et al., 2012) was defined as HvKP that acquired a bla_{KPC} gene.

String Test

Overnight cultured *K. pneumoniae* colonies on sheep blood agar plates were stretched outward using an inoculation loop as described previously (Shon et al., 2013). The string test was considered positive when a viscous string produced was over 5 mm in length. Strain NTUH-K2044 was used as a positive control and HS11286 was used as a negative control.

Capsule Staining

Capsule staining of *K. pneumoniae* strains was performed according to the manufacturer's instructions (catalog number: BA-4039; BASO, Zhuhai, China). NTUH-K2044 was used as a positive control and HS11286 was used as a negative control.

Periodic Acid-Schiff Staining

Periodic acid-Schiff staining was performed according to the manufacturer's protocol (catalog number: BA4080A; BASO, Zhuhai, China). Strains NTUH-K2044 and HS11286 were used as positive and negative controls, respectively.

Fitness Analysis

A growth curve was generated to evaluate the fitness of *K. pneumoniae* strains (Liu et al., 2016). These strains were cultured overnight in Luria-Bertani broth, diluted to an optical density at 600 nm (OD_{600}) of 0.001, and cultured at 37°C under

aerobic conditions (BioTek Synergy H1, Winooski, VT, USA). The OD_{600} values were measured every 30 min and plotted as a curve. Strains NTUH-K2044 and HS11286 were used as positive and negative controls, respectively.

Quantitative PCR Analysis

Quantitative PCR analysis of *galF* mRNA together with 16S rRNA was performed using an Applied Biosystems 7500 system (Applied Biosystems, San Ramon, CA, USA). The primers used are shown in **Table S1**. Strains NTUH-K2044 and HS11286 were used as positive and negative controls, respectively. The analyses were performed according to the manufacturer's protocol (catalog number: FS-Q1002; FOREVER STAR, Beijing, China).

Mouse Lethality Test

Mouse experiments were approved by the Institutional Animal Care and Use Committee of the School of Pharmacy, Fudan University (Shanghai, China) (ethical approval document NO. 201603-TY-MQ-01). Pathogen-free female BALB/c mice (age, 6 weeks), four per group, were intraperitoneally inoculated with 100 μL of *K. pneumoniae* strains at the mid-logarithmic growth phase (Mizuta et al., 1983). Before inoculation, *K. pneumoniae* strains were washed twice with normal saline and centrifuged at 10,621 × *g* for 4 min. A 0.6 McFarland standard equivalent to 2.0×10^8 colony forming units (CFU)/mL was prepared. The final inoculation was 10^2–10^7 CFU/mL. The mice were observed for 14 d after inoculation. LD_{50} was determined according to a previous study (Reed and Muench, 1938). Strains NTUH-K2044 and HS11286 were used as positive and negative controls. *K. pneumoniae* strains with $LD_{50} \leq 10$ times of that of NTUH-K2044 were regarded as hypervirulent; those with $LD_{50} > 10$ times of that of NTUH-K2044 were denoted as hypovirulent.

Statistical Analysis

GraphPad Prism 8 software (GraphPad Software Inc., Sand Diego, CA, USA) was used to perform Chi-square test, one-way ANOVA, and Kruskal-Wallis test between groups; $p < 0.05$ was considered significant.

RESULTS

Distribution of Key Virulence Genes

A varying distribution of virulence genes was observed, ranging from 0.0% (*c-rmpA*) to 100.0% (*entB*) (**Figure 2**). The 13 virulence genes could be classified into 4 categories based on rates of distribution: ≤ 10.0% (*allS*, *wzy-K1*, and *c-rmpA*), approximately 11.0–30.0% (*peg-344*, *p-rmpA*, *p-rmpA2*, *iucA*, and *iroN*), approximately 50.0–80.0% (*irp2*), and approximately 81.0–100.0% (*fimH*, *mrkD*, *entB*, and *wzi*).

Distribution of Predicted HvKP, *bla*$_{KPC}$(+)-KP, *bla*$_{KPC}$(+)-HvKP, and Hv-*bla*$_{KPC}$(+)-KP

In total, 127 (29.1%), 186 (42.7%), 9 (2.1%), and 26 (6.0%) strains were putatively denoted as HvKP, *bla*$_{KPC}$(+)-KP, *bla*$_{KPC}$(+)-HvKP, and Hv-*bla*$_{KPC}$(+)-KP strains, respectively.

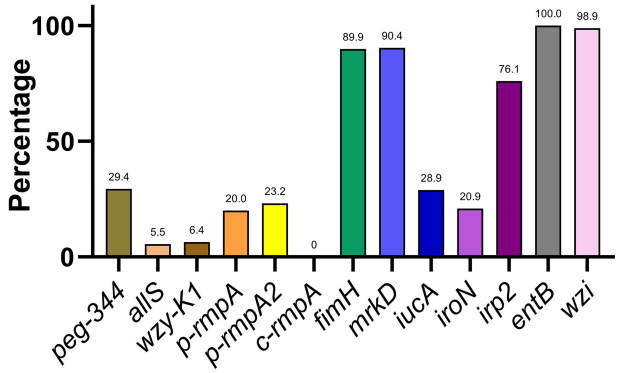

FIGURE 2 | Distribution of 13 key virulence genes among the *Klebsiella pneumoniae* isolates.

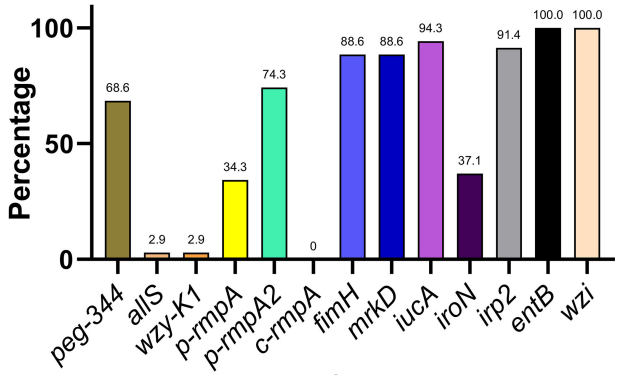

FIGURE 3 | Distribution of key virulence genes among putative *bla*$_{KPC}$(+)-HvKP and Hv-*bla*$_{KPC}$(+)-KP strains. *bla*$_{KPC}$, beta-lactamase *K. pneumoniae* carbapenemase gene; *bla*$_{KPC}$(+)-HvKP, *bla*$_{KPC}$(+) hypervirulent *K. pneumoniae*; Hv-*bla*$_{KPC}$(+)-KP, hypervirulent *bla*$_{KPC}$(+) *K. pneumoniae*.

Distribution of Key Virulence Genes in Putative *bla*$_{KPC}$(+)-HvKP and Hv-*bla*$_{KPC}$(+)-KP

The distribution of 13 key virulence genes among the putative *bla*$_{KPC}$(+)-HvKP and Hv-*bla*$_{KPC}$(+)-KP strains is shown in **Figure 3**. The 13 virulence genes were classified into four categories based on the rates of distribution: ≤ 10.0% (*allS*, *wzy-K1*, and *c-rmpA*), approximately 31.0–50.0% (*p-rmpA* and *iroN*), approximately 51.0–80.0% (*peg-344* and *p-rmpA2*), and approximately 81.0–100.0% (*fimH*, *mrkD*, *iucA*, *irp2*, *entB*, and *wzi*).

Morphological Characteristics

In total, 34 putative *bla*$_{KPC}$(+)-HvKP and Hv-*bla*$_{KPC}$(+)-KP strains, except for *bla*$_{KPC}$(+)-HvKP strain JS184, demonstrated negative string test results. No hypercapsule was found among the 35 putative *bla*$_{KPC}$(+)-HvKP and Hv-*bla*$_{KPC}$(+)-KP strains (**Figure 4**). No exopolysaccharides were found to be produced by

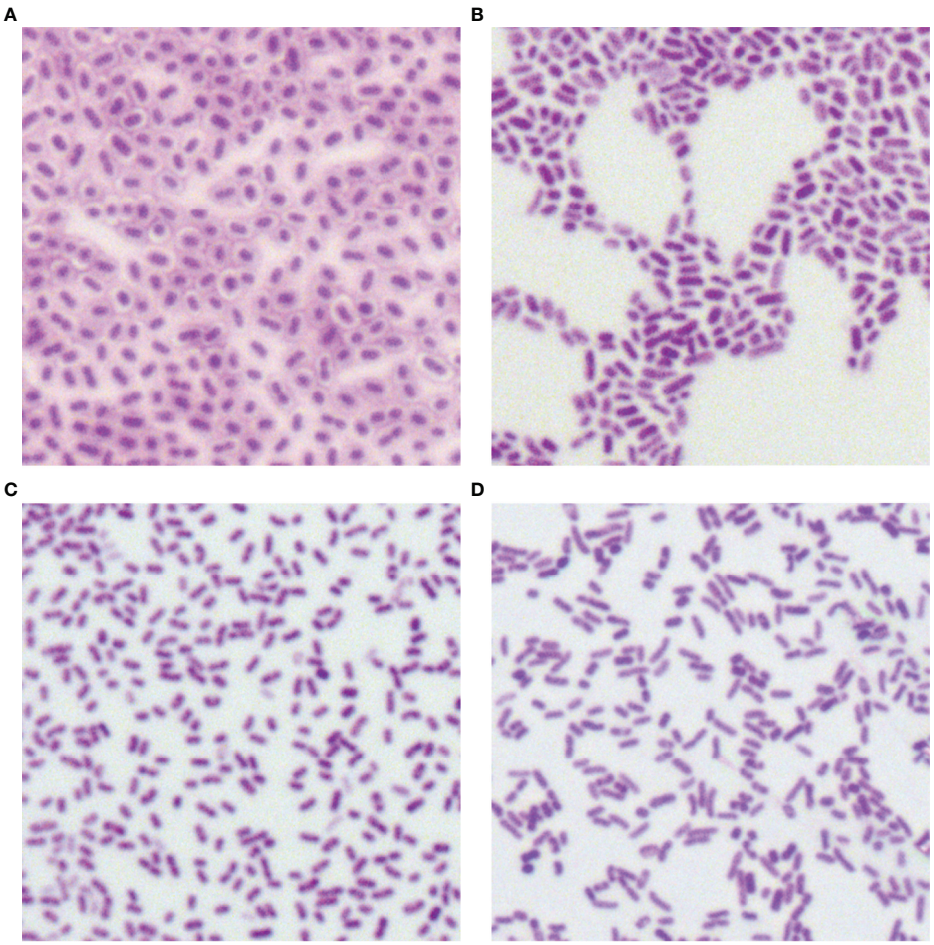

FIGURE 4 | Capsule staining of 35 putative *bla*$_{KPC}$(+)-HvKP and Hv-*bla*$_{KPC}$(+)-KP strains. **(A)** *Klebsiella pneumoniae* NTUH-K2044, **(B)** *K. pneumoniae* HS11286, **(C)** JS184, and **(D)** TZ20. *K. pneumoniae* strains are purple and rod-shaped, and their transparent surroundings are hypercapsules (×1000). *bla*$_{KPC}$, beta-lactamase *K. pneumoniae* carbapenemase gene; *bla*$_{KPC}$(+)-HvKP, *bla*$_{KPC}$(+) hypervirulent *K. pneumoniae*; Hv-*bla*$_{KPC}$(+)-KP, hypervirulent *bla*$_{KPC}$(+) *K. pneumoniae*.

the putative *bla*$_{KPC}$(+)-HvKP and Hv-*bla*$_{KPC}$(+)-KP strains, except for JS184 (**Figure 5**).

Fitness Analysis

Among the 9 putative *bla*$_{KPC}$(+)-HvKP and 26 Hv-*bla*$_{KPC}$(+)-KP strains, 8 strains were chosen to represent each serotype: JS184 (K2, ST65), JS185 (K2, ST977), JS210 (K47, ST11), TZ16 (K64, ST11), TZ19 (K20, ST81), TZ20 (K20, ST81), TZ58 (K57, ST not defined), and JSH17 (K24, ST15). One-way ANOVA analysis indicated F = 0.9081 and p = 0.5178, which demonstrated similar growth and no fitness cost for the 8 strains (**Figure 6**).

Expression of *galF*

Figure 7 shows the relative expression of *galF* in the putative strains compared to that in the control strains NTUH-K2044 and HS11286. JS184, TZ20, JSH17, and HS11286 showed high *galF* expression.

Mouse Lethality Tests

The survival curve for mice inoculated (10^6 CFU) with the two *bla*$_{KPC}$(+)-HvKP strains, JS184 and TZ20, is shown in **Figure 8**. Log-rank (Mantel-Cox) test yielded values of χ^2 = 11.4286, p = 0.0096 for the four groups (JS184, TZ20, HS11286, and NTUH-K2044); χ^2 = 1.5521, p = 0.4602 for three groups (JS184, TZ20, and NTUH-K2044). Therefore, the virulence of JS184 and TZ20 was similar to that of NTUH-K2044, and was higher than that of HS11286. The LD_{50} values were 10^6 CFU for NTUH-K2044, 10^3 CFU for JS184, < 10^6 CFU for TZ20, > 10^7 CFU for HS11286 and the other 33 putative *bla*$_{KPC}$(+)-HvKP/Hv-*bla*$_{KPC}$(+)-KP strains.

Traits of Confirmed *bla*$_{KPC}$(+)-HvKP Strains

The two confirmed *bla*$_{KPC}$(+)-HvKP strains, JS184 and TZ20, showed differences in ST, *irp2* expression, and serotype (**Table 1**).

DISCUSSION

A combination of carbapenem resistance and hypervirulence in õõõõõ*K. pneumoniae* strains has been recently reported (Gu et al., 2018). However, the epidemiology of CR-HvKP and

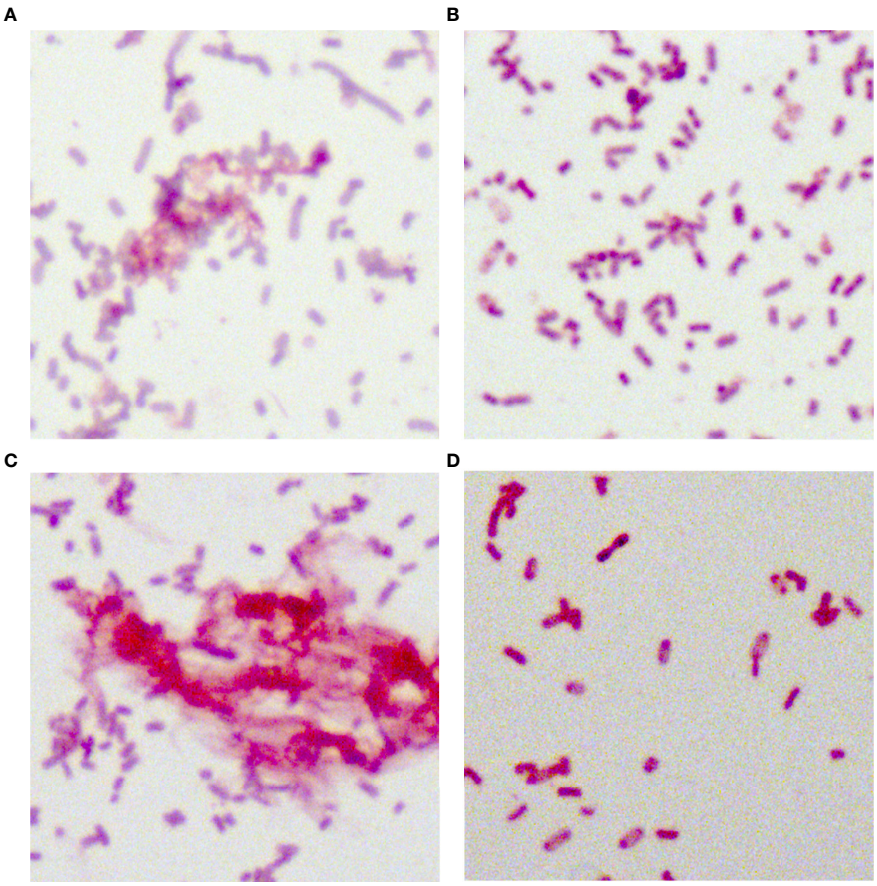

FIGURE 5 | Periodic acid-Schiff staining of 35 putative *bla*$_{KPC}$(+)-HvKP and Hv-*bla*$_{KPC}$(+)-KP strains. **(A)** *Klebsiella pneumoniae* NTUH-K2044, **(B)** *K. pneumoniae* HS11286, **(C)** JS184, and **(D)** TZ20. *K. pneumoniae* strains were purple/red and rod-shaped; the red fluffy masses were exopolysaccharides. *bla*$_{KPC}$, beta-lactamase *K. pneumoniae* carbapenemase gene; *bla*$_{KPC}$(+)-HvKP, *bla*$_{KPC}$(+) hypervirulent *K. pneumoniae*; Hv-*bla*$_{KPC}$(+)-KP, hypervirulent *bla*$_{KPC}$(+) *K. pneumoniae.*

Hv-CRKP has not been extensively studied. To our knowledge, this is the first epidemiological surveillance study on *bla*$_{KPC}$(+)-HvKP and Hv-*bla*$_{KPC}$(+)-KP strains in China using a mouse lethality test to evaluate their prevalence.

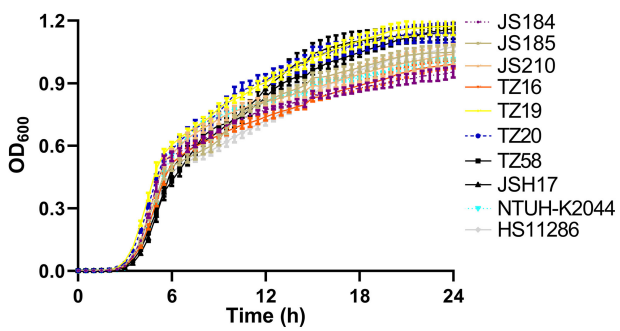

FIGURE 6 | Growth curves of 10 putative *bla*$_{KPC}$(+)-HvKP and Hv-*bla*$_{KPC}$(+)-KP strains. *bla*$_{KPC}$, beta-lactamase *K. pneumoniae* carbapenemase gene; *bla*$_{KPC}$(+)-HvKP, *bla*$_{KPC}$(+) hypervirulent *K. pneumoniae*; Hv-*bla*$_{KPC}$(+)-KP, hypervirulent *bla*$_{KPC}$(+) *K. pneumoniae*; OD$_{600}$, optical density at 600 nm.

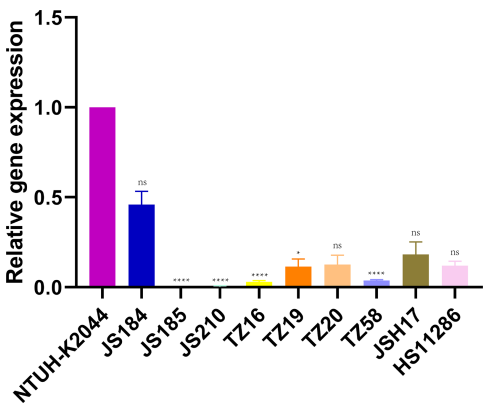

FIGURE 7 | Expression of *galF* among 35 putative *bla*$_{KPC}$(+)-HvKP and Hv-*bla*$_{KPC}$(+)-KP strains. *Klebsiella pneumoniae* NTUH-K2044 was used as the standard to which others were compared. Kruskal-Wallis test was used for comparison. *bla*$_{KPC}$, beta-lactamase *K. pneumoniae* carbapenemase gene; *bla*$_{KPC}$(+)-HvKP, *bla*$_{KPC}$(+) hypervirulent *K. pneumoniae*; Hv-*bla*$_{KPC}$(+)-KP, hypervirulent *bla*$_{KPC}$(+) *K. pneumoniae*; ns, not significant; ****, $p < 0.0001$; *, $p < 0.05$.

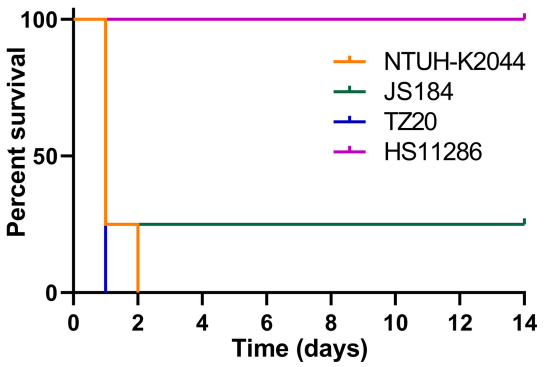

FIGURE 8 | Survival curves of mice inoculated with two bla_{KPC}(+)-HvKP strains. bla_{KPC}(+)-HvKP, beta-lactamase *K. pneumoniae* carbapenemase gene-positive hypervirulent *Klebsiella pneumoniae*.

In total, 13 key virulence genes in *K. pneumoniae* were investigated in this study; **Figure 2** shows a remarkable divergence in their distribution. The extremely high detection rates of *fimH*, *mrkD*, *entB*, and *wzi* indicate ubiquitous production of type 1 fimbriae, type 2 fimbriae, enterobactins, and capsules. Another siderophore gene *irp2* was present in a large proportion of the strains (76.1%), and is typically carried by ICE*Kp*1 in the chromosome; The remaining 2 siderophore genes *iucA* and *iroN* showed detection rates of approximately 20.0–30.0%, and are usually harboured by pK2044 and pLVPK-like virulence plasmids (Struve et al., 2015). The virulence genes *peg-344*, *p-rmpA*, and *p-rmpA2* are also present in pK2044- and pLVPK-like virulence plasmids (Russo and Marr, 2019), and therefore yielded similar detection rates to those of *iucA* and *iroN* ($p > 0.05$). The *c-rmpA* gene is present in the chromosome and often found in PLA specimens (Hsu et al., 2011). No such specimens were included in this study, which may explain the detection rate of 0.0%. The low detection rate of *wzy-K1* (6.4%) suggests the rarity of K1 *K. pneumoniae* in clinical practice.

Various molecular factors were evaluated to screen for CR-HvKP and Hv-CRKP. Zhang et al. previously evaluated *iucA*, *iroN*, *rmpA*, and *rmpA2* to check for the presence of virulence plasmids, and performed the *G. mellonella* lethality test to identify CR-HvKP, which yielded a rate of 5.2% (55/1052) for CR-HvKP (Zhang et al., 2020). We previously defined HvKP as: positive *wzy-K1*, ≥3 positive siderophore genes (*entB*, *irp2*, *iroN*, and *iucA*), or ≥1 positive capsule-regulating genes (*p-rmpA2*, *c-rmpA/A2*, and *p-rmpA*), and estimated a rate of 5.6% (29/521) for Hv-bla_{KPC}(+)-KP (Shon et al., 2013), which was also applied in this study. Harada et al. defined HvKP as strains carrying virulence genes, *rmpA*, *rmpA2*, *iroBCDN*, *iucABCD*, or *iutA* (Harada et al., 2019). Russo et al. confirmed that the *G. mellonella* lethality experiment cannot accurately differentiate HvKP from cKP (Russo and MacDonald, 2020). Thus, the mouse lethality test may represent the only approach to determine the exact prevalence of CR-HvKP/Hv-CRKP. In this study, only two bla_{KPC}(+)-HvKP strains, but no Hv-bla_{KPC}(+)-KP strains, were eventually confirmed using a mouse lethality test, showing a rate of 0.5% (2/436) for CR-HvKP which was far lower than that reported in other studies (Zhang et al., 2020; Hu et al., 2021). Owing to the predominance of KPC-induced carbapenem resistance (Lin et al., 2018), the actual prevalence of CR-HvKP should be approximately 0.5–1.0% in mainland China in 2017. The considerable difference in prevalence rates determined between this study and other reports highlights the need to elucidate why such biomarkers are not reliable and the difference between mouse and *G. mellonella* lethality tests. Zhang et al., reported that only one *K. pneumoniae* strain has been confirmed as CR-HvKP among three strains that harbour *rmpA* based on a mouse lethality test (Zhang et al., 2015). The fact that *rmpA* genes are non-functional in cKP may be attributed to different genetic backgrounds, although *rmpA*-related genes, such as *kvrA*, *kvrB*, and *rcsB* (Palacios et al., 2018; Walker et al., 2019), were found to be widely distributed in both cKP and HvKP (data not shown).

Although Hv-CRKP and CR-HvKP strains are currently emerging worldwide (Gu et al., 2018; Karlsson et al., 2019), our study revealed that the emergence of CR-HvKP is a relatively greater concern owing to its prevalence. In this study, two confirmed bla_{KPC}(+)-HvKP strains were found, including JS184 (K2) and TZ20 (K20), which showed no fitness cost, no hypercapsule production, and high expression of *galF* which is responsible for the synthesis of capsule precursor (Peng et al., 2018; Walker et al., 2019). However, JS184 showed a positive string test and exopolysaccharide production in contrast to TZ20. The reason for this is not known. In addition, JS184 and TZ20 also showed different ST and *irp2* expression.

This study had a few limitations. First, only typical siderophore genes were referred to, but not their expression. Second, capsule staining is not sufficient to differentiate capsules of various thicknesses, which may impact virulence.

Taken together, our findings indicate that CR-HvKP may emerge more often than Hv-CRKP; the former accounted for less than 1.0% of the strains evaluated *via* mouse lethality tests among clinical *K. pneumoniae* strains in mainland China in 2017.

TABLE 1 | Traits of confirmed bla_{KPC}(+)-HvKP strains.

strain	ST	*peg-344*	*allS*	*wzy-K1*	*p-rmpA*	*p-rmpA2*	*c-rmpA*	*fimH*	*mrkD*	*iucA*	*iroN*	*irp2*	*entB*	serotype
JS184	65	+	−	−	+	+	−	+	+	+	+	−	+	K2
TZ20	81	+	−	−	+	+	−	+	+	+	+	+	+	K20

+, positive; -, negative; bla_{KPC}(+)-HvKP, beta-lactamase Klebsiella pneumoniae carbapenemase gene-positive hypervirulent Klebsiella pneumoniae; ST, sequence type.

DATA AVAILABILITY STATEMENT

The datasets presented in this study can be found in online repositories. The names of the repository/repositories and accession number(s) can be found in the article/ **Supplementary Material**.

ETHICS STATEMENT

The animal study was reviewed and approved by the Institutional Animal Care and Use Committee of the School of Pharmacy, Fudan University (Shanghai, China).

AUTHOR CONTRIBUTIONS

DH, WC, and QZ contributed to conception of the study. ML, LY, ZY, YW, YH, GL, and XJ collected and identified the strains. DH, WC, QZ, PF, DT, and WW performed PCR and MLST analyses, string tests, capsular staining, periodic acid-Schiff staining, and fitness tests. PR and QM performed mouse lethality tests. DH, WC, and QZ wrote the manuscript which was revised by XJ and LY. All authors read and approved the final manuscript.

FUNDING

This study was supported by research grants from the National Natural Science Foundation of China (grants 81871692, 82172315, 82172315 and 81572031), Shanghai Municipal Key Clinical Specialty (Laboratory Medicine, No. shslczdzk03303), and the Shanghai Municipal Science and Technology Commission (grant number 19JC1413002).

ACKNOWLEDGMENTS

We thank Professor Jin-Town Wang from the Department of Internal Medicine, National Taiwan University Hospital, for providing the strain NTUH-K2044.

SUPPLEMENTARY MATERIAL

The Supplementary Material for this article can be found online at: https://www.frontiersin.org/articles/10.3389/fcimb.2022.882210/full#supplementary-material

REFERENCES

Adeolu, M., Alnajar, S., Naushad, S., and Gupta, R. (2016). Genome-Based Phylogeny and Taxonomy of the 'Enterobacteriales': Proposal for Enterobacterales Ord. Nov. Divided Into the Families Enterobacteriaceae, Erwiniaceae Fam. Nov., Pectobacteriaceae Fam. Nov., Yersiniaceae Fam. Nov., Hafniaceae Fam. Nov., Morganellaceae Fam. Nov., and Budviciaceae Fam. Nov. *Int. J. Syst. Evol. Microbiol.* 66 (12), 5575–5599. doi: 10.1099/ijsem.0.001485

Brisse, S., Passet, V., Haugaard, A. B., Babosan, A., Kassis-Chikhani, N., Struve, C., et al. (2013). Wzi Gene Sequencing, a Rapid Method for Determination of Capsular Type for *Klebsiella* Strains. *J. Clin. Microbiol.* 51 (12), 4073–4078. doi: 10.1128/JCM.01924-13

Chen, Y. C., Lin, C. H., Chang, S. N., and Shi, Z. Y. (2016). Epidemiology and Clinical Outcome of Pyogenic Liver Abscess: An Analysis From the National Health Insurance Research Database of Taiwan, 2000–2011.J. *Microbiol. Immunol. Infect.* 49 (5), 646–653. doi: 10.1016/j.jmii.2014.08.028

Compain, F., Babosan, A., Brisse, S., Genel, N., Audo, J., Ailloud, F., et al. (2014). Multiplex PCR for Detection of Seven Virulence Factors and K1/K2 Capsular Serotypes of Klebsiella Pneumoniae. *J. Clin. Microbiol.* 52 (12), 4377–4380. doi: 10.1128/JCM.02316-14

Diancourt, L., Passetet, V., Verhoef, J., Grimont, P. A., and Brisse, S. (2005). Multilocus Sequence Typing of *Klebsiella Pneumoniae* Nosocomial Isolates. *J. Clin. Microbiol.* 43 (8), 4178–4182. doi: 10.1128/JCM.43.8.4178-4182.2005

Effah, C. Y., Sun, T., Liu, S., and Wu, Y. (2020). *Klebsiella Pneumoniae: An* Increasing Threat to Public Health. *Ann. Clin. Microbiol. Antimicrob.* 19 (1), 1. doi: 10.1186/s12941-019-0343-8

Fang, C. T., Chuang, Y. P., Shun, C. T., Chang, S. C., and Wang, J. T. (2004). A Novel Virulence Gene in *Klebsiella Pneumoniae* Strains Causing Primary Liver Abscess and Septic Metastatic Complications. *J. Exp. Med.* 199 (5), 697–705. doi: 10.1084/jem.20030857

Gu, D., Dong, N., Zheng, Z., Lin, D., Huang, M., Wang, L., et al. (2018). A Fatal Outbreak of ST11 Carbapenem-Resistant Hypervirulent Klebsiella Pneumoniae in a Chinese Hospital: A Molecular Epidemiological Study. *Lancet Infect. Dis.* 18 (1), 37–46. doi: 10.1016/S1473-3099(17)30489-9

Harada, S., Aoki, K., Yamamoto, S., Ishii, Y., Sekiya, N., Kurai, H., et al. (2019). Clinical and Molecular Characteristics of *Klebsiella Pneumoniae* Isolates Causing Bloodstream Infections in Japan: Occurrence of Hypervirulent Infections in Health Care. *J. Clin. Microbiol.* 57 (11), e01206-19. doi: 10.1128/JCM.01206-19

Hauck, C., Cober, E., Richter, S. S., Perez, F., Salata, R. A., Kalayjian, R. C., et al. (2016). Spectrum of Excess Mortality Due to Carbapenem-Resistant *Klebsiella Pneumoniae* Infections. *Clin. Microbiol. Infect.* 22 (6), 513–519. doi: 10.1016/j.cmi.2016.01.023

Hsu, C. R., Lin, T. L., Chen, Y. C., Chou, H. C., and Wang, J. T. (2011). The Role of Klebsiella Pneumoniae rmpA in Capsular Polysaccharide Synthesis and Virulence Revisited. *Microbiology.* 157 (12), 3446–3457. doi: 10.1099/mic.0.050336-0

Huang, W., Qiao, F., Zhang, Y., Huang, J., Deng, Y., Li, J., et al. (2018). In-Hospital Medical Costs of Infections Caused by Carbapenem-Resistant *Klebsiella Pneumoniae*. *Clin. Infect. Dis.* 67 (suppl_2), S225–S230. doi: 10.1093/cid/ciy642

Hu, D., Li, Y., Ren, P., Tian, D., Chen, W., Fu, P., et al. (2021). Molecular Epidemiology of Hypervirulent Carbapenemase-Producing Klebsiella Pneumoniae. *Front. Cell. Infect. Microbiol.* 11, 256. doi: 10.3389/fcimb.2021.661218

Karampatakis, T., Antachopoulos, C., and Iosifidis, E. (2016). Molecular Epidemiology of Carbapenem-Resistant *Klebsiella Pneumoniae* in Greece. *Future Microbiol.* 11, 809–823. doi: 10.2217/fmb-2016-0042

Karlsson, M., Stanton, R. A., Ansari, U., McAllister, G., Chan, M. Y., Sula, E., et al. (2019). Identification of a Carbapenemase-Producing Hypervirulent *Klebsiella Pneumoniae* Isolate in the United States. *Antimicrob. Agents Chemother.* 63 (7), e00519-19. doi: 10.1128/AAC.00519-19

Lee, C. R., Lee, J. H., Park, K. S., Kim, Y. B., Jeong, B. C., and Lee, S. H. (2016). Global Dissemination of Carbapenemase-Producing *Klebsiella Pneumoniae:* Epidemiology, Genetic Context, Treatment Options, and Detection Methods. *Front. Microbiol.* 7, 895. doi: 10.3389/fmicb.2016.00895

Lin, D., Chen, J., Yang, Y., Cheng, J., and Sun, C. (2018). Epidemiological Study of Carbapenem-Resistant Klebsiella Pneumoniae. *Open Med.* 13, 460–466. doi: 10.1515/med-2018-0070

Lin, L., Xiao, X., Wang, X., Xia, M., and Liu, S. (2020). In Vitro Antimicrobial Susceptibility Differences Between Carbapenem-Resistant KPC-2-Producing and NDM-1-Producing *Klebsiella Pneumoniae* in a Teaching Hospital in Northeast China. *Microb. Drug Resist.* 26 (2), 94–99. doi: 10.1089/mdr.2018.0398

Liu, Y. C., Cheng, D. L., and Lin, C. L. (1986). *Klebsiella Pneumoniae* Liver Abscess Associated With Septic Endophthalmitis. *Arch. Intern. Med.* 146 (10), 1913–1916. doi: 10.1001/archinte.1986.00360220057011

Liu, P., Li, P., Jiang, X., Bi, D., Xie, Y., Tai, C., et al. (2012). Complete Genome Sequence of Klebsiella Pneumoniae Subsp. *Pneumoniae* HS11286, a Multidrug-Resistant Strain Isolated From Human Sputum. *J. Bacteriol.* 194 (7), 1841–1842. doi: 10.1128/JB.00043-12

Liu, D., Liu, Z. S., Hu, P., Cai, L., Fu, B. Q., Li, Y. S., et al. (2016). Characterization of Surface Antigen Protein 1 (SurA1) From Acinetobacter Baumannii and its Role in Virulence and Fitness. *Vet. Microbiol.* 186, 126–138. doi: 10.1016/j.vetmic.2016.02.018

Mizuta, K., Ohta, M., Mori, M., Hasegawa, T., Nakashima, I., and Kato, N. (1983). Virulence for Mice of Klebsiella Strains Belonging to the O1 Group: Relationship to Their Capsular (K) Types. *Infect. Immun.* 40 (1), 56–61. doi: 10.1128/iai.40.1.56-61.1983

Paczosa, M. K., and Mecsas, J. (2016). Klebsiella Pneumoniae: Going on the Offense With a Strong Defense. *Microbiol. Mol. Biol. Rev.* 80 (3), 629–661. doi: 10.1128/MMBR.00078-15

Palacios, M., Miner, T. A., Frederick, D. R., Sepulveda, V. E., Quinn, J. D., Walker, K. A., et al. (2018). Identification of Two Regulators of Virulence That Are Conserved in *Klebsiella Pneumoniae* Classical and Hypervirulent Strains. *mBio.* 9 (4), e01443-18. doi: 10.1128/mBio.01443-18

Pendleton, J. N., Gorman, S. P., and Gilmore, B. F. (2013). Clinical relevance of the ESKAPE pathogens. *Expert Rev. Anti Infect. Ther.* 11 (3), 297–308. doi: 10.1586/eri.13.12

Peng, D., Li, X., Liu, P., Zhou, X., Luo, M., Su, K., et al. (2018). Transcriptional Regulation of galF by RcsAB Affects Capsular Polysaccharide Formation in *Klebsiella Pneumoniae* NTUH-K2044. *Microbiol. Res.* 216, 70–78. doi: 10.1016/j.micres.2018.08.010

Reed, L. J., and Muench, H. (1938). A Simple Method of Estimating Fifty Percent Endpoints. *Am. J. Hyg.* 27 (3), 493–497. doi: 10.1093/oxfordjournals.aje.a118408

Russo, T. A., and MacDonald, U. (2020). The *Galleria Mellonella* Infection Model Does Not Accurately Differentiate Between Hypervirulent and Classical Klebsiella Pneumoniae. *mSphere.* 5 (1), e00850-19. doi: 10.1128/mSphere.00850-19

Russo, T. A., and Marr, C. M. (2019). Hypervirulent *Klebsiella Pneumoniae*. *Clin. Microbiol. Rev.* 32 (3), e00001-19. doi: 10.1128/CMR.00001-19

Russo, T. A., Olson, R., Fang, C. T., Stoesser, N., Miller, M., MacDonald, U., et al. (2018). Identification of Biomarkers for Differentiation of Hypervirulent Klebsiella Pneumoniae From Classical *K. Pneumoniae*. *J. Clin. Microbiol.* 56 (9), e00776-18. doi: 10.1128/JCM.00776-18

Shon, A. S., Bajwa, R. P., and Russo, T. A. (2013). Hypervirulent (Hypermucoviscous) Klebsiella Pneumoniae: A New and Dangerous Breed. *Virulence.* 4 (2), 107–118. doi: 10.4161/viru.22718

Siu, L. K., Yeh, K. M., Lin, J. C., Fung, C. P., and Chang, F. Y. (2012). Klebsiella Pneumoniae Liver Abscess: A New Invasive Syndrome. *Lancet Infect. Dis.* 12 (11), 881–887. doi: 10.1016/S1473-3099(12)70205-0

Struve, C., Roe, C. C., Stegger, M., Stahlhut, S. G., Hansen, D. S., Engelthaler, D. M., et al. (2015). Mapping the Evolution of Hypervirulent Klebsiella Pneumoniae. *mBio.* 6 (4), e00630. doi: 10.1128/mBio.00630-15

Walker, K. A., Miner, T. A., Palacios, M., Trzilova, D., Frederick, D. R., Broberg, C. A., et al. (2019). A *Klebsiella Pneumoniae* Regulatory Mutant Has Reduced Capsule Expression But Retains Hypermucoviscosity. *mBio* 10 (2), e00089-19. doi: 10.1128/mBio.00089-19

Wong, J. S., Chan, T. K., Lee, H. M., and Chee, S. P. (2000). Endogenous Bacterial Endophthalmitis: An East Asian Experience and a Reappraisal of a Severe Ocular Affliction. *Ophthalmology* 107 (8), 1483–1491. doi: 10.1016/S0161-6420(00)00216-5

World Health Organization. (2017). *Global Priority List of Antibiotic-Resistant Bacteria to Guide Research, Discovery, and Development of New Antibiotics*. (Geneva, Swiss).

Yang, C. S., Tsai, H. Y., Sung, C. S., Lin, K. H., Lee, F. L., and Hsu, W. M. (2007). Endogenous Klebsiella Endophthalmitis Associated With Pyogenic Liver Abscess. *Ophthalmology* 114 (5), 876–880. doi: 10.1016/j.ophtha.2006.12.035

Yigit, H., Queenan, A. M., Anderson, G. J., Domenech-Sanchez, A., Biddle, J. W., Steward, C. D., et al. (2001). Novel Carbapenem-Hydrolyzing Beta-Lactamase, KPC-1, From a Carbapenem-Resistant Strain of Klebsiella Pneumoniae. *Antimicrob. Agents Chemother.* 45 (4), 1151–1161. doi: 10.1128/AAC.45.4.1151-1161.2001

Zhan, L., Wang, S., Guo, Y., Jin, Y., Duan, J., Hao, Z., et al. (2017). Outbreak by Hypermucoviscous *Klebsiella Pneumoniae* ST11 Isolates With Carbapenem Resistance in a Tertiary Hospital in China. *Front. Cell Infect. Microbiol.* 7, 182. doi: 10.3389/fcimb.2017.00182

Zhang, Y., Jin, L., Ouyang, P., Wang, Q., Wang, R., Wang, J., et al. (2020). Evolution of Hypervirulence in Carbapenem-Resistant Klebsiella Pneumoniae in China: A Multicentre, Molecular Epidemiological Analysis. *J. Antimicrob. Chemother.* 75 (2), 327–336. doi: 10.1093/jac/dkz446

Zhang, Y., Zeng, J., Liu, W., Zhao, F., Hu, Z., Zhao, C., et al. (2015). Emergence of a Hypervirulent Carbapenem-Resistant Klebsiella Pneumoniae Isolate From Clinical Infections in China. *J. Infect.* 71 (5), 553–560. doi: 10.1016/j.jinf.2015.07.010

Conflict of Interest: The authors declare that the research was conducted in the absence of any commercial or financial relationships that could be construed as a potential conflict of interest.

Publisher's Note: All claims expressed in this article are solely those of the authors and do not necessarily represent those of their affiliated organizations, or those of the publisher, the editors and the reviewers. Any product that may be evaluated in this article, or claim that may be made by its manufacturer, is not guaranteed or endorsed by the publisher.

frontiers | Frontiers in Cellular and Infection Microbiology

TYPE Original Research
PUBLISHED 08 August 2022
DOI 10.3389/fcimb.2022.936649

OPEN ACCESS

EDITED BY
Milena Dropa,
University of São Paulo, Brazil

REVIEWED BY
Monique Tiba,
Adolfo Lutz Institute, Brazil
Asad U. Khan,
Aligarh Muslim University, India

*CORRESPONDENCE
Heping Xu
xmsunxhp@163.com
Xiaoyan Li
xiaoyanli@gzhmu.edu.cn

†These authors have contributed equally to this work and share first authorship

SPECIALTY SECTION
This article was submitted to Clinical Microbiology, a section of the journal Frontiers in Cellular and Infection Microbiology

RECEIVED 05 May 2022
ACCEPTED 11 July 2022
PUBLISHED 08 August 2022

CITATION
Huang Y, Ma X, Zeng S, Fu L, Xu H and Li X (2022) Emergence of a *Salmonella* Rissen ST469 clinical isolate carrying bla_{NDM-13} in China.
Front. Cell. Infect. Microbiol. 12:936649.
doi: 10.3389/fcimb.2022.936649

Emergence of a *Salmonella* Rissen ST469 clinical isolate carrying bla_{NDM-13} in China

Yulan Huang[1†], Xiaobo Ma[2,3†], Shihan Zeng[1†], Liang Fu[1], Heping Xu[2,3*] and Xiaoyan Li[1*]

[1]Department of Clinical Laboratory, Fifth Affiliated Hospital, Southern Medical University, Guangzhou, China, [2]Department of Clinical Laboratory, the First Affiliated Hospital of Xiamen University (Xiamen Key Laboratory of Genetic Testing), School of medicine, Xiamen University, Xiamen, China, [3]School of Public Health, Xiamen University, Xiamen, China

New Delhi metallo-β-lactamase-13 (NDM-13) is an NDM variant that was first identified in 2015 and has not been detected in *Salmonella* species prior to this study. Here we describe the first identification of a *Salmonella* Rissen strain SR33 carrying bla_{NDM-13}. The aim of this study was to molecularly characterize SR33's antimicrobial resistance and virulence features as well as investigate the genetic environment of bla_{NDM-13}. The *Salmonella* Rissen SR33 strain was isolated from a patient with fever and diarrhea. SR33 belonged to ST469, and it was found to be multidrug-resistant (MDR) and to carry many virulence genes. Phylogenetic analysis showed that SR33 shared a close relationship with most of the Chinese *S*. Rissen ST469 strains. bla_{NDM-13} was located in a transmissible IncI1 plasmid pNDM13-SR33. Sequence analysis of bla_{NDM-13}-positive genomes downloaded from GenBank revealed that a genetic context (ΔIS*Aba125*-bla_{NDM-13}-ble_{MBL}-trpF) and a hybrid promoter (consisting of –35 sequences provided by IS*Aba125* and –10 sequences) were conserved. IS*Aba125* was truncated by IS*1294* in three plasmids carrying bla_{NDM-13}, including pNDM13-SR33. To our knowledge, this is the first report of bla_{NDM-13} carried by *Salmonella*. The emergence of bla_{NDM-13} in a clinical MDR *S*. Rissen ST469 strain highlights the critical need for monitoring and controlling the dissemination of bla_{NDM-13}. bla_{NDM-13} carried by a transmissible IncI1 plasmid may result in an increased risk of bla_{NDM-13} transmission. IS*1294* may be involved in the movement of bla_{NDM-13}.

KEYWORDS

bla_{NDM-13}, *Salmonella* Rissen, ST469, IS*Aba125*, IS*1294*

Introduction

Carbapenems have been used for decades to treat severe gram-negative bacterial infections, particularly in resistant and multidrug-resistant (MDR) infections (Hansen, 2021). According to the World Health Organization's Global Priority List, carbapenem-resistant Enterobacteriaceae (CRE) pose a growing threat to public health worldwide (Tacconelli et al., 2018). New Delhi metallo-β-lactamase (NDM) is a subclass B1 metallo-β-lactamase that is capable of hydrolyzing almost all β-lactams including carbapenems (Yong et al., 2009; Nordmann et al., 2011). Worse still, clinically available β-lactamase inhibitors are ineffective in preventing carbapenem hydrolysis by NDM enzymes (Wu et al., 2019). NDM-positive strains are usually resistant to most of antimicrobial agents, due to coexistence of other resistance mechanisms (Nordmann et al., 2011), leading to a variety of infections that are associated with high mortality (Guducuoglu et al., 2017). Since NDM-1 was first identified in clinical isolates in India in 2008 (Yong et al., 2009), 31 variants have been reported worldwide, representing a significant challenge for public health and clinical management (Moellering, 2010; Dortet et al., 2014; Li et al., 2021). Of these, NDM-13 is a variant that has two amino acid substitutions (D95N and M154L) compared with NDM-1, resulting in the increased hydrolytic activity against cefotaxime (Shrestha et al., 2015). NDM-13 has been detected in five *Escherichia coli* strains obtained from Nepal (n = 1) (Shrestha et al., 2015), China (n = 3) (Lv et al., 2016), and Korea (n = 1) (Kim et al., 2019). Here we aim to characterize a $bla_{\text{NDM-13}}$-positive *Salmonella* Rissen strain SR33 isolated in China. To our knowledge, this is the first report of $bla_{\text{NDM-13}}$ detected in *Salmonella*.

Materials and methods

Bacterial strain

Strain SR33 was isolated from a fecal sample of an old patient. This patient was hospitalized due to occasional fever and diarrhea. During hospitalization, cefixime was ineffective against this infection, but it improved after treatment with levofloxacin. SR33 was identified by the VITEK-2 COMPACT automatic microbial identification system (bioMérieux, Marcy-l'Étoile, France), and its serotype was confirmed by slide agglutination technique (Kauffmann-White-Le Minor scheme) (Grimont and Weill, 2007)

Antimicrobial susceptibility testing

The minimum inhibitory concentrations (MICs) for imipenem, ertapenem, ceftazidime, ceftriaxone, cefepime, amoxicillin/clavulanic acid, piperacillin/tazobactam, trimethoprim/sulfamethoxazole, levofloxacin, ampicillin, tetracycline, ciprofloxacin, chloramphenicol, and azithromycin were determined by broth microdilution following the CLSI guidelines, and MIC results were interpreted according to the CLSI breakpoints (Wayne, 2021).

Whole-genome sequencing and bioinformatics analysis

The genomic DNA of SR33 was extracted by the bacterial genomic DNA extraction kit (Tiangen, Beijing, China) and sequenced on an Oxford Nanopore platform (Novogene, Tianjin, China). Sequence reads were assembled by Unicycler 0.4.8 (Wick et al., 2017) and annotated by Prokka 1.14.5 (Seemann,, 2014). The serotype was further confirmed by SISTR 1.1.1 (Yoshida et al., 2016), and the sequence type (ST) was determined using MLST 2.18.0 (Larsen et al., 2012). The distance matrix based on the core-genome single-nucleotide polymorphism (SNP) profiles of 37 Chinese *S.* Rissen ST469 isolates was generated using Parsnp and HarvestTools (Treangen et al., 2014). The phylogenetic tree was constructed by MEGA X (Kumar et al., 2018). Resistance genes and plasmid replicons were identified using Abricate (https://github.com/tseemann/abricate) with the ResFinder (Zankari et al., 2012) and PlasmidFinder (Carattoli et al., 2014) databases, respectively. The filtering criteria of antimicrobial resistance genes were >90% identity and >90% coverage. The virulence genes were analyzed by the database of Virulence Factors of Pathogenic Bacteria (VFDB) using BLASTn with a threshold of >70% identity and >70% coverage (Chen et al., 2016). The presence of *Salmonella* pathogenicity islands (SPIs) was explored by SPIFinder (https://cge.cbs.dtu.dk/services/SPIFinder/). Circular maps of plasmids were generated using the BLAST Ring Image Generator (BRIG) tool (Alikhan et al., 2011). Transposon and insertion sequence (IS) elements were scanned using the ISFinder database (Siguier et al., 2006). BLASTn (Altschul et al., 1990) was used to determine the identity of the genetic environment between NDM-13-positive sequences. The genetic environment was visualized by EasyFig (Sullivan et al., 2011).

Plasmid conjugation experiments

Transferability of plasmid harboring $bla_{\text{NDM-13}}$ was assessed by the conjugation experiment, using rifampin-resistant *E. coli* C600 as the recipient strain. Transconjugants were selected on Luria-Bertani agar plates containing rifampin (100 μg/ml) and imipenem (2 μg/ml). Transconjugants containing the $bla_{\text{NDM-13}}$ gene were verified by PCR sequencing (forward primer sequence: ATGGAATTGCCCAATATTATGCAC and reverse primer sequence: TCAGCGCAGCTTGTCGGC). The antimicrobial susceptibility of the transconjugant was confirmed by the broth microdilution method.

Nucleotide sequence accession number

The whole-genome sequence of SR33 has been submitted to the GenBank database with accession numbers CP092911–CP092914. The nucleotide sequence of plasmid pNDM13-SR33 has been deposited under accession number CP092912.

Results

Antimicrobial susceptibility testing and antimicrobial resistance genes

As shown in Table 1, SR33 was multidrug resistant to all tested β-lactams, trimethoprim/sulfamethoxazole, and tetracycline and was susceptible to quinolones (levofloxacin and ciprofloxacin), azithromycin, and chloramphenicol. In addition to $bla_{\text{NDM-13}}$, SR33 carried genes that mediate resistance to β-lactams ($bla_{\text{TEM-1}}$), bleomycin (ble_{MBL}), streptomycin (*aadA1*, *aadA2*), chloramphenicol (*cmlA1*), trimethoprim (*dfrA12*), sulfonamide (*sul3*), and tetracycline [*tet(A)*]. The information of resistance genes detected in SR33 is listed in Supplementary Table S1.

Whole-genome sequencing (WGS) showed that $bla_{\text{NDM-13}}$ and ble_{MBL} were located on an IncI1 plasmid designated as pNDM13-SR33, which is 88,258 bp in length with an average GC content of 50.37%. The other resistance genes were found on the chromosome. pNDM13-SR33 was successfully self-transferred into C600, and the transconjugant SR33-C600 was resistant to all tested β-lactams (Table 1).

Characterization of the SR33 strain and phylogenetic analysis of Chinese *S.* Rissen ST469 isolates

The serotype and sequence type of SR33 were determined to be serovar Rissen and ST469. Phylogenetic analysis of SR33 with other 36 Chinese *S.* Rissen ST469 isolates (retrieved and downloaded from EnteroBase in February 2022, https://enterobase.warwick.ac.uk/species/index/senterica) revealed that SR33 differed from the other isolates by 41–418 SNPs (Figure 1). The information of these strains is listed in Supplementary Table S2. Besides, these strains were mainly isolated from food, poultry, and humans. Meanwhile, the majority of Chinese *S.* Rissen ST469 strains were MDR. The drug resistance profiles of these MDR strains were similar, and common drug resistance genes include *aadA1*, *aadA2*, $bla_{\text{TEM-1}}$, *cmlA1*, *sul3*, *dfrA12*, and *tet(A)*. Since the common drug resistance genes in SR33 were located on chromosomes, and 29/37 Chinese *S.* Rissen ST469 isolates did not carry resistance plasmids, we speculated that the antimicrobial resistance genes were mainly located on the chromosomes of these closely related MDR strains.

Salmonella pathogenicity islands and virulence-associated genes

According to SPIFinder, SR33 contained SPI-1 to SPI-5, SPI-8, and SPI-9. All VFDB-annotated genes are listed in Table 2. Based on the annotation of the VFDB database, SR33 harbored 124 virulence genes. The virulence genes are

TABLE 1 MIC values of antimicrobials for SR33 and its transconjugant.

Antimicrobials	SR33		C600		SR33-C600	
	MIC values (μg/mL)	Interpretation	MIC values (μg/mL)	Interpretation	MIC values (μg/mL)	Interpretation
Imipenem	≥16	R	≤1	S	≥16	R
Ertapenem	≥8	R	≤0.5	S	≥8	R
Ceftazidime	≥64	R	≤4	S	≥64	R
Ceftriaxone	≥64	R	≤1	S	≥64	R
Cefepime	16	R	≤2	S	16	R
Amoxicillin/clavulanic acid	≥32	R	≤4	S	≥32	R
Piperacillin/tazobactam	≥128	R	≤16	S	≥128	R
Trimethoprim/sulfamethoxazole	≥320	R	≤20	S	≤20	S
Levofloxacin	≤0.12	S	≤0.5	S	0.5	S
Ampicillin	≥32	R	≤8	S	≥32	R
Tetracycline	≥16	R	≤4	S	≤4	S
Ciprofloxacin	≤0.06	S	≤0.25	S	≤0.25	S
Chloramphenicol	≤8	S	≤8	S	≤8	S
Azithromycin	≤16	S	≤16	S	≤16	S

MIC, minimum inhibitory concentration; R, resistant; I, intermediate; S, sensitive.

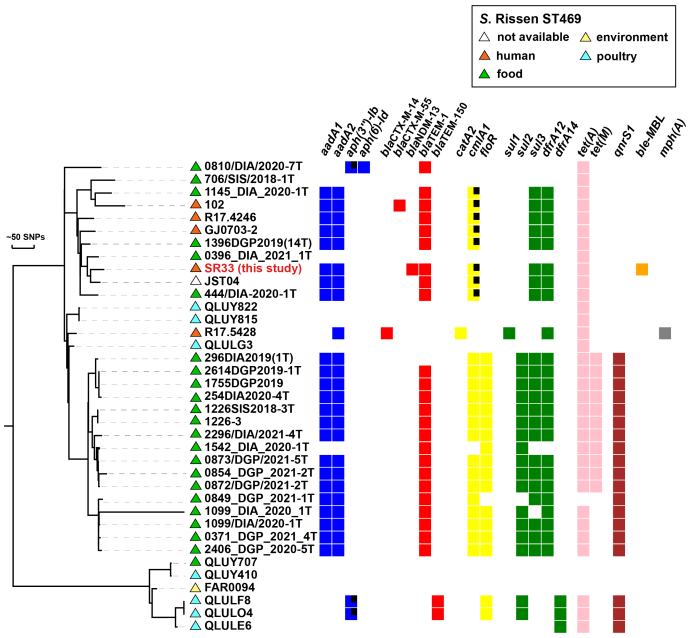

FIGURE 1
Phylogenetic distribution of antimicrobial resistance genes of SR33 of this study and other Chinese *S.* Rissen ST469 isolates. Antimicrobial resistant genes are represented by colored squares, genes with partial deletions are marked with black squares. The source of each isolate is shown with colored triangles. Bars represent unit distance of 50 SNPs.

involved in adhesion systems, iron uptake, magnesium uptake, macrophage, flagella, type III secretion systems (T3SS), and serum resistance.

Plasmid analysis of $bla_{\text{NDM-13}}$-positive isolates

NDM-13 has been identified in plasmids of three *E. coli* stains, including an IncX3 plasmid pNDM13-DC33(accession no. KX094555), an IncFIB plasmid pSECR18-0956 (accession no. MK157018), and an IncI1 plasmid pHNAHS65I-1 (accession no. MN219406). Of note, pNDM13-SR33 shared 99% coverage and 100% identity with an IncI1-$bla_{\text{NDM-13}}$ plasmid pHNAHS65I (accession no. MN219406) of *E. coli* discovered in 2020 (Figure 2), which has a truncated ble_{MBL}.

Comparative analysis of the genetic environment of $bla_{\text{NDM-13}}$

As shown in Figure 3, the $bla_{\text{NDM-13}}$-producing strains shared a conserved genetic structure (Δ*ISAba125*-$bla_{\text{NDM-13}}$-ble_{MBL}-trpF). The conserved region was found involved in various genetic contexts with different insertion sequences. The genetic context of $bla_{\text{NDM-13}}$ in SR33 was highly similar to pHNAHS65I-1 (no. MN219406) with Δ*ISAba125* truncated by the insertion of an IS*1294* upstream, which was also detected in pSECR18-0956 (no. MK157018). In L704 (no. RIZT01000075) and pSECR18-0956 (no. MK157018), the $bla_{\text{NDM-13}}$ region was adjacent to an IS*CR1* complex class 1 integron (IS*CR1-sul1-qacEΔ1-IntI1*). The sequences of L704 and IOMTU558 (accession no. LC012596) were flanked by IS*26* and IS*3000*, respectively. In addition, a cluster (IS*3000*-Δ*ISAba125-IS5*-Δ*ISAba125*) was found upstream of $bla_{\text{NDM-13}}$ in pNDM13-DC33 (no. KX094555). Moreover, a hybrid promoter (consisting of −35 sequences within the inverted repeat left of *ISAba125* and −10 sequences) located upstream of $bla_{\text{NDM-13}}$ was conservative in $bla_{\text{NDM-13}}$-producing strains.

Discussion

To date, New Delhi metallo-β-lactamase-13 (NDM-13) has been detected in five *E. coli* stains with different genetic backgrounds. Here, we report the emergence of an NDM-13-positive *Salmonella* strain SR33. The serotype of SR33 was determined to be serovar Rissen, which is regarded as one of the 20 most common serovars to cause human salmonellosis (European Food Safety Authority, E.C.f.D.P.a.C, 2017). SR33 was assigned to ST469, an MDR clone that has been reported in multiple countries (Campos et al., 2019).

10.3389/fcimb.2022.936649

TABLE 2 Virulence-associated genes in SR33.

VF classes	Virulence factors	Genes
Fimbrial adherence determinants	Agf (thin aggregative fimbriae/curli)	*csg*ABCDEFG, *ste*ABC
	Lpf (long polar fimbriae)	*lpf*ABCE
	Type 1 fimbriae	*fim*CDFHI
Non-fimbrial adherence determinants	MisL	*mis*L
	SinH	*sin*H
Iron uptake	Enterobactin	*ent*ABCES, *fep*ABCDG
	Salmochelin	*iro*BCN
Magnesium uptake	Magnesium uptake/transporter	*mgt*BC
Macrophage inducible gene	Mig-14	*mig*-14
Motility	Flagella	*che*WY, *flg*GH, *fli*AGMP
Secretion system	T3SS (SPI-1 encoded)	*inv*ABCEFGHIJ, *org*ABC, *prg*HIJK, *sic*AP, *sip*D, *spa*OPQRS
	T3SS-1 translocated effectors	*avr*A, *sip*ABC/*ssp*ABC, *sop*ABDE2, *spt*P, *slr*P
	T3SS (SPI-2 encoded)	*ssa*CDEGHIJKLMNOPQRSTUV, *ssc*AB, *sse*ABCDE
	T3SS-2 translocated effectors	*pip*BB2, *sif*ABH, *sop*D2, *sse*FGJK1K2L, *spi*C/*ssa*B
Serum resistance	OmpA (Outer membrane protein A)	*omp*A
Others	Lipooligosaccharide	*gmh*A/*lpc*A
	Lipopolysaccharide	*gtr*AB

VF, virulence factors.

SR33 was found to be MDR and to harbor nine resistance genes. These resistance genes were consistent with the phenotypes except for *cmlA1*. SR33 remained sensitive to chloramphenicol, which might be due to the fact that the *cmlA1* gene had a sequence deletion of 96 bp. Since SR33 was resistant to all β-lactams and susceptible to quinolones, it explains well why cefixime was ineffective against this infection and levofloxacin was effective.

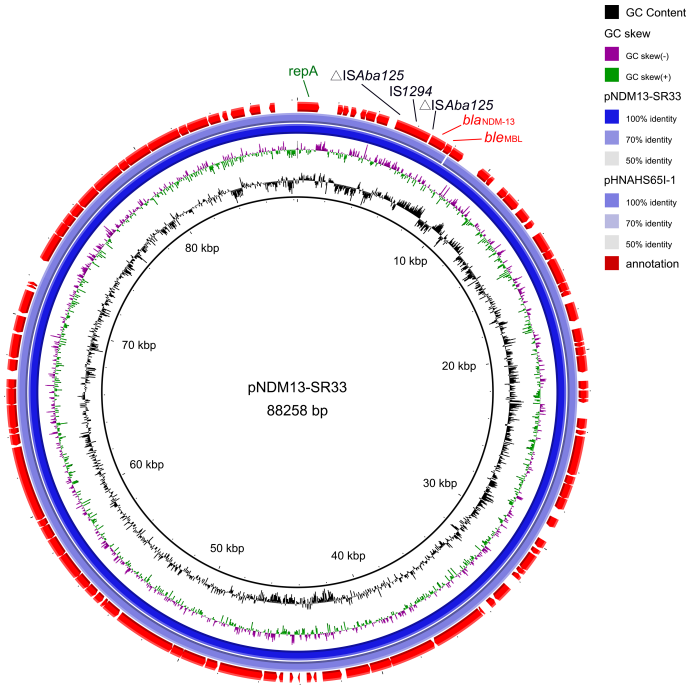

FIGURE 2
Genetic map of pNDM13-SR33 (no. CP092912) and pHNAHS65I-1 (no. MN219406). The repA, IS elements, resistance genes are annotated by green, black, red fonts, respectively.

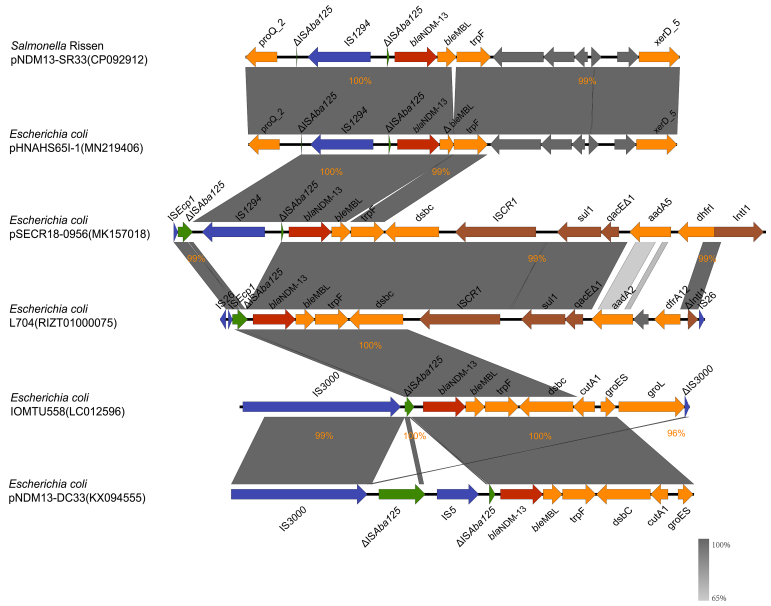

FIGURE 3
bla$_{NDM-13}$ flanking sequence of pNDM13-SR33 (no. CP092912), pHNAHS65I-1 (no. MN219406), L704 (no. RIZT01000075), pSECR18-0956 (no. MK157018), IOMTU558 (no. LC012596), and pNDM13-DC33 (no. KX094555). The *bla*$_{NDM-13}$ gene, IS*Aba125*, other insertion sequences, integron elements, and genes encoding hypothetical proteins are shown in red, green, blue, brown, and gray, respectively. The rest of genes are colored in orange. Δ; indicates a truncated gene or mobile element. The percentages signify the genetic identity between these sequences.

Based on phylogenetic analysis, SR33 was closely related to the majority of the Chinese *S.* Rissen ST469 strains downloaded from EnteroBase. Since the available 37 Chinese *S.* Rissen ST469 isolates were mostly isolated from food, poultry, and humans, it is in agreement with the idea that *S.* Rissen infection occurs in humans as a zoonosis through food chain transmission (Xu et al., 2020). Therefore, it is possible that this patient had a foodborne infection. Another important finding is that most Chinese *S.* Rissen ST469 strains were MDR and shared similar drug resistance profiles. Since the antimicrobial resistance genes were mainly located on chromosomes, we should pay close attention to the vertical transmission of MDR *S.* Rissen ST469 strains. These observations emphasize the necessity of the surveillance of *S.* Rissen ST469 pathogens.

SPIs are gene clusters located on chromosomes and encode various virulence components (Foley et al., 2008). SR33 contained five important SPIs (SPI-1 to SPI-5) that are correlated with the pathogenesis of *Salmonella* (Cui et al., 2021) and additional two SPIs (SPI-8, SPI-9). Based on the annotation of the VFDB database, most of the virulence genes carried by SR33 are associated with flagella, type III secretion systems (T3SS), and adhesion systems, which have been demonstrated to play a variety of roles in the pathogenesis of *Salmonella* (Jajere, 2019). Of these, T3SS is regarded as the most important virulence factor of *Salmonella* (Lou et al., 2019). In general, MDR strain SR33 possessed important pathogenicity islands and many virulence-associated genes, which highlights the pathogenesis of SR33.

NDM-13 was first identified on the chromosome of *E. coli* IOMUT558 (ST101) from Nepal (Shrestha et al., 2015), and it was subsequently detected in four *E. coli* stains, namely, an IncFIB plasmid pSECR18-0956 of SECR18-0956 (ST8499) from Korea (Kim et al., 2019), an IncX3 plasmid pNDM13-DC33 carried by DC33 (ST5138) (Lv et al., 2016), an IncI1 plasmid pHNAHS65I-1 of AHS8C65RI, and L704 strain (the location of *bla*$_{NDM-13}$ is unclear) from China. In our study, *bla*$_{NDM-13}$ was found in a transmissible IncI1 plasmid pNDM13-SR33 of *S.* Rissen (ST469). The high coverage and identity between pNDM13-SR33 and pHNAHS65I-1 suggest that cross-species dissemination of *bla*$_{NDM-13}$ plasmids had occurred. The *bla*$_{NDM}$-carrying plasmids mostly belong to IncX3, IncFII, and IncC replicon types (Wu et al., 2019), indicating that the vector of NDM-13 may be different from the other variants. Previous studies showed that the IncI1 plasmids are often associated with clinically relevant strains (García-Fernández et al., 2008) and it is the major vehicle of extended spectrum β-lactamase (Carattoli et al., 2021). Thus, *bla*$_{NDM-13}$ in SR33 carried by an IncI1 transmissible plasmid may result in an increased risk of *bla*$_{NDM-13}$ transmission.

Comparative analysis of the *bla*$_{NDM-13}$ genetic contents revealed that *bla*$_{NDM-13}$ was bracketed by multi-insertional sequences. Of these, IS*Aba125* was conservative in *bla*$_{NDM-13}$-positive isolates. It is consistent with the finding that IS*Aba125* (intact or truncated) upstream of *bla*$_{NDM}$ is common in *bla*$_{NDM}$

genetic contexts (Ahmad et al., 2018; Pérez-Vázquez et al., 2019; Das et al., 2019; Wu et al., 2019), implying a role in the transmission of bla_{NDM}. IS*3000*, IS*26*, and IS*5* have also been reported to be associated with dissemination of NDM-encoding genes, while the role of IS*1294* is still unclear (Zhao et al., 2021; Acman et al., 2022). IS*1294* belongs to the IS*91* family, and previous reports demonstrated that the disruption of the IS*Ecp1* element by IS*1294* was linked to the promotion of bla_{CMY-2} (Sidjabat et al., 2014; Tagg et al., 2014) and bla_{CTX-55} (Pan et al., 2013; Hu et al., 2018) gene dissemination. In this study, ΔIS*Aba125* truncated by IS*1294* was found in three bla_{NDM-13}-harboring plasmids including pNDM13-SR33. We thus suspected that IS*1294* may be involved in the mobilization and dissemination of bla_{NDM-13}.

Expression of the bla_{NDM-1} gene is under the control of a hybrid promoter (consisting of −35 sequences within the inverted repeat left of IS*Aba125* and −10 sequences) located upstream of bla_{NDM-1} (Poirel et al., 2011). BLASTn analysis revealed that this hybrid promoter was also conservative in bla_{NDM-13}-producing strains. This finding further supports that bla_{NDM-13} is derived from bla_{NDM-1} (Lv et al., 2016; Wu et al., 2019).

Conclusion

To the best of our knowledge, this study first reports an NDM-13-producing *Salmonella* isolate. The emergence of bla_{NDM-13} in a clinical MDR *Salmonella* Rissen ST469 strain poses a significant threat to public health. Most of the *S.* Rissen ST469 strains isolated from China were MDR, which highlights the importance of the surveillance for *S.* Rissen ST469. The bla_{NDM-13} carried by a transmissible IncI1 plasmid may cause an increased risk of bla_{NDM-13} transmission. IS*1294* may be involved in the mobilization and dissemination of bla_{NDM-13}.

Data availability statement

The datasets presented in this study can be found in online repositories. The names of the repository/repositories and accession number(s) can be found below: https://www.ncbi.nlm.nih.gov/genbank/, CP092911-CP092914.

Ethics statement

The studies involving human participant were reviewed and approved by the Ethics Committee of the First Affiliated Hospital of Xiamen University. The participant provided his written informed consent to participate in this study.

Author contributions

HX and XL contributed to the conception and design of the study. HX and XM provided this strain. YH and SZ performed laboratory experiments. YH, XM, SZ, and LF analyzed the data. YH wrote the manuscript. XL revised the manuscript. All authors have read and approved the manuscript.

Funding

This study was funded by the Youth Foundation of the National Natural Science Foundation of China (81902104), Basic and Applied Basic Research Foundation of Guangdong Province (2021A1515220153), Basic and Applied Basic Research Foundation of Guangdong Province Natural Science Foundation (2022A1515012481), and Joint Research Projects of Health and Education Commission of Fujian Province (2019-WJ-42).

Acknowledgments

We thank Dr. Kai Zhou (Shenzhen Institute of Respiratory Diseases, The First Affiliated Hospital (Shenzhen People's Hospital), Southern University of Science and Technology, Shenzhen, China) for his revision of the manuscript.

Conflict of interest

The authors declare that the research was conducted in the absence of any commercial or financial relationships that could be construed as a potential conflict of interest.

Publisher's note

Supplementary material

The Supplementary Material for this article can be found online at: https://www.frontiersin.org/articles/10.3389/fcimb.2022.936649/full#supplementary-material

References

Acman, M., Wang, R., van Dorp, L., Shaw, L. P., Wang, Q., Luhmann, N., et al. (2022). Role of mobile genetic elements in the global dissemination of the carbapenem resistance gene bla(NDM). *Nat. Commun.* 13 (1), 1131. doi: 10.1038/s41467-022-28819-2

Ahmad, N., Ali, S.M., and Khan, A.U.. (2018). Detection of New Delhi Metallo-β-Lactamase Variants NDM-4, NDM-5, and NDM-7 in Enterobacter aerogenes Isolated from a Neonatal Intensive Care Unit of a North India Hospital: A First Report. *Microb. Drug Resist.* 24 (2), 161–165. doi: 10.1089/mdr.2017.0038

Alikhan, N.F., Petty, N.K., Ben Zakour, N.L., and Beatson, S.A.. (2011). BLAST Ring Image Generator (BRIG): Simple prokaryote genome comparisons. *BMC Genomics* 12, 402. doi: 10.1186/1471-2164-12-402

Altschul, S. F., Gish, W., Miller, W., Myers, E. W., and Lipman, D. J. (1990). Basic local alignment search tool. *J. Mol. Biol.* 215 (3), 403–410. doi: 10.1016/s0022-2836(05)80360-2

Campos, J., Mourão, J., Peixe, L., and Antunes, P. (2019). Non-typhoidal salmonella in the pig production chain: a comprehensive analysis of its impact on human health. *Pathogens* 8 (1), 19. doi: 10.3390/pathogens8010019

Carattoli, A., Villa, L., Fortini, D., and García-Fernández, A. (2021). Contemporary IncI1 plasmids involved in the transmission and spread of antimicrobial resistance in enterobacteriaceae. *Plasmid* 118, 102392. doi: 10.1016/j.plasmid.2018.12.001

Carattoli, A., Zankari, E., García-Fernández, A., Voldby Larsen, M., Lund, O., Villa, L., et al. (2014). *In silico* detection and typing of plasmids using PlasmidFinder and plasmid multilocus sequence typing. *Antimicrob. Agents Chemother.* 58 (7), 3895–3903. doi: 10.1128/aac.02412-14

Chen, L., Zheng, D., Liu, B., Yang, J., and Jin, Q. (2016). VFDB 2016: hierarchical and refined dataset for big data analysis–10 years on. *Nucleic Acids Res.* 44 (D1), D694–D697. doi: 10.1093/nar/gkv1239

Cui, L., Wang, X., Zhao, Y., Peng, Z., Gao, P., Cao, Z., et al. (2021). Virulence comparison of salmonella enterica subsp. enterica isolates from chicken and whole genome analysis of the high virulent strain s. enteritidis 211. *Microorganisms* 9 (11), 2239. doi: 10.3390/microorganisms9112239

Das, U. N., Singh, A. S., Lekshmi, M., Nayak, B. B., and Kumar, S. (2019). Characterization of bla(NDM)-harboring, multidrug-resistant Enterobacteriaceae isolated from seafood. *Environ Sci Pollut Res Int* 26 (3), 2455–2463. doi: 10.3390/microorganisms9112239

Dortet, L., Poirel, L., and Nordmann, P. (2014). Worldwide dissemination of the NDM-type carbapenemases in Gram-negative bacteria. *Biomed Res. Int.* 2014, 249856. doi: 10.1155/2014/249856

European Food Safety Authority, E.C.f.D.P.a.C (2017). The European union summary report on trends and sources of zoonoses, zoonotic agents and food-borne outbreaks in 2016. *Efsa J.* 15 (12), e05077. doi: 10.2903/j.efsa.2017.5077

Foley, S. L., Lynne, A. M., and Nayak, R. (2008). Salmonella challenges: prevalence swine poultry potential pathogenicity such isolates. *J. Anim. Sci.* 86 (14 Suppl), E149–E162. doi: 10.2527/jas.2007-0464

García-Fernández, A., Chiaretto, G., Bertini, A., Villa, L., Fortini, D., Ricci, A., et al. (2008). Multilocus sequence typing of IncI1 plasmids carrying extended-spectrum beta-lactamases in escherichia coli and salmonella of human and animal origin. *J. Antimicrob. Chemother.* 61 (6), 1229–1233. doi: 10.1093/jac/dkn131

Grimont, P. A., and Weill, F. X.. Antigenic formulae of the Salmonella serovars. *WHO collaborating centre for reference and research on Salmonella* 9 1–166. Available online at: https://www.scacm.org/free/Antigenic%20Formulae%20of%20the%20Salmonella%20Serovars%202007%209th%20edition.pdf.

Hansen, G. T. (2021). Continuous evolution: perspective on the epidemiology of carbapenemase resistance among enterobacterales and other gram-negative bacteria. *Infect. Dis. Ther.* 10 (1), 75–92. doi: 10.1007/s40121-020-00395-2

Hu, X., Gou, J., Guo, X., Cao, Z., Li, Y., Jiao, H., et al. (2018). Genetic contexts related to the diffusion of plasmid-mediated CTX-M-55 extended-spectrum beta-lactamase isolated from enterobacteriaceae in China. *Ann. Clin. Microbiol. Antimicrob.* 17 (1), 12. doi: 10.1186/s12941-018-0265-x

Guducuoglu, H., Gursoy, N.C., Yakupogullari, Y., Parlak, M., Karasin, G., Sunnetcioglu, M., et al. (2017). Hospital outbreak of a colistin-resistant, NDM-1- and OXA-48-Producing klebsiella pneumoniae: High mortality from pandrug resistance. *Microbial Drug resistance (Larchmont N.Y.)* 24 (7), 966–972. doi: 10.1089/mdr.2017.0173

Jajere, S. M. (2019). A review of salmonella enterica with particular focus on the pathogenicity and virulence factors, host specificity and antimicrobial resistance including multidrug resistance. *Vet. World* 12 (4), 504–521. doi: 10.14202/vetworld.2019.504-521

Kim, J. S., Jin, Y. H., Park, S. H., Han, S., Kim, H. S., Park, J. H., et al. (2019). Emergence of a multidrug-resistant clinical isolate of escherichia coli st8499 strain producing ndm-13 carbapenemase in the republic of Korea. *Diagn. Microbiol. Infect. Dis.* 94 (4), 410–412. doi: 10.1016/j.diagmicrobio.2019.02.013

Kumar, S., Stecher, G., Li, M., Knyaz, C., and Tamura, K. (2018). MEGA X: Molecular evolutionary genetics analysis across computing platforms. *Mol. Biol. Evol.* 35 (6), 1547–1549. doi: 10.1093/molbev/msy096

Larsen, M. V., Cosentino, S., Rasmussen, S., Friis, C., Hasman, H., Marvig, R. L., et al. (2012). Multilocus sequence typing of total-genome-sequenced bacteria. *J. Clin. Microbiol.* 50 (4), 1355–1361. doi: 10.1128/jcm.06094-11

Li, X., Zhao, D., Li, W., Sun, J., and Zhang, X. (2021). Enzyme inhibitors: The best strategy to tackle superbug NDM-1 and its variants. *Int. J. Mol. Sci.* 23 (1) , 197. doi: 10.3390/ijms23010197

Lou, L., Zhang, P., Piao, R., and Wang, Y. (2019). Salmonella pathogenicity island 1 (SPI-1) and its complex regulatory network. *Front. Cell Infect. Microbiol.* 9, 270. doi: 10.3389/fcimb.2019.00270

Lv, J., Qi, X., Zhang, D., Zheng, Z., Chen, Y., Guo, Y., et al. (2016). First report of complete sequence of a bla(ndm-13)-harboring plasmid from an escherichia coli st5138 clinical isolate. *Front. Cell Infect. Microbiol.* 6, 130. doi: 10.3389/fcimb.2016.00130

Moellering, R. C.Jr. (2010). NDM-1–a cause for worldwide concern. *N Engl. J. Med.* 363 (25), 2377–2379. doi: 10.1056/NEJMp1011715

Nordmann, P., Poirel, L., Walsh, T. R., and Livermore, D. M. (2011). The emerging NDM carbapenemases. *Trends Microbiol.* 19 (12), 588–595. doi: 10.1016/j.tim.2011.09.005

Pan, Y. S., Liu, J. H., Hu, H., Zhao, J. F., Yuan, L., Wu, H., et al. (2013). Novel arrangement of the blaCTX-M-55 gene in an escherichia coli isolate coproducing 16S rRNA methylase. *J. Basic Microbiol.* 53 (11), 928–933. doi: 10.1002/jobm.201200318

Pérez-Vázquez, M., Sola Campoy, P.J., Ortega, A., Bautista, V., Monzón, S., Ruiz-Carrascoso, G., et al. (2019). Emergence of NDM-producing Klebsiella pneumoniae and Escherichia coli in Spain: Phylogeny, resistome, virulence and plasmids encoding blaNDM-like genes as determined by WGS. *J Antimicrob Chemother* 74 (12), 3489–3496. doi: 10.1093/jac/dkz366

Poirel, L., Bonnin, R.A., and Nordmann, P.. (2011). Analysis of the resistome of a multidrug-resistant NDM-1-producing Escherichia coli strain by high-throughput genome sequencing.. *Antimicrob Agents Chemother* 45 (9), 4224–4229. doi: 10.1128/aac.00165-11

Shrestha, B., Tada, T., Miyoshi-Akiyama, T., Shimada, K., Ohara, H., Kirikae, T., et al. (2015). Identification of a novel NDM variant, NDM-13, from a multidrug-resistant escherichia coli clinical isolate in Nepal. *Antimicrob. Agents Chemother.* 59 (9), 5847–5850. doi: 10.1128/aac.00332-15

Sidjabat, H. E., Seah, K. Y., Coleman, L., Sartor, A., Derrington, P., Heney, C., et al. (2014). Expansive spread of IncI1 plasmids carrying blaCMY-2 amongst escherichia coli. *Int. J. Antimicrob. Agents* 44 (3), 203–208. doi: 10.1016/j.ijantimicag.2014.04.016

Siguier, P., Perochon, J., Lestrade, L., Mahilon, J., and Chandler, M. (2006). ISfinder: The reference centre for bacterial insertion sequences. *Nucleic Acids Res.* 34, D32–36. doi: 10.1093/nar/gkj014

Sullivan, M. J., Petty, N. K., and Beatson, S. A. (2011). Easyfig: A genome comparison visualizer. *Bioinf. (Oxford England)* 27 (7), 1009–1010. doi: 10.1093/bioinformatics/btr039

Tacconelli, E., Carrara, E., Savoldi, A., Harbarth, S., Mendelson, M., Monnet, D. L., et al. (2018). Discovery, research, and development of new antibiotics: the WHO priority list of antibiotic-resistant bacteria and tuberculosis. *Lancet Infect. Dis.* 18 (3), 318–327. doi: 10.1016/s1473-3099(17)30753-3

Tagg, K. A., Iredell, J. R., and Partridge, S. R. (2014). Complete sequencing of IncI1 sequence type 2 plasmid pJIE512b indicates mobilization of blaCMY-2 from an IncA/C plasmid. *Antimicrob. Agents Chemother.* 58 (8), 4949–4952. doi: 10.1128/aac.02773-14

Seemann, T (2014). Prokka: rapid prokaryotic genome annotation. *Bioinf. (Oxford England)* 30 (14) 2068–2069. doi: 10.1093/bioinformatics/btu153.

Treangen, T. J., Ondov, B. D., Koren, S., and Phillippy, A. M. (2014). The harvest suite for rapid core-genome alignment and visualization of thousands of intraspecific microbial genomes. *Genome Biol.* 15 (11), 524. doi: 10.1186/s13059-014-0524-x

Wayne, P. (2021). Performance Standards for Antimicrobial Susceptibility Testing. *31st ed CLSI supplement M100*, (USA: Clinical and Laboratory Standards Institute).

Wick, R. R., Judd, L. M., Gorrie, C. L., and Holt, K. E. (2017). Unicycler: Resolving bacterial genome assemblies from short and long sequencing reads. *PloS Comput. Biol.* 13 (6), e1005595. doi: 10.1371/journal.pcbi.1005595

Wu, W., Feng, Y., Tang, G., Qiao, F., McNally, A., Zong, Z., et al (2019). NDM metallo-β-Lactamases and their bacterial producers in health care settings. *Clin. Microbiol. Rev.* 32 (2), e00115–18. doi: 10.1128/cmr.00115-18

Xu, X., Biswas, S., Gu, G., Elbediwi, M., Li, Y., and Yue, M. (2020). Characterization of multidrug resistance patterns of emerging salmonella enterica serovar rissen along the food chain in China. *Antibiotics (Basel)* 9 (10), 660. doi: 10.3390/antibiotics9100660

Yong, D., Toleman, M. A., Giske, C. G., Cho, H. S., Sundman, K., Lee, K., et al. (2009). Characterization of a new metallo-beta-lactamase gene, bla(NDM-1), and a novel erythromycin esterase gene carried on a unique genetic structure in klebsiella pneumoniae sequence type 14 from India. *Antimicrob. Agents Chemother.* 53 (12), 5046–5054. doi: 10.1128/aac.00774-09

Yoshida, C. E., Peter, K., Laing, C. R., Lingohr, E. J., Gannon, V. P., Nash, J. H. E., et al (2016). The salmonella *in silico* typing resource (sistr): An open web-accessible tool for rapidly typing and subtyping draft salmonella genome assemblies. *PloS One* 11 (1), e0147101. doi: 10.1371/journal.pone.0147101

Zankari, E., Hasman, H., Cosentino, S., Vestergaard, M., Rasmussen, S., Lund, O., et al. (2012). Identification of acquired antimicrobial resistance genes. *J. Antimicrob. Chemother.* 67 (11), 2640–2644. doi: 10.1093/jac/dks261

Zhao, Q. Y., Zhu, J. H., Cai, R. M., Zheng, X. R., Zhang, L. J., Chang, M. X., et al. (2021). IS26 is responsible for the evolution and transmission of bla(NDM)-harboring plasmids in escherichia coli of poultry origin in China. *mSystems* 6 (4), e0064621. doi: 10.1128/mSystems.00646-21

frontiers | Frontiers in Cellular and Infection Microbiology

TYPE Original Research
PUBLISHED 12 August 2022
DOI 10.3389/fcimb.2022.943735

OPEN ACCESS

EDITED BY
Milena Dropa,
Faculty of Public Health, University of São Paulo, Brazil

REVIEWED BY
Jose Ramos-Vivas,
Universidad Europea del Atlántico, Spain
Payam Behzadi,
Islamic Azad University, Iran
Eduardo Rodriguez-Noriega,
Civil Hospital of Guadalajara, Mexico

*CORRESPONDENCE
Siwei Wang
358031289@qq.com

†These authors have contributed equally to this work

SPECIALTY SECTION
This article was submitted to Clinical Microbiology, a section of the journal Frontiers in Cellular and Infection Microbiology

RECEIVED 14 May 2022
ACCEPTED 12 July 2022
PUBLISHED 12 August 2022

CITATION
Tian C, Xing M, Fu L, Zhao Y, Fan X and Wang S (2022) Emergence of uncommon KL38-OCL6-ST220 carbapenem-resistant *Acinetobacter pittii* strain, co-producing chromosomal NDM-1 and OXA-820 carbapenemases.
Front. Cell. Infect. Microbiol. 12:943735.
doi: 10.3389/fcimb.2022.943735

Emergence of uncommon KL38-OCL6-ST220 carbapenem-resistant *Acinetobacter pittii* strain, co-producing chromosomal NDM-1 and OXA-820 carbapenemases

Chongmei Tian[1†], Mengyu Xing[2†], Liping Fu[1], Yaping Zhao[1], Xueyu Fan[3] and Siwei Wang[4*]

[1]Department of Pharmacy, Shaoxing Hospital of Traditional Chinese Medicine Affiliated to Zhejiang Chinese Medical University, Shaoxing, China, [2]Department of Pharmacy, Affiliated Hangzhou First People's Hospital, Zhejiang University School of Medicine, Hangzhou, China, [3]Department of Clinical Laboratory, Quzhou People's Hospital, Quzhou Affiliated Hospital of Wenzhou Medical University, Quzhou, China, [4]Core Facility, Quzhou People's Hospital, Quzhou Affiliated Hospital of Wenzhou Medical University, Quzhou, China

Objective: To characterize one KL38-OCL6-ST220 carbapenem-resistant *Acinetobacter pittii* strain, co-producing chromosomal NDM-1 and OXA-820 carbapenemases.

Methods: *A. pittii* TCM strain was isolated from a bloodstream infection (BSI). Antimicrobial susceptibility tests were conducted *via* disc diffusion and broth microdilution. Stability experiments of bla_{NDM-1} and $bla_{OXA-820}$ carbapenemase genes were further performed. Whole-genome sequencing (WGS) was performed on the Illumina and Oxford Nanopore platforms. Multilocus sequence typing (MLST) was analyzed based on the Pasteur and Oxford schemes. Resistance genes, virulence factors, and insertion sequences (ISs) were identified with ABRicate based on ResFinder 4.0, virulence factor database (VFDB), and ISfinder. Capsular polysaccharide (KL), lipooligosaccharide outer core (OCL), and plasmid reconstruction were tested using *Kaptive* and PLACNETw. PHASTER was used to predict prophage regions. A comparative genomics analysis of all ST220 *A. pittii* strains from the public database was carried out. Point mutations, average nucleotide identity (ANI), DNA–DNA hybridization (DDH) distances, and pan-genome analysis were performed.

Results: *A. pittii* TCM was $ST220^{Pas}$ and $ST1818^{Oxf}$ with KL38 and OCL6, respectively. It was resistant to imipenem, meropenem, and ciprofloxacin but still susceptible to amikacin, colistin, and tigecycline. WGS revealed that *A. pittii* TCM contained one circular chromosome and four plasmids. The Tn*125* composite transposon, including bla_{NDM-1}, was located in the chromosome with 3-bp target site duplications (TSDs). Many virulence factors and the $bla_{OXA-820}$ carbapenemase gene were also identified. The stability assays revealed that

bla$_{NDM-1}$ and *bla*$_{OXA-820}$ were stabilized by passage in an antibiotic-free medium. Moreover, 12 prophage regions were identified in the chromosome. Phylogenetic analysis showed that there are 11 ST220 *A. pittii* strains, and one collected from Anhui, China was closely related. All ST220 *A. pittii* strains presented high ANI and DDH values; they ranged from 99.85% to 100% for ANI and from 97.4% to 99.9% for DDH. Pan-genome analysis revealed 3,200 core genes, 0 soft core genes, 1,571 shell genes, and 933 cloud genes among the 11 ST220 *A. pittii* strains.

Conclusions: The coexistence of chromosomal NDM-1 and OXA-820 carbapenemases in *A. pittii* presents a huge challenge in healthcare settings. Increased surveillance of this species in hospital and community settings is urgently needed.

KEYWORDS

Acinetobacter pittii, chromosomal NDM-1, OXA-820, Tn125, ST220, BSI

Introduction

The genus *Acinetobacter* is ubiquitous in diverse environments and clinical settings. The species belonging to the *Acinetobacter calcoaceticus–Acinetobacter baumannii* complex (ACB complex) including *A. calcoaceticus*, *A. baumannii*, *A. dijkshoorniae*, *A. lactucae*, *A. nosocomialis*, *A. pittii*, and *A. seifertii* are of great importance (Sarshar et al., 2021). Among these species, *A. pittii* is an important opportunistic pathogen that mainly causes healthcare-associated infections, including bloodstream infections (BSIs), pneumonia, and urinary tract infections (UTIs) (Pailhories et al., 2018; Chopjitt et al., 2021). One important contributing factor to these nosocomial infections is their ability to survive in stressful environments and, consequently, how difficult they are to eradicate (Chapartegui-Gonzalez et al., 2022). These difficult to eradicate strains then lead to nosocomial infections, particularly in immunocompromised patients in intensive care units (Ding et al., 2022).

Carbapenems are still the main antimicrobial agents for the treatment of infections with multidrug-resistant *Acinetobacter* spp., including *A. pittii* (Hirschberg and Kopple, 1989; Bassetti et al., 2021). However, reports of carbapenem resistance are increasing recently and have created a huge therapeutic challenge for clinicians (Bonnin et al., 2014; Wang et al., 2016). Comprehensive understanding of these resistance mechanisms has been accelerated by advancements in whole-genome sequencing (WGS) technologies (Javkar et al., 2021).

Carbapenem resistance in *A. pittii* is mainly caused by class D carbapenemases such as OXA-23, OXA-40, and OXA-58 and, in some cases, by metallo-b-lactamases (MBLs), including the New Delhi metallo-β-lactamase (NDM) (Kaase et al., 2014). NDM could mediate resistance to most β-lactam antimicrobial agents, including penicillins, cephalosporins, and carbapenems (Feng et al., 2021). NDM in *A. pittii* strains was relevant to sporadic human infection with high mortality rates and hospital transmissions in various countries, and serves as a potential reservoir for the *bla*$_{NDM-1}$-carrying plasmids. However, co-harboring of *bla*$_{NDM-1}$ and *bla*$_{OXA-820}$ in the chromosome of *A. pittii* has not been reported until now.

Apart from resistance, virulence also plays a key role in environmental persistence and the epidemic spread of disease (Chin et al., 2018). However, *A. baumannii* is commonly considered to be a low virulent pathogen (Chapartegui-Gonzalez et al., 2021), and studies regarding the virulence attributes of *A. pittii* are rarer (Cosgaya et al., 2019). Recently, a study from France described one case of *A. pittii* community-acquired pneumonia with a low virulence profile (Larcher et al., 2017). Considering the fact that various virulence factors can be found in *A. pittii* strains, studying its virulence and discussing its pathogenesis are still crucial in the pursuit of treating patients.

In this study, we investigate the characteristics of one sequence of type 220 A. *pittii* strain isolated from a bloodstream infection (BSI) in China. To the best of our knowledge, this is the first description of an ST220 *A. pittii* strain in which co-harboring *bla*$_{NDM-1}$ and *bla*$_{OXA-820}$ carbapenemase genes resided on the chromosome. A combination of Illumina and MinION whole-genome sequencing was conducted to provide comprehensive insight into the genomic and chromosome structure features.

Materials and methods

Flow chart indicating the process of this study

A flow chart (Figure 1) was built to show all the experiments and employed procedures of this study using CmapTools v6.04 (https://cmap.ihmc.us) (Behzadi and Gajdacs, 2021). Based on the different parts of the experiments, sequencing, and bioinformatic sections, this study was divided into two parts (Ranjbar et al., 2017).

Bacterial isolation, identification, and characterization of *A. pittii* isolate

A. pittii TCM strain was isolated from a BSI during routine diagnostic analysis on 19 January 2018 in Hangzhou, China. Isolate identification to species level was conducted by matrix-assisted laser desorption ionization–time of flight mass spectrometry (MALDI-TOF MS, Bruker Daltonik GmbH, Bremen, Germany) and confirmed by 16S rRNA gene-based sequencing (Nagy et al., 2009; Nagy et al., 2012).

Antimicrobial susceptibility testing

Minimum inhibitory concentrations (MICs) for *A. pittii* TCM strain against multiple antibiotics were tested by using disk diffusion and broth microdilution. It interpreted breakpoints for *Acinetobacter* spp. according to the recommendations from the Clinical and Laboratory Standards Institute (CLSI), 2021 guidelines and European Committee on Antimicrobial Susceptibility Testing (EUCAST), 2021. Because there is no tigecycline breakpoint for *Acinetobacter*, MIC was interpreted according to the guidelines of EUCAST for *Enterobacterales* (with MIC breakpoint value ≤0.5 mg/L denoting susceptibility and >0.5 mg/L denoting resistance). The antibiotic disks used in this study included imipenem (IPM, 10 μg, Oxoid, Cheshire, UK), meropenem (MEM, 10 μg, Oxoid, Cheshire, UK), Amikacin (AMI, 30 μg, Oxoid, Cheshire, UK), and ciprofloxacin (CIP, 5 μg, Oxoid, Cheshire, UK) in a Mueller-Hinton agar (MHA) culture medium (Oxoid, Cheshire, UK). In addition to the antibiotics mentioned above, colistin (COL, Sigma-Aldrich, St. Louis, MO, USA) and tigecycline (TGC, Sigma-Aldrich, St. Louis, MO, USA) were also investigated using broth microdilution. *Escherichia coli* ATCC 25922 served as the quality control strain.

Stability experiments of bla_{NDM-1} and $bla_{OXA-820}$ carbapenemase genes

A. pittii TCM strain was grown overnight in three separate cultures at 37°C in 2 ml of Luria broth (LB) without antibiotics, followed by serial passage of 2 μl of overnight culture into 2 ml of LB daily, yielding 10 generations each lasting 7 days (Lv et al., 2020). On the last day, samples were collected and streaked on antibiotic-free MHA plates. Colonies were selected randomly, and the presence of bla_{NDM-1} and $bla_{OXA-820}$ was confirmed *via*

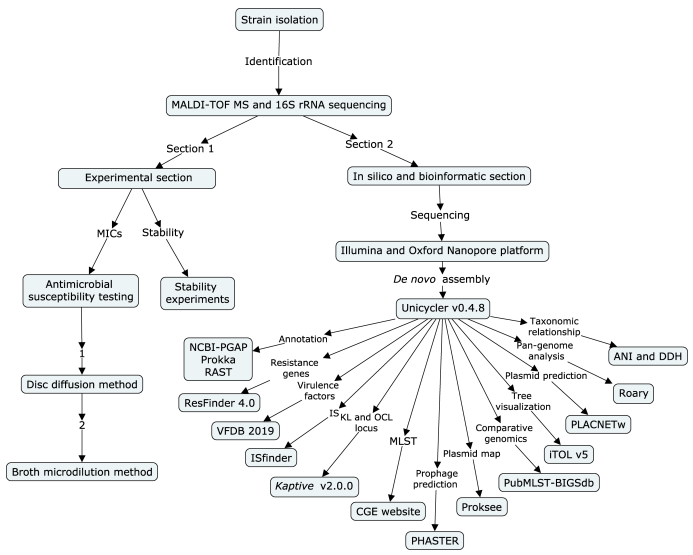

FIGURE 1
Flow chart of all experiments and employed procedures in this study. The flow chart was built using CmapTools v6.04. It is divided into an experimental section and a bioinformatic section.

PCR. Primers were designed based on the full-length sequences of bla_{NDM-1} and $bla_{OXA-820}$ on the *A. pittii* TCM chromosome (GenBank accession number: *CP095407*) using Snapgene (Dotmatics, USA) BLAST (NCBI, USA) 2.3.2 and BLAST software. Primers are listed in Table S1.

Whole-genome sequencing and bioinformatics analysis

Genomic DNA was extracted from the *A. pittii* TCM strain using a Qiagen minikit (Qiagen, Hilden, Germany) in accordance with the manufacturer's recommendations. Whole-genome sequencing was performed using both the Illumina HiSeq platform (Illumina, San Diego, CA, USA) and the Oxford Nanopore MinION platform (Nanopore, Oxford, UK). *De novo* assembly of the reads of Illumina and MinION was constructed using Unicycler v0.4.8 (Wick et al., 2017). The prediction and annotation of genome sequences were performed using the National Center for Biotechnology Information's (NCBI) Prokaryotic Genome Annotation Pipeline (PGAP) updated in 2018 (Tatusova et al., 2016); Prokka v.1.13 (Seemann, 2014) and rapid annotations were done using the subsystems technology (RAST) server (Overbeek et al., 2014). Antimicrobial resistance genes were identified using the ABRicate v0.8.13 program (https://github.com/tseemann/abricate) based on ResFinder 4.0 updated in 2020 (http://genomicepidemiology.org/) (Zankari et al., 2012; Bortolaia et al., 2020). The point mutations were identified using the fIDBAC server and manual comparison (Liang et al., 2021). Bacterial virulence factors were identified through the virulence factor database updated in 2019 (VFDB 2019, http://www.mgc.ac.cn/VFs/) (Liu et al., 2022). Insertion sequences (ISs) were identified using the Isfinder updated in 2022 (Siguier et al., 2006). Capsular polysaccharide (K locus, KL) and lipooligosaccharide (OC locus, OCL) were tested using *Kaptive* v2.0.0 updated in 2021 (Wyres et al., 2020; Lam et al., 2022). Multilocus sequence typing (MLST) was performed *via* the Center for Genomic Epidemiology (CGE) website updated in 2020 (https://cge.cbs.dtu.dk/services/MLST/). The Phage Search Tool (PHASTER) updated in 2016 was used for the prediction of bacteriophages (Zhou et al., 2011; Arndt et al., 2016).

Plasmid reconstruction was conducted using the PLACNETw tool (Vielva et al., 2017). Plasmid structure was visualized using Proksee (https://proksee.ca/) (Stothard et al., 2019). Comparative genomics analysis of all 11 ST220 *A. pittii* strains from the PubMLST database (https://pubmlst.org/) was further performed using the Bacterial Isolate Genome Sequence Database (BIGSdb) (Jolley et al., 2018). The generation tree file was visualized using the Interactive Tree of Life updated in 2021 (iTOL v5, https://itol.embl.de/) (Letunic and Bork, 2021). Default parameters were used for all software packages.

The taxonomic relationships among these isolates were further evaluated using the average nucleotide identity (ANI) (Luis and Konstantinos, 2016) and DNA–DNA hybridization (DDH) distances (Meier-Kolthoff et al., 2013), with *A. pittii* HUMV-6483 as the reference strain and species positive control (Chapartegui-Gonzalez et al., 2017). Pan-genome analysis was performed *via* the Roary software (Page et al., 2015) and visualized using Phandango (https://jameshadfield.github.io/phandango/#/main).

Results

Genome annotations and subsystem categories

The genome and protein-coding sequences (CDS) were annotated and predicted using PGAP and RAST. According to PGAP annotation, there are 4,330 genes, of which 4,102 are protein-coding genes, 131 are pseudogenes, and the remaining 97 are predicted RNA-coding genes, composed of 74 tRNAs, 18 rRNAs and 5 ncRNAs.

In contrast to PGAP, 4,280 genes that belonged to 313 subsystems were annotated using RAST. The subsystem each CDS was classified into is shown in Figure 2. Most of them belonged to metabolism (443) and amino acids and derivatives (307). Additionally, 45 CDS were sorted into virulence, disease, and defense categories.

Susceptibility to antimicrobial agents

The antimicrobial susceptibility testing results revealed the *A. pittii* TCM strain possessed a multidrug-resistant (MDR) profile when both CLSI and EUCAST breakpoints were used. The inhibition zone diameters of imipenem, meropenem, ciprofloxacin, and amikacin were 17 mm (R), 13 mm (R), 7 mm (R), and 21 mm (S), respectively. The broth microdilution results showed that the MICs of imipenem and meropenem were 8 and 16 mg/L, respectively. *A. pittii* TCM strain also exhibited a resistance to ciprofloxacin (32 mg/L). In our case, *A. pittii* TCM was still susceptible to amikacin (2 mg/L), colistin (1 mg/L), and tigecycline (0.5 mg/L). The susceptibility of the *A. pittii* TCM strain against the antimicrobial agents above was consistent when the isolate was classified as resistant or susceptible using CLSI and EUCAST breakpoints.

Antimicrobial resistance determinants, point mutations, and virulence profiles

Analysis of the genome of the *A. pittii* TCM strain revealed that in addition to co-harboring bla_{NDM-1} and $bla_{OXA-820}$, a series of genes conferring resistance to β-lactams (blaADC-43), bleomycin (*ble-MBL*), streptomycin [*ant(2")-Ia*], sulfonamides

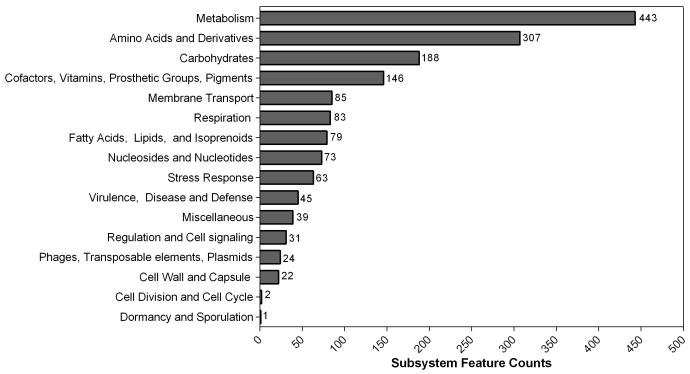

FIGURE 2
Counts of protein-coding sequences distributed in each subsystem feature based on RAST annotation. The number of each subsystem category is shown on the right of each column.

(*sul2*), and macrolide [*msr(IE)* and *mph(E)*] were also identified (Table 1). Regarding fluoroquinolones resistance, serine by lysine at position 81 (S81L) in the *gyrA* (DNA gyrase) was found. However, no *pmrAB* and *lpxACD* mutations were identified in this strain. Based on these results, the genotype and the phenotype were consistent.

Many virulence factors were identified in the *A. pittii* TCM strain. One was the outer membrane protein *ompA* gene *pga* operon (*pgaABCD*) encoding poly-β-1,6-N-acetyl-d-glucosamine (PNAG), which is important for biofilm development. Others were *csu* operon encoding Csu pili and *pbpG* encoding PbpG for serum resistance—a quite important two-component regulatory system *bfmRS* involved in Csu expression. Then, finally, there were *lpxABC* and *lpxL* encoding lipopolysaccharide (LPS) and many genes (*bauABCDEF*, *basABCDEFGHIJ*, and *barAB*) encoding Acinetobactin for iron uptake.

Stability of $bla_{\text{NDM-1}}$ and $bla_{\text{OXA-820}}$

The stability assays revealed that $bla_{\text{NDM-1}}$ and $bla_{\text{OXA-820}}$ were quite stable even after 70 samples under antibiotics-free condition. These results were confirmed with PCR (Supplementary Figure 1).

Multilocus sequence typing, lipooligosaccharide outer core, and capsular polysaccharide

Based on the Pasteur MLST scheme, the *A. pittii* TCM strain was typed into a sequence type 220 (*cpn60*-45, *fusA*-20, *gltA*-44, *pyrG*-16, *recA*-20, *rplB*-29, *rpoB*-20). According to the Oxford MLST schemes, it belonged to ST1818 (*cpn60*-52, *gdhB*-141, *gltA*-62, *gpi*-247, *gyrB*-129, *recA*-7, *rpoD*-10). The specific positions of all housekeeping genes are shown in Figure 3A.

Kaptive showed that the *A. pittii* TCM strain contains OC locus 6 (OCL-6), matching the 98.98% coverage of reference sequence with 80.55% nucleotide identity. The K locus in the *A. pittii* TCM strain is KL38. It matches 100% of the locus with an overall nucleotide identity of 96.89%.

Chromosome and Tn*125* composite transposon structure

The hybrid assembly of Illumina and MinION reads showed that the *A. pittii* TCM strain had a 4,250,902-bp circular chromosome (Figure 3A) with guanine cytosine (GC) content of 39.00% (Table 1).

TABLE 1 Molecular characterization of genomes from the *A. pittii* TCM strain.

Genome	Size(bp)	GCcontent	Resistancegenes	Accession numbers
chromosome	4,250,902	39.00%	$bla_{\text{NDM-1}}$, $bla_{\text{OXA-820}}$, blaADC-43, *ble-MBL*,	*CP095407*
pTCM-1	84,108	39.54%	sul2	*CP095408*
pTCM-2	11,346	33.29%	ND	*CP095409*
pTCM-3	8,505	35.49%	msr*(E)*, mph*(E)*	*CP095410*
pTCM-4	6,078	39.19%	*ant(2")-Ia*	*CP095411*

ND, not detected.

The bla_{NDM-1} gene cluster was arranged sequentially as IS*Aba125*, bla_{NDM-1}, and *ble-MBL* elements (Figure 3B). The bla_{NDM-1} gene was embedded in the composite transposon Tn*125*, bracketed by two copies of the IS*Aba125* orientated in the same direction, and flanked by 3-bp (AAG) possible target site duplications (TSDs). Moreover, the composite transposon structure of Tn*125* with another 3-bp (AAA) TSD in the plasmid pDETAB2 (GenBank accession number: CP047975), which was isolated from a rectal swab sample in China, is identical to this Tn*125* with a percentage of 99.99% (Figure 3B).

Plasmid prediction and genetic analysis of plasmids

To identify the contigs that may belong to a plasmid, the PLACNETw software was used based on the Illumina sequencing data. Result showed that the *A. pittii* TCM strain had a chromosome of 3.9 Mb and three predicted plasmids with 20.22, 11.45, and 6.27 kb, respectively (Figure 4).

We further assembled the complete genome with both short-read Illumina sequencing data and long-read Oxford Nanopore sequencing data. To visualize the plasmid maps of the *A. pittii* TCM strain, a member of the CGView (Circular Genome Viewer) software family, Proksee, was utilized for generating high-quality, navigable maps of circular genomes. This tool is a Java program and originally intended for bacterial genomes. In our case, four plasmids were identified in the *A. pittii* TCM strain, namely pTCM-1 to pTCM-4, with sizes between 6,078 and 84,108 bp and GC contents ranging from 33.29% to 39.54% (Table 1). Different kinds of resistance genes were carried by pTCM-1, pTCM-3, and pTCM-1 and showed in the plasmid maps (Figures 5A, C, D). However, pTCM-2 does not carry any resistance genes (Figure 5B).

Prophage regions in the chromosome

Prophage regions were predicted by the PHASTER tool. The results showed six intact, four questionable, and two incomplete regions in the chromosome (Figure 6A). Regions 3, 5, 7, 10, 11, and 12 were 71.5, 39.1, 50.8, 43.4, 22.5, and 30.8 kb long with GC contents of 39.27%, 40.92%, 38.10%, 39.60%, 38.25%, and 40.27%, respectively. Based on the PHASTER

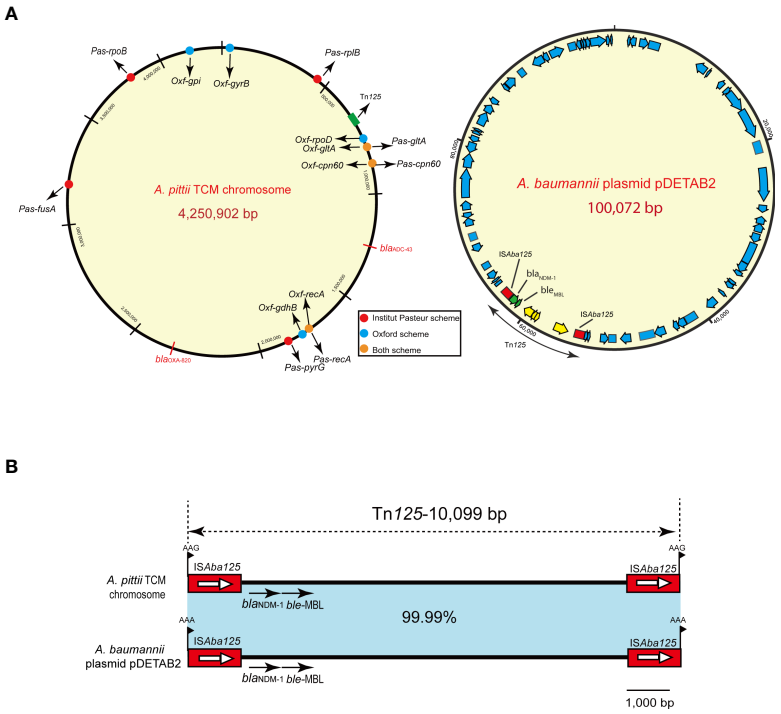

FIGURE 3
A. pittii TCM strain chromosome circular map and Tn*125* composite transposon structure. **(A)** Circular map of the *A. pittii* TCM chromosome. Housekeeping genes of Pasteur and Oxford schemes are indicated by various colors. On the right panel of **(A)**, *A. baumannii* plasmid pDETAB2 and Tn*125* composite transposon structure are shown. **(B)** Structure of Tn*125* composite transposon compared with plasmid pDETAB2 (CP047975). Horizontal arrows represent the direction of the genes, with black arrows indicating resistance genes. Light blue shades indicate regions with 99.99%–100% identity. Target site duplication (TSD) is shown as flag in black.

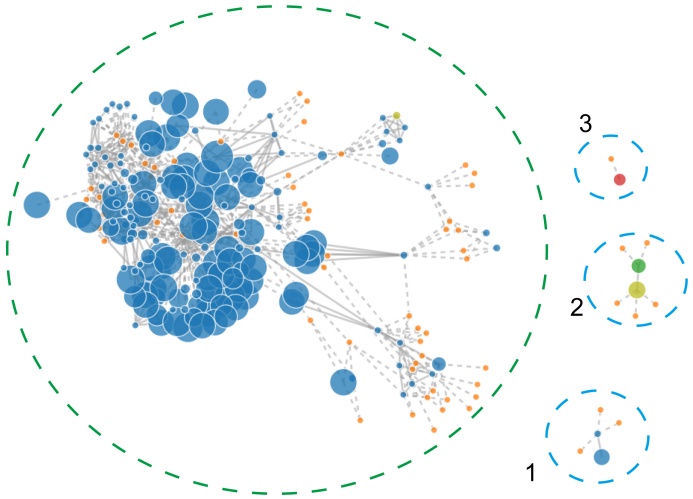

FIGURE 4
PLACNETw was used for plasmid reconstruction from the A. pittii TCM strain draft genomes. The contigs node's sizes are proportional to their length. Blue nodes represent contigs of *A. pittii* TCM genomes, and orange nodes indicate the reference genomes. Contigs nodes' sizes are proportional to their length. Color nodes represent contigs with special function proteins: yellow-green (replication initiation protein), red (relaxases), and green represents both. The green-dotted line shows the chromosome and the three blue-dotted lines show the plasmids.

tool, all six regions above were predicted to be intact due to having scores of >90. The gene function of the six intact prophage regions, known to be essential for phage activity such as specifying attachment, structural components, phage integration, and cell lysis were identified (Figure 6B). In addition, regions 1, 6, 8, and 9 were classified as questionable due to their scores of 70 or 80. However, there were also two incomplete prophage regions with scores of 20 and 30, respectively.

Comparative genomics analysis of all ST220 *A. pittii* strains in public database

We further queried the PubMLST database, and the information of 10 other ST220 *A. pittii* strains was obtained. Strains were collected from several different sources, including blood, sputum, abscesses, and the upper respiratory tract of patients and environmental sinks (Figure 7). Their hosts were isolated in various cities in the USA, Japan, China, and Thailand. Comparative genomics analysis showed that there is a very close relationship between the *A. pittii* strain YB45 and the *A. pittii* TCM strain used in this study. Moreover, the *A. pittii* AP864 and AP984 strains collected from Thailand were of the same branch. Furthermore, three strains isolated from Chengdu in China, namely WCHAP100010, WCHAP100007, and WCHAP100022, were closely related.

Taxonomic relationship and pan-genome analysis

Public genomes were reannotated using Prokka, and then a gene presence/absence analysis was performed on the basis of the annotated protein sequences. As shown in Figure 8A, 3,200 core genes, 0 soft core genes, 1,571 shell genes, and 933 cloud genes were defined. The presence/absence of all the genes were further visualized with the phylogenetic tree (Figure 8B). From that tree, the close relationship between *A. pittii* strain YB45 and *A. pittii* TCM strain was also observed.

To further compare the taxonomic relationship among all ST220 *A. pittii* strains and *A. pittii* HUMV-6483 reference strain, both ANI and DDH distances were calculated. All ST220 *A. pittii* strains presented high ANI and DDH values, ranging from 99.85% to 100% for ANI and from 97.4% to 99.9% for DDH (Figure 8C). Furthermore, the reference strain averaged 96.47% for ANI and 70.9% for DDH among the isolates used in this study (Figure 8C).

Discussion

The presence of carbapenemase-producing *Acinetobacter* spp., including *A. baumanii*, *A. lwoffii*, and *A. pittii*, has become dominant in several countries, and they are increasingly being considered quite important nosocomial pathogens (Wisplinghoff et al., 2012; Mohd Rani et al., 2017;

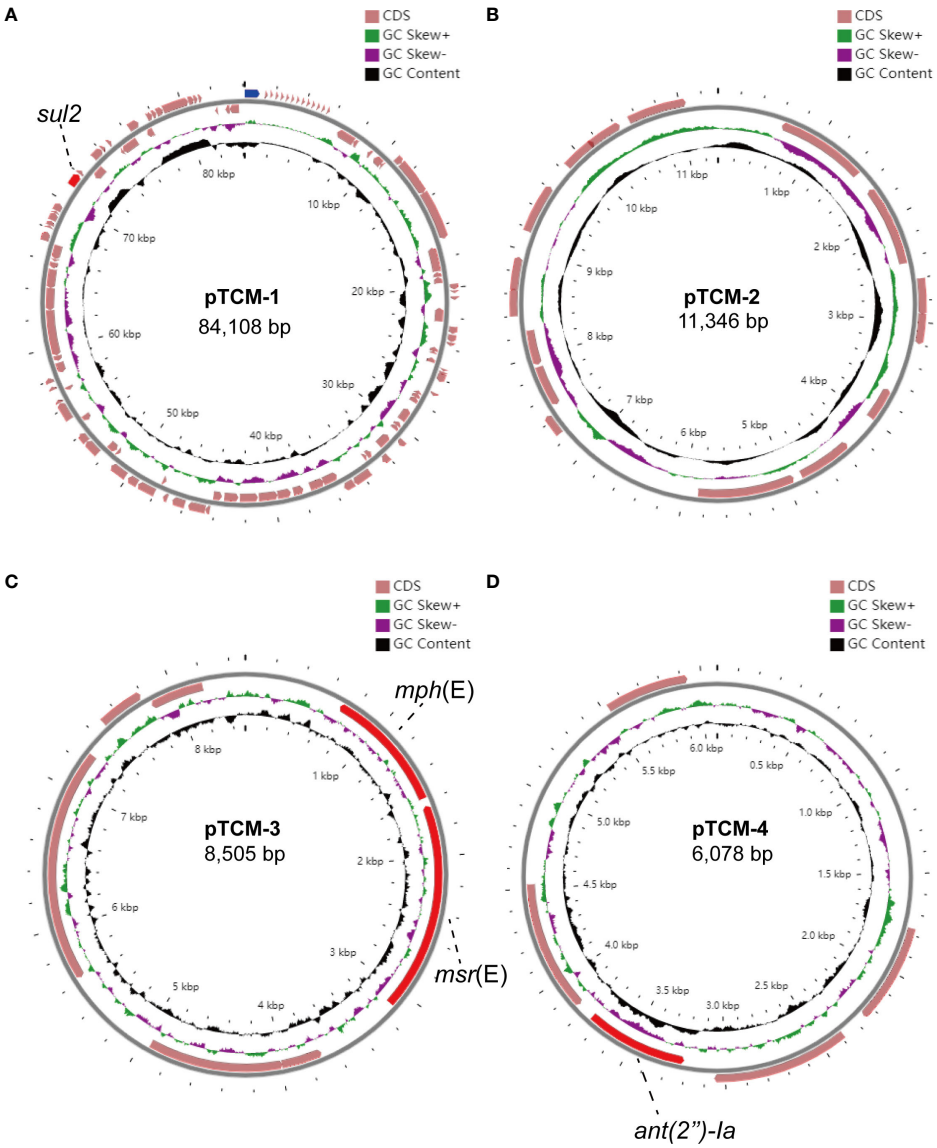

FIGURE 5
Four circular plasmid maps in *A. pittii* TCM strain. Red arrows indicate the antimicrobial resistance genes. Pink arrows indicate the other open reading frames (ORFs). Antimicrobial resistance genes carried by the plasmid are labeled. **(A)** Circular plasmid map of pTCM-1. **(B)** Circular plasmid map of pTCM-2. **(C)** Circular plasmid map of pTCM-3. **(D)** Circular plasmid map of pTCM-4.

Mulani et al., 2019; Kiyasu et al., 2020). Although carbapenemases (especially for OXA-23, OXA-24/40, OXA-58) are widely disseminated among *Acinetobacter* species, few data are available for pathogenic *A. pittii* strains harboring carbapenemase except for sporadic reports (Sung et al., 2015).

Metallo-ß-lactamases (MBLs) (e.g., NDM-1) could neutralize the activity of ß-lactam antibiotics *via* hydrolyzing amide bonds. The spread of MBLs worldwide is the result of the lack of appropriate inhibitors and the transfer of the resistance genes that are located in the composite transposon structure. Hence, MBLs are known to support bacterial survival as powerful weapons against antibiotics (Behzadi et al., 2020). In previous studies, Yang et al. (2012) found MBL-producing *A. pittii* (NDM-1-positive) disseminated predominantly within the ICU in China. However, limited data and knowledge concerning NDM-1-positive *A. pittii*-causing BSI have been acquired to date in China (Yang et al., 2021). Authors' study, one carbapenem-resistant *A. pittii* strain from BSI was isolated. To promote understanding regarding the genomic function of our *A. pittii* strain, the RAST software was utilized to classify the different CDS into subsystems according to their function (Aziz et al., 2008). Consistent with other published studies, the majority of

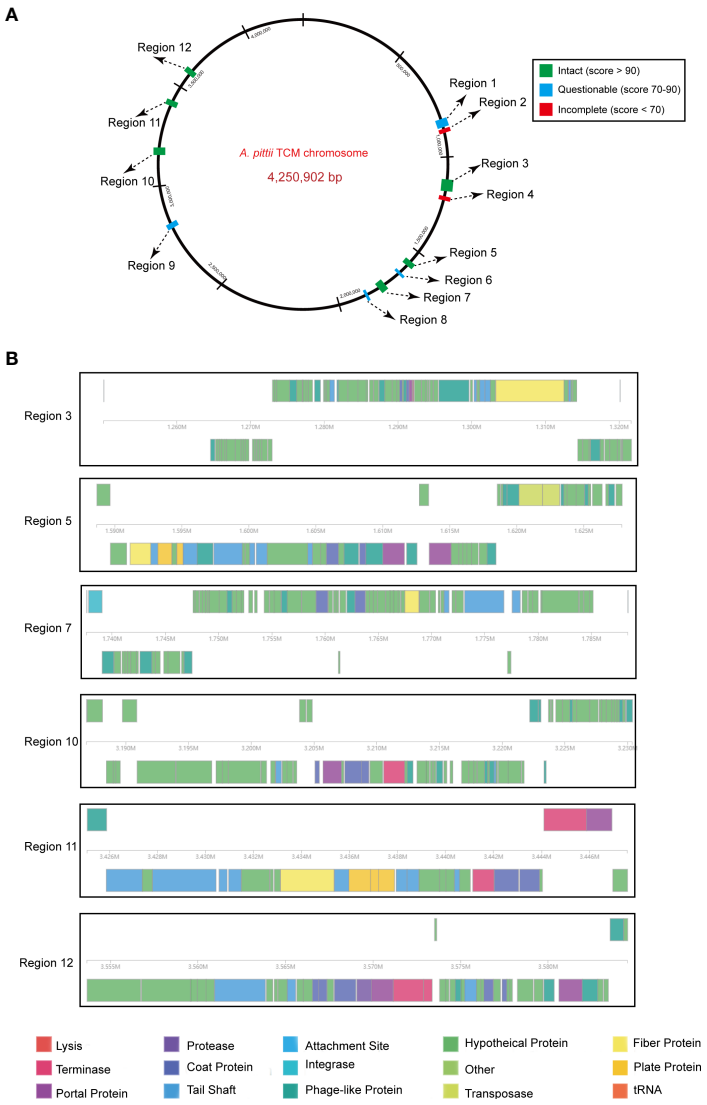

FIGURE 6
Predicted prophage regions within the *A. pittii* TCM chromosome. **(A)** A total of 12 prophage regions are positioned in the chromosome. Green means the intact prophage regions (score >90), blue means the questionable prophage regions (score 70–90), and red means the incomplete prophage regions (score <70). **(B)** Structure of six intact prophage regions. Genes are colored based on predicted functions.

the genes belong to "Metabolism," followed by features with cellular components (amino acids, carbohydrates) (Chapartegui-Gonzalez et al., 2022).

Regarding the carbapenem-resistant *A. pittii* isolates, an outbreak of ST63 clone that carried a 45-kb bla_{NDM-1}-bearing plasmid was reported in an ICU in China (Yang et al., 2012). In addition, Chopjitt et al. (2021) reported the ST63, ST396, and ST220 carbapenem-resistant *A. pittii* strains from the perspective of clinical characteristics and genome-based single nucleotide polymorphism (SNP). However, no studies completely clarify the chromosome and plasmid structures of bla_{NDM-1}-positive carbapenem-resistant *A. pittii* strain. Few studies highlight the importance of mobile genetic elements (MGEs) in *A. pittii*. MGEs, including insertion sequences (ISs), integrons, and transposons, play a particularly important role in the resistance gene transfer between plasmid and chromosomes (Gorbunova et al., 2021). One study from Chapartegui-González et al. (2022) revealed that various ISs were found in all five *A. pittii* isolates. In particular, IS*Aba125* was found in a HUMV0315 *A. pittii* strain that was collected from Santander, Spain. In the current study, we, for the first time, found bla_{NDM-1} in the chromosome that mediated two IS*Aba125*-based Tn*125* composite transposons, highlighting the importance of IS*Aba125*-mediated transfer of resistance determinants. The

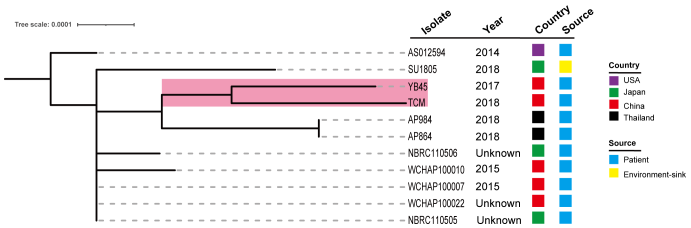

FIGURE 7
Phylogenetic analysis of 11 ST220 *A. pittii* strains based on the public database. The tree was built *via* the PubMLST database and visualized with iTOL v5. Isolates name, isolation date, country, and collection sources are shown in each isolate. The filled boxes reveal the different countries or sources based on different colors. The PubMLST ID and GenBank accession numbers of 10 ST220 *A. pittii* strains are shown as follows: AS012594 (ID: 6032, GenBank accession number: VLVU00000000), SU1805 (ID: 5840, GenBank accession number: JACWEV000000000), YB45 (ID: 5339, GenBank accession number: CP029610), AP984 (ID: 5927, GenBank accession number: JAEHOG000000000), AP864 (ID: 5924, GenBank accession number: JAEFCW000000000), NBRC110506 (ID: 5858, GenBank accession number: BBTY00000000), WCHAP100010 (ID: 5991, GenBank accession number: SGTJ00000000), WCHAP100007 (ID: 6001, GenBank accession number: SGTM00000000), WCHAP100022 (ID: 6006, GenBank accession number: SGSZ00000000), and NBRC110505 (ID: 5861, GenBank accession number: BBTX00000000).

genetic structure of Tn*125* composite transposon was highly related (99.99% identity) to a previously described $bla_{\text{NDM-1}}$-$bla_{\text{OXA-58}}$-harboring plasmid from an *A. baumannii* strain isolated from the rectal swab of a hospitalized patient in an ICU in Hangzhou, China (Liu et al., 2021a). Considering that these two strains had the same geographic location, there is a possibility that Tn*125* transfers between the chromosomes and plasmids of two species *via* one translocation event. In addition to resistance gene transfer mediated by composite transposons, XerC, and XerD, site-specific tyrosine recombinases (XerC/D-like sites) and a 28-bp recombination site *dif*, could play key roles in the resistance genes transfer of $bla_{\text{OXA-40-like}}$, $bla_{\text{OXA-499}}$, and $bla_{\text{OXA-58}}$ (Cameranesi et al., 2018). *A. pittii* could be a crucial source of resistant genes and lead to the dissemination of resistant genes among species.

The degree of *A. pittii* virulence remains poorly understood. *ompA*, *pgaABCD*, and *bfmRS* are identified in our strain, which are able to promote adhesion and biofilm formation (Geisinger et al., 2018). This is a crucial pathogenic feature of many bacteria, facilitating colonization on the surface of biological materials, leading to further medical device-associated infections and promoting the evasion of the host immune system *in vivo* (Gordon and Wareham, 2010; Harding et al., 2018). More importantly, many virulence factors encoding Acinetobactin were found. Conde-Pérez et al. (2021) uncovered the essential role of Acinetobactin in the pathogenicity. Additionally, OCL and KL gene clusters, which also represent the virulence factor and are responsible for the biosynthesis of the outer core of lipooligosaccharide and capsules, are potentially useful epidemiological markers and may perform a key role in vaccine and biomarker development (Wyres et al., 2020). In our study, KL38 had a quite high identity. Whether all $bla_{\text{NDM-1}}$-positive carbapenem-resistant *A. pittii* strains belong to this kind of KL type still needs further study. There are 12 prophage regions identified in the chromosome. A previous study from Krahn et al. (2016) demonstrated that transposon Tn*125*, which embedded the $bla_{\text{NDM-1}}$ gene, could transfer *via* phage-mediated transduction within the species of *A. baumannii*. Thus, prophages may play a key role in the horizontal gene transfer (HGT) of carbapenems resistance genes, such as $bla_{\text{NDM-1}}$ and $bla_{\text{OXA-23}}$ (Krahn et al., 2016; Abouelfetouh et al., 2022). Another study from Loh et al. (2020) in China showed a wide variation in the number of prophages in *A. baumannii* genomes. Several phages carry carbapenems resistance genes, including $bla_{\text{NDM-1}}$ and $bla_{\text{OXA-23}}$, demonstrating the importance of lysogenic phages in the transfer of resistance genes. However, an important limitation of our study is that the activities of these prophages were not confirmed through induced experiments for prophages.

Acinetobacter spp. have a relatively small genome size compared to the other Gram-negative pathogens Therefore, there are fewer CDS (Chapartegui-Gonzalez et al., 2021; Chapartegui-Gonzalez et al., 2022). We further analyzed the genome features of all ST220 *A. pittii* strains based on the public database, in particular with the NDM-1 type carbapenemase. Zhang and Zhou (2018) reported the draft genome sequence of an NDM-1-, OXA-421-, and AmpC-producing ST220 *A. pittii* YB45 strain in Anhui Province, China. Based on the comparative genomics analysis, there is a very close relationship between *A. pittii* strain YB45 and *A. pittii* TCM strain. These strains may be spreading among different provinces in China, and they require early recognition and detection of carbapenemases. All AP864, AP984, and SU1805 isolates collected from Thailand and Japan carried NDM-1. Therefore, we speculated that carbapenem-resistant *A. pittii* strains, which were isolated in Asia, seemed to be more likely to harbor NDM-1. These genome data might facilitate further understanding of the genomic feature of NDM-1-positive *A. pittii* strains.

This study provides a comprehensive pan-genome analysis. Among the analyzed strains, all ST220 strains have high ANI

10.3389/fcimb.2022.943735

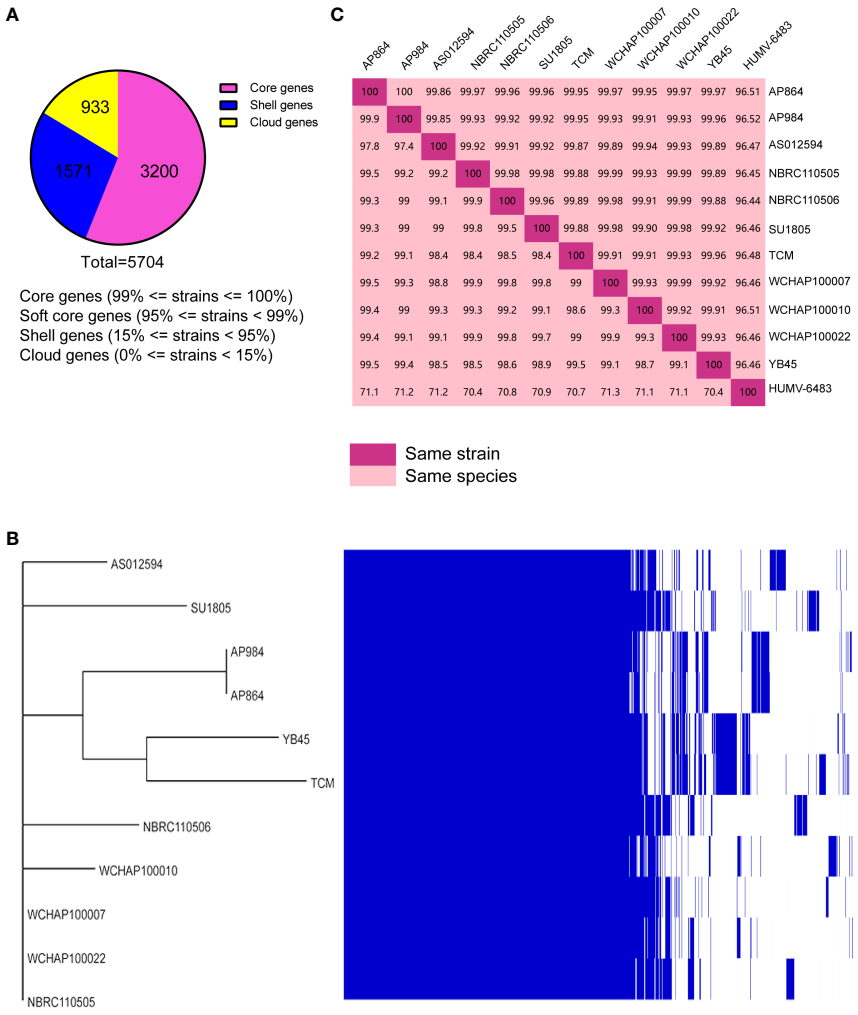

FIGURE 8
Pan-genome analysis of ST220 *A. pittii* strains using Roary. **(A)** Number of genes belonging to the core, the shell, or the cloud is shown as a pie chart. **(B)** Matrix of the presence/absence of genes generated with Roary and the phylogenetic tree of 11 ST220 *A. pittii* strains is also shown. The figure was visualized using Phandango. **(C)** Matrix distance values among *A. pittii* strains. The upper part shows average nucleotide identity (ANI) values; the lower part indicates DNA–DNA hybridization (DDH) values. A reference strain, namely *A. pittii* HUMV-6483, is also included to confirm the bacterial species. The threshold to belong to the same species is considered to be 95% for ANI values, whereas >70% is the threshold for DDH values. Diagonal 100% means the same strain.

and DDH values, suggesting a close genetic relationship. The numerous genes on the core genome compared with the pan-genome also highlight the similarity among these sequenced strains. In other studies, pan-genome and core-genome sizes vary and possess pan-genome values between 3,000 and 6,500, similar to our genome data (Chapartegui-Gonzalez et al., 2021).

It is worth noting that current treatment options for carbapenem-resistant Gram-negative infections are limited and need new antibiotics (Bassetti et al., 2021; Tamma et al., 2021). Novel therapeutic options against resistant microorganisms such as cefiderocol, GSK-3342830, eravacycline, WCK 5153 with sulbactam, apramycin, and bacteriophage therapy should be considered to overcome the problematic Gram-negative pathogens (Isler et al., 2019). Additionally, high-dose sulbactam combined with either levofloxacin, minocycline, or tigecycline may promote superior rates of clinical improvement and clinical cure, especially for multidrug-resistant or extensively drug-resistant *Acinetobacter* spp. (Liu et al., 2021b).

Conclusion

This study is the first to report co-producing chromosomal NDM-1 and OXA-820 carbapenemases in *A. pittii* collected

from a BSI patient in China. This discovery highlights the clinical importance of this species. The complete structures of the chromosome and plasmids were analyzed. Tn*125* composite transposon could transfer *via* a translocation event, and this species also may disseminate among different provinces in China. Therefore, surveillance is warranted, and early detection of carbapenemase genes is recommended to avoid a major spread in healthcare settings, especially in the ICU.

Data availability statement

The complete sequences of the chromosome of *A. pittii* TCM strain and plasmids pTCM-1, pTCM-2, pTCM-3, and pTCM-4 have been deposited in GenBank under accession numbers CP095407-CP095411, respectively.

Ethics statement

This study was approved by the local Ethics Committees of the Hospital with a waiver ofinformed consent due to this study mainly focused on bacterial genome and the retrospective nature of the study.

Author contributions

CT and MX designed the experiments, analyzed the data, and wrote the paper. CT, MX, LF, and YZ performed the majority of the experiments. MX isolated the bacteria. XF and SW supervised this study and reviewed and edited the paper. All authors read and approved the final version of the manuscript.

Funding

This work was supported by the Medical Health Science and Technology Project of Zhejiang Provincial Health Commission (2022RC278) and the Natural Science Foundation of Zhejiang Province (LGF20H300003, LGF20H280002, and LQ19H160002).

Conflict of interest

The authors declare that the research was conducted in the absence of any commercial or financial relationships that could be construed as a potential conflict of interest.

Publisher's note

All claims expressed in this article are solely those of the authors and do not necessarily represent those of their affiliated organizations, or those of the publisher, the editors and the reviewers. Any product that may be evaluated in this article, or claim that may be made by its manufacturer, is not guaranteed or endorsed by the publisher.

Supplementary material

The Supplementary Material for this article can be found online at: https://www.frontiersin.org/articles/10.3389/fcimb.2022.943735/full#supplementary-material

SUPPLEMENTARY FIGURE 1
PCR confirmation of bla_{NDM-1} and $bla_{OXA-820}$. Colony PCR was performed on an *A. pittii* TCM strain and cultured without any antibiotics using specific primers. Blank is the no-template control.

References

Abouelfetouh, A., Mattock, J., Turner, D., Li, E., and Evans, B. A. (2022). Diversity of carbapenem-resistant acinetobacter baumannii and bacteriophage-mediated spread of the Oxa23 carbapenemase. *Microb. Genom.* 8. doi: 10.1099/mgen.0.000752

Arndt, D., Grant, J. R., Marcu, A., Sajed, T., Pon, A., Liang, Y., et al. (2016). PHASTER: a better, faster version of the PHAST phage search tool. *Nucleic Acids Res.* 44, W16–W21. doi: 10.1093/nar/gkw387

Aziz, R. K., Bartels, D., Best, A. A., Dejongh, M., Disz, T., Edwards, R. A., et al. (2008). The RAST server: rapid annotations using subsystems technology. *BMC Genomics* 9, 75. doi: 10.1186/1471-2164-9-75

Bassetti, M., Echols, R., Matsunaga, Y., Ariyasu, M., Doi, Y., Ferrer, R., et al. (2021). Efficacy and safety of cefiderocol or best available therapy for the treatment of serious infections caused by carbapenem-resistant gram-negative bacteria (CREDIBLE-CR): a randomised, open-label, multicentre, pathogen-focused, descriptive, phase 3 trial. *Lancet Infect. Dis.* 21, 226–240. doi: 10.1016/S1473-3099(20)30796-9

Behzadi, P., and Gajdacs, M. (2021). Writing a strong scientific paper in medicine and the biomedical sciences: a checklist and recommendations for early career researchers. *Biol. Futur.* 72, 395–407. doi: 10.1007/s42977-021-00095-z

Behzadi, P., Garcia-Perdomo, H. A., Karpinski, T. M., and Issakhanian, L. (2020). Metallo-ss-lactamases: a review. *Mol. Biol. Rep.* 47, 6281–6294. doi: 10.1007/s11033-020-05651-9

Bonnin, R. A., Docobo-Perez, F., Poirel, L., Villegas, M. V., and Nordmann, P. (2014). Emergence of OXA-72-producing acinetobacter pittii clinical isolates. *Int. J. Antimicrob. Agents* 43, 195–196. doi: 10.1016/j.ijantimicag.2013.10.005

Bortolaia, V., Kaas, R. S., Ruppe, E., Roberts, M. C., Schwarz, S., Cattoir, V., et al. (2020). ResFinder 4.0 for predictions of phenotypes from genotypes. *J. Antimicrob. Chemother.* 75, 3491–3500. doi: 10.1093/jac/dkaa345

Cameranesi, M. M., Moran-Barrio, J., Limansky, A. S., Repizo, G. D., and Viale, A. M. (2018). Site-specific recombination at XerC/D sites mediates the formation and resolution of plasmid Co-integrates carrying a blaOXA-58- and TnaphA6-resistance module in acinetobacter baumannii. *Front. Microbiol.* 9, 66. doi: 10.3389/fmicb.2018.00066

Chapartegui-Gonzalez, I., Lazaro-Diez, M., and Ramos-Vivas, J. (2022). Genetic resistance determinants in clinical acinetobacter pittii genomes. *Antibiotics (Basel)* 11. doi: 10.3390/antibiotics11050676

Chapartegui-Gonzalez, I., Lazaro-Diez, M., Redondo-Salvo, S., Alted-Perez, L., Ocejo-Vinyals, J. G., Navas, J., et al. (2017). Whole-genome sequence of

acinetobacter pittii HUMV-6483 isolated from human urine. *Genome Announc.* 5. doi: 10.1128/genomeA.00658-17

Chapartegui-Gonzalez, I., Lazaro-Diez, M., Redondo-Salvo, S., Navas, J., and Ramos-Vivas, J. (2021). Antimicrobial resistance determinants in genomes and plasmids from acinetobacter baumannii clinical isolates. *Antibiotics (Basel)* 10. doi: 10.3390/antibiotics10070753

Chin, C. Y., Tipton, K. A., Farokhyfar, M., Burd, E. M., Weiss, D. S., and Rather, P. N. (2018). A high-frequency phenotypic switch links bacterial virulence and environmental survival in acinetobacter baumannii. *Nat. Microbiol.* 3, 563–569. doi: 10.1038/s41564-018-0151-5

Chopjitt, P., Putthanachote, N., Ungcharoen, R., Hatrongjit, R., Boueroy, P., Akeda, Y., et al. (2021). Genomic characterization of clinical extensively drug-resistant acinetobacter pittii isolates. *Microorganisms* 9. doi: 10.3390/microorganisms9020242

CLSI (2021). *Performance standards for antimicrobial susceptibility testing, M100, 31st ed* (Wayne, PA: Clinical and Laboratory Standards Institute).

Conde-Perez, K., Vazquez-Ucha, J. C., Alvarez-Fraga, L., Ageitos, L., Rumbo-Feal, S., Martinez-Guitian, M., et al. (2021). In-depth analysis of the role of the acinetobactin cluster in the virulence of acinetobacter baumannii. *Front. Microbiol.* 12, 752070. doi: 10.3389/fmicb.2021.752070

Cosgaya, C., Ratia, C., Mari-Almirall, M., Rubio, L., Higgins, P. G., Seifert, H., et al. (2019). *In vitro* and *in vivo* virulence potential of the emergent species of the acinetobacter baumannii (Ab) group. *Front. Microbiol.* 10, 2429. doi: 10.3389/fmicb.2019.02429

Ding, Z., Li, Z., Zhao, Y., Hao, J., Li, T., Liu, Y., et al. (2022). Phenotypic and genotypic characteristics of a tigecycline-resistant acinetobacter pittii isolate carrying bla NDM-1 and the novel bla OXA allelic variant bla OXA-1045. *Front. Microbiol.* 13, 868152. doi: 10.3389/fmicb.2022.868152

European Committee on Antimicrobial Susceptibility Testing *Breakpoint tables for interpretation of MICs and zone diameters version 11.0, valid from 2021-01-01*. Available at: http://www.eucast.org.

Feng, Y., Xue, G., Feng, J., Yan, C., Cui, J., Gan, L., et al. (2021). Rapid detection of new Delhi metallo-beta-Lactamase gene using recombinase-aided amplification directly on clinical samples from children. *Front. Microbiol.* 12, 691289. doi: 10.3389/fmicb.2021.691289

Geisinger, E., Mortman, N. J., Vargas-Cuebas, G., Tai, A. K., and Isberg, R. R. (2018). A global regulatory system links virulence and antibiotic resistance to envelope homeostasis in acinetobacter baumannii. *PloS Pathog.* 14, e1007030. doi: 10.1371/journal.ppat.1007030

Gorbunova, V., Seluanov, A., Mita, P., Mckerrow, W., Fenyo, D., Boeke, J. D., et al. (2021). The role of retrotransposable elements in ageing and age-associated diseases. *Nature* 596, 43–53. doi: 10.1038/s41586-021-03542-y

Gordon, N. C., and Wareham, D. W. (2010). Multidrug-resistant acinetobacter baumannii: mechanisms of virulence and resistance. *Int. J. Antimicrob. Agents* 35, 219–226. doi: 10.1016/j.ijantimicag.2009.10.024

Harding, C. M., Hennon, S. W., and Feldman, M. F. (2018). Uncovering the mechanisms of acinetobacter baumannii virulence. *Nat. Rev. Microbiol.* 16, 91–102. doi: 10.1038/nrmicro.2017.148

Hirschberg, R., and Kopple, J. D. (1989). Evidence that insulin-like growth factor I increases renal plasma flow and glomerular filtration rate in fasted rats. *J. Clin. Invest.* 83, 326–330. doi: 10.1172/JCI113878

Isler, B., Doi, Y., Bonomo, R. A., and Paterson, D. L. (2019). New treatment options against carbapenem-resistant acinetobacter baumannii infections. *Antimicrob. Agents Chemother.* 63. doi: 10.1128/AAC.01110-18

Javkar, K., Rand, H., Hoffmann, M., Luo, Y., Sarria, S., Thirunavukkarasu, N., et al. (2021). Whole-genome assessment of clinical acinetobacter baumannii isolates uncovers potentially novel factors influencing carbapenem resistance. *Front. Microbiol.* 12, 714284. doi: 10.3389/fmicb.2021.714284

Jolley, K. A., Bray, J. E., and Maiden, M. C. J. (2018). Open-access bacterial population genomics: BIGSdb software, the PubMLST.org website and their applications. *Wellcome Open Res.* 3, 124. doi: 10.12688/wellcomeopenres.14826.1

Kaase, M., Szabados, F., Pfennigwerth, N., Anders, A., Geis, G., Pranada, A. B., et al. (2014). Description of the metallo-beta-lactamase GIM-1 in acinetobacter pittii. *J. Antimicrob. Chemother.* 69, 81–84. doi: 10.1093/jac/dkt325

Kiyasu, Y., Hitomi, S., Funayama, Y., Saito, K., and Ishikawa, H. (2020). Characteristics of invasive acinetobacter infection: A multicenter investigation with molecular identification of causative organisms. *J. Infect. Chemother.* 26, 475–482. doi: 10.1016/j.jiac.2019.12.010

Krahn, T., Wibberg, D., Maus, I., Winkler, A., Bontron, S., Sczyrba, A., et al. (2016). Intraspecies transfer of the chromosomal acinetobacter baumannii blaNDM-1 carbapenemase gene. *Antimicrob. Agents Chemother.* 60, 3032–3040. doi: 10.1128/AAC.00124-16

Lam, M. M. C., Wick, R. R., Judd, L. M., Holt, K. E., and Wyres, K. L. (2022). Kaptive 2.0: updated capsule and lipopolysaccharide locus typing for the klebsiella pneumoniae species complex. *Microb. Genom.* 8. doi: 10.1099/mgen.0.000800

Larcher, R., Pantel, A., Arnaud, E., Sotto, A., and Lavigne, J. P. (2017). First report of cavitary pneumonia due to community-acquired acinetobacter pittii, study of virulence and overview of pathogenesis and treatment. *BMC Infect. Dis.* 17, 477. doi: 10.1186/s12879-017-2589-0

Letunic, I., and Bork, P. (2021). Interactive tree of life (iTOL) v5: an online tool for phylogenetic tree display and annotation. *Nucleic Acids Res.* 49, W293–W296. doi: 10.1093/nar/gkab301

Liang, Q., Liu, C., Xu, R., Song, M., Zhou, Z., Li, H., et al. (2021). fIDBAC: A platform for fast bacterial genome identification and typing. *Front. Microbiol.* 12, 723577. doi: 10.3389/fmicb.2021.723577

Liu, H., Moran, R. A., Chen, Y., Doughty, E. L., Hua, X., Jiang, Y., et al. (2021a). Transferable acinetobacter baumannii plasmid pDETAB2 encodes OXA-58 and NDM-1 and represents a new class of antibiotic resistance plasmids. *J. Antimicrob. Chemother.* 76, 1130–1134. doi: 10.1093/jac/dkab005

Liu, J., Shu, Y., Zhu, F., Feng, B., Zhang, Z., Liu, L., et al. (2021b). Comparative efficacy and safety of combination therapy with high-dose sulbactam or colistin with additional antibacterial agents for multiple drug-resistant and extensively drug-resistant acinetobacter baumannii infections: A systematic review and network meta-analysis. *J. Glob. Antimicrob. Resist.* 24, 136–147. doi: 10.1016/j.jgar.2020.08.021

Liu, B., Zheng, D., Zhou, S., Chen, L., and Yang, J. (2022). VFDB 2022: a general classification scheme for bacterial virulence factors. *Nucleic Acids Res.* 50, D912–D917. doi: 10.1093/nar/gkab1107

Loh, B., Chen, J., Manohar, P., Yu, Y., Hua, X., and Leptihn, S. (2020). A biological inventory of prophages in a. baumannii genomes reveal distinct distributions in classes, length, and genomic positions. *Front. Microbiol.* 11, 579802. doi: 10.3389/fmicb.2020.579802

Luis, M. R., and Konstantinos, T. K. (2016). The enveomics collection: A toolbox for specialized analyses of microbial genomes and metagenomes. *PeerJ. Prepr.* 4, e1900v1.

Lv, L., Wan, M., Wang, C., Gao, X., Yang, Q., Partridge, S. R., et al. (2020). Emergence of a plasmid-encoded resistance-Nodulation-Division efflux pump conferring resistance to multiple drugs, including tigecycline, in klebsiella pneumoniae. *mBio* 11. doi: 10.1128/mBio.02930-19

Meier-Kolthoff, J. P., Auch, A. F., Klenk, H. P., and Goker, M. (2013). Genome sequence-based species delimitation with confidence intervals and improved distance functions. *BMC Bioinf.* 14, 60. doi: 10.1186/1471-2105-14-60

Mohd Rani, F., Ni, A. R., Ismail, S., Alattraqchi, A. G., Cleary, D. W., Clarke, S. C., et al. (2017). Acinetobacter spp. infections in Malaysia: A review of antimicrobial resistance trends, mechanisms and epidemiology. *Front. Microbiol.* 8, 2479. doi: 10.3389/fmicb.2017.02479

Mulani, M. S., Kamble, E. E., Kumkar, S. N., Tawre, M. S., and Pardesi, K. R. (2019). Emerging strategies to combat ESKAPE pathogens in the era of antimicrobial resistance: A review. *Front. Microbiol.* 10, 539. doi: 10.3389/fmicb.2019.00539

Nagy, E., Becker, S., Kostrzewa, M., Barta, N., and Urban, E. (2012). The value of MALDI-TOF MS for the identification of clinically relevant anaerobic bacteria in routine laboratories. *J. Med. Microbiol.* 61, 1393–1400. doi: 10.1099/jmm.0.043927-0

Nagy, E., Maier, T., Urban, E., Terhes, G., Kostrzewa, M.Bacteria, E.S.G.O.a.R.I.A (2009). Species identification of clinical isolates of bacteroides by matrix-assisted laser-desorption/ionization time-of-flight mass spectrometry. *Clin. Microbiol. Infect.* 15, 796–802. doi: 10.1111/j.1469-0691.2009.02788.x

Overbeek, R., Olson, R., Pusch, G. D., Olsen, G. J., Davis, J. J., Disz, T., et al. (2014). The SEED and the rapid annotation of microbial genomes using subsystems technology (RAST). *Nucleic Acids Res.* 42, D206–D214. doi: 10.1093/nar/gkt1226

Page, A. J., Cummins, C. A., Hunt, M., Wong, V. K., Reuter, S., Holden, M. T., et al. (2015). Roary: rapid large-scale prokaryote pan genome analysis. *Bioinformatics* 31, 3691–3693. doi: 10.1093/bioinformatics/btv421

Pailhories, H., Tiry, C., Eveillard, M., and Kempf, M. (2018). Acinetobacter pittii isolated more frequently than acinetobacter baumannii in blood cultures: the experience of a French hospital. *J. Hosp. Infect.* 99, 360–363. doi: 10.1016/j.jhin.2018.03.019

Ranjbar, R., Behzadi, P., Najafi, A., and Roudi, R. (2017). DNA Microarray for rapid detection and identification of food and water borne bacteria: From dry to wet Lab. *Open Microbiol. J.* 11, 330–338. doi: 10.2174/1874285801711010330

Sarshar, M., Behzadi, P., Scribano, D., Palamara, A. T., and Ambrosi, C. (2021). Acinetobacter baumannii: An ancient commensal with weapons of a pathogen. *Pathogens* 10. doi: 10.3390/pathogens10040387

Seemann, T. (2014). Prokka: rapid prokaryotic genome annotation. *Bioinformatics* 30, 2068–2069. doi: 10.1093/bioinformatics/btu153

Siguier, P., Perochon, J., Lestrade, L., Mahillon, J., and Chandler, M. (2006). ISfinder: the reference centre for bacterial insertion sequences. *Nucleic Acids Res.* 34, D32–D36. doi: 10.1093/nar/gkj014

Stothard, P., Grant, J. R., and Van Domselaar, G. (2019). Visualizing and comparing circular genomes using the CGView family of tools. *Brief Bioinform.* 20, 1576–1582. doi: 10.1093/bib/bbx081

Sung, J. Y., Koo, S. H., Kim, S., and Kwon, G. C. (2015). Emergence of acinetobacter pittii harboring new Delhi metallo-beta-lactamase genes in daejeon, Korea. *Ann. Lab. Med.* 35, 531–534. doi: 10.3343/alm.2015.35.5.531

Tamma, P. D., Aitken, S. L., Bonomo, R. A., Mathers, A. J., Van Duin, D., and Clancy, C. J. (2021). Infectious diseases society of America guidance on the treatment of extended-spectrum beta-lactamase producing enterobacterales (ESBL-e), carbapenem-resistant enterobacterales (CRE), and pseudomonas aeruginosa with difficult-to-Treat resistance (DTR-p. aeruginosa). *Clin. Infect. Dis.* 72, e169–e183. doi: 10.1093/cid/ciaa1478

Tatusova, T., Dicuccio, M., Badretdin, A., Chetvernin, V., Nawrocki, E. P., Zaslavsky, L., et al. (2016). NCBI prokaryotic genome annotation pipeline. *Nucleic Acids Res.* 44, 6614–6624. doi: 10.1093/nar/gkw569

Vielva, L., De Toro, M., Lanza, V. F., and de la Cruz, F. (2017). PLACNETw: a web-based tool for plasmid reconstruction from bacterial genomes. *Bioinformatics* 33, 3796–3798. doi: 10.1093/bioinformatics/btx462

Wang, J., Wu, L., Xu, L., Chen, Y., and Chen, Y. (2016). Draft genome sequence of a multidrug-resistant new Delhi metallo-beta-lactamase NDM-1-producing acinetobacter pittii sequence type 207 isolate from China. *J. Glob. Antimicrob. Resist.* 6, 88–89. doi: 10.1016/j.jgar.2016.04.003

Wick, R. R., Judd, L. M., Gorrie, C. L., and Holt, K. E. (2017). Unicycler: Resolving bacterial genome assemblies from short and long sequencing reads. *PloS Comput. Biol.* 13, e1005595. doi: 10.1371/journal.pcbi.1005595

Wisplinghoff, H., Paulus, T., Lugenheim, M., Stefanik, D., Higgins, P. G., Edmond, M. B., et al. (2012). Nosocomial bloodstream infections due to acinetobacter baumannii, acinetobacter pittii and acinetobacter nosocomialis in the united states. *J. Infect.* 64, 282–290. doi: 10.1016/j.jinf.2011.12.008

Wyres, K. L., Cahill, S. M., Holt, K. E., Hall, R. M., and Kenyon, J. J. (2020). Identification of acinetobacter baumannii loci for capsular polysaccharide (KL) and lipooligosaccharide outer core (OCL) synthesis in genome assemblies using curated reference databases compatible with kaptive. *Microb. Genom.* 6. doi: 10.1099/mgen.0.000339

Yang, J., Chen, Y., Jia, X., Luo, Y., Song, Q., Zhao, W., et al. (2012). Dissemination and characterization of NDM-1-producing acinetobacter pittii in an intensive care unit in China. *Clin. Microbiol. Infect.* 18, E506–E513. doi: 10.1111/1469-0691.12035

Yang, L., Dong, N., Xu, C., Ye, L., and Chen, S. (2021). Emergence of ST63 pandrug-resistant acinetobacter pittii isolated from an AECOPD patient in China. *Front. Cell Infect. Microbiol.* 11, 739211. doi: 10.3389/fcimb.2021.739211

Zankari, E., Hasman, H., Cosentino, S., Vestergaard, M., Rasmussen, S., Lund, O., et al. (2012). Identification of acquired antimicrobial resistance genes. *J. Antimicrob. Chemother.* 67, 2640–2644. doi: 10.1093/jac/dks261

Zhang, Y., and Zhou, S. (2018). Draft genome sequence of an NDM-1-, OXA-421- and AmpC-producing acinetobacter pittii ST220 in anhui province, China. *J. Glob. Antimicrob. Resist.* 14, 176–177. doi: 10.1016/j.jgar.2018.07.008

Zhou, Y., Liang, Y., Lynch, K. H., Dennis, J. J., and Wishart, D. S. (2011). PHAST: a fast phage search tool. *Nucleic Acids Res.* 39, W347–W352. doi: 10.1093/nar/gkr485

frontiers | Frontiers in Cellular and Infection Microbiology

TYPE Original Research
PUBLISHED 25 August 2022
DOI 10.3389/fcimb.2022.892126

OPEN ACCESS

EDITED BY
Milena Dropa,
Faculty of Public Health, University of São Paulo, Brazil

REVIEWED BY
Sameh AbdelGhani,
Beni-Suef University, Egypt
Chaitra Shankar,
Christian Medical College & Hospital, India
Mariana Andrea Papalia,
Facultad de Farmacia y Bioquímica, Universidad de Buenos Aires, Argentina

*CORRESPONDENCE
Volkhard A. J. Kempf
volkhard.kempf@kgu.de
Moses Masika
mosmasika@uonbi.ac.ke

†These authors have contributed equally to this work and share first authorship

SPECIALTY SECTION
This article was submitted to Clinical Microbiology, a section of the journal Frontiers in Cellular and Infection Microbiology

RECEIVED 08 March 2022
ACCEPTED 05 August 2022
PUBLISHED 25 August 2022

CITATION
Villinger D, Schultze TG, Musyoki VM, Inwani I, Aluvaala J, Okutoyi L, Ziegler A-H, Wieters I, Stephan C, Museve B, Kempf VAJ and Masika M (2022) Genomic transmission analysis of multidrug-resistant Gram-negative bacteria within a newborn unit of a Kenyan tertiary hospital: A four-month prospective colonization study. *Front. Cell. Infect. Microbiol.* 12:892126. doi: 10.3389/fcimb.2022.892126

Genomic transmission analysis of multidrug-resistant Gram-negative bacteria within a newborn unit of a Kenyan tertiary hospital: A four-month prospective colonization study

David Villinger[1,2,3†], Tilman G. Schultze[1,2,3†], Victor M. Musyoki[4†], Irene Inwani[5], Jalemba Aluvaala[5], Lydia Okutoyi[6], Anna-Henriette Ziegler[1], Imke Wieters[2,7], Christoph Stephan[2,7], Beatrice Museve[8], Volkhard A. J. Kempf[1,2,3*] and Moses Masika[4*]

[1]Institute of Medical Microbiology and Infection Control, University Hospital Frankfurt, Frankfurt am Main, Hesse, Germany, [2]University Center of Infectious Diseases, University Hospital Frankfurt, Frankfurt am Main, Hesse, Germany, [3]University Center of Competence for Infection Control, Frankfurt, Hesse, Germany, [4]Department of Medical Microbiology, University of Nairobi, Nairobi, Kenya, [5]Pediatrics Department, Kenyatta National Hospital, Nairobi, Kenya, [6]Quality Health Department, Kenyatta National Hospital, Nairobi, Kenya, [7]Center of Internal Medicine/Infectious Diseases Unit, University Hospital Frankfurt, Frankfurt am Main, Hesse, Germany, [8]Department of Laboratory Medicine, Kenyatta National Hospital, Nairobi, Kenya

Objective: Multidrug-resistant organisms (MDRO), especially carbapenem-resistant organisms (CRO), represent a threat for newborns. This study investigates the colonization prevalence of these pathogens in a newborn unit at a Kenyan tertiary hospital in an integrated approach combining routine microbiology, whole genome sequencing (WGS) and hospital surveillance data.

Methods: The study was performed in the Kenyatta National Hospital (KNH) in 2019 over a four-month period and included 300 mother-baby pairs. A total of 1,097 swabs from newborns (weekly), mothers (once) and the hospital environment were taken. Routine clinical microbiology methods were applied for surveillance. Of the 288 detected MDRO, 160 isolates were analyzed for antimicrobial resistance genes and phylogenetic relatedness using whole genome sequencing (WGS) and bioinformatic analysis.

Results: In maternal vaginal swabs, MDRO detection rate was 15% (n=45/300), including 2% CRO (n=7/300). At admission, MDRO detection rate for neonates was 16% (n=48/300), including 3% CRO (n=8/300) with a threefold increase for MDRO (44%, n=97/218) and a fivefold increase for CRO (14%, n=29/218) until discharge. Among CRO, *K. pneumoniae* harboring bla_{NDM-1} (n=20) or bla_{NDM-5} (n=16) were most frequent. WGS analysis revealed 20 phylogenetically related

transmission clusters (including five CRO clusters). In environmental samples, the MDRO detection rate was 11% (n=18/164), including 2% CRO (n=3/164).

Conclusion: Our study provides a snapshot of MDRO and CRO in a Kenyan NBU. Rather than a large outbreak scenario, data indicate several independent transmission events. The CRO rate among newborns attributed to the spread of NDM-type carbapenemases is worrisome.

KEYWORDS

multidrug resistance, colonization, sub-Sahara, whole genome sequencing, NDM, carbapenemase

Introduction

Neonatal mortality rates in sub-Sahara Africa, including Kenya, continue to be among the highest worldwide (Gage et al., 2021) and severe newborn infections are accountable for 37% of these deaths (Ahmed et al., 2018). Due to limited medical infrastructure, reduced treatment options and high patient vulnerability (Laxminarayan and Bhutta, 2016), patients in newborn units (NBU) are at high risk for infections with multidrug-resistant organisms (MDRO). A WHO-report of 2017 classifies certain Gram-negative bacteria as critical priority (World Health Organization, 2017) with carbapenem-resistant *Acinetobacter baumannii*, carbapenem-resistant or 3rd generation-cephalosporin resistant *Enterobacteriaceae* and carbapenem-resistant *Pseudomonas aeruginosa* as highest concern. Especially, carbapenem-resistant *A. baumannii* and *Enterobacteriaceae* are prone to cause long-lasting outbreaks in hospital settings (Khalid et al., 2020). Methicillin-resistant *Staphylococcus aureus* (MRSA) are other pathogens often involved in hospital-acquired infections (Schuetz et al., 2021). Surveillance data of MDRO, MRSA and their transmission routes is scarce in low-and middle-income countries (Huynh et al., 2015) but knowledge about it is essential to initiate appropriate infection control measures. In this study, we identified clusters of MDRO and carbapenem-resistant organisms (CRO) at the NBU of the Kenyatta National Hospital (KNH) in Nairobi, Kenya, by an integrated approach combining patient data, routine microbiology results, bacterial genome sequences and infection epidemiology analysis.

Material and methods

Study design

This was a prospective study conducted in a newborn unit at KNH between January and April 2019. Rectal swabs from newborns, vaginal swabs from mothers and environmental samples from surfaces and medical equipment (on study days d55-57 and d89) were taken over a period of four months. These samples were analyzed for the presence of MDRO (Department of Medical Microbiology, University of Nairobi (UoN) and the Department of Laboratory Medicine, KNH). For a subset of MDRO, whole-genome-sequencing was performed, and phylogenetic relatedness of the bacterial isolates was assessed (Institute of Medical Microbiology and Infection Control, University Hospital Frankfurt am Main, Germany). Clusters were analyzed by integrated metadata analysis (sampling, location within the hospital).

Study participants

In this study, 300 mother-newborn pairs over a period of 110 days were included. Inclusion criteria were (i) admission to the NBU and (ii) given informed consent. Exclusion criteria was any given medical or ethical contradiction to rectal swabs of newborns or vaginal swabs of mothers. Ethical approval was given by KNH – UoN Ethics & Research Committee (KNH/UoN-ERC: P208/04/2018; University of Nairobi, Kenya, College of Health Sciences, July 11th, 2018) and by the Ethics Committee of the Medical Faculty Goethe University Frankfurt am Main, Germany (FKZ 01KA1772; 15/05/2018).

Study site

At KNH NBU, 200 to 300 newborns per month receive medical care. NBU is organized into nine sub-units. At admission, newborns are examined in the admission room. Medical care is provided in newborn intensive care units (NICU1, NICU2, NICU3), in nurseries (nursery B1, nursery B2, nursery B3) or in an isolation room. Nursery D is reserved for newborns with improved health condition. The delivery

ward is separated from NBU by two floors. Mothers stay in different post-natal wards and visit the NBU every three hours to (breast-)feed their babies.

Sample collection

Vaginal swabs (MK Plast, New Delhi, India) were collected from mothers once at the day their newborns were admitted (according to the ethics proposal KNH/UoN-ERC: P208/04/2018). Rectal swabs of newborns were taken at the day of admission, weekly during their stay at NBU and at discharge from the NBU. Due to ethical reasons, no sample was taken from deceased newborns. Environmental samples were categorized as (i) medical devices (e.g., ventilators, ultrasound transducer), (ii) near patient (e.g., cots, incubators), (iii) far from patient (e.g., desks, computer equipment) or (iv) unclean areas (e.g., surfaces, sinks), and were taken on d55-57 and d89.

Routine microbiology testing

Bacterial cultures were incubated for 24 hours at 35-37°C on selective chromogenic ESBL agar (CHROMagar, Mast, Paris, France). Identification (ID) and antimicrobial susceptibility testing (AST) was done via VITEK-2 (bioMérieux SA, Marcy-l'Étoile, France) using GN83 and P580 cards and imipenem E-test strips (Liofilchem, Roseto degli Abruzzi, Italy) according to Clinical Laboratory Standards Institute (CLSI) guidelines (Clinical and Laboratory Standards Institute (CLSI), 2019). Each ID and AST included a purity control on Columbia blood agar. All MDRO isolates were stored at -80°C in CRYOBANK™ medium (Mast).

Sequencing

Due to the agreements of the ethics proposal (KNH/UoN-ERC: P208/04/2018), 160 bacterial isolates (including 51/63 CRO) were selected from 288 detected MDRO for whole genome sequencing (WGS) prioritized by the following criteria: (i) carbapenem-resistant phenotype, (ii) culturable bacterial status upon arrival in Germany and (iii) likeliness of transmission onto or among newborns. Isolates were shipped on dry ice in CRYOBANK medium to Frankfurt am Main, Germany and were phenotypically re-assessed upon arrival using routine microbiology methods. Identification and AST were confirmed using Vitek-2, ID MALDI-ToF MS (bioMérieux SA, Nürtingen, Germany) according to European Committee on Antimicrobial Susceptibility Testing (EUCAST) guidelines version 8.0 (accessible via https://www.eucast.org/clinical_breakpoints/). Lateral flow assays (Hardy, Santa Maria, USA) were used to detect the following carbapenemases: NDM, KPC, OXA-48, VIM and IMP. All laboratory testing was performed under strict quality control criteria (laboratory accreditation according to ISO 15189:2011 standards) at the Institute for Medical Microbiology and Infection Control, University Hospital Frankfurt am Main, Germany. Isolates with inconsistent AST, unclear documented origin and copy strains (meaning that the same pathogen was detected in the same newborn multiple times) were excluded from further analysis.

DNA of cultured bacteria was extracted using DNeasy UltraClean 96 Kit (Qiagen, Venlo, Netherlands). Library preparation and sequencing was performed by a commercial service provider (Novogene, Cambridge, UK) using Illumina chemistry. Sequencing was carried out on a NovaSeq 6000 flow cell using a paired-end sequencing strategy of 2x150 bp. Details for *in silico*-sequence analysis is described in the Supplementary Information.

Software/Statistics

Research Electronic Data Capture software (REDCap, Vanderbilt University, Nashville, USA) was used to capture and store sample metadata (e.g., sample type, sampling date and time, location) and resistance phenotype (including ID, AST and subcultures). Confidence intervals (CI) were calculated using Newcombe-Wilson (Newcombe, 1998) method and the Relative Risk (RR) was determined using the Armitage -Berry Methods (Armitage et al., 2008).

Results

Sample collection and phenotypic determination of antimicrobial resistance

A total of 300 mother-newborn pairs were included in this study. The median age of the mothers was 27 years, and the range of newborn gestation age was between 25 weeks+6 days to 42 weeks+0 days. These newborns were admitted to the NBU at the day of delivery (or immediately after referral from other hospitals).

In total, 1,097 swabs were obtained, including 164 environmental samples (Figure 1A). Among the 288 detected MDRO, the most frequent species was *K. pneumoniae* (n=155) followed by *E. coli* (n=83) and *A. baumannii* (n=7). Multidrug-resistant *P. aeruginosa* isolates were not detected in any sample. Furthermore, 63 bacterial isolates were identified as CRO (*K. pneumoniae*: n=35; *E. coli*: n=13; *A. baumannii*: n=5).

At admission to NBU (after delivery or after referral from another hospital), MDRO were detected from 16% of newborns (n=48/300; 16%; CI 12-21%), including 3% CRO (n=8/300; 3%; CI 1-5%). Among mothers, a 15% MDRO rate (n=45/300; 15%; CI 11-19%), including 2% CRO (n=7/300; 2%; CI 1-5%) was

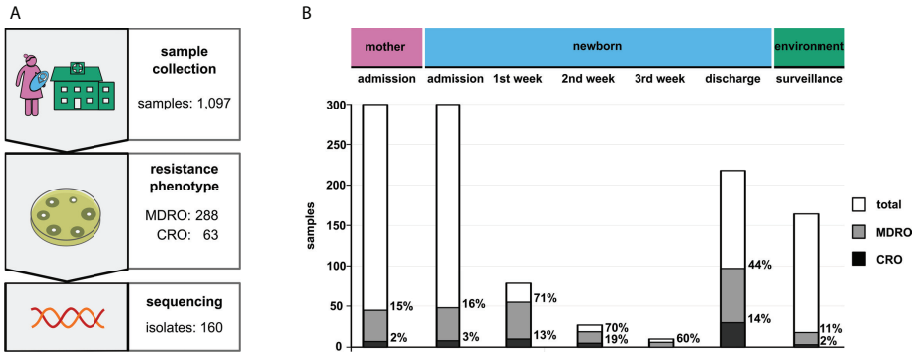

FIGURE 1
Results of the surveillance study. **(A)** Study design including the respective sample numbers (MDRO, multidrug-resistant organisms; CRO, carbapenem-resistant organisms). **(B)** Total prevalence of the identified bacteria grouped by sample type. "Admission" and "discharge" refer to the particular hospital stays of patients. Column sizes indicate absolute numbers, while percentages of MDRO and CRO are given next to the respective columns.

observed. The rates for mothers and newborns at admission were similar (MDRO: RR 0.94; CI 0.65-1.36; CRO: RR 0.88; CI 0.32-2.38). For newborns, the rate of MDRO increased from admission to discharge from 16% to 44% (n=97/218; 44%; CI 38-51%), and for CRO from 3% to 14% (n=29/218; 14%; CI 9-18%) indicating that 49 newborns became colonized with MDRO and of these, 21 newborns with CRO. This represents a three-fold increase of MDRO and a five-fold increase of CRO (MDRO: RR 2.78; CI 2.06-3.75; CRO: RR 4.99 CI 2.33-10.70). The highest increase was observed in the first week after admission to NBU (see Figure 1B).

MDRO and CRO isolates were obtained from medical devices (n=9), unclean areas (n=6) and near patient areas (n=3). Rates in NBU-environmental samples were 11% (n=18/164; 11%; CI 7-17%) for MDRO and 2% (n=3/164; 2%; CI 1-5%) for CRO.

Genomic characterization and phylogenetic analysis of MDRO and CRO

Of all sequenced *Enterobacteriaceae*, 89% (n=137/154) harbored an extended spectrum β-lactamase (ESBL) type $bla_{\text{CTX-M-15}}$. For 42/51 sequenced CRO, a bla_{NDM}-type carbapenemase gene was identified. These were distributed among *K. pneumoniae* (n=25; $bla_{\text{NDM-1}}$: n=14, $bla_{\text{NDM-5}}$: n=10, $bla_{\text{NDM-7}}$: n=1), *E. coli* (n=11; $bla_{\text{NDM-5}}$: n=6, $bla_{\text{NDM-7}}$: n=5) and other *Enterobacteriaceae* (n=6; all harboring $bla_{\text{NDM-1}}$). For all four *A. baumannii* isolates, a $bla_{\text{OXA-23}}$ carbapenemase was detected; one of those additionally harbored $bla_{\text{OXA-66}}$, two others $bla_{\text{OXA-69}}$ and one $bla_{\text{OXA-365}}$. Other detected carbapenemases include $bla_{\text{OXA-232}}$ and $bla_{\text{OXA-181}}$ (each found in one *K. pneumoniae* isolate, respectively). Detailed information regarding sequence type and antimicrobial resistance genes is given in Supplementary Table 1.

A phylogenetic analysis of the 160 selected isolates was carried out. Copy strains (n=17) were excluded once confirmed by sequence analysis. Results revealed 20 clusters of closely related isolates, including five CRO clusters. Of these, 19 were formed by *K. pneumoniae* (CRO clusters: n=4) and one cluster was formed by *E. coli* (see Figure 2 and Supplementary Table 2).

Among these clusters, cluster I and II as well as cluster VI, VII and VIII consist of isolates of the same sequence type. The median difference between isolates of cluster VI and VII is 132 SNVs (min: 130; max: 133), of cluster VI and VIII 182 SNVs (min: 175; max: 184) and of cluster VII and VIII 191 SNVs (min: 183; max: 193), respectively. Similarly, cluster I and II both belong to ST39, with a median difference between the isolates of 2,380 SNVs (min: 2,380, max: 2,384). These results demonstrate that these clusters VI, VII and VIII are distinguishable within ST 17 and clusters I and II within ST 39.

Cluster I, which consist of *K. pneumoniae* ST39 with $bla_{\text{CTX-M-15}}$, represents the largest cluster (n=15). The isolates spanned the complete investigated period (d14 until d106) and were obtained from 15 neonates in seven of the nine NBU-subunits (except isolation room and NICU3).

Cluster VIII, formed by *K. pneumoniae* isolates of ST17 carrying $bla_{\text{NDM-5}}$, was the largest CRO cluster (Figure 3). The respective isolates derived from nine different newborns and were obtained from three different subunits (Supplementary Figure 1). The initial isolate was sampled on Nursery B3 on d46. Six isolates were detected in Nursery D (on d74 (n=2), d82, d85 (n=2) and d96) and two in NICU2 on d90 and d95, respectively.

Clusters indicating transmissions among mothers and newborns were rarely found (only cluster XIII and XIV). Only in three cases, bacteria of the same species (*K. pneumoniae* with MDRO status) were detected in mothers and their respective newborns but none of these bacteria were phylogenetically

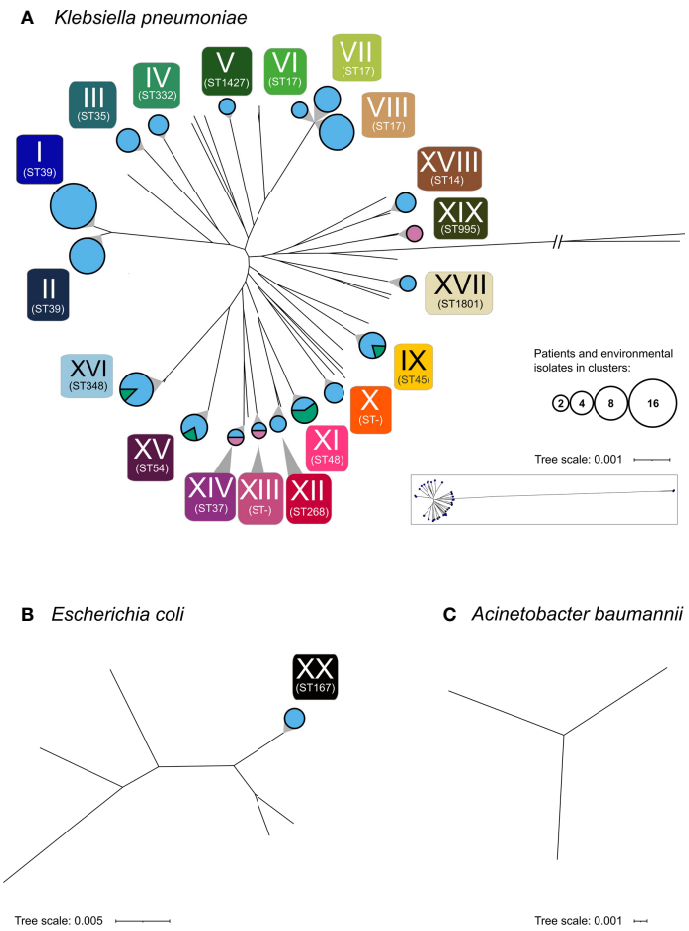

FIGURE 2
Phylogenetic analysis of the 160 sequenced isolates. Phylogenetic analysis revealed 20 clusters (I-XX) depicted as circles. **(A)** *K. pneumoniae*, **(B)** *E. coli*, **(C)** *A. baumannii*. Circle areas represent the number of patients and environmental samples forming the cluster, while the circle color indicates the respective sample types (rose, maternal; light blue, neonatal; green, environmental). Multilocus sequence types (ST) of clusters are shown below each cluster. Non-typable sequence types are designated as "ST-". Sequence types of all particular isolates are given in Supplementary Table 1.

closely related (pairwise SNP distance: 16,780, 16,583 and >133k SNPs, respectively) excluding vertical transmission from mother to child. Clusters consisting of isolates obtained from the NBU-environment and among newborn samples (cluster IX) as well as clusters consisting exclusively of samples from mothers (cluster XIX) were detected. Besides the already mentioned ST39 (n=26; cluster I: n=15, cluster II: n=9; no cluster: n=2), ST17 (n=17; including the NDM-5-positive cluster VIII: n=9) and ST348 (n=13; no carbapenemase detected) were the most frequently found *K. pneumoniae* sequence types.

Plasmid MLST analysis and genomic assessment of those regions flanking carbapenemase genes indicate that transmission of bacteria rather than plasmid hospitalism is the dominant mechanism for the spread of carbapenemases and the occurrence of CRO (see Supplementary Figure 2, Supplementary Figure 3).

Discussion

This report focusses on MDRO colonization prevalence among newborns in a tertiary hospital in Kenya with a special emphasis on carbapenem resistance. Data revealed a five-fold increase of CRO from 3% at admission to 14% at discharge underlining the need for appropriate infection control actions. Genomic analysis revealed 20 MDRO clusters and, in particular, five heterogeneous CRO clusters (clusters: VIII: n=9 isolates; XV: n=5; IV: n=3; XX: n=3; XIII: n=2; see Supplementary Table 2) within the relatively short study period. These results indicate not one ongoing outbreak scenario but several individual transmissions and emphasize a need for multiform counteractions which are not easy to implement in clinical routine patient care.

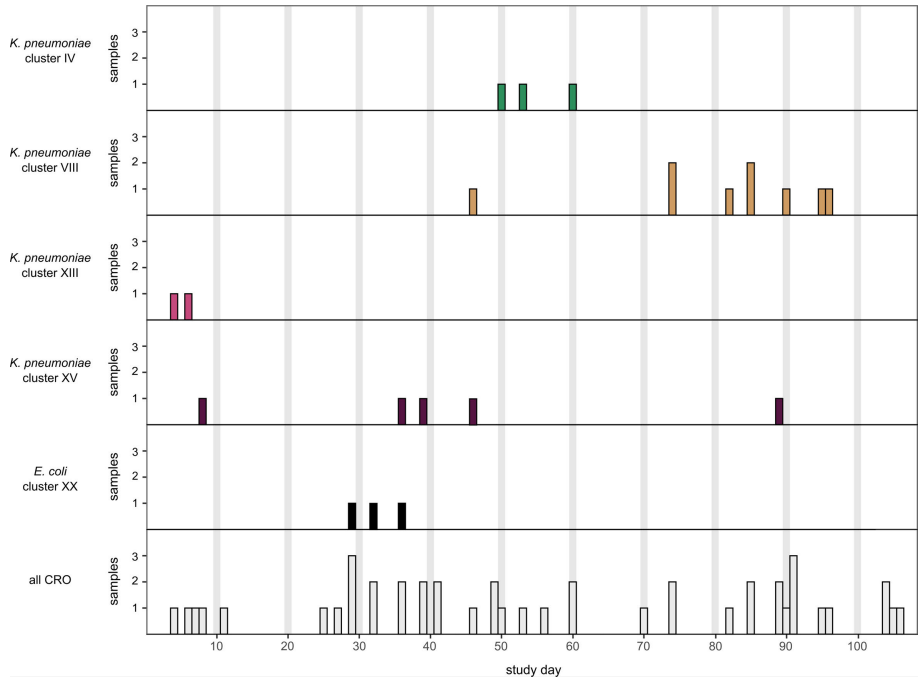

FIGURE 3
Surveillance timeline of CRO over 110 study days. From 51 detected CRO, seven copy strains were excluded resulting in 44 unique isolates. In separate rows, the *K. pneumoniae clusters* IV, VIII, XIII, XV and the *E. coli* cluster XX are displayed.

Data on MDRO colonization prevalence among NBUs in low- and middle-income countries is limited (Huynh et al., 2015) and studies are often focussed on clinical infections while the colonisation status (a prerequisite for infection) is not reported. The most prevalent sepsis-causing pathogens in NBUs in sub-Saharan Africa are *S. aureus*, *Klebsiella spp.* and *E. coli* (Okomo et al., 2019). In our study, screening did not detect any MRSA (data not shown). While similar to our findings, a previous study from two hospitals in Nairobi, Kenya (Omuse et al., 2015) reported only a low MRSA prevalence (3.7%), in our study only vaginal and rectal swabs were included, which are known to be of limited sensitivity for MRSA detection (Bitterman et al., 2010). The absence of multidrug-resistant *P. aeruginosa* in other sub-Saharan NBUs (Ghana) is also consistent with our results (Labi et al., 2020).

An earlier Kenyan study reported ESBL colonization rates of 10% at admission to NBU with an incidence of acquisition of 21.4% per day resulting in more than half of the neonates to be colonized with ESBL within the first three days upon admission (Kagia et al., 2019). In Ghana (Labi et al., 2020), 75% of the *Klebsiella spp.* from NBUs were ESBL positive and the carriage rate of carbapenemase-producing *Klebsiella spp.* was 8%. This shows that, the MDRO colonization rate among newborns in this study is high but within the reported range from sub-Saharan Africa (Kagia et al., 2019; Labi et al., 2020). In contrast, a study from a German NBUs disclosed Denkel et al., 2014 (Rettedal et al., 2015) found 2.9% of mothers to be colonized with ESBL.

The high rate of CRO-colonized newborns at discharge (14%) is alarming but in range with results from other sub-Saharan studies (8-9% in South Africa (Ballot et al., 2019) and Ghana (Labi et al., 2020)). Consistently, when looking at neonatal sepsis, an increase of CRO from about 3% (2013) to 9% (2015) was detected in South Africa due to NDM-producing *K. pneumoniae* (Ballot et al., 2019) but the underlying NDM-subtype remained unreported. Also, high CRO rates (e.g. 24% carbapenem resistance among *K. pneumoniae*) in clinical isolates at KNH have been described earlier (Wangai et al., 2019). These reports indicate that CRO represent a significant threat for patients and, in particular, for newborns in Kenya and other sub-Saharan African countries.

K. pneumoniae NDM-1 was initially detected in Nairobi in the year 2007 (Poirel et al., 2011). Among more than 200 studies from 2010 to 2019 analysing the prevalence of NDM in Africa, NDM-1 was dominating by far (93%) with much lower rates for NDM-5 (4%) and NDM-7 (2%) (Safavi et al., 2020). *Enterobacteriaceae* from Kenyan hospitals were reported earlier to harbor NDM-1 and NDM-5 and for *A. baumannii* OXA-23 was found to be most prevalent (Musila et al., 2021). This carbapenemase pattern is widely reflecting the distribution of CRO characterized in our study.

MDRO outbreaks in NBUs are frequently reported and whole genome sequence analysis has proven a powerful tool for outbreak analysis (Mammina et al., 2007; Dramowski et al., 2017; Johnson and Quach, 2017; Brinkac et al., 2019; Okomo et al., 2020). Usually,

problems in basic hygiene and increased exposure to medical procedures are significantly associated with MDRO infections (Haller et al., 2015). Such basic hygiene problems (possibly originating from medical staff or mothers, or visitors) are reflected by the high rate of MDRO/CRO detections from environmental samples (MDRO: n=18/164; CRO: n=3/164) and are difficult to overcome.

Shortcomings in basic hygiene contributed, e.g., to a *K. pneumoniae* ST39 outbreak in Gambia (Okomo et al., 2020) and this sequence type was also the prevalent among MDRO isolates (cluster I and II; n=25) in our study. In KNH, we found 20 different clusters suggesting several independently occurring transmission events over all NBU subunits with MDRO isolates from mothers and environmental samples (see Supplementary Figure 1). Unfortunately, exact transmission routes could not be reconstructed as this topic was not part of the initial study protocol. Clearly, the high MDRO entry by mothers (15% MDRO, 2% CRO) and newborns (16% MDRO, 3% CRO) at admission is a challenge for any infection control team.

To mitigate against this threat to newborns, staff at the KNH NBU have implemented multiple infection control measures (e.g., infection control team with weekly ward rounds, antibiotic stewardship team with daily consultations) and supported the analysis of the MDRO/CRO prevalence and transmission events strongly. Also, transmission events were clearly detected at the NBU, the successful work of the team is reflected by the fact that 56% of the newborns were not colonized with MDRO at discharge.

The herein described MDRO and CRO prevalence at the NBUs of KNH is worrisome and needs further attention (i) to clarify transmission routes and (ii) to implement further infection control measures. Generally, the limited MDRO surveillance data from sub-Saharan Africa indicate an increase of CRO infections in recent years but studies analysing colonization rather than infections are scarce (Okomo et al., 2019). It must be assumed that the extend of antibiotic resistance in Kenya is underestimated.

Data availability statement

Sequence data generated in this study was deposited in the NCBI Sequence Read Archive (SRA) under BioProject accession PRJNA804332.

Ethics statement

Ethical approval was given by KNH – UoN Ethics & Research Committee (KNH/UoN-ERC: P208/04/2018; University of Nairobi, Kenya, College of Health Sciences, July 11th, 2018) and by the Ethics Committee of the Medical Faculty Goethe University Frankfurt am Main, Germany (FKZ 01KA1772; 15/05/2018).

Authors contributions

General conceptualization: DV, VK, II, IW, and LO. Concept design and project management: DV and MM. Data collection and bacteriology: DV, MM, A-HZ, BM, VM, JA, IW, and LO. Data analysis non-WGS: DV, VM, A-HZ, TS, and VK. Data analysis WGS and Figure design: TS and DV. Writing of the manuscript DV, TS, VK, MM, and CS, II. All authors contributed to the article and approved the submitted version.

Funding

The authors have no competing interests to disclose. Funding for this study was provided by DLR (Deutsches Zentrum für Luft- und Raumfahrt) in cooperation with German Federal Ministry of Education and Research (BMBF; grant number 01KA1772) and partially by the LOEWE Center DRUID (Novel Drug Targets against Poverty-Related and Neglected Tropical Infectious Diseases). Findings and conclusions of this study do not necessarily represent views of the University.

Acknowledgments

We thank all laboratory and clinical staff at KNH and UHF involved in the study, in particular G. Revathi (Aga Khan University Hospital) and B. Maugo, M. Alacoque, S. Kinara and C. Onsinyo (all KNH).

Conflict of interest

The authors declare that the research was conducted in the absence of any commercial or financial relationships that could be construed as a potential conflict of interest.

Publisher's note

All claims expressed in this article are solely those of the authors and do not necessarily represent those of their affiliated

organizations, or those of the publisher, the editors and the reviewers. Any product that may be evaluated in this article, or claim that may be made by its manufacturer, is not guaranteed or endorsed by the publisher.

Supplementary material

The Supplementary Material for this article can be found online at: https://www.frontiersin.org/articles/10.3389/fcimb.2022.892126/full#supplementary-material

References

Ahmed, I., Ali, S. M., Amenga-Etego, S., Ariff, S., Bahl, R., Baqui, A. H., et al. (2018). Population-based rates, timing, and causes of maternal deaths, stillbirths, and neonatal deaths in south Asia and sub-Saharan Africa: a multi-country prospective cohort study. *Lancet Global Health* 6, e1297–e1308. doi: 10.1016/S2214-109X(18)30385-1

Armitage, P., Berry, G., and Matthews, J. N. S. (2008). *Statistical methods in medical research. 4th ed* (Oxford: Blackwell Science).

Ballot, D. E., Bandini, R., Nana, T., Bosman, N., Thomas, T., Davies, V. A., et al. (2019). A review of -multidrug-resistant enterobacteriaceae in a neonatal unit in Johannesburg, south Africa. *BMC Pediatr.* 19. doi: 10.1186/s12887-019-1709-y

Bitterman, Y., Laor, A., Itzhaki, S., and Weber, G. (2010). Characterization of the best anatomical sites in screening for methicillin-resistant staphylococcus aureus colonization. *Eur. J. Clin. Microbiol. Infect. Dis.* 29, 391–397. doi: 10.1007/s10096-009-0869-3

Brinkac, L. M., White, R., D'Souza, R., Nguyen, K., Obaro, S. K., and Fouts, D. E. (2019). Emergence of New Delhi Metallo-β-Lactamase (NDM-5) in *Klebsiella quasipneumoniae* from Neonates in a Nigerian Hospital. *mSphere* 4, 525–527. doi: 10.1128/mSphere.00685-18

Clinical and Laboratory Standards Institute (CLSI) (2019). *Performance standards for antimicrobial susceptibility testing. M100 29th edition*. Wayne, Pennsylvania, USA: Clinical and Laboratory Standards Institute.

Denkel, L. A., Schwab, F., Kola, A., Leistner, R., Garten, L., von Weizsäcker, K., et al. (2014). The mother as most important risk factor for colonization of very low birth weight (VLBW) infants with extended-spectrum β-lactamase-producing enterobacteriaceae (ESBL-e). *J. Antimicrob. Chemother.* 69, 2230–2237. doi: 10.1093/jac/dku097

Dramowski, A., Aucamp, M., Bekker, A., and Mehtar, S. (2017). Infectious disease exposures and outbreaks at a south African neonatal unit with review of neonatal outbreak epidemiology in Africa. *Int. J. Infect. Dis.* 57, 79–85. doi: 10.1016/j.ijid.2017.01.026

Gage, A. D., Fink, G., Ataguba, J. E., and Kruk, M. E. (2021). Hospital delivery and neonatal mortality in 37 countries in sub-Saharan Africa and south Asia: An ecological study. *PloS Med.* 18, e1003843. doi: 10.1371/journal.pmed.1003843

Haller, S., Eller, C., Hermes, J., Kaase, M., Steglich, M., Radonic, A., et al. (2015). What caused the outbreak of ESBL-producing klebsiella pneumoniae in a neonatal intensive care unit, Germany 2009 to 2012? reconstructing transmission with epidemiological analysis and whole-genome sequencing. *BMJ Open* 5, e007397–e007397. doi: 10.1136/bmjopen-2014-007397

Huynh, B. T., Padget, M., Garin, B., Herindrainy, P., Kermorvant-Duchemin, E., Watier, L., et al. (2015). Burden of bacterial resistance among neonatal infections in low income countries: How convincing is the epidemiological evidence? *BMC Infect. Dis.* 15. doi: 10.1186/s12879-015-0843-x

Johnson, J., and Quach, C. (2017). Outbreaks in the neonatal ICU: A review of the literature. *Curr. Opin. Infect. Dis.* 30, 395–403. doi: 10.1097/QCO.0000000000000383

Kagia, N., Kosgei, P., Ooko, M., Wafula, L., Mturi, N., Anampiu, K., et al. (2019). Carriage and acquisition of extended-spectrum β-lactamase-producing enterobacterales among neonates admitted to hospital in kilifi, Kenya. *Clin. Infect. Dis.* 69, 751–759. doi: 10.1093/cid/ciy976

Khalid, S., Ahmad, N., Ali, S. M., and Khan, A. U. (2020). Outbreak of efficiently transferred carbapenem-resistant bla NDM -producing gram-negative bacilli isolated from neonatal intensive care unit of an Indian hospital. *Microbial Drug Resistance* 26, 284–289. doi: 10.1089/mdr.2019.0092

Labi, A. K., Bjerrum, S., Enweronu-Laryea, C. C., Ayibor, P. K., Nielsen, K. L., Marvig, R. L., et al. (2020). High carriage rates of multidrug-resistant gram-negative bacteria in neonatal intensive care units from Ghana. *Open Forum Infect. Dis.* 7. doi: 10.1093/OFID/OFAA109

Laxminarayan, R., and Bhutta, Z. A. (2016). Antimicrobial resistance–a threat to neonate survival. *Lancet Global Health* 4, e676–e677. doi: 10.1016/S2214-109X(16)30221-2

Mammina, C., di Carlo, P., Cipolla, D., Giuffrè, M., Casuccio, A., di Gaetano, V., et al. (2007). Surveillance of multidrug-resistant gram-negative bacilli in a neonatal intensive care unit: prominent role of cross transmission. *Am. J. Infection Control* 35, 222–230. doi: 10.1016/j.ajic.2006.04.210

Musila, L., Kyany'a, C., Maybank, R., Stam, J., Oundo, V., and Sang, W. (2021). Detection of diverse carbapenem and multidrug resistance genes and high-risk strain types among carbapenem non-susceptible clinical isolates of target gram-negative bacteria in Kenya. *PloS One* 16. doi: 10.1371/journal.pone.0246937

Newcombe, R. G. (1998). Interval estimation for the difference between independent proportions: comparison of eleven methods. *Stat Med.* 17, 873–890. doi: 10.1002/(SICI)1097-0258(19980430)17:8<873::AID-SIM779>3.0.CO;2-I

Okomo, U., Akpalu, E. N. K., le Doare, K., Roca, A., Cousens, S., Jarde, A., et al. (2019). Aetiology of invasive bacterial infection and antimicrobial resistance in neonates in sub-Saharan Africa: a systematic review and meta-analysis in line with the STROBE-NI reporting guidelines. *Lancet Infect. Dis.* 19, 1219–1234. doi: 10.1016/S1473-3099(19)30414-1

Okomo, U., Senghore, M., Darboe, S., Bojang, E., Zaman, S. M. A., Hossain, M. J., et al. (2020). Investigation of sequential outbreaks of burkholderia cepacia and multidrug-resistant extended spectrum β-lactamase producing klebsiella species in a West African tertiary hospital neonatal unit: a retrospective genomic analysis. *Lancet Microbe* 1, e119–e129. doi: 10.1016/S2666-5247(20)30061-6

Omuse, G., Kabera, B., and Revathi, G. (2015). Low prevalence of methicillin resistant as determined by an automated identification system in two private hospitals in Nairobi, Kenya: A cross sectional study. *BMC Infect. Dis.* 14. doi: 10.1186/s12879-014-0669-y

Poirel, L., Revathi, G., Bernabeu, S., and Nordmann, P. (2011). Detection of NDM-1-producing klebsiella pneumoniae in Kenya. *Antimicrob. Agents Chemother.* 55, 934–936. doi: 10.1128/AAC.01247-10

Rettedal, S., Löhr, I. H., Bernhoff, E., Natås, O. B., Sundsfjord, A., and Øymar, K. (2015). Extended-spectrum β-lactamase-producing enterobacteriaceae among pregnant women in Norway: Prevalence and maternal-neonatal transmission. *J. Perinatol.*, 907–912. doi: 10.1038/jp.2015.82

Safavi, M., Bostanshirin, N., Hajikhani, B., Yaslianifard, S., van Belkum, A., Goudarzi, M., et al. (2020). Global genotype distribution of human clinical isolates of new Delhi metallo-β-lactamase-producing klebsiella pneumoniae; a systematic review. *J. Global Antimicrob. Resistance* 23, 420–429. doi: 10.1016/j.jgar.2020.10.016

Schuetz, C. R., Hogan, P. G., Reich, P. J., Halili, S., Wiseman, H. E., Boyle, M. G., et al. (2021). Factors associated with progression to infection in methicillin-resistant staphylococcus aureus-colonized, critically ill neonates. *J. Perinatol.* 41, 1285–1292. doi: 10.1038/s41372-021-00944-8

Wangai, F. K., Masika, M. M., Lule, G. N., Karari, E. M., Maritim, M. C., Jaoko, W. G., et al. (2019). Bridging antimicrobial resistance knowledge gaps: The East African perspective on a global problem. *PloS One* 14. doi: 10.1371/journal.pone.0212131

World Health Organization (2017). *Prioritization of pathogens to guide discovery, research and development of new antibiotics for drug-resistant bacterial infections, including tuberculosis* (Geneva). Available at: https://apps.who.int/iris/handle/10665/311820.

frontiers | Frontiers in Cellular and Infection Microbiology

TYPE Original Research
PUBLISHED 16 September 2022
DOI 10.3389/fcimb.2022.964539

OPEN ACCESS

EDITED BY
Milena Dropa,
Faculty of Public Health, University of São Paulo, Brazil

REVIEWED BY
Stefania Zanetti,
University of Sassari, Italy
Carolina Silva Nodari,
Institut Pasteur, France

*CORRESPONDENCE
Yung-Chih Wang
wystwyst@gmail.com
Yi-Tzu Lee
s851009@yahoo.com.tw

†These authors have contributed equally to this work

SPECIALTY SECTION
This article was submitted to Clinical Microbiology, a section of the journal Frontiers in Cellular and Infection Microbiology

RECEIVED 08 June 2022
ACCEPTED 31 August 2022
PUBLISHED 16 September 2022

CITATION
Chiang T-T, Huang T-W, Sun J-R, Kuo S-C, Cheng A, Liu C-P, Liu Y-M, Yang Y-S, Chen T-L, Lee Y-T and Wang Y-C (2022) Biofilm formation is not an independent risk factor for mortality in patients with *Acinetobacter baumannii* bacteremia. *Front. Cell. Infect. Microbiol.* 12:964539. doi: 10.3389/fcimb.2022.964539

Biofilm formation is not an independent risk factor for mortality in patients with *Acinetobacter baumannii* bacteremia

Tsung-Ta Chiang[1], Tzu-Wen Huang[2,3], Jun-Ren Sun[1,4], Shu-Chen Kuo[5], Aristine Cheng[6,7], Chang-Pan Liu[8,9], Yuag-Meng Liu[10], Ya-Sung Yang[1], Te-Li Chen[11], Yi-Tzu Lee[12,13]*† and Yung-Chih Wang[1]*†

[1]Division of Infectious Diseases and Tropical Medicine, Department of Internal Medicine, Tri-Service General Hospital, National Defense Medical Center, Taipei, Taiwan, [2]Department of Microbiology and Immunology, School of Medicine, College of Medicine, Taipei Medical University, Taipei, Taiwan, [3]Graduate Institute of Medical Sciences, College of Medicine, Taipei Medical University, Taipei, Taiwan, [4]Institute of Preventive Medicine, National Defense Medical Center, Taipei, Taiwan, [5]National Institute of Infectious Diseases and Vaccinology, National Health Research Institute, Maoli County, Taiwan, [6]Department of Internal Medicine, National Taiwan University Hospital, Taipei, Taiwan, [7]College of Medicine, National Taiwan University, Taipei, Taiwan, [8]Division of Infectious Diseases, Department of Internal Medicine, Mackay Memorial Hospital, Taipei, Taiwan, [9]Department of Medical Research, Mackay Memorial Hospital, Taipei, Taiwan, [10]Division of Infectious Diseases, Department of Internal Medicine, Changhua Christian Hospital, Changhua, Taiwan, [11]Graduate Institute of Life Sciences, National Defense Medical Center, Taipei, Taiwan, [12]Department of Emergency Medicine, Taipei Veterans General Hospital, Taipei, Taiwan, [13]Faculty of Medicine, School of Medicine, National Yang-Ming University, Taipei, Taiwan

In the past decades, due to the high prevalence of the antibiotic-resistant isolates of *Acinetobacter baumannii*, it has emerged as one of the most troublesome pathogens threatening the global healthcare system. Furthermore, this pathogen has the ability to form biofilms, which is another effective mechanism by which it survives in the presence of antibiotics. However, the clinical impact of biofilm-forming *A. baumannii* isolates on patients with bacteremia is largely unknown. This retrospective study was conducted at five medical centers in Taiwan over a 9-year period. A total of 252 and 459 patients with bacteremia caused by biofilm- and non-biofilm-forming isolates of *A. baumannii*, respectively, were enrolled. The clinical demographics, antimicrobial susceptibility, biofilm-forming ability, and patient clinical outcomes were analyzed. The biofilm-forming ability of the isolates was assessed using a microtiter plate assay. Multivariate analysis revealed the higher APACHE II score, shock status, lack of appropriate antimicrobial therapy, and carbapenem resistance of the infected strain were independent risk factors of 28-day mortality in the patients with *A. baumannii* bacteremia. However, there was no significant difference between the 28-day survival and non-survival groups, in terms of the biofilm forming ability. Compared to the patients infected with non-biofilm-forming isolates, those infected with biofilm-forming isolates had a lower in-hospital mortality rate.

Patients with either congestive heart failure, underlying hematological malignancy, or chemotherapy recipients were more likely to become infected with the biofilm-forming isolates. Multivariate analysis showed congestive heart failure was an independent risk factor of infection with biofilm-forming isolates, while those with arterial lines tended to be infected with non-biofilm-forming isolates. There were no significant differences in the sources of infection between the biofilm-forming and non-biofilm-forming isolate groups. Carbapenem susceptibility was also similar between these groups. In conclusion, the patients infected with the biofilm-forming isolates of the *A. baumannii* exhibited different clinical features than those infected with non-biofilm-forming isolates. The biofilm-forming ability of *A. baumannii* may also influence the antibiotic susceptibility of its isolates. However, it was not an independent risk factor for a 28-day mortality in the patients with bacteremia.

KEYWORDS

***Acinetobacter baumannii*, bacteremia, biofilm, carbapenem resistance, mortality**

Introduction

Acinetobacter baumannii is an important pathogen responsible for various nosocomial infections and leads to high rates of mortality and morbidity in the infected patients (Cisneros et al., 1996; Dijkshoorn et al., 2007). Its emergence as a drug-resistant pathogen has made the treatment of infected patients difficult (Dijkshoorn et al., 2007; Peleg et al., 2008). Moreover, *A. baumannii* has been found to have the ability to form biofilms, which is another effective way for the bacteria to survive in the presence of antibiotics (Villegas and Hartstein, 2003; Martí et al., 2011). Biofilm, a three-dimensional structure constructed by the bacterial community, is encased in an extracellular polymeric matrix (Hall-Stoodley et al., 2004). Biofilms may act as a barrier against the penetration of antimicrobials, to alter their metabolism and effects, resulting in antimicrobial resistance (Harrison et al., 2007). However, some studies have shown that biofilm-forming isolates exhibit variations in drug resistance (Rodríguez-Baño et al., 2008; Qi et al., 2016; Donadu et al., 2021). These findings suggest that the biofilm-forming ability of bacterial isolates may contribute to differences in drug resistance. Moreover, biofilm- and non-biofilm-forming isolates could show different virulence.

A. baumannii can cause various biofilm-associated infections, such as chronic wound infections, ventilator-associated pneumonia, infective endocarditis, and catheter-related infections (Høiby et al., 2015; Gedefie et al., 2021). Although biofilm-associated infections are considered the cause of morbidity and mortality in patients, several studies have reported that infections caused by them are not associated with worse outcomes (Rodríguez-Baño et al., 2008; Barsoumian et al., 2015; Wang et al., 2018). Therefore, the clinical impact of the biofilm-forming ability of the pathogen remains elusive. In previous studies, we found that biofilm formation was not associated with worse outcomes in *A. baumannii* bacteremic pneumonia (Wang et al., 2018). However, different types of biofilm-associated infections may result in different clinical outcomes. Limited data are available regarding the clinical impacts of biofilm-forming ability of the isolates of *A. baumannii*. This study aimed to establish a correlation between the biofilm-forming ability of *A. baumannii* and the clinical outcomes in patients with *A. baumannii* bacteremia.

Materials and methods

Hospital setting and study population

This retrospective study was conducted from January 2010 to December 2019 at five medical centers in Taiwan, namely (alphabetically) Changhua Christian Hospital (CCH, 1676 beds) in Central Taiwan, Mackay Memorial Hospital (MMH, 2055 beds), National Taiwan University Hospital (NTUH, 2245 beds), Taipei Veterans General Hospital (TVGH, 2900 beds), and Tri-Service General Hospital (TSGH, 1712 beds) of National Defense Medical Center in Northern Taiwan. Patients who had at least one positive blood culture for *A. baumannii* and who simultaneously had symptoms and signs of infection were enrolled. In patients with two or more positive blood cultures, only the first blood culture was included. Patients under 20 years of age and with incomplete medical records were excluded. The study protocol was approved by the institutional review board

(IRB) of each hospital (approval numbers: CCH: IRB No. 140514, MKH: IRB No. 14MMHIS125, NTU: IRB No. 201008047R, TSGH: IRB No. 1-103-05-100, and TVGH: IRB No. 2015-04-003C).

An episode of *A. baumannii* bacteremia was defined as the isolation of *A. baumannii* from a blood culture on one or more occasions. The onset of bacteremia was defined as the day when the blood culture that eventually yielded *A. baumannii* was obtained. Bacteremia episodes in the intensive care unit (ICU) were defined as having occurred within 48 h of ICU admission. A previous stay in the ICU was defined as admission to the ICU within 30 days prior to the bacteremia onset. Previous use of antimicrobials was defined as the use of antimicrobials, 30 days preceding the date of bacteremia onset. Those who received immunosuppressant agents within 2 weeks or corticosteroids at a dosage equivalent to or higher than 15 mg of prednisolone daily for 1 week within 4 weeks prior to the bacteremia onset were considered to have received immunosuppressant therapy. Chemotherapy use was defined as the administration of cytotoxic agents within 6 weeks prior to the onset of bacteremia. Recent surgery was defined as a surgery performed within 4 weeks prior to the onset of bacteremia. The source of bacteremia was determined according to the US Centers for Disease Control and Prevention definitions (Garner et al., 1988). The Acute Physiology and Chronic Health Evaluation (APACHE) II score within 24 h prior to the bacteremia onset was used to assess the severity of the disease. The all-cause 28-day mortality was defined as death occurring within 28 days of the onset of bacteremia and was set as the endpoint. The survival status of those who were discharged before the 28-day period was determined by contacting the patient or reviewing their medical records. None of the patients in this group were lost to follow-up.

Bacterial identification and antimicrobial susceptibility testing

Presumptive identification of the isolates at the *A. baumannii* complex (Abc) level was performed using the Vitek 2 system (bioMérieux, Marcy l'Etoile, France). The multiplex polymerase chain reaction was carried out to identify *A. baumannii* at the level of genomic species (Chen et al., 2007). The minimum inhibitory concentrations (MICs) of antimicrobial agents were determined by broth microdilution (Wayne and CLSI., 2006) and interpreted according to the standards given by the Clinical and Laboratory Standards Institute (CLSI) standards (Wayne and CLSI., 2020).

Biofilm cultivation and measurement

Biofilm-forming capability was quantitatively estimated using the crystal violet staining method (O'Toole et al., 1999; Wang et al., 2016). However, minor modifications in the procedure were made. Briefly, the bacterial strains were cultured at 37°C for 24 h in 5 mL Luria-Bertani (LB) broth supplemented with 1% D–glucose (LBglu). The cultures were diluted in LBglu to achieve an optical density (OD) of 0.03 at a wavelength of 570 nm. Aliquots of 200 µL of the final solution were added to each well of a 96-well tissue culture polystyrene microtiter plate. After incubation with agitation for 48 h at 37°C, the suspensions were removed and the wells were washed with phosphate-buffered saline (PBS), followed by the addition of 200 µL of 0.1% crystal violet to stain the cells. The plates were then incubated for 20 min with gentle agitation and washed. The crystal violet of the stained biofilms were solubilized with 200 µL of 95% ethanol for 10 min with agitation. The amount of biofilm formed was quantified by measuring the optical density at 570 nm (OD_{570}). All experiments were performed in triplicates and repeated on three separate occasions. The OD_{570} values of the well with un-inoculated LB medium were used as a negative control. Those with OD_{570} values at least twice that of the negative controls on at least two separate occasions were considered as biofilm formation positive (Rodríguez-Baño et al., 2008).

Statistical analyses

The data were analyzed using the statistical package PASW for the Windows version 26 (SPSS, Chicago, IL, USA). The χ^2 test with Yate's correction or Fisher's exact test was used to compare the categorical differences. Continuous variables were analyzed using the Student's *t* test and data were presented as median and interquartile range (IQR). The time to mortality, defined as the interval between bacteremia onset and death, was analyzed using Kaplan–Meier survival analysis, and log-rank test was used to compare the univariate survival distribution between different groups of patients. The logistic regression model was used to explore independent prognostic factors associated with the 28-day mortality. Univariate analyses were performed for each of the risk factors to ascertain the odds ratio (OR) and 95% confidence interval (CI). All biologically plausible variables with a $P < 0.10$ in the univariate analysis were considered for inclusion in the multivariate logistic regression model with a backward selection process. A $P < 0.05$ was considered statistically significant.

Results

Patients who had experienced at least one episode of the *A. baumannii* complex monomicrobial bacteremia during the 9-year period were enrolled for evaluation. Those with bacteremia caused by non-*baumannii Acinectobacter* spp. were excluded from the analysis. Ultimately, of 711 patients that were enrolled, 385 (54.15%) survived and 326 (45.85%) died within 28 days of the onset of *A. baumannii* bacteremia. The demographic and clinical features of the 28-days survivors and non-survivors are presented in Table 1. Multivariate logistic regression analysis was carried out (Table 2) to delineate the independent risk factors of 28-day mortality due to *A. baumannii* bacteremia. Previous exposure to fluoroquinolones (OR, 2.052; CI 1.182–3.564; $P = 0.011$), liver cirrhosis (OR, 2.395; CI, 1.196–4.796; $P = 0.014$), higher disease severity (APACHE II score) (OR, 1.147; CI, 1.116–1.178; $P < 0.001$), shock (OR, 1.863; CI, 1.179–2.944; $P = 0.008$), receipt of a thoracic drain (OR, 5.502; CI, 1.889–16.021; $P = 0.002$), infection by carbapenem-resistant isolates (OR, 2.425; CI, 1.524–3.858; $P < 0.001$), and receipt of inappropriate antimicrobial therapy (OR, 1.670; CI, 1.051–2.655; $P = 0.030$) were independent risk factors of 28-day mortality. In contrast, those who had hypertension (OR, 0.523; CI, 0.336–0.815; $P = 0.004$), cerebrovascular disease (OR, 0.296; CI, 0.171–0.512; $P < 0.001$), underwent a surgery within the past 4 weeks (OR, 0.492; CI, 0.288–0.840; $P = 0.009$), and those who had developed bacteremia as a consequence of a urinary tract infection (OR, 0.381; CI, 0.161–0.904; $P = 0.029$) were more likely to survive the 28-days after developing bacteremia. The proportion of infection caused by biofilm formation isolates was not significant differed between survivors and non-survivors within 28 days. (38.4% *vs.* 31.9%, $P = 0.071$).

To further explore the risk of the infection by biofilm-forming isolates, we divided the patients into two groups according to the biofilm-forming ability of the bacterial isolates. The demographic and clinical characteristics of patients with *A. baumannii* bacteremia caused by the biofilm-forming (n = 252, 35.44%) and non-biofilm-forming (n = 459, 64.56%) isolates are listed in Table 3. Those who became infected with biofilm-forming isolates were less likely to contract the infection in the ICU (40.1% *vs.* 49.9%, $P = 0.015$), more likely to have congestive heart failure (19.0% *vs.* 12.9%, $P = 0.029$), less likely to be exposed previously to penicillin (8.3% *vs.* 13.7%, $P= 0.039$), more likely to have hematological malignancy (10.3% *vs.* 5.2%, $P = 0.014$), more likely to receive chemotherapy (12.7% *vs.* 7.8%, $P = 0.045$), less likely to receive a central venous catheter insertion (28.2% *vs.* 46.2%, $P < 0.001$), less likely to receive an arterial line insertion (9.5% *vs.* 26.8%, $P < 0.001$), less likely to be on a ventilator (44% *vs.* 56.6%, $P = 0.002$), and less likely to receive a thoracic drain insertion (2% *vs.* 5.9%, $P = 0.022$). The resistance rates to carbapenems were similar for both biofilm-forming and non-biofilm-forming isolates (56.7% *vs.* 59.3%, $P = 0.525$). Furthermore, there was no significant difference in their 14-day and 28-day mortality rates (Figure 1). The overall mortality rate was higher in the non-biofilm-forming group by a borderline statistical difference, compared with the biofilm-forming group (58.4% *vs.* 50.4%, $P = 0.048$). Logistic regression analysis was performed to delineate the independent risk factors for the infection by the biofilm-forming isolates. As shown in Table 4, congestive heart failure was a risk factor of infection with biofilm-forming isolates (OR, 1.918; CI, 1.221–3.012; $P = 0.005$). However, those who received an arterial line were less likely to be infected with biofilm-forming isolates (OR, 0.416; CI, 0.240–0.721; $P = 0.002$).

We further stratified the strains according to the infection foci that resulted in bacteremia (Table 5). Pneumonia was the most common source of infection, followed by primary bacteremia and catheter-related bloodstream infections. There were no significant difference in the sources of bacteremia between the biofilm-forming and non-biofilm-forming isolates.

A subgroup analysis was conducted to assess the risk factors of 28-day mortality in the patients infected with biofilm-forming isolates (Supplementary Table S1). Those who had developed bacteremia in the ICU, had previous exposure to fluoroquinolones, had collagen vascular disease, were recipients of immunosuppressant therapy, had hematological malignancy, had previous ICU admission history, were recipients of ventilator support, were infected with carbapenem-resistant isolates, had presented with shock, had higher APACHE II score, had bacteremia secondary to pneumonia, or had a multisite infection, were associated with a higher 28-day mortality rate. In contrast, those who underwent surgery within 4 weeks prior to the onset of bacteremia, those who had received appropriate antimicrobial therapy, those who had bacteremia secondary to urinary tract infection were associated with lower 28-day mortality rates. In the logistic regression analysis, those who had hematological malignancy (OR, 3.636; CI, 1.011–13.072; $P = 0.048$), infected with carbapenem-resistant isolates (OR, 2.945; CI, 1.344–6.453; $P = 0.007$), and had higher APACHE II score (OR, 1.151; CI, 1.098–1.206; $P < 0.001$) were independently associated with the 28-day mortality rates (Supplementary Table S2).

Discussion

This study revealed that there were no significant differences in the 14-day and 28-day mortality rates between patients infected with the biofilm-forming and non-biofilm-forming isolates of *A. baumannii*. Previous exposure to fluoroquinolones, liver cirrhosis, higher APACHE II score, shock status, infection with carbapenem-resistant isolates, and receipt of inappropriate antimicrobial therapy were independent risk factors of 28-day mortality in patients with *A. baumannii*

10.3389/fcimb.2022.964539

TABLE 1 Clinical characteristics and outcomes of patients with *Acinetobacter baumannii* bloodstream infections who survived or died within 28 days of bacteremia onset.

Variables	Survivors (n = 385)	Non-survivors (n =326)	P value
Demographic characteristics			
Age, median (IQR), years	71 (58–80)	72 (57–81)	0.722
Male sex, No. (%)	261 (67.8)	235 (72.1)	0.220
Acquired in ICU, No. (%)	151 (39.2)	179 (54.9)	< 0.001
Length of hospitalization before bacteremia, median (IQR), days	14 (5–32)	20 (9–38)	0.190
Previous use of antibiotics, No. (%)			
Aminoglycosides	41 (10.6)	27 (8.3)	0.308
Penicillins	47 (12.2)	37 (11.3)	0.816
β-lactam/β-lactamase inhibitors (except sulbactam)	43 (11.2)	46 (14.1)	0.256
Sulbactam	15 (3.9)	13 (4.0)	1.000
Non-anti-pseudomonas Cephalosporins	84 (21.8)	57 (17.5)	0.158
Anti-pseudomonas Cephalosporins	61 (15.8)	78 (23.9)	0.008
Group 2 carbapenems	61 (15.8)	71 (21.8)	0.043
Fluoroquinolones	41 (10.6)	83 (25.5)	< 0.001
Tigecycline	12 (3.1)	27 (8.3)	0.003
Colistin	7 (1.8)	18 (5.5)	0.013
Teicoplanin	53 (13.8)	72 (22.1)	0.004
Fluconazole	31 (8.1)	44 (13.5)	0.020
Comorbid condition, No. (%)			
Liver cirrhosis	27 (7.0)	47 (14.4)	0.002
Chronic obstructive pulmonary disease	62 (16.1)	66 (20.2)	0.170
Chronic kidney disease	110 (28.6)	111 (34.0)	0.123
Type 2 diabetes mellitus	125 (32.5)	95 (29.1)	0.371
Hypertension	158 (41.0)	104 (31.9)	0.013
Coronary artery disease	38 (9.9)	38 (11.7)	0.466
Congestive heart failure	53 (13.8)	54 (16.6)	0.344
Cerebrovascular accident	104 (27.0)	43 (13.2)	< 0.001
Collagen vascular disease	6 (1.6)	22 (6.7)	< 0.001
Immunosuppressant therapy	73 (19.0)	89 (27.3)	0.009
Solid tumor	74 (19.2)	62 (19.0)	1.000
Hematological malignancy	18 (4.7)	32 (9.8)	0.008
Chemotherapy	38 (9.9)	30 (9.2)	0.799
Trauma	19 (4.9)	5 (1.5)	0.012
Recent surgery	113 (29.4)	47 (14.4)	< 0.001
Previous ICU admission	179 (46.5)	190 (58.3)	0.002
Charlson comorbidity index, median (IQR)	3 (1–5)	3 (1–5)	0.279
APACHE II score, median (IQR)	18 (12–24)	29 (21–38)	< 0.001
Shock	76 (19.7)	153 (46.9)	< 0.001
Invasive Procedures, No. (%)			
Central venous catheter	139 (36.1)	144 (44.2)	0.031
Arterial line	67 (17.4)	80 (24.5)	0.020
Tracheostomy	41 (10.6)	33 (10.1)	0.902
Ventilator use	168 (43.6)	203 (62.3)	< 0.001
Hemodialysis	32 (8.3)	46 (14.1)	0.016
Thoracic drain	8 (2.1)	24 (7.4)	0.001
Abdominal drain	32 (8.3)	23 (7.1)	0.575
Total parental nutrition	23 (6.0)	27 (8.3)	0.242
Source of bacteremia, No. (%)			

(Continued)

TABLE 1 Continued

Variables	Survivors (n = 385)	Non-survivors (n =326)	P value
Pneumonia	154 (40.0)	188 (57.7)	< 0.001
Catheter related bloodstream infection	63 (16.4)	47 (14.4)	0.533
Urinary tract infection	46 (11.9)	13 (4.0)	< 0.001
Intra-abdominal infection	35 (9.1)	23 (7.1)	0.339
Skin and soft tissue infection	22 (5.7)	12 (3.7)	0.222
Primary bacteremia	79 (20.5)	69 (21.2)	0.853
Surgical site infection	2 (0.5)	3 (0.9)	0.665
Central nerve system infection	3 (0.8)	2 (0.6)	1.000
Multisite infection	16 (4.2)	22 (6.7)	0.135
Biofilm formation, No. (%)	148 (38.4)	104 (31.9)	0.071
Carbapenem-resistance isolates	174 (45.2)	241 (73.9)	< 0.001
Inappropriate antimicrobial therapy, No. (%)	244 (63.4)	251 (77.0)	< 0.001

IQR, interquartile range; ICU, intensive care unit; APACHE II, Acute Physiology and Chronic Health Evaluation II.

bacteremia. Congestive heart failure was an independent risk factor of infection with biofilm-forming isolates, while the patients with an arterial line were more likely to be infected with non-biofilm-forming isolates.

It is not surprising that shock status, higher APACHE II score, infection with carbapenem-resistant *A. baumannii*, and inappropriate treatment were independent risk factors for mortality, which is consistent with previous findings (Peleg et al., 2008; Lee et al., 2012; Wong et al., 2017). Those with liver cirrhosis had a higher 28-day mortality in this study. Our previous study also demonstrated a higher 30-day mortality rate in patients with liver cirrhosis compared to those without cirrhosis;, however, there was no significant difference (Liu et al., 2019). That study investigated all *Acinetobacter* species and enrolled a relatively small number of patients with *A. baumannii* bacteremia. The relatively small population of patients with *A. baumannii* bacteremia in that study may have contributed to the insignificance.

Patients with a previous exposure to fluoroquinolones had worse clinical outcomes. Although there is limited research regarding the correlation between fluoroquinolone exposure and outcomes in patients with *A. baumannii* bacteremia, one study concluded that exposure to fluoroquinolones is an independent risk factor for the development of carbapenem-resistant *A. baumannii* bacteremia (Kopterides et al., 2007). This may explain the risk of mortality in patients with *A. baumannii* bacteremia in our study.

The components of biofilms and their unique environment overpower most antimicrobials used for treating biofilm-associated infections (Høiby et al., 2010; Del Pozo, 2018; Law and Tan, 2022). The biofilm-associated infections can subsequently induce chronic infections, resulting in a considerable burden on the global healthcare system (Hall-Stoodley et al., 2004; Høiby et al., 2015). However, there is limited research regarding the clinical implications of biofilm formation. A previous study demonstrated that those infected with biofilm-forming isolates of *A. baumannii* had a probable history of ICU admission, use of antibiotics, and lesser severity of disease (Zhang et al., 2016). The study did not demonstrate an influence of biofilm formation on the clinical outcomes in the patients. A single-institute study documented that the mortality during an initial infection was significantly more common in patients with the biofilm-forming isolates, compared with those with the non-biofilm-forming isolates (Barsoumian et al., 2015). However, the low attributable mortality (7.1%) among the study population made it difficult to draw any conclusions regarding the clinical outcomes of biofilm formation ability of *A. baumannii* (Barsoumian et al., 2015). Recently, in a cohort study involving 273 patients, we found that biofilm formation was not associated with worse outcomes in patients with *A. baumannii* bacteremic pneumonia (Wang et al., 2018). As *A. baumannii* contributes to a variety of biofilm-associated infections, we included all types of infections to delineate the effects of biofilm formation on the clinical outcomes in this study. We found that biofilm formation capability was not an independent risk factor of 14-day and 28-day mortality in patients with *A. baumannii* bacteremia.

Bacterial cells embedded in the biofilms are known to be resistant to antimicrobials through several mechanisms, including limited penetration of the antimicrobials, slow growth rate of the bacterial cells in biofilms, physiological heterogeneity of the biofilms, and the expression of some resistance genes (Lewis, 2001; Mah and O'Toole, 2001; Harrison et al., 2007; Olsen, 2015). These conditions make biofilms difficult to eradicate and therefore, the correlation between resistance to individual antibiotics and biofilm formation remains elusive. While some studies have shown a positive correlation between resistance to individual antibiotics and biofilm formation (Rao et al., 2008; Badave and Kulkarni, 2015), others have found a negative correlation between the

Table 2 Logistic regression analysis for the risk of 28-day mortality in patients with *Acinetobacter baumannii* bloodstream infections.

Variables	Crude model		Model 1*	
	OR (95% CI)	*P*	OR (95% CI)	*P*
Acquired in ICU	1.887 (1.399–2.545)	< 0.001	1.045 (0.659–1.656)	0.852
Previous use of antibiotics				
Anti-pseudomonas Cephalosporins	1.671 (1.150–2.427)	0.007	1.511 (0.899–2.538)	0.119
Group 2 carbapenems	1.479 (1.012–2.161)	0.043	0.914 (0.532–1.570)	0.745
Fluoroquinolones	2.866 (1.905–4.312)	< 0.001	2.085 (1.182–3.564)	0.011
Tigecycline	2.807 (1.3.98–5.634)	0.004	1.042 (0.414–2.624)	0.931
Colistin	3.156 (1.301–7.653)	0.011	2.447 (0.779–7.687)	0.126
Teicoplanin	1.776 (1.202–2.624)	0.004	1.120 (0.627–2.001)	0.701
Fluconazole	1.782 (1.096–2.895)	0.020	0.670 (0.346–1.299)	0.236
Comorbid condition				
Liver cirrhosis	2.234 (1.357–3.677)	0.002	2.395 (1.196–4.796)	0.014
Hypertension	0.673 (0.494–0.917)	0.012	0.523 (0.336–0.815)	0.004
Cerebrovascular accident	0.411 (0.277–0.607)	< 0.001	0.296 (0.171–0.512)	< 0.001
Collagen vascular disease	4.571 (1.830–11.416)	0.001	2.729 (0.804–9.265)	0.108
Immunosuppressant therapy	1.605 (1.128–2.283)	0.009	1.159 (0.678–1.955)	0.581
Hematological malignancy	2.219 (1.221–4.034)	0.009	1.497 (0.627–3.572)	0.364
Trauma	0.300 (0.111–0.813)	0.018	0.887 (0.273–2.877)	0.842
Recent surgery	0.405 (0.278–0.592)	< 0.001	0.492 (0.288–0.840)	0.009
Previous ICU admission	1.608 (1.194–2.165)	0.002	1.068 (0.642–1.777)	0.800
APACHE II score, median (IQR)	1.135 (1.112–1.158)	< 0.001	1.147 (1.116–1.179)	< 0.001
Shock	3.596 (2.580–5.012)	< 0.001	1.863 (1.179–2.944)	0.008
Invasive Procedures, No. (%)				
Central venous catheter	1.400 (1.036–1.893)	0.029	0.753 (0.440–1.230)	0.241
Arterial line	1.544 (1.072–2.223)	0.020	0.647 (0.348–1.204)	0.169
Ventilator use	2.132 (1.577–2.881)	< 0.001	0.700 (0.423–1.160)	0.166
Hemodialysis	1.812 (1.124–2.922)	0.015	0.900 (0.474–1.711)	0.748
Thoracic drain	3.745 (1.659–8.455)	0.001	5.502 (1.889–16.021)	0.002
Source of bacteremia				
Pneumonia	2.043 (1.514–2.758)	< 0.001	0.930 (0.594–1.458)	0.752
Urinary tract infection	0.306 (0.162–0.577)	< 0.001	0.381 (0.161–0.904)	0.029
Carbapenem-resistance isolates	3.438 (2.500–4.728)	< 0.001	2.425 (1.524–3.858)	< 0.001
Inappropriate antimicrobial therapy	1.934 (1.389–2.693)	< 0.001	1.670 (1.051–2.655)	0.030

OR, odds ratio; CI, confidence interval; ICU, intensive care unit; APACHE II, Acute Physiology and Chronic Health Evaluation II.*Adjusted by all factors included in the table.

biofilm formation ability and carbapenem resistance (Rodríguez-Baño et al., 2008; Qi et al., 2016; Wang et al., 2018). Our previous studies have also demonstrated that most carbapenem-resistant *A. baumannii* transformants exhibit reduced biofilm-forming abilities (Wang et al., 2018). Our current study has shown similar findings, as the biofilm-forming isolates exhibited lower rates of carbapenem-resistance than the non-biofilm-forming isolates (56.7% *vs.* 59.3%). These findings suggest that the complexity of biofilm composition, and not of the bacteria themselves in the biofilms, may contribute to the antibiotic resistance of the biofilms (Lewis, 2001; Mah and O'Toole, 2001; Harrison et al., 2007; Olsen, 2015). Further studies are needed to elucidate the detailed mechanisms of antimicrobial resistance in the biofilms.

A major strength of this study was the larger sample size of patients who were enrolled from multiple medical centers. In order to exclude colonized isolates, all the bacterial strains collected in this study were isolated from blood samples. We enrolled patients with *A. baumannii* bacteremia caused by different sources of infection to represent the real-world clinical situations. Another strength was the use of multivariate analysis to delineate the risk factors for mortality in patients with bacteremia caused by biofilm-forming isolates of *A. baumannii*.

This retrospective study had several limitations, including selection bias and inconsistencies in patient care among the different hospitals. Another key limitation is that the *in vitro* formation of biofilms does not represent the actual *in vivo*

10.3389/fcimb.2022.964539

TABLE 3 Clinical characteristics of patients and clinical isolates with biofilm-forming and non-biofilm-forming *Acinetobacter baumannii* blood stream infections.

	Biofilm-forming (*n* = 252)	Non-biofilm-forming (*n* = 459)	*P* value
Demographic characteristics			
Age, median (IQR), years	71 (57–81)	72 (57–80)	0.132
Male sex, No. (%)	171 (67.9)	325 (70.8)	0.443
Acquired in ICU, No. (%)	101 (40.1)	229 (49.9)	0.015
Length of hospitalization before bacteremia, median (IQR), days	16 (6.25–34)	18 (7–33)	0.231
Previous use of antibiotics, No. (%)			
Aminoglycosides	20 (7.9)	48 (10.5)	0.290
Penicillins	21 (8.3)	63 (13.7)	0.039
β-lactam/β-lactamase inhibitors (except sulbactam)	32 (12.7)	57 (12.4)	0.906
Sulbactam	11 (4.4)	17 (3.7)	0.689
Non-anti-pseudomonas Cephalosporins	46 (18.3)	95 (20.7)	0.491
Anti-pseudomonas Cephalosporins	52 (19.0)	87 (20.6)	0.621
Group 2 Carbapenems	38 (15.1)	94 (20.5)	0.087
Fluoroquinolones	39 (15.5)	85 (18.5)	0.353
Tigecycline	12 (4.8)	27 (5.9)	0.608
Colistin	6 (2.4)	19 (4.1)	0.289
Teicoplanin	36 (14.3)	89 (19.4)	0.099
Fluconazole	22 (8.7)	53 (11.5)	0.254
Comorbid condition, No. (%)			
Liver cirrhosis	27 (10.7)	47 (10.2)	0.898
Chronic obstructive pulmonary disease	40 (15.9)	88 (19.2)	0.308
Chronic kidney disease	84 (33.3)	137 (29.8)	0.352
Type 2 diabetes mellitus	74 (29.4)	146 (31.8)	0.553
Hypertension	87 (34.5)	175 (38.1)	0.372
Coronary artery disease	28 (11.1)	48 (10.5)	0.800
Congestive heart failure	48 (19.0)	59 (12.9)	0.029
Cerebrovascular accident	50 (19.8)	97 (21.1)	0.700
Collagen vascular disease	14 (5.6)	14 (3.1)	0.110
Immunosuppressant therapy	61 (24.2)	101 (22.0)	0.514
Solid tumor	57 (22.6)	79 (17.2)	0.090
Hematological malignancy	26 (10.3)	24 (5.2)	0.014
Chemotherapy	32 (12.7)	36 (7.8)	0.045
Recent surgery	48 (19.0)	112 (24.4)	0.111
Previous ICU admission	126 (50.0)	243 (52.9)	0.480
Charlson comorbidity index, median (IQR)	2 (1-5)	3 (2-6)	0.113
APACHE II score, median (IQR)	21 (14-29)	24 (17-31)	0.650
Shock, No. (%)	81 (32.1)	148 (32.2)	1.000
Invasive Procedures, No. (%)			
Central venous catheter	71 (28.2)	212 (46.2)	<0.001
Arterial line	24 (9.5)	123 (26.8)	<0.001
Tracheostomy	52 (11.3)	22 (8.7)	0.306
Ventilator use	111 (44.0)	260 (56.6)	0.002
Hemodialysis	20 (7.9)	58 (12.6)	0.060
Thoracic drain	5 (2.0)	27 (5.9)	0.022
Abdominal drain	13 (5.2)	42 (9.2)	0.058
Total parental nutrition	17 (6.7)	33 (7.2)	0.879
Carbapenem resistance, No. (%)	143 (56.7)	272 (59.3)	0.525
Appropriate antimicrobial therapy	87 (34.5)	129 (28.1)	0.088

(Continued)

TABLE 3 Continued

	Biofilm-forming (n = 252)	Non-biofilm-forming (n = 459)	P value
Outcome			
14-day mortality, No. (%)	87 (34.5)	180 (39.2)	0.226
28-day mortality, No. (%)	104 (41.3)	222 (48.4)	0.071
Overall Mortality, No. (%)	127 (50.4)	268 (58.4)	0.048

IQR, interquartile range; ICU, intensive care unit; APACHE II, Acute Physiology and Chronic Health Evaluation II.

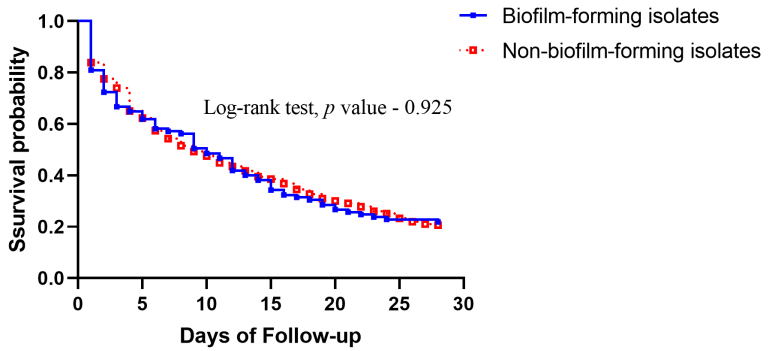

FIGURE 1
Comparison of Kaplan–Meier survival curves, at 28 days, between patients with *Acinetobacter baumannii* bacteremia caused by biofilm-forming isolates and non-biofilm-forming isolates.

TABLE 4 Logistic regression analysis of predictors for patients infected with biofilm-forming *Acinetobacter baumannii*.

Characteristic	Univariate analysis		Multivariate analysis	
	Crude OR (95% CI)	p	Adjusted OR (95% CI)	p
Acquired in ICU	0.672 (0.492–0.917)	0.012		
Previous use of penicillins	0.571 (0.340–0.961)	0.035		
Previous use of group 2 Carbapenems	0.690 (0.456–1.042)	0.078		
Previous use of teicoplanin	0.693 (0.454–1.057)	0.088		
Congestive heart failure	1.595 (1.052–2.420)	0.028	1.918 (1.221–3.012)	0.005
Solid tumor	1.406 (0.960–2.060)	0.080		
Hematological malignancy	2.085 (1.170–3.715)	0.013		
Chemotherapy	1.709 (1.033–2.827)	0.037		
Central venous catheter	0.457 (0.329–0.636)	<0.001		
Arterial line	0.288 (0.180–0.459)	<0.001	0.416 (0.240–0.721)	0.002
Ventilator use	0.603 (0.442–0.821)	0.001		
Hemodialysis	0.596 (0.350–1.016)	0.057		
Thoracic drain	3.087 (1.174–8.120)	0.022		
Abdominal drain	0.540 (0.284–1.026)	0.060		

ICU, intensive care unit; CI, confidence interval; OR, odds ratio.

TABLE 5 Types of infections caused by biofilm-forming and non-biofilm-forming isolates of *Acinetobacter baumannii*.

Sources of bacteremia	Biofilm-forming (n = 252)	Non-biofilm-forming (n = 459)	P-value	Overall Mortality	28-day Mortality
Pneumonia, No. (%)	111 (44.0)	231 (50.3)	0.117	67.8%	55.0%
Catheter related bloodstream infection, No. (%)	45 (17.9)	65 (14.2)	0.195	48.2%	42.7%
Urinary tract infection, No. (%)	25 (9.9)	34 (7.4)	0.257	28.8%	22.0%
Intra-abdominal infection, No. (%)	27 (10.7)	31 (6.8)	0.085	48.3%	39.7%
Skin and soft tissue infection, No. (%)	11 (4.4)	23 (5.0)	0.855	52.9%	35.3%
Primary bacteremia, No. (%)	56 (22.2)	92 (20.0)	0.500	52.0%	46.6%
Central nerve system infection, No. (%)	0 (0.0)	5 (1.1)	0.167	60.0%	40.0%
Surgical site infection, No. (%)	2 (0.8)	3 (0.7)	1.000	80.0%	60.0%
Multisite infection, No. (%)	19 (7.5)	19 (4.1)	0.057	71.1%	57.9%

conditions. Although there are several methods for the detecting *in vitro* biofilm formation, there is currently no gold-standard protocol for its quantification. Furthermore, it is challenging to assess the biofilm formation inside the human body. In addition, the *in vitro* conditions may be quite different from those of the human environment.

In conclusion, this is the first large sample size study on the clinical outcomes of patients with *A. baumannii* bacteremia. Our results demonstrated that the biofilm-forming ability was not an independent risk factor for mortality in patients with *A. baumannii* bacteremia. Patients with *A. baumannii* bacteremia with a greater severity of disease, who were infected with carbapenem-resistant isolates, or had received an inappropriate antimicrobial therapy had worse outcomes. Patients with congestive heart failure were more likely to be infected with biofilm-forming isolates, while those with an arterial line were less likely to be infected with them. Among the patients infected with biofilm-forming isolates, those with hematological malignancies, infected with carbapenem-resistant isolates, and those with greater severity of disease (higher APACHE II scores) were associated with worse clinical outcomes. Further studies are required to establish the optimal treatment for bacteremia caused by the biofilm-forming isolates of *A. baumannii*.

Data availability statement

The raw data supporting the conclusions of this article will be made available by the authors, without undue reservation.

Ethics statement

The studies involving human participants were reviewed and approved by Changhua Christian Hospital (140514) Mackay Memorial Hospital (14MMHIS125) National Taiwan University Hospital (201008047R) Taipei Veterans General Hospital (2015-04-003C) Tri-Service General Hospital (1-103-05-100). Written informed consent for participation was not required for this study in accordance with the national legislation and the institutional requirements.

Author contributions

Conceptualization, T-TC, Y-TL, and Y-CW; Data curation, AC, C-PL, Y-ML, and Y-SY; Formal analysis, T-TC, T-WH, and J-RS; Funding acquisition, Y-TL and Y-CW; Investigation, S-CK, AC, and C-PL; Methodology, T-TC, Y-TL, and Y-CW; Project administration, Y-TL, and Y-CW; Resources, Y-ML, Y-SY, and T-LC; Software, T-WH, J-RS, and S-CK; Supervision, T-LC, Y-TL, and Y-CW; Validation, T-LC, Y-TL, and Y-CW; Visualization, C-PL, Y-ML, and Y-SY; Writing – original draft, T-TC, Y-TL, and Y-CW; Writing – review and editing, T-TC, Y-TL, and Y-CW. All authors contributed to the article and approved the submitted version.

Funding

This work was supported by grants from Taipei Veterans General Hospital [V108C-012, VTA108-T-2-3, VTA109-T-3-2, VTA110-V4-5-2, VTA111-T-3-3], Tri-Service General Hospital [TSGH-E-109237, TSGH-E-110205, TSGH-E-111245], and the Ministry of Science and Technology [MOST-108-2314-B-016 -029, MOST-109-2314-B-016 -056, MOST-110-2314-B-016-063, MOST-110-2314-B-075-072, MOST 108-2314-B-075-034-MY3, MOST 107-2314-B-075-066-MY3].

Conflict of interest

The authors declare that the research was conducted in the absence of any commercial or financial relationships that could be construed as a potential conflict of interest.

Publisher's note

All claims expressed in this article are solely those of the authors and do not necessarily represent those of their affiliated organizations, or those of the publisher, the editors and the reviewers. Any product that may be evaluated in this article, or claim that may be made by its manufacturer, is not guaranteed or endorsed by the publisher.

Supplementary material

The Supplementary Material for this article can be found online at: https://www.frontiersin.org/articles/10.3389/fcimb.2022.964539/full#supplementary-material

References

Badave, G. K., and Kulkarni, D. (2015). Biofilm producing multidrug resistant acinetobacter baumannii: An emerging challenge. *J. Clin. Diagn. Res.* 9, DC08–DC10. doi: 10.7860/JCDR/2015/11014.5398

Barsoumian, A. E., Mende, K., Sanchez, C. J.Jr., Beckius, M. L., Wenke, J. C., Murray, C. K., et al. (2015). Clinical infectious outcomes associated with biofilm-related bacterial infections: a retrospective chart review. *BMC Infect. Dis.* 15, 223. doi: 10.1186/s12879-015-0972-2

Chen, T.-L., Sin, L.-K., Wu, R. C.-C., Shaio, M.-F., Huang, L.-Y., Fung, C.-P., et al. (2007). Comparison of one-tube multiplex PCR, automated ribotyping and intergenic spacer (ITS) sequencing for rapid identification of *Acinetobacter baumannii*. clin. *Microbiol. Infect.* 13, 801–806. doi: 10.1111/j.1469-0691.2007.01744.x

Cisneros, J. M., Reyes, M. J., Pachón, J., Becerril, B., Caballero, F. J., García-Garmendia, J. L., et al. (1996). Bacteremia due to acinetobacter baumannii: epidemiology, clinical findings, and prognostic features. *Clin. Infect. Dis.* 22, 1026–1032. doi: 10.1093/clinids/22.6.1026

CLSI (2006). *Methods for dilution antimicrobial susceptibility tests for bacteria that grow aerobically: Approved standard M7-A7*. Wayne, PA: Clinical and Laboratory Standards Institute.

CLSI (2020). *Performance Standards for Antimicrobial Susceptibility Testing. 30th Ed. CLSI Supplement M100.* Wayne, PA: Clinical and Laboratory Standards Institute.

Del Pozo, J. L. (2018). Biofilm-related disease. *Expert Rev. Anti-Infect Ther.* 16, 51–65. doi: 10.1080/14787210.2018.1417036

Dijkshoorn, L., Nemec, A., and Seifert, H. (2007). An increasing threat in hospitals: multidrug-resistant acinetobacter baumannii. *Nat. Rev. Microbiol.* 5, 939–951. doi: 10.1038/nrmicro1789

Donadu, M. G., Mazzarello, V., Cappuccinelli, P., Zanetti, S., Madléna, M., Nagy, ÁL., et al. (2021). Relationship between the biofilm-forming capacity and antimicrobial resistance in clinical acinetobacter baumannii isolates: results from a laboratory-based *in vitro* study. *Microorganisms* 9(11):2384. doi: 10.3390/microorganisms9112384

Garner, J. S., Jarvis, W. R., Emori, T. G., Horan, T. C., and Hughes, J. M. (1988). CDC Definitions for nosocomial infections, 1988. *Am. J. Infect. Control.* 16, 128–140. doi: 10.1016/0196-6553(88)90053-3

Gedefie, A., Demsis, W., Ashagrie, M., Kassa, Y., Tesfaye, M., Tilahun, M., et al. (2021). Acinetobacter baumannii biofilm formation and its role in disease pathogenesis: A review. *Infect. Drug Resist.* 14, 3711–3719. doi: 10.2147/IDR.S332051

Høiby, N., Bjarnsholt, T., Givskov, M., Molin, S., and Ciofu, O. (2010). Antibiotic resistance of bacterial biofilms. *Int. J. Antimicrob. Agents.* 35, 322–332. doi: 10.1016/j.ijantimicag.2009.12.011

Høiby, N., Bjarnsholt, T., Moser, C., Bassi, G. L., Coenye, T., Donelli, G., et al. (2015). ESCMID guideline for the diagnosis and treatment of biofilm infections 2014. *Clin. Microbiol. Infect.* 21 Suppl 1, S1–25. doi: 10.1016/j.cmi.2014.10.024

Høiby, N., Bjarnsholt, T., Moser, C., Bassi, G. L., Coenye, T., Donelli, G., et al. (2015). ESCMID guideline for the diagnosis and treatment of biofilm infections 2014. *Clin. Microbiol. Infect.* 21, S1–25. doi: 10.1016/j.cmi.2014.10.024

Hall-Stoodley, L., Costerton, J. W., and Stoodley, P. (2004). Bacterial biofilms: from the natural environment to infectious diseases. *Nat. Rev. Microbiol.* 2, 95–108. doi: 10.1038/nrmicro821

Harrison, J. J., Ceri, H., and Turner, R. J. (2007). Multimetal resistance and tolerance in microbial biofilms. *Nat. Rev. Microbiol.* 5, 928–938. doi: 10.1038/nrmicro1774

Kopterides, P., Koletsi, P. K., Michalopoulos, A., and Falagas, M. E. (2007). Exposure to quinolones is associated with carbapenem resistance among colistin-susceptible acinetobacter baumannii blood isolates. *Int. J. Antimicrob. Agents.* 30, 409–414. doi: 10.1016/j.ijantimicag.2007.06.026

Law, S. K. K., and Tan, H. S. (2022). The role of quorum sensing, biofilm formation, and iron acquisition as key virulence mechanisms in acinetobacter baumannii and the corresponding anti-virulence strategies. *Microbiol. Res.* 260, 127032. doi: 10.1016/j.micres.2022.127032

Lee, Y. T., Kuo, S. C., Yang, S. P., Lin, Y. T., Tseng, F. C., Chen, T. L., et al. (2012). Impact of appropriate antimicrobial therapy on mortality associated with acinetobacter baumannii bacteremia: Relation to severity of infection. *Clin. Infect. Dis.* 55, 209–215. doi: 10.1093/cid/cis385

Lewis, K. (2001). Riddle of biofilm resistance. *Antimicrob. Agents Chemother.* 45, 999–1007. doi: 10.1128/AAC.45.4.999-1007.2001

Liu, C. P., Chiang, T. T., Liu, Y. M., Kuo, S. C., Yang, Y. S., Lee, Y. T., et al. (2019). A multicenter study on clinical characteristics of acinetobacter bacteremia in patients with liver cirrhosis. *J. Microbiol. Immunol. Infect. Wei mian yu gan ran za zhi.* 52, 956–965. doi: 10.1016/j.jmii.2018.03.001

Mah, T. F., and O'Toole, G. A. (2001). Mechanisms of biofilm resistance to antimicrobial agents. *Trends Microbiol.* 9, 34–39. doi: 10.1016/s0966-842x(00)01913-2

Martí, S., Rodríguez-Baño, J., Catel-Ferreira, M., Jouenne, T., Vila, J., Seifert, H., et al. (2011). Biofilm formation at the solid–liquid and air–liquid interfaces by acinetobacter species. *BMC Res. Notes.* 4, 5. doi: 10.1186/1756-0500-4-5

Olsen, I. (2015). Biofilm-specific antibiotic tolerance and resistance. *Eur. J. Clin. Microbiol. Infect. Dis.* 34, 877–886. doi: 10.1007/s10096-015-2323-z

O'Toole, G. A., Pratt, L. A., Watnick, P. I., Newman, D. K., Weaver, V. B., and Kolter, R. (1999). Genetic approaches to study of biofilms. *Methods Enzymol.* 310, 91–109. doi: 10.1016/s0076-6879(99)10008-9

Peleg, A. Y., Seifert, H., and Paterson, D. L. (2008). *Acinetobacter baumannii*: emergence of a successful pathogen. *Clin. Microbiol. Rev.* 21, 538–582. doi: 10.1128/CMR.00058-07

Qi, L., Li, H., Zhang, C., Liang, B., Li, J., Wang, L., et al. (2016). Relationship between antibiotic resistance, biofilm formation, and biofilm-specific resistance in acinetobacter baumannii. *Front. Microbiol.* 7. doi: 10.3389/fmicb.2016.00483

Rao, R. S., Karthika, R. U., Singh, S. P., Shashikala, P., Kanungo, R., Jayachandran, S., et al. (2008). Correlation between biofilm production and multiple drug resistance in imipenem resistant clinical isolates of acinetobacter baumannii. *Indian J. Med. Microbiol.* 26, 333–337. doi: 10.4103/0255-0857.43566

Rodríguez-Baño, J., Martí, S., Soto, S., Fernández-Cuenca, F., Cisneros, J. M., Pachón, J., et al. (2008). Biofilm formation in acinetobacter baumannii: Associated features and clinical implications. *Clin. Microbiol. Infect.* 14, 276–278. doi: 10.1111/j.1469-0691.2007.01916.x

Villegas, M. V., and Hartstein, A. I. (2003). Acinetobacter outbreaks, 1977–2000. *Infect. Control Hosp. Epidemiol.* 24, 284–295. doi: 10.1086/502205

Wang, Y. C., Huang, T. W., Yang, Y. S., Kuo, S. C., Chen, C. T., Liu, C. P., et al. (2018). Biofilm formation is not associated with worse outcome in acinetobacter baumannii bacteraemic pneumonia. *Sci. Rep.* 8, 7289. doi: 10.1038/s41598-018-25661-9

Wang, Y. C., Kuo, S. C., Yang, Y. S., Lee, Y. T., Chiu, C. H., Chuang, M. F., et al. (2016). Individual or combined effects of meropenem, imipenem, sulbactam, colistin, and tigecycline on biofilm-embedded acinetobacter baumannii and biofilm architecture. *Antimicrob. Agents Chemother.* 60, 4670–4676. doi: 10.1128/AAC.00551-16

Wong, D., Nielsen, T. B., Bonomo, R. A., Pantapalangkoor, P., Luna, B., and Spellberg, B. (2017). Clinical and pathophysiological overview of *Acinetobacter* infections: a century of challenges. *Clin. Microbiol. Rev.* 30, 409–447. doi: 10.1128/CMR.00058-16

Zhang, D., Xia, J., Xu, Y., Gong, M., Zhou, Y., Xie, L., et al. (2016). Biological features of biofilm-forming ability of acinetobacter baumannii strains derived from 121 elderly patients with hospital-acquired pneumonia. *Clin. Exp. Med.* 16, 73–80. doi: 10.1007/s10238-014-0333-2

frontiers | Frontiers in Cellular and Infection Microbiology

TYPE Original Research
PUBLISHED 24 October 2022
DOI 10.3389/fcimb.2022.951049

OPEN ACCESS

EDITED BY
Milena Dropa,
Faculty of Public Health, University of São Paulo, Brazil

REVIEWED BY
Rafael Vignoli,
Universidad de la República, Uruguay
Helia Magaly Bello-Toledo,
University of Concepcion, Chile

*CORRESPONDENCE
Daniela Centrón
dcentron@gmail.com

SPECIALTY SECTION
This article was submitted to Clinical Microbiology, a section of the journal Frontiers in Cellular and Infection Microbiology

RECEIVED 23 May 2022
ACCEPTED 29 September 2022
PUBLISHED 24 October 2022

CITATION
Knecht CA, García Allende, N, Álvarez VE, Prack McCormick B, Massó MG, Piekar M, Campos J, Fox B, Camicia G, Gambino AS, Leguina ACdV, Donis N, Fernández-Canigia L, Quiroga MP and Centrón D (2022) Novel insights related to the rise of KPC-producing *Enterobacter cloacae* complex strains within the nosocomial niche. *Front. Cell. Infect. Microbiol.* 12:951049. doi: 10.3389/fcimb.2022.951049

Novel insights related to the rise of KPC-producing *Enterobacter cloacae* complex strains within the nosocomial niche

Camila A. Knecht[1], Natalia García Allende[2], Verónica E. Álvarez[1], Barbara Prack McCormick[1,3], Mariana G. Massó[1], María Piekar[1], Josefina Campos[4], Bárbara Fox[5], Gabriela Camicia[1], Anahí S. Gambino[1], Ana Carolina del Valle Leguina[1], Nicolás Donis[1], Liliana Fernández-Canigia[5], María Paula Quiroga[1] and Daniela Centrón[1]*

[1]Laboratorio de Investigaciones en Mecanismos de Resistencia a Antibióticos, Instituto de Investigaciones en Microbiología y Parasitología Médica, Facultad de Medicina, Universidad de Buenos Aires - Consejo Nacional de Investigaciones Científicas y Técnicas (IMPaM, UBA-CONICET), Ciudad Autónoma de Buenos Aires, Argentina, [2]Servicio de Infectología y Epidemiología Hospitalaria, Hospital Alemán, Ciudad Autónoma de Buenos Aires, Buenos Aires, Argentina, [3]Facultad de Ciencias Agrarias, Universidad Nacional de Lomas de Zamora (FCA, UNLZ), Lomas de Zamora, Argentina, [4]Plataforma de Genómica y Bioinformática, Instituto Nacional de Enfermedades Infecciosas-Administración Nacional de Laboratorios e Institutos de Salud (INEI-ANLIS), Ciudad Autónoma de Buenos Aires, Argentina, [5]Departamento de Microbiología, Hospital Alemán, Ciudad Autónoma de Buenos Aires, Buenos Aires, Argentina

According to the World Health Organization, carbapenem-resistant *Enterobacteriaceae* (CRE) belong to the highest priority group for the development of new antibiotics. Argentina-WHONET data showed that Gram-negative resistance frequencies to imipenem have been increasing since 2010 mostly in two CRE bacteria: *Klebsiella pneumoniae* and *Enterobacter cloacae* Complex (ECC). This scenario is mirrored in our hospital. It is known that *K. pneumoniae* and the ECC coexist in the human body, but little is known about the outcome of these species producing KPC, and colonizing or infecting a patient. We aimed to contribute to the understanding of the rise of the ECC in Argentina, taking as a biological model both a patient colonized with two KPC-producing strains (one *Enterobacter hormaechei* and one *K. pneumoniae*) and *in vitro* competition assays with prevalent KPC-producing ECC (KPC-ECC) versus KPC-producing *K. pneumoniae* (KPC-Kp) high-risk clones from our institution. A KPC-producing *E. hormaechei* and later a KPC-Kp strain that colonized a patient shared an identical novel conjugative IncM1 plasmid harboring bla_{KPC-2}. In addition, a total of 19 KPC-ECC and 58 KPC-Kp strains isolated from nosocomial infections revealed that high-risk clones KPC-ECC ST66 and ST78 as well as KPC-Kp ST11 and ST258 were prevalent and selected for competition assays. The competition assays with KCP-ECC ST45, ST66, and ST78 versus KPC-Kp ST11, ST18, and ST258 strains analyzed here showed no statistically significant difference. These assays evidenced that high-risk clones of KPC-ECC and KPC-Kp can coexist in the same hospital environment

including the same patient, which explains from an ecological point of view that both species can exchange and share plasmids. These findings offer hints to explain the worldwide rise of KPC-ECC strains based on the ability of some pandemic clones to compete and occupy a certain niche. Taken together, the presence of the same new plasmid and the fitness results that showed that both strains can coexist within the same patient suggest that horizontal genetic transfer of bla_{KPC-2} within the patient cannot be ruled out. These findings highlight the constant interaction that these two species can keep in the hospital environment, which, in turn, can be related to the spread of KPC.

KEYWORDS

***Klebsiella pneumoniae*, *Enterobacter cloacae* complex, carbapenem-resistance, bla_{KPC-2}, Argentina**

Introduction

Since 2017, the World Health Organization has classified pathogens depending on their priority for the development of new antibiotics as critical, high, and medium (World Health Organization, 2017). Carbapenem-resistant *Enterobacteriaceae* (CRE) were categorized as critical priority pathogens. This group includes bacteria that have become resistant to the best antibiotic options treatment available: carbapenems and third-generation cephalosporins. These bacteria pose a threat in healthcare facilities, especially among patients whose care requires invasive devices (Wang et al., 2016). In Argentina, carbapenem-resistant isolates rose from 10% to 32.7% in the case of *K. pneumoniae* and from 5% to 12% in the case of *Enterobacter cloacae* Complex (ECC) from 2010 until 2021 (Red WHONET Argentina). Accordingly, ECC has been reported as the second most common CRE in several countries (Tavares et al., 2015; Jia et al., 2018; Annavajhala et al., 2019; Falco et al., 2021; Hansen, 2021), with *E. cloacae* and *E. hormaechei* being the prevalent multidrug-resistant (MDR) clinical isolates (Annavajhala et al., 2019). *Enterobacter hormaechei* is part of the ECC together with 22 other species that are closely genotypically related, and little is known about its fitness within the nosocomial environment (Davin-Regli et al., 2019). Total genome sequences of various *Enterobacter* spp. have shown that *E. hormaechei* has often been misidentified by routine identification techniques (Davin-Regli et al., 2019). Therefore, its importance in the clinical environment could have been underestimated; however, outbreaks of *E. hormaechei* have been reported in the past (Campos et al., 2007; Paauw et al., 2009).

Among the plasmid-born resistance mechanisms that account for carbapenem resistance, the production of KPC has remained predominant (Bonomo et al., 2018). The most common variants of the gene that codifies for KPC are bla_{KPC-2} and bla_{KPC-3} (Brandt et al., 2019), which have become endemic in several countries (Frost et al., 2019). Argentina is among these countries, and apart from clinical isolates, bla_{KPC-2} has also been recently detected in sewage (Ghiglione et al., 2021). The bla_{KPC} genes have been found in more than 257 different representative KPC plasmids (Brandt et al., 2019) belonging to diverse Inc groups and sizes, and with several features that account for their success. Carbapenem-resistant (CR) *Klebsiella pneumoniae* (CRKP) strains carrying KPC (KPC-Kp) have been long known to represent a threat to human health causing severe infections that are difficult to treat (Heiden et al., 2020). Also, the ECC has lately awoken interest due to its increasing resistance to carbapenems codified by several genes found in isolates all over the globe (Annavajhala et al., 2019). Outbreaks take place mainly in low- and middle-income countries (BARNARDS Group et al., 2021) and are particularly dangerous for children and newborns (Girlich et al., 2021). Unlike KPC-Kp, not only stable bla_{KPC}–high-risk clones associations account for the spread of KPC-ECC but also the acquisition of plasmids by diverse clones (Annavajhala et al., 2019). To be considered high-risk clones, the lineages must meet several characteristics: to be globally distributed, to possess several acquired antimicrobial resistance genes, to be able to colonize and persist in hosts for long periods, to be transmitted effectively among hosts, to cause severe and/or recurrent infections, and to have enhanced pathogenicity and fitness (Mathers et al., 2015).

Fitness is a fundamental notion in evolutionary biology. When compared with their less-fit competitors, genotypes with better fitness tend to produce more offspring and hence increase in frequency over time (Wiser and Lenski, 2015). High-risk clones are likely to have advantageous biological traits that boost their fitness, giving them an evolutionary advantage over other isolates of the same species (Pitout and Finn, 2020). Such traits provide them with the capacity to outperform competing bacteria and to establish as the dominant component of the

bacterial community. Even though there are several methods to quantify microbial fitness, the approach that most closely corresponds to the meaning of fitness in evolutionary theory uses a competition assay (Wiser and Lenski, 2015). Competition assays between isogenic strains are common (Sander et al., 2002; Guo et al., 2012), but much less is explored about lineages or interspecies competitions that share the same ecological niche (Hafza et al., 2018; Ávarez et al., 2020).

The aim of this study was to investigate the interplay of KPC-ECC challenged with prevalent high-risk KPC-Kp clones from our institution including strains isolated from the same patient to understand if fitness contributes to the success of KPC-ECC within the nosocomial niche.

Results

Epidemiology of carbapenem-resistant *Enterobacteriaceae* strains isolated from nosocomial infections from October 2018 until December 2020 in our institution

From October 2018 until December 2020, a study with surveillance purposes identified 153 CRE strains isolated from nosocomial infections in our institution. This survey revealed that *K. pneumoniae* accounted for 85% of CRE, 12% were the ECC, and the remaining 3% were other CRE species. Whole-genome sequencing (WGS) of KPC-Kp (n = 58) and KPC-ECC (n = 19) nosocomial strains was sequenced by Illumina MiSeq-I (n = 77). Their MLST profiles were assigned using the pubMLST database (Table S1; Jolley et al., 2018). We identified that high-risk clones KPC-Kp ST258 and ST11, and KPC-ECC ST66 and ST78 were found among infected patients (Table S1). Also, for the taxonomical identification of ECC strains, we combined the results obtained with rMLST, which identified the HA2pEho, HAC11Eho, and HA58Eho strains as *E. hormaechei*, with those obtained by Kraken 2 (Wood et al., 2019); the same outcome was obtained with some extra information about the subspecies and the absence of contaminations (Table S7). By ANI (Jain et al., 2018) and *in silico* DNA–DNA hybridization (Meier-Kolthoff et al, 2022), we obtained additional information on the subspecies, identifying *E. hormaechei* HA2pEho ST45, HAC11Eho ST78, and HA58Eho ST66 as belonging to different subspecies (Tables S8 and S9). These results were also in agreement with those obtained with Kraken 2. The KPC-producing *E. hormaechei* HAC11Eho subspecies *hoffmannii* (ST78), *E. hormaechei* HA58Eho subspecies *xiangfangensis* (ST66), *K. pneumoniae* HA3pKpn (ST258), and *K. pneumoniae* HA15pKpn (ST11) strains from this survey were chosen for fitness assays.

Novel and conjugative IncM1 pDCCK1-KPC plasmid carrying bla_{KPC-2} shared by both KPC-producing strains colonizing the same patient

On 20 November 2018, a 71-year-old man (patient M71) was admitted to our hospital with febrile syndrome (Figure S1). After 1 week of hospitalization, surgical debridement of sacral pressure ulcer was performed. A carbapenemase-producing strain was isolated from a vital tissue wound swab. After a new hospitalization in January 2019, a rectal swab was taken for surveillance purposes; a carbapenem-resistant strain was isolated. Through WGS, the first colonizing strain was identified as *E. hormaechei* subspecies *steigerwaltii* belonging to the ST45 (HA2pEho). The second strain was identified as KPC-Kp belonging to the sequence type ST18 (HA7pKpn).

The outcome of the search for antibiotic resistance genes (ARGs) and the determination of antibiotype profiles are shown in Figure 1. Genome analysis and phenotypic resistance profile showed that both strains were MDR, i.e., resistant to more than three classes of antibiotics but still susceptible to more than two classes of antibiotics (Magiorakos et al., 2012). Apart from bla_{KPC-2}, two other genes were shared by both strains, *aph(3")-Ib* and *aph(6)-Id*, conferring resistance to streptomycin. Besides the ARG they had in common, *E. hormaechei* HA2pEho carried bla_{ACT-70} (naturally harbored by the species), bla_{TEM-1}, *catA2*, *qnrB19*, and *sul2*. The gene cassette *dfrA14* was identified in the variable region of a class 1 integron. *K. pneumoniae* HA7pKpn carried $bla_{SHV-215}$ (naturally harbored by the species), *fosA5*, *oqxA*, *oqxB*, and *tet*(C). In addition, the gene cassette *dfrA5* was found within the variable region of a clinical class 1 integron with the 3′-conserved sequence harboring *qacEΔ1* and *sul1*. Minimum inhibitory concentrations (MICs) are shown in Table S2.

Genome analysis revealed that *E. hormaechei* HA2pEho and *K. pneumoniae* HA7pKpn strains carried several plasmids (Table S3). A virulence multireplicon IncHI1B/IncFIB plasmid was found in *K. pneumoniae* HA7pKpn, and a Col(pHAD28), an IncFIB(pECLA), an IncFII(pECLA), and a pKP1433 were found in *E. hormaechei* HA2pEho. In addition, a novel IncM1 plasmid named pDCCK1-KPC carrying bla_{KPC-2} was identical in both strains (Figure 2). In both cases, the whole sequence of the plasmid pDCCK1-KPC was on a single contig. In the case of *E. hormaechei* HA2pEho, the contig was 76,978 bp long, and in the case of *K. pneumoniae* HA7pKpn, it was 77,218 bp. The contiguousness of the extremes of the contigs was verified by PCR using specially designed primers. The best hit of pDCCK1-KPC against the BLAST database was plasmid pIP69 (MN626603.1) with 81% of cover and 99.98% identity. This plasmid was isolated in 1969 from a *Salmonella paratyphi* strain (Chabbert et al., 1972), and in comparison with pDCCK1-KPC, pIP69 lacked the bla_{KPC-2} gene and its flanking sequences (16,008 bp) (Neil et al., 2020). Although the plasmid

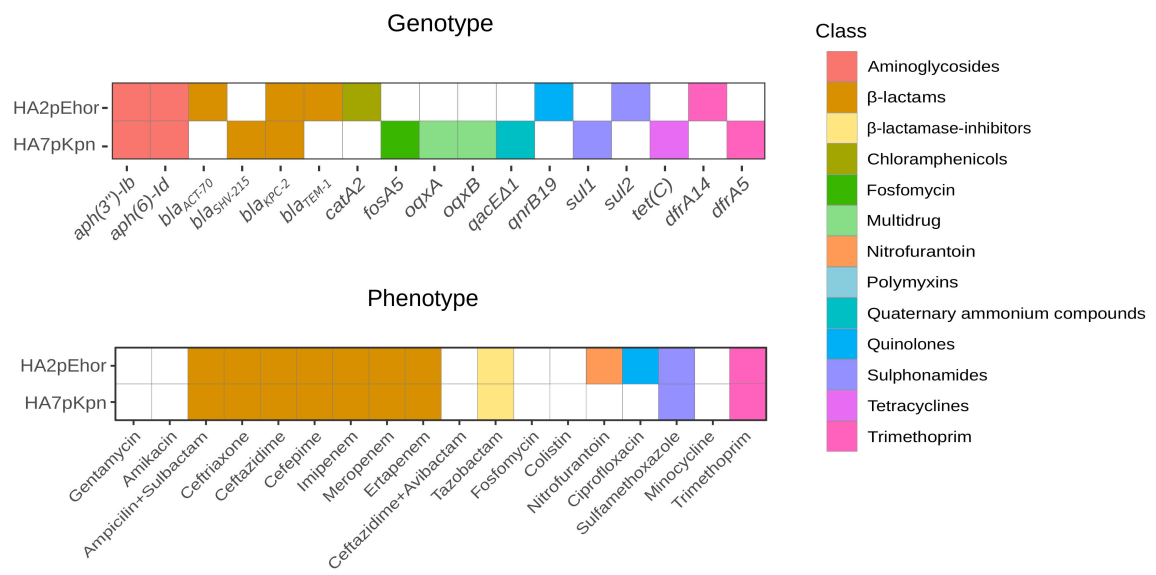

FIGURE 1
Antibiotic resistance genes and antibiotype profiles of *E. hormaechei* HA2pEho, *K. pneumoniae*, and HA7pKpn strains isolated from colonizations. Colored cell means presence and different colors indicate the antibiotic class for which the ARG codifies. The lower panel shows the resistance phenotype, and the upper panel shows the resistance genotype. The figure was made in R using the package ggplot2.

pECL189-1 (CP047966.1) covers the whole region, which was absent in plasmid pIP69, the genetic arrangement was different, and the genes, in that case, were not contiguous. Apart from the bla_{KPC-2} gene, the pDCCK1-KPC plasmid carried several genes that likely account for its success such as a mercury resistance island, the gene *parM*, a toxin–antitoxin system *pemI–pemK*, and the *umuCD* operon. Conjugation assays were carried out between *E. hormaechei* HA2pEho and *K. pneumoniae* HA7pKpn as donor strains and *Escherichia coli* J53 as a recipient strain. Both assays were positive, confirming that pDCCK1-KPC can be horizontally transferred. Determination of MIC of transconjugants revealed that pDCCK1-KPC only transfers resistance to β-lactams including carbapenems (Table S2). This result is in agreement with the composition of pDCCK1-KPC that only carries one ARG, the bla_{KPC-2} gene.

A genetic platform of 17,092 bp involved in the dissemination of bla_{KPC-2} was identified as Tn*3*-IS*Apu1*-IS*Apu2*-IS*Kpn27*-bla_{KPC-2}-IS*Kpn6*-*korC*-orf-*klcA*-*repB*-*hin*-Tn*3* in pDCCK1-KPC showing some differences with sequences available at the NCBI database (Figure S2). A very closely related core platform Tn*3*-IS*Kpn27*-Δbla_{TEM-1}-bla_{KPC-2}-IS*Kpn6*-*korC*-orf-*klcA*-*repB* was described by Shen et al. (2009) and was later called variant 1. Also, a similar genetic platform was described in Argentina in 2011 (Gomez et al., 2011), in 2018 (De Belder et al., 2018), and more recently in 2021 (Ghiglione et al., 2021), whereas an identical platform was found in our institution (Knecht et al, 2022). In the genetic platform of both *K. pneumoniae* HA7pKpn and *E. hormaechei* HA2pEho, Δbla_{TEM-1} was missing, and nucleotides between IS*Kpn27* and bla_{KPC-2} were only 254 bp. Moreover, a related genetic platform with the gene *hin* upstream from *repB*, more similar to our platform, was found by Dong et al. (2020). In all these cases, the genetic platform carrying bla_{KPC-2} was in IncP or IncR plasmids, as the main difference with pDCCK1-KPC, which corresponded to an IncM1 replicon. Although these genetic platforms are not the most frequent for the dissemination of bla_{KPC-2}, they were identified in clinical and environmental isolates on a global scale (Table S4). The sequences found in the NCBI database that were most similar to the genetic platform found in pDCCK1-KPC covered 13,475 bp of the platform (Table S4). This search resulted in 111 hits, 89 of which were *Enterobacteriaceae*, and among them, 73 were *K. pneumoniae* and 2 were *E. cloacae*. Other bacteria belonging to different taxa with 99%–100% of query cover were two *Pseudomonas aeruginosa* and eight *Aeromonas* spp.

In vitro competition between high-risk clones of KPC-producing strains of *Enterobacter cloacae* Complex and *Klebsiella pneumoniae*

To understand the interplay in the success of the two prevalent CRE in the nosocomial niche from our institution, we compared the fitness of prevalent high-risk clones of KPC-ECC and KPC-Kp strains. The study of clonal competition was

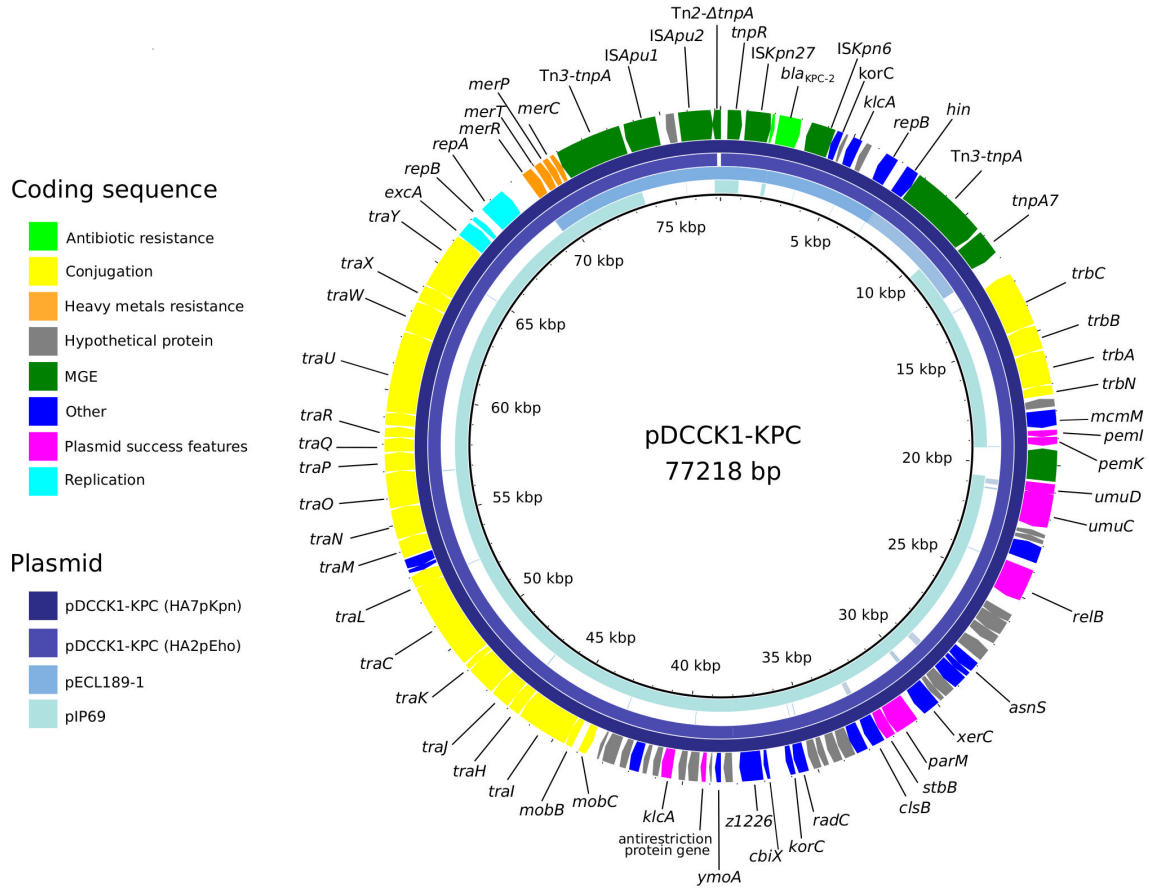

FIGURE 2
Fitness assays between KPC-ECC and KPC-Kp clones. KPC-*E. hormaechei* ST45 (HA2pEho), ST66 (HA58Eho), and ST78 (HAC11Eho) were set to compete with KPC-*K. pneumoniae* ST11 (HA15pKpn), ST18 (HA7pKpn), and ST258 (HA3pKpn). *E. hormaechei* ST45 and *K. pneumoniae* ST18 are the sequenced strains described in this study, and the other STs are high-risk clones found in our institution during a surveillance program (Table S1). In the cases where the values are above zero, it can be interpreted that ECC clones outcompete *K. pneumoniae* clones. The figure was made in R using the package ggplot2.

carried out in a biological model without antibiotic pressure in order to replicate what can happen in the hospital environment, in which there are niches where an antibiotic pressure is not exerted directly, for example, on abiotic surfaces.

We carried out *in vitro* competition of KPC-producing *E. hormaechei* HA2pEho ST45, *E. hormaechei* HA58Eho ST66, and *E. hormaechei* HAC11Eho ST78 versus *K. pneumoniae* HA15pKpn ST11, *K. pneumoniae* HA7pKpn ST18, and *K. pneumoniae* HA3pKpn ST258 in the absence of antimicrobial pressure (Figure 3; Tables S5 and S6). In addition, maintenance assays of bla_{KPC-2} showed that this gene remains present in the absence of selective pressure for all these strains during the time of competitions. Both *E. hormaechei* ST66 and ST78, and *K. pneumoniae* ST258 and ST11 represent high-risk international clones and are also the most frequently found in our institution, in contrast to the other high-risk clone analyzed here, *E. hormaechei* ST45 (Table S1). Taking into account the clonal competitions involving *E. hormaechei* HA2pEho ST45, with *K. pneumoniae* HA7pKpn ST18 or with *K. pneumoniae* HA3pKpn ST258, we found that *E. hormaechei* HA2pEho ST45 showed a positive S value and fitness cost of −2.874 and −5,981%, respectively. These results indicate that *E. hormaechei* HA2pEho ST45 has a competitive advantage over these two *K. pneumoniae* ST18 and ST258 isolates. The opposite was shown for the clonal competition of *E. hormaechei* HA2pEho ST45 with *K. pneumoniae* HA15pKpn ST11. For the clonal competitions of *E. hormaechei* HAC11Eho ST78 with the three *K. pneumoniae* ST11, ST18, and ST258 strains, the S values and fitness costs obtained were opposite of those obtained for *E. hormaechei* HA2pEho ST45. The clonal competitions carried out showed only tendencies, since none of the results obtained were statistically significant. The clearer differences were obtained for *E. hormaechei* ST66 over *K. pneumoniae* ST18 and for *K. pneumoniae* ST258 over *E. hormaechei* ST78, which showed a

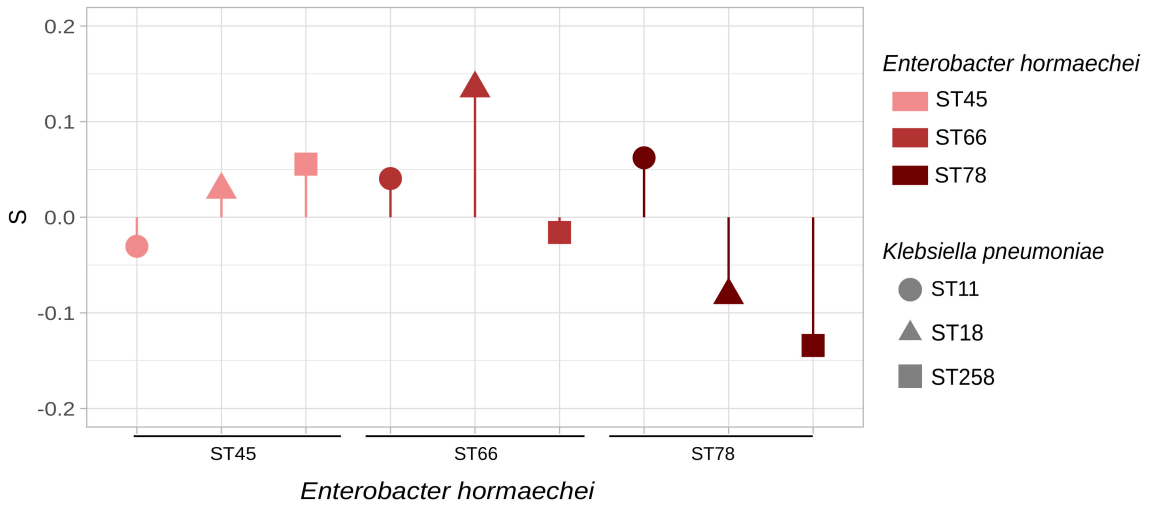

FIGURE 3
Plasmid pDCCK1-KPC from *E. hormaechei* HA2pEho and *K. pneumoniae* HA7pKpn strains and genetic platform of bla_{KPC-2}. Alignment of the novel plasmid pDCCK1-KPC against pIP69 (MN626603.1) and pECL189-1 (CP047966.1). The figure was made using BRIG.

fitness cost >10% (13,919% and −13,476, respectively). Previous studies reported that the greater the difference in growth rate between two strains, the greater the bacterial load difference over time (Guo et al., 2012). This fact was not confirmed in the case of competitions with *E. hormaechei* ST45, ST66, and ST78, and the *K. pneumoniae* ST11, ST18, and ST258 strains analyzed here. This indicates that competitions between clones have emerging properties resulting from their interactions while growing in the same niche.

Although general comparisons can shed light on the reasons for the prevalence of particular clones, the acquired antimicrobial resistance and virulence genes of a particular strain will also determine why it surpasses another under specific conditions. It has been proposed that differences in antimicrobial resistance and virulence factors such as secretion systems should be under consideration altogether and that even small genomic modifications play a role in determining the clonal competence of pathogens (Álvarez et al., 2020). Therefore, we investigated the presence of secretion systems in the two KPC strains isolated from patient M71. Twelve core genes (*gspCDEFGHIJKLMNO*) of a type II secretion system were identified in both strains colonizing patient M71. *K. pneumoniae* HA7pKpn carried type I and type II secretion system components, and *E. hormaechei* HA2pEho also encoded for proteins related to secretion system type IV. The type I secretion system was represented by the genes *hlyB*, *hlyD*, *prsE*, *tolC*, *macA*, and *macB* in HA2pEho and by *tolC*, *macA*, and *macB* in *K. pneumoniae* HA7pkpn. The type IV secretion system is related to the conjugation system of bacteria and directly transfers effector proteins to the host cytosol through a central pore (Voth et al., 2012). All the genes of the *virB*/*D4* complex that constitute one type of secretion system IVA were found in *E. hormaechei* HA2pEho except for *virB7* and *virD4*.

Discussion

Our results contribute to the understanding of both the dissemination of the most clinically relevant carbapenemase, bla_{KPC-2} in the ECC, and the role of fitness of high-risk clones in the rise of KPC-ECC within the nosocomial environment in colonized as well as in infected patients. Since phenotypic methods or even the traditionally employed 16S rRNA gene typing is insufficient to resolve the species identification of the ECC strains (Annavajhala et al., 2019), little is known concerning their dissemination in Latin America. The molecular survey performed during the period from October 2018 until December 2020 at our institution allowed us to infer the first data on circulating clones in our geographical region, which detected high-risk clones *E. hormaechei* ST45 (subspecies *steigerwaltii*), ST66 (subspecies *xiangfangensis*), and ST78 (subspecies *hoffmannii*). Interestingly, the same STs were also the most prevalent found among carbapenem-resistant ECC (CRECC) isolates in France, but in that case, the carbapenemase genes responsible for the phenotype were alleles of the gene bla_{VIM} (Emeraud et al., 2022). As expected, despite constant changes regarding nomenclature within the ECC, *E. cloacae* and *E. hormaechei* continue to prevail among multidrug clinical isolates (Annavajhala et al., 2019). *E. hormaechei* ST171, ST114, and ST66 belong to CC114 and

have been found to be widespread among global CRECC isolates from several countries (Peirano et al., 2018). On the other hand, *E. hormaechei* ST78 was identified as a high-risk clone among both extended-spectrum β-lactamase-producing ECC and CRECC (Gomez-Simmonds et al., 2018; Emeraud et al., 2022). *E. hormaechei* ST45 is recognized as a high-risk clone (Izdebski et al., 2015) reported in Australia (Sidjabat et al., 2015), Colombia (Falco et al., 2021), Chile (Wozniak et al., 2021), Germany (Heiden et al., 2020), Spain (Fernández et al., 2015), and other countries in Europe (Izdebski et al., 2015). As a whole, these results suggest that the establishment of successful high-risk clones of *E. hormaechei* in the nosocomial niche provides the opportunity to evolve to MDR phenotypes mediated by the acquisition and maintenance of diverse plasmids, which may have been substantial contributors to the continuous rise of CRECC.

The gene bla_{KPC-2} was in the same conjugative plasmid in both strains from inpatient M71. The novel plasmid that we called pDCCK1-KPC belongs to the IncM1 incompatibility group. According to a review on bla_{KPC} plasmids (Brandt et al., 2019), IncM plasmids were unusual at least until 2019, when just 7 out of 435 plasmids belonged to this incompatibility group. Plasmid pDCCK1-KPC is a novel rearrangement between plasmids leading to the acquisition of a new KPC-2 genetic platform by an IncM1 plasmid. These multiple events of loss and/or gain of mobile genetic elements that also include insertions, deletions, or homologous recombination coincide with what was identified for the dissemination of bla_{KPC-2} in previous works. Similar plasmids show traces of multiple events, with partial mobile genetic elements scattered throughout its genetic platform (Botts et al., 2017; Brandt et al., 2019; Ghiglione et al., 2021).

It cannot be ruled out that pDCCK1-KPC might have been transferred from *E. hormaechei* HA2pEho to *K. pneumoniae* HA7pKpn within the patient, although it is not possible to confirm it. Putative HGT of bla_{KPC-2} has been previously reported to have taken place intrapatient (Anchordoqui et al., 2015; Wozniak et al., 2021). The study by Anchordoqui et al. (2015) was also carried out in Argentina, and HGT was reported to have taken place between *E. coli* and *K. pneumoniae*, *E. cloacae* and *K. pneumoniae*, and *Citrobacter freundii* and *Klebsiella oxytoca*. In this case, the STs of strains were not determined, and plasmids belonged to different incompatibility groups including IncM/L but were not sequenced.

A very closely related genetic platform carrying bla_{KPC-2} was found contemporary to strains isolated from inpatient M71 in environmental strains *Enterobacter absuriae* WW14A and *Klebsiella quasipneumoniae* subsp. *quasipneumoniae* WW19C, which were recovered from the same sewage network of our institution in 2018 (Ghiglione et al., 2021). Therefore, our study also reinforces the need for studying the spread of critical acquired ARG within the One Health perspective. Since it is not possible to identify the direction of the ARG flow, the role of the environment either as a source or as a reservoir of the bla_{KPC-2} gene is confirmed in our findings. The platform Tn*3*-IS*Apu1*-IS*Apu2*-IS*Kpn27*-bla_{KPC-2}-IS*Kpn6*-*korC*-orf-*klcA*-*repB*-*hin*-Tn*3* (17092 bp) was identical to the one recently found in another clinical isolate from our institution (Knecht et al., 2022). In comparison with the platform in sewage strains, both its location in a different plasmid and the lack of Δbla_{TEM-1} highlight the ability of bla_{KPC-2}-flanking sequences to evolve, extending the spreading range.

The competition assays with *E. hormaechei* ST45, ST66, and ST78, and the *K. pneumoniae* ST11, ST18, and ST258 strains analyzed here showed only slight differences in the values obtained. The results obtained for the clonal competitions of the three high-risk clones of *E. hormaechei* with no statistically significant difference with the *K. pneumoniae* ST11, ST18, and ST258 strains analyzed could explain in part the co-occurrence of KPC-Kp and KPC-ECC in clinical isolates. As a consequence, these species can share the same plasmids such as pDCCK1-KPC as the main contributors to the global spread of KPC.

The fact that high-risk international clones of KPC-ECC and KPC-Kp can coexist successfully within the nosocomial niche is in agreement with the steady rise of KPC-ECC observed in Argentina since 2010 (WHONET Argentina Network) and other countries like Brazil (Tavares et al., 2015), Colombia (Falco et al., 2021), USA (Annavajhala et al., 2019; Hansen, 2021), China (Jia et al., 2018), Portugal, and India (Center for Disease Dynamics, Economics & Policy). Accordingly, a decrease in KPC-ECC strains in our hospital is not expected despite the prevalence and fruitful spread of high-risk international clones of KPC-Kp ST258 and ST11. Since both these high-risk clones are disseminated worldwide, a replica of this scenario is likely to occur in other regions.

Considering that fitness studies have previously helped to understand the emergence of relevant antimicrobial-resistant lineages (Luo et al., 2005; Otto, 2013; Ávarez et al., 2020; Hertz et al., 2022), it would be interesting to deeply investigate the interplay of most common KPC-producing clones from other institutions. Studying the ecological behavior of high-risk clones coexisting within the same hospital and their changing epidemiological patterns over time could contribute to identifying possible competitive emerging clones as well as prevent the further spread of KPC-producing strains.

Materials and methods

Bacterial strains and antibiotic susceptibility assays

Strains *E. hormaechei* HA2pEho and *K. pneumoniae* HA7pKpn were colonizing strains isolated from the same patient as indicated in the *Results* section. The rest of the strains were part of a surveillance program of CRE infecting strains carried out in our institution during the period October 2018 until December 2020

(Table S1). Strains were isolated in blood agar and EMB agar media. The first identification was achieved by MALDI-TOF. Antibiotic susceptibility profiles were determined with the BD Phoenix system according to the guidelines and interpretation criteria of the Clinical and Laboratory Standards Institute (CLSI, 2022). Susceptibility to colistin was done by the pre-diffusion method according to the National Antimicrobial Reference Laboratory, Malbrán Institute, INEI-ANLIS, Argentina (http://antimicrobianos.com.ar/ATB/wp-content/uploads/2017/09/Protocolo-Predifusion-Tabletas-COL-Rosco-version2-Agosto2017.pdf).

Although fosfomycin breakpoint is only for *E. coli*, we extrapolated it to *K. pneumoniae* and the ECC. The KPC-producing *E. hormaechei* HAC11Eho (ST78), *E. hormaechei* HA58Eho (ST66), *K. pneumoniae* HA3pKpn (ST258), and *K. pneumoniae* HA15pKpn (ST11) strains from this survey were chosen for fitness assays.

DNA sequencing and bioinformatic analysis

Genomic DNA extraction was performed using a QIAamp® DNA Mini QIAcube Kit, and libraries were prepared with COVIDSeq Test (Illumina, San Diego, CA, USA) starting from the library preparation step. The libraries were sequenced at the Malbrán Institute in Argentina on Illumina MiSeq-I (Illumina, San Diego, CA, USA) with a MiSeq Reagent Kits v2 cartridge with 500 cycles in the case of HA2pEho and 300 in the case of HA7pKpn.

Quality inspection of the reads was performed using FASTQC v0.11.9 (Wingett and Andrews, 2018), while Trimmomatic v0.39 (Bolger et al., 2014) was used for adapter clipping and trimming low-quality reads. SPAdes v3.15.3 (Prjibelski et al., 2020) was used for genome assembly, and QUAST v5.0.2 was used for assessing the quality of the assembly (Quast et al., 2012). Prokka v1.14.5 was used for genome annotation (Seemann, 2014). Some of these tools were run at the European Galaxy server (Afgan et al., 2016). The number of reads for *E. hormaechei* HA2pEho was 1,355,790 with a length of 250 bp, and that for *K. pneumoniae* HA7pKpn was 1,542,461 with an average of 150 bp. The assembly size was 4,907,320 bp in 88 contigs for *E. hormaechei* HA2pEho and 5,581,104 in 161 contigs for *K. pneumoniae* HA7pKpn. The N50 was 327,017 for *E. hormaechei* HA2pEho and 181,947 for *K. pneumoniae* HA7pKpn.

Based on the information from WGS, further identification of the strains was carried out using several *in silico* molecular methods: rMLST (Jolley et al., 2018), Kraken 2 (which also analyzes the presence of contaminations; Wood et al., 2019), average nucleotide identity (ANI) (Jain et al., 2018), and *in silico* DNA–DNA hybridization (Meier-Kolthoff et al., 2022) (Tables S8 and S9). Whole-genome sequences of type strains were downloaded from the NCBI database based on the studies from Cho et al. (2021) and Wu et al. (2020).

Antibiotic resistance genes were searched using Resfinder (Bortolaia et al., 2020) and CARD (Alcock et al., 2019), and plasmids were found with PlasmidFinder. The identity of β-lactamases was refined using the β-lactamase database (Naas et al., 2017). Plasmids were further analyzed using BLAST (Altschu et al., 1990). The whole sequence of pDCCK1-KPC was on a single contig for both strains. The contiguousness of the extremes of the contig was verified by PCR using specially designed primers. In the case of HA2pEho, primers used were pDCCK1-F: CTGTACATGAAGGCGAAATGTCC and pDCCK1-R: CCTCATTCGTGCGCTCTAGG, and for HA7pKpn, the following primers were used: pDCCK-1B-F: GCGTGTAATGCAGATGGCAG and pDCCK-1B-R: ATGTATCTGCGTCCTGAGCG.

Figures 1 and 2 were made using the ggplot2 (Alboukadel, 2018) package in R (R Core Team, 2020), and Figure 3 was made using BRIG (Alikhan et al., 2011).

Conjugation assays

Briefly, mid-log cultures of donor (HA2pEho and HA7pKpn) and recipient (*E. coli* J53) strains were mixed in LB broth (Laboratorios Britania S.A., Argentina). The mating culture was then incubated overnight at 37°C using the drop plate method. Four replicas were used in each conjugation: only LB, LB with the addition of meropenem (8 μg/ml), sodium azide (80 μg/ml), or a combination of both. To verify that colonies growing on both antibiotics were transconjugant *E. coli* J53, they were grown on EMB agar (Laboratorios Britania S.A., Argentina). bla_{KPC-2} PCR was carried out with the primers KPC-F: CCGTCAGTTCTGCTGTC and KPC-R: CGTTGTCATCCTCGTTAG (Ramírez et al., 2013) using GoTaq® enzyme (Promega, Madison, WI).

In vitro competition and fitness measurements

Growth rate and generation times were calculated by measuring DO at 600 nm. This was done in triplicate. All experiments involved in competition assays were carried out without selective pressure. To test plasmid stability in the absence of selective pressure, we carried out plasmid stability assays. This consisted of subculturing the isolates without antibiotics for 120 h. A single colony was picked from an agar plate containing 8 μg/ml of meropenem with the clone and left to grow overnight (ON) in 5 ml of LB media without the addition of antibiotics. After 24 h, 50 μl of ON culture was inoculated in 5 ml of LB media. After repeating this procedure four times, 100 μl of a 1E-07 dilution was plated on an LB agar plate, and 30 colonies were randomly picked. The presence of bla_{KPC-2} was determined by PCR.

For competitions, isolates were diluted to 1.6E+08 (OD 600 0.2) colony-forming units (CFU)/ml, and equal volumes were combined; thus, the initial ratio of the isolate pairs was close to 1:1; then, 10 µl of the mixture was added to 20 ml of LB broth and grown at 37°C with agitation at 180 rpm. At 24-h intervals, 10 µl of bacterial subcultures was transferred to 20 ml of fresh LB broth. This was done in triplicate. At 72 and 96 h, 100 µl was inoculated on EMB agar plates and left to grow ON at 37°C. The CFU of HA7pKpn and HA2pEho were counted, and after 96 h, the adaptive difference was calculated with the equation

$$S = \ln\left[\left(\frac{\frac{ECC_t}{Kpn_t}}{\frac{ECCt_{t-1}}{Kpn_{t-1}}}\right)^{\frac{1}{y}}\right]$$

and fitness F = 1 + S, where S is the selection coefficient and shows the difference in fitness between two competing strains at time t, ECC_t = number of *E. hormaechei* colonies, Kpn_t = number of *K. pneumoniae* colonies, and ECC_{t-1} and Kpn_{t-1} are the number of ECC and *K. pneumoniae* at the previous time, respectively. The quotient of the ratios of the cell numbers was standardized with 1/y, where "y" is the number of bacterial generations during the assay (Sander et al., 2002; Guo et al., 2012). Here, the exponent was 1/9 because cell numbers were determined every nine generations. The terms Kpn_t/Kpn_{t-1} and ECC_t/ECC_{t-1} give the growth rates for *K. pneumoniae* and ECC strains, respectively. Hence, S is the natural logarithm of the quotient of the growth rates of the competing strains. S is positive if the ECC bacterial fitness is increased compared with that of the *K. pneumoniae* competitor strain. Sander et al. (2002) applied this method to make comparisons between resistant and susceptible strains of a single species. In this case, we did not count resistant bacteria but counted the CFU of the different strains in the absence of antibiotics, as colonies could be differentiated thanks to their different ability to ferment lactose. In the case where colonies could not be differentiated, we randomly picked 15 colonies from each plate and did PCR with primers specific for *K. pneumoniae* (Kaushik and Balasubramanian, 2012). We then calculated the frequency of each species and multiplied it by the CFU number to obtain the CFU number of each species. Statistical analysis was done using ANOVA with an alpha value of 0.05.

Data availability statement

The data presented in the study is deposited in GenBank, accession number PRJNA841267.

Author contributions

DC and MPQ contributed to the conception and design of the study. CAK, NGA, BF, LF-C, ASG, ND, and GC performed the experimental assays. CAK, VEA, BPM, ACdVL, MP, MGM, and JC carried out bioinformatics analysis. DC structured the work, wrote and coordinated the drafts of the manuscript, and did the final edition. CAK, MPQ, NGA, and DC wrote the Results section. All the authors contributed to the analysis of the data and manuscript revision, read, and approved the submitted version.

Funding

MPQ and DC are members of the career investigator of CONICET, Argentina. CAK, AcdVL, and VEA have a Posdoctoral Fellowship from CONICET. MP is recipient of an Universidad de Buenos Aires´s doctoral fellowship and ASG has a Doctoral Fellowship from CONICET. NGA is an infectious diseases specialist. BF and LF-C are clinical microbiology specialists. Aires doctoral fellowship. NA is an infectious diseases doctor. BF and LF-C are clinical microbiology specialists. This study was supported by grants ISID/Pfizer 2019 (#56570859) and PUE 2522 from CONICET given to DC and IMPaM, respectively.

Acknowledgments

We would like to thank Andrea Aguilar and Nicolás Mendiondo for their work on bioinformatic analysis.

Conflict of interest

MPQ and DC are members of the career investigator of CONICET, Argentina. CAK and VEA have a Posdoctoral Fellowship from CONICET, and ASG have a Doctoral Fellowship from CONICET. NGA is an infectious diseases specialist. This study was supported by grants ISID/Pfizer 2019 (#56570859) and PUE 2522 from CONICET given to DC, and IMPaM, respectively. The funders were not involved in the study design, collection, analysis, interpretation of data, the writing of this article or the decision to submit it for publication. All authors declare no other competing interests.

Publisher's note

Supplementary material

The Supplementary Material for this article can be found online at: https://www.frontiersin.org/articles/10.3389/fcimb.2022.951049/full#supplementary-material

References

Afgan, E., Baker, D., van den Beek, M., Blankenberg, D., Bouvier, D., Čech, M., et al. (2016). The galaxy platform for accessible, reproducible and collaborative biomedical analyses: 2016 update. *Nucleic Acids Res.* 44, W3–W10. doi: 10.1093/nar/gkw343

Alboukadel, K. (2018) *Ggpubr: "ggplot2" based publication ready plots. r package version 0.2.* Available at: https://CRAN.R-project.org/package=ggpubr.

Alcock, B. P., Raphenya, A. R., Lau, T. T. Y., Tsang, K. K., Bouchard, M., Edalatmand, A., et al. (2019). CARD 2020: antibiotic resistome surveillance with the comprehensive antibiotic resistance database. *Nucleic Acids Res.* 48, gkz935. doi: 10.1093/nar/gkz935

Alikhan, N.-F., Petty, N. K., Ben Zakour, N. L., and Beatson, S. A. (2011). BLAST ring image generator (BRIG): simple prokaryote genome comparisons. *BMC Genomics* 12, 402. doi: 10.1186/1471-2164-12-402

Altschu, P. S. F., Gish, W., Miller, W., Myers, E. W., and Lipman, D. J. (1990). Basic local alignment search tool. 8. *J. Mol. Biol.* 215 (3), 403–410. doi: 10.1016/S0022-2836(05)80360-2

Ávarez, V. E., Quiroga, M. P., Galán, A. V., Vilacoba, E., Quiroga, C., Ramírez, M. S., et al. (2020). Crucial Role of the Accessory Genome in the Evolutionary Trajectory of Acinetobacter baumannii Global Clone 1. *Front. Microbiol.* 11, 342. doi: 10.3389/fmicb.2020.00342

Anchordoqui, M. S., De Belder, D., Lucero, C., Rapoport, M., Faccone, D., Rodriguez, A., et al. (2015). *In vivo* horizontal dissemination of the bla_{KPC-2} gene carried on diverse genetic platforms among clinical isolates of *Enterobacteriaceae*. *J. Global Antimicrob. Resist.* 3, 210–213. doi: 10.1016/j.jgar.2015.05.001

Annavajhala, M. K., Gomez-Simmonds, A., and Uhlemann, A.-C. (2019). Multidrug-resistant *Enterobacter cloacae* complex emerging as a global, diversifying threat. *Front. Microbiol.* 10. doi: 10.3389/fmicb.2019.00044

BARNARDS Group, Sands, K., Carvalho, M. J., Portal, E., Thomson, K., Dyer, C., et al. (2021). Characterization of antimicrobial-resistant gram-negative bacteria that cause neonatal sepsis in seven low- and middle-income countries. *Nat. Microbiol.* 6, 512–523. doi: 10.1038/s41564-021-00870-7

Bolger, A. M., Lohse, M., and Usadel, B. (2014). Trimmomatic: A flexible trimmer for illumina sequence data. *Bioinformatics* 30, 2114–2120. doi: 10.1093/bioinformatics/btu170

Bonomo, R. A., Burd, E. M., Conly, J., Limbago, B. M., Poirel, L., Segre, J. A., et al. (2018). Carbapenemase-producing organisms: A global scourge. *Clin. Infect. Dis.* 66, 1290–1297. doi: 10.1093/cid/cix893

Bortolaia, V., Kaas, R. S., Ruppe, E., Roberts, M. C., Schwarz, S., Cattoir, V., et al. (2020). ResFinder 4.0 for predictions of phenotypes from genotypes. *J. Antimicrob. Chemother.* 75, 3491–3500. doi: 10.1093/jac/dkaa345

Botts, R. T., Apffel, B. A., Walters, C. J., Davidson, K. E., Echols, R. S., Geiger, M. R., et al. (2017). Characterization of four multidrug resistance plasmids captured from the sediments of an urban coastal wetland. *Front. Microbiol.* 8, 1922. doi: 10.3389/fmicb.2017.01922

Brandt, C., Viehweger, A., Singh, A., Pletz, M. W., Wibberg, D., Kalinowski, J., et al. (2019). Assessing genetic diversity and similarity of 435 KPC-carrying plasmids. *Sci. Rep.* 9, 11223. doi: 10.1038/s41598-019-47758-5

Campos, L. C., Lobianco, L. F., Seki, L. M., Santos, R. M. R., and Asensi, M. D. (2007). Outbreak of *Enterobacter hormaechei* septicaemia in newborns caused by contaminated parenteral nutrition in Brazil. *J. Hosp. Infect.* 66, 95–97. doi: 10.1016/j.jhin.2007.02.013

Center for Disease Dynamics, Economics & Policy *ResistanceMap*. Available at: https://resistancemap.cddep.org/About.php.

Chabbert, Y. A., Scavizzi, M. R., Witchitz, J. L., Gerbaud, G. R., and Bouanchaud, D. H. (1972). Incompatibility groups and the classification of *fi* ¯ resistance factors. *J. Bacteriol.* 112, 666–675. doi: 10.1128/jb.112.2.666-675.1972

Cho, G.-S., Stein, M., Fiedler, G., Igbinosa, E. O., Koll, L. P., Brinks, E., et al. (2021). Polyphasic study of antibiotic-resistant enterobacteria isolated from fresh produce in Germany and description of enterobacter vonholyi sp. nov. isolated from marjoram and enterobacter dykesii sp. nov. isolated from mung bean sprout. *System. Appl. Microbiol.* 44, 126174. doi: 10.1016/j.syapm.2020.126174

CLSI (2022). *Performance Standards for Antimicrobial Susceptibility Testing, supplement M100. 32nd ed.* (USA: Clinical and Laboratory Standards Institute).

Davin-Regli, A., Lavigne, J.-P., and Pagès, J.-M. (2019). *Enterobacter* spp.: Update on taxonomy, clinical aspects, and emerging antimicrobial resistance. *Clin. Microbiol. Rev.* 32, e00002–19. doi: 10.1128/CMR.00002-19

De Belder, D., Lucero, C., Rapoport, M., Rosato, A., Faccone, D., Petroni, A., et al. (2018). Genetic diversity of KPC-producing *Escherichia coli, klebsiella oxytoca, serratia marcescens*, and *Citrobacter freundii* isolates from Argentina. *Microb. Drug Resist.* 24, 958–965. doi: 10.1089/mdr.2017.0213

Dong, D., Mi, Z., Li, D., Gao, M., Jia, N., Li, M., et al. (2020). Novel IncR/IncP6 hybrid plasmid pCRE3-KPC recovered from a clinical KPC-2-Producing citrobacter braakii isolate. *mSphere* 5 ,e00891–19. doi: 10.1128/mSphere.00891-19

Emeraud, C., Petit, C., Gauthier, L., Bonnin, R. A., Naas, T., and Dortet, L. (2022). Emergence of VIM-producing enterobacter cloacae complex in France between 2015 and 2018. *J. Antimicrob. Chemother.* 77, 944–951. doi: 10.1093/jac/dkab471

Falco, A., Guerrero, D., García, I., Correa, A., Rivera, S., Olaya, M. B., et al. (2021). Molecular characterization of KPC-2-Producing *Enterobacter cloacae* complex isolates from cali, Colombia. *Antibiotics* 10, 694. doi: 10.3390/antibiotics10060694

Fernández, J., Montero, I., Martínez, Ó., Fleites, A., Poirel, L., Nordmann, P., et al. (2015). Dissemination of multiresistant *Enterobacter cloacae* isolates producing OXA-48 and CTX-M-15 in a Spanish hospital. *Int. J. Antimicrob. Agents* 46, 469–474. doi: 10.1016/j.ijantimicag.2015.07.003

Frost, I., Van Boeckel, T. P., Pires, J., Craig, J., and Laxminarayan, R. (2019). Global geographic trends in antimicrobial resistance: the role of international travel. *J. Travel Med.* 26, taz036. doi: 10.1093/jtm/taz036

Ghiglione, B., Haim, M. S., Penzotti, P., Brunetti, F., D´Amico González, G., Di Conza, J., et al. (2021). Characterization of emerging pathogens carrying bla_{KPC-2} gene in IncP-6 plasmids isolated from urban sewage in Argentina. *Front. Cell. Infect. Microbiol.* 11. doi: 10.3389/fcimb.2021.722536

Girlich, D., Ouzani, S., Emeraud, C., Gauthier, L., Bonnin, R. A., Le Sache, N., et al. (2021). Uncovering the novel *Enterobacter cloacae* complex species responsible for septic shock deaths in newborns: A cohort study. *Lancet Microbe* 2, e536–e544. doi: 10.1016/S2666-5247(21)00098-7

Gomez, S. A., Pasteran, F. G., Faccone, D., Tijet, N., Rapoport, M., Lucero, C., et al. (2011). Clonal dissemination of *Klebsiella pneumoniae* ST258 harbouring KPC-2 in Argentina. *Clin. Microbiol. Infect.* 17, 1520–1524. doi: 10.1111/j.1469-0691.2011.03600.x

Gomez-Simmonds, A., Annavajhala, M. K., Wang, Z., Macesic, N., Hu, Y., Giddins, M. J., et al. (2018). Genomic and geographic context for the evolution of high-risk carbapenem-resistant *Enterobacter cloacae* complex clones ST171 and ST78. *mBio* 9 ,e00542–18. doi: 10.1128/mBio.00542-18

Guo, B., Abdelraouf, K., Ledesma, K. R., Nikolaou, M., and Tam, V. H. (2012). Predicting bacterial fitness cost associated with drug resistance. *J. Antimicrob. Chemother.* 67, 928–932. doi: 10.1093/jac/dkr560

Hafza, N., Challita, C., Dandachi, I., Bousaab, M., Dahdouh, E., and Daoud, Z. (2018). Competition assays between ESBL-producing *E. coli* and *K. pneumoniae* isolates collected from Lebanese elderly: An additional cost on fitness. *J. Infect. Public Health* 11, 393–397. doi: 10.1016/j.jiph.2017.09.010

Hansen, G. T. (2021). Continuous evolution: Perspective on the epidemiology of carbapenemase resistance among *Enterobacterales* and other gram-negative bacteria. *Infect. Dis. Ther.* 10, 75–92. doi: 10.1007/s40121-020-00395-2

Heiden, S. E., Hübner, N.-O., Bohnert, J. A., Heidecke, C.-D., Kramer, A., Balau, V., et al. (2020). A *Klebsiella pneumoniae* ST307 outbreak clone from Germany demonstrates features of extensive drug resistance, hypermucoviscosity, and enhanced iron acquisition. *Genome Med.* 12, 113. doi: 10.1186/s13073-020-00814-6

Hertz, F. B., Marvig, R. L., Frimodt-Møller, N., and Nielsen, K. L. (2022). *In vitro* relative fitness, *in vivo* intestinal colonization and genomic differences of *Escherichia coli* of ST131 carrying $bla_{CTX-M-15}$. *Front. Microbiol.* 12. doi: 10.3389/fmicb.2021.798473

Izdebski, R., Baraniak, A., Herda, M., Fiett, J., Bonten, M. J. M., Carmeli, Y., et al. (2015). MLST reveals potentially high-risk international clones of *Enterobacter cloacae*. *J. Antimicrob. Chemother.* 70, 48–56. doi: 10.1093/jac/dku359

Jain, C., Rodriguez, -R. L. M., Phillippy, A. M., Konstantinidis, K. T., and Aluru, S.. (2018). High throughput ANI analysis of 90K prokaryotic genomes reveals clear species boundaries. *Nat. Commun.* 9, 5114. doi: 10.1038/s41467-018-07641-9

Jia, X., Dai, W., Ma, W., Yan, J., He, J., Li, S., et al. (2018). Carbapenem-resistant *E. cloacae* in southwest China: Molecular analysis of resistance and risk factors for infections caused by NDM-1-Producers. *Front. Microbiol.* 9. doi: 10.3389/fmicb.2018.00658

Jolley, K. A., Bray, J. E., and Maiden, M. C. J. (2018). Open-access bacterial population genomics: BIGSdb software, the PubMLST.org website and their applications. *Wellcome Open Res.* 3, 124. doi: 10.12688/wellcomeopenres.14826.1

Kaushik, R., and Balasubramanian, R. (2012). Assessment of bacterial pathogens in fresh rainwater and airborne particulate matter using real-time PCR. *Atmospheric Environ.* 46, 131–139. doi: 10.1016/j.atmosenv.2011.10.013

Knecht, C. A., Allende, N. G., Álvarez, V. E., Cormick, B. P. M., Massó, M. G., Campos, J., et al. (2022). New sequence type of an enterobacter cloacae complex

strain with the potential to become a high-risk clone. *J. Global Antimicrob. Resist.* 31, 162–164. doi: 10.1016/j.jgar.2022.08.015. S2213716522002065.

Luo, N., Pereira, S., Sahin, O., Lin, J., Huang, S., Michel, L., et al. (2005). Enhanced *in vivo* fitness of fluoroquinolone-resistant *Campylobacter jejuni* in the absence of antibiotic selection pressure. *Proc. Natl. Acad. Sci. U.S.A.* 102, 541–546. doi: 10.1073/pnas.0408966102

Magiorakos, A.-P., Srinivasan, A., Carey, R. B., Carmeli, Y., Falagas, M. E., Giske, C. G., et al. (2012). Multidrug-resistant, extensively drug-resistant and pandrug-resistant bacteria: An international expert proposal for interim standard definitions for acquired resistance. *Clin. Microbiol. Infect.* 18, 268–281. doi: 10.1111/j.1469-0691.2011.03570.x

Mathers, A. J., Peirano, G., and Pitout, J. D. D. (2015). The role of epidemic resistance plasmids and international high-risk clones in the spread of multidrug-resistant *Enterobacteriaceae*. *Clin. Microbiol. Rev.* 28, 565–591. doi: 10.1128/CMR.00116-14

Meier-Kolthoff, J. P., Carbasse, J. S., Peinado-Olarte, R. L., and Göker, M. (2022). TYGS and LPSN: A database tandem for fast and reliable genome-based classification and nomenclature of prokaryotes. *Nucleic Acids Res.* 50, D801–D807. doi: 10.1093/nar/gkab902

Naas, T., Oueslati, S., Bonnin, R. A., Dabos, M. L., Zavala, A., Dortet, L., et al. (2017). Beta-lactamase database (BLDB) – structure and function. *J. Enzyme Inhibition Medicinal Chem.* 32, 917–919. doi: 10.1080/14756366.2017.1344235

Neil, K., Allard, N., Grenier, F., Burrus, V., and Rodrigue, S. (2020). Highly efficient gene transfer in the mouse gut microbiota is enabled by the Incl2 conjugative plasmid TP114. *Commun. Biol.* 3, 523. doi: 10.1038/s42003-020-01253-0

Otto, M. (2013). Community-associated MRSA: What makes them special? *Int. J. Med. Microbiol.* 303, 324–330. doi: 10.1016/j.ijmm.2013.02.007

Paauw, A., Caspers, M. P. M., Leverstein-van Hall, M. A., Schuren, F. H. J., Montijn, R. C., Verhoef, J., et al. (2009). Identification of resistance and virulence factors in an epidemic *Enterobacter hormaechei* outbreak strain. *Microbiology* 155, 1478–1488. doi: 10.1099/mic.0.024828-0

Peirano, G., Matsumura, Y., Adams, M. D., Bradford, P., Motyl, M., Chen, L., et al. (2018). Genomic epidemiology of global carbapenemase-producing enterobacter spp. 2008–2014. *Emerg. Infect. Dis.* 24, 1010–1019. doi: 10.3201/eid2406.171648

Pitout, J. D. D., and Finn, T. J. (2020). The evolutionary puzzle of *Escherichia coli* ST131. *Infect. Genet. Evol.* 81, 104265. doi: 10.1016/j.meegid.2020.104265

Prjibelski, A., Antipov, D., Meleshko, D., Lapidus, A., and Korobeynikov, A. (2020). Using SPAdes *De novo* assembler. *Curr. Protoc. Bioinf.* 70, e102. doi: 10.1002/cpbi.102

Quast, C., Pruesse, E., Yilmaz, P., Gerken, J., Schweer, T., Yarza, P., et al. (2012). The SILVA ribosomal RNA gene database project: improved data processing and web-based tools. *Nucleic Acids Res.* 41, D590–D596. doi: 10.1093/nar/gks1219

Ramírez, D. G., Nicola, F., Zarate, S., Relloso, S., Smayevsky, J., and Arduino, S. (2013). Emergence of *Pseudomonas aeruginosa* with KPC-type carbapenemase in a teaching hospital: An 8-year study. *J. Med. Microbiol.* 62, 1565–1570. doi: 10.1099/jmm.0.059923-0

R Core Team (2020). *R: A language and environment for statistical computing* (Vienna, Austria: R Foundation for Statistical Computing). Available at: https://www.R-project.org/.

Red WHONET Argentina *Vigilancia de la resistencia a los antimicrobianos red WHONET Argentina 2010-2021*. Available at: https://antimicrobianos.com.ar (Accessed May 10, 2022).

Sander, P., Springer, B., Prammananan, T., Sturmfels, A., Kappler, M., Pletschette, M., et al. (2002). Fitness cost of chromosomal drug resistance-conferring mutations. *Antimicrob. Agents Chemother.* 46, 1204–1211. doi: 10.1128/AAC.46.5.1204-1211.2002

Seemann, T. (2014). Prokka: rapid prokaryotic genome annotation. *Bioinformatics* 30, 2068–2069. doi: 10.1093/bioinformatics/btu153

Shen, P., Wei, Z., Jiang, Y., Du, X., Ji, S., Yu, Y., et al. (2009). Novel genetic environment of the carbapenem-hydrolyzing β-lactamase KPC-2 among *Enterobacteriaceae* in China. *Antimicrob. Agents Chemother.* 53, 4333–4338. doi: 10.1128/AAC.00260-09

Sidjabat, H. E., Townell, N., Nimmo, G. R., George, N. M., Robson, J., Vohra, R., et al. (2015). Dominance of IMP-4-Producing *Enterobacter cloacae* among carbapenemase-producing *Enterobacteriaceae* in Australia. *Antimicrob. Agents Chemother.* 59, 4059–4066. doi: 10.1128/AAC.04378-14

Tavares, C. P., Pereira, P. S., Marques, E., de, A., Faria, C., de Souza, M., et al. (2015). Molecular epidemiology of KPC-2–producing *Enterobacteriaceae* (non–*Klebsiella pneumoniae*) isolated from Brazil. *Diagn. Microbiol. Infect. Dis.* 82, 326–330. doi: 10.1016/j.diagmicrobio.2015.04.002

Voth, D. E., Broederdorf, L. J., and Graham, J. G. (2012). Bacterial type IV secretion systems: versatile virulence machines. *Future Microbiol.* 7, 241–257. doi: 10.2217/fmb.11.150

Wang, Q., Zhang, Y., Yao, X., Xian, H., Liu, Y., Li, H., et al. (2016). Risk factors and clinical outcomes for carbapenem-resistant *Enterobacteriaceae* nosocomial infections. *Eur. J. Clin. Microbiol. Infect. Dis.* 35, 1679–1689. doi: 10.1007/s10096-016-2710-0

Wingett, S., and Andrews, S. (2018). FastQ screen: A tool for multi-genome mapping and quality control. *F1000Res* 7. doi: 10.12688/f1000research.15931.2

Wiser, M. J., and Lenski, R. E. (2015). A comparison of methods to measure fitness in *Escherichia coli*. *PloS One* 10, e0126210. doi: 10.1371/journal.pone.0126210

Wood, D. E., Lu, J., and Langmead, B. (2019). Improved metagenomic analysis with kraken 2. *Genome Biol.* 13, 257–270. doi: 10.1186/s13059-019-1891-0

World Health Organization (2017) *WHO publishes list of bacteria for which new antibiotics are urgently needed*. Available at: https://www.who.int/news/item/27-02-2017-who-publishes-list-of-bacteria-for-which-new-antibiotics-are-urgently-needed.

Wozniak, A., Figueroa, C., Moya-Flores, F., Guggiana, P., Castillo, C., Rivas, L., et al. (2021). A multispecies outbreak of carbapenem-resistant bacteria harboring the bla_{KPC} gene in a non-classical transposon element. *BMC Microbiol.* 21, 107. doi: 10.1186/s12866-021-02169-3

Wu, W., Feng, Y., and Zong, Z. (2020). Precise species identification for *Enterobacter*: A genome sequence-based study with reporting of two novel species, *Enterobacter quasiroggenkampii* sp. nov. and *Enterobacter quasimori* sp. nov. *mSystems* 5, e00527–e00520. doi: 10.1128/mSystems.00527-20

frontiers | Frontiers in Cellular and Infection Microbiology

TYPE Original Research
PUBLISHED 27 October 2022
DOI 10.3389/fcimb.2022.998578

OPEN ACCESS

EDITED BY
Milena Dropa,
Faculty of Public Health, University of São Paulo, Brazil

REVIEWED BY
Farzad Badmasti,
Pasteur Institute of Iran, Iran
Yancheng Yao,
University of Giessen, Germany

*CORRESPONDENCE
Jianjun Gou
jianjung@zzu.edu.cn
Beiwen Zheng
zhengbw@zju.edu.cn

†These authors have contributed equally to this work and share first authorship

SPECIALTY SECTION
This article was submitted to Clinical Microbiology, a section of the journal Frontiers in Cellular and Infection Microbiology

RECEIVED 20 July 2022
ACCEPTED 13 October 2022
PUBLISHED 27 October 2022

CITATION
Qiao J, Ge H, Xu H, Guo X, Liu R, Li C, Chen R, Zheng B and Gou J (2022) Detection of IMP-4 and SFO-1 co-producing ST51 *Enterobacter hormaechei* clinical isolates. *Front. Cell. Infect. Microbiol.* 12:998578. doi: 10.3389/fcimb.2022.998578

Detection of IMP-4 and SFO-1 co-producing ST51 *Enterobacter hormaechei* clinical isolates

Jie Qiao[1,2†], Haoyu Ge[1,2†], Hao Xu[2], Xiaobing Guo[1], Ruishan Liu[2], Chenyu Li[1], Ruyan Chen[1], Beiwen Zheng[2,3,4*] and Jianjun Gou[1*]

[1]Department of Laboratory Medicine, The First Affiliated Hospital of Zhengzhou University, Zhengzhou, China, [2]Collaborative Innovation Center for Diagnosis and Treatment of Infectious Diseases, State Key Laboratory for Diagnosis and Treatment of Infectious Diseases, The First Affiliated Hospital, College of Medicine, Zhejiang University, Hangzhou, China, [3]Department of Structure and Morphology, Jinan Microecological Biomedicine Shandong Laboratory, Jinan, Shandong, China, [4]Research Units of Infectious Diseases and Microecology, Chinese Academy of Medical Sciences, Beijing, China

Purpose: To explore the genetic characteristics of the IMP-4 and SFO-1 co-producing multidrug-resistant (MDR) clinical isolates, *Enterobacter hormaechei* YQ13422hy and YQ13530hy.

Methods: MALDI-TOF MS was used for species identification. Antibiotic resistance genes (ARGs) were tested by PCR and Sanger sequencing analysis. In addition to agar dilution, broth microdilution was used for antimicrobial susceptibility testing (AST). Whole-genome sequencing (WGS) analysis was conducted using the Illumina NovaSeq 6000 and Oxford Nanopore platforms. Annotation was performed by RAST on the genome. The phylogenetic tree was achieved using kSNP3.0. Plasmid characterization was conducted using S1-pulsed-field gel electrophoresis (S1-PFGE), Southern blotting, conjugation experiments, and whole genome sequencing (WGS). An in-depth study of the conjugation module was conducted using the OriTFinder website. The genetic context of bla_{IMP-4} and bla_{SFO-1} was analyzed using BLAST Ring Image Generator (BRIG) and Easyfig 2.3.

Results: YQ13422hy and YQ13530hy, two MDR strains of ST51 *E. hormaechei* harboring bla_{IMP-4} and bla_{SFO-1}, were identified. They were only sensitive to meropenem, amikacin and polymyxin B, and were resistant to cephalosporins, aztreonam, piperacillin/tazobactam and aminoglycosides, intermediate to imipenem. The genetic context surrounding bla_{IMP-4} was 5′CS-*hin-1*-IS*26*-Int*I1*-bla_{IMP-4}-IS*6100*-*ecoRII*. The integron of bla_{IMP-4} is In*823*, which is the array of gene cassettes of 5′CS-bla_{IMP-4}. Phylogenetic analysis demonstrated that *E. hormaechei* YQ13422hy and YQ13530hy belonged to the same small clusters with a high degree of homology.

Conclusion: This observation revealed the dissemination of the bla_{IMP-4} gene in *E. hormaechei* in China. We found that bla_{IMP-4} and bla_{SFO-1} co-exist in MDR clinical *E. hormaechei* isolates. This work showed a transferable IncN-type

plasmid carrying the bla_{IMP-4} resistance gene in *E. hormaechei*. We examined the potential resistance mechanisms of pYQ13422-IMP-4 and pYQ13422-SFO-1, along with their detailed genetic contexts.

KEYWORDS

Enterobacter hormaechei, ST51, bla_{IMP-4}, bla_{SFO-1}, IncN, multidrug-resistant, genomics

Introduction

Enterobacter cloacae complex (ECC) is the most common group of species among the genus *Enterobacter*, including six closely related species: *E. cloacae*, *E. asburiae*, *E. hormaechei*, *E. kobei*, *E. ludwigii*, and *E. nimipressuralis* (Mezzatesta et al., 2012). *Enterobacter hormaechei* can be widely found in different environments such as the nature (Osei Sekyere and Reta, 2021), feces of humans or animals. But it is also an important pathogenic bacteria in hospitals, which can be responsible for nosocomial infections, such as wounds, urinary tract, and soft tissue infections (Xu et al., 2015). The horizontal spread of bacterial resistance genes, especially the carbapenemase-encoding gene, has brought great difficulties to clinical treatment (Annavajhala et al., 2019).

Since bla_{IMP-1} was firstly declared in Japan in 1991 (Watanabe et al., 1991), IMP- producing ECC has been playing an increasingly significant role in the world antibiotic resistance stage, like Malaysia (Liew et al., 2018), Portugal (Goncalves et al., 2021), and Korea (Lee et al., 2017). As time progressed, more and more IMP variants appeared in China, including IMP-2 (Riccio et al., 2000), IMP-8 (Yan et al., 2001), IMP-4 (Chu et al., 2001), IMP-26 (Gou et al., 2020). In China, IMP-4-positive carbapenemase-producing *Enterobacterales* (CPE) have become important carbapenem-resistant bacteria (Hu et al., 2014), since it was first discovered in Hongkong (Chu et al., 2001) in 2001. The bla_{IMP-4} is mainly found in *Pseudomonas aeruginosa*, but has been gradually reported in Enterobacteriaceae (Matsumura et al., 2017), such as *E. hormaechei* (Chen et al., 2022). More importantly, the coincidence of bla_{IMP} and other antibiotic resistance genes is becoming increasingly common, such as co-carrying bla_{IMP-4} and bla_{NDM-1} (Zhang et al., 2021a), further increasing the tremendous pressure of clinical treatment.

In 1999, a clinical *E. cloacae* 8009 isolate possessing a transferable plasmid harboring bla_{SFO-1} was reported in Japan (Matsumoto and Inoue, 1999). The reports of bla_{SFO-1} and coexisting antibiotic resistance genes have recently increased in China (Zhou et al., 2020). In comparison with other broad-spectrum-beta-lactamases, the bla_{SFO-1} gene has a low occurrence of antimicrobial resistance that has been ignored by routine monitoring. We found a carbapenem-resistant *E. hormaechei* clinical isolate co-harboring bla_{SFO-1} and bla_{IMP-4}.

There are few studies on the transmission of bla_{SFO-1} and bla_{IMP-4} in ECC in China, especially *E. hormaechei*. Therefore, it is vital to further explore the genome and phenotypic characteristics of the bla_{SFO-1} and bla_{IMP-4} in *E. hormaechei* in China. We identified clinical isolates of *E. hormaechei* YQ13422hy and YQ13530hy co-producing bla_{IMP-4} and bla_{SFO-1}, and described the detailed content of a conjugative IncN-plasmid. Furthermore, we revealed the underlying transmission mechanisms of bla_{IMP-4}.

Materials and methods

Bacterial strains

We continuously collected ECC clinical isolates from a tertiary hospital affiliated to Wenzhou Medical University from 2015 to 2017 for routine surveillance. A total of eight carbapenemase producing ECC clinical isolates have been identified using the MALDI-TOF MS (Bruker, Bremen, Germany). Among them, the two isolates of IMP-4-producing *E. hormaechei* strains (25%) were identified using PCR and next-generation sequencing (NGS), designated as YQ13422hy and YQ13530hy.

Multilocus sequence typing and antimicrobial susceptibility testing

As described previously, multilocus sequence typing (MLST) was conducted (Gou et al., 2020). A new sequence type has been submitted to MLST and have been approved by PubMLST (http://pubmlst.org/ecloacae). Agar dilution and broth microdilution were used for antimicrobial susceptibility testing (AST), and *Escherichia coli* ATCC 25922 was used as control. AST results were interpreted based on the Clinical and Laboratory Standards Institute (CLSI) 2021 standards, while tigecycline and colistin clinical breakpoints were based on the 2022 EUCAST (http://www.eucast.org). Sixteen antimicrobial

resistance genes were searched using PCR, including bla_{KPC}, bla_{NDM}, bla_{IMP}, bla_{OXA-23}, bla_{OXA-48}, bla_{VIM}, and *mcr*-1-10.

Plasmid characterization and conjugation assays

Pulsed-field gel electrophoresis (PFGE) was used to determine the homology between strains YQ13422hy and YQ13530hy. PFGE was undertaken on the CHEF-DR III system (Bio-Rad. Hercules, CA, United States), and patterns were evaluated and interpreted according to the published guidelines (Xu et al., 2018). The profiles of plasmids in strains YQ13422hy and YQ13530hy were analyzed by the S1-PFGE, as previously described (Wang et al., 2019). Then we used a digoxigenin-labeled bla_{IMP-4} probe made by a dig-high prime DNA Labeling and Detection Starter Kit II (Roche Diagnostics) to determine the location of plasmid harboring bla_{IMP-4} *via* southern blotting and hybridization. The transferability of plasmids was investigated by using *E. coli* J53, a NaN_3-resistant standard strain, as a receptor for conjugation assays. Subsequently, transconjugants carrying bla_{IMP-4} were first selected using Mueller-Hinton agar (OXOID, Hampshire, United Kingdom) plates containing both 1 mg/L meropenem and 200 mg/L NaN_3. Further, the selected conjugates were confirmed by MALDI-TOF/MS, PCR identified the bla_{IMP-4} gene, and AST was used to confirm the expression of drug resistance genes.

Whole genome sequencing and *in silico* analyses

Genomic DNA was extracted using a Genomic DNA Isolation Kit (QIAGEN, Hilden, Germany) and sequenced using Illumina Novaseq 6000 (Illumina, San Diego, CA, United States) and Oxford Nanopore platforms (Oxford Nanopore Technologies, Oxford, United Kingdom). RAST 2.0 was used to annotate the draft genomes obtained by SPAdes version 3.9.1 (Aziz et al., 2008) (http://rast.nmpdr.org/). ISfinder and INTEGRALL were used to detect insertion sequence elements and integrons (https://www-is.biotoul.fr/). Antimicrobial resistance genes (ARGs) were identified by Resfinder (https://cge.cbs.dtu.dk/services/ResFinder/). Different plasmid genome sequences were compared by BLAST Ring Image Generator (Alikhan et al., 2011) (BRIG). The figures about the genetic context surrounding the antibiotic resistance genes were drawn by Easyfig 2.3 (Sullivan et al., 2011). To verify whether the plasmids pYQ13422-IMP-4, pYQ13530-IMP-4, pYQ13422-SFO-1 and pYQ13530-SFO-1 were conjugative plasmids, we used the OriTFinder website (https://tool-mml.sjtu.edu.cn/oriTfinder/oriTfinder.html).

Phylogenetic analysis

We downloaded all available IMP-carrying ECC from the NCBI genome database in May 2022 to study the phylogenetic relationships of YQ13422hy and YQ13530hy with other ECC. KSNP3.0 (Gardner et al., 2015) was used to construct the phylogenetic tree based on the previously-mentioned downloaded data *via* SNPS. ITOL was used to visualize and modify the phylogenetic tree (https://itol.embl.de/).

Results

Species confirmation and homology analysis

The YQ13422hy strain was isolated from a sputum specimen of a 36-year-old male suffering from hypoxic encephalopathy on March 12, 2017. YQ13530hy was isolated from a sputum specimen of a 60-year-old male with brain herniation on April 2, 2017. The patient carrying YQ13422hy was hospitalized for 3 months, from March 01, 2017 to June 10, 2022. The patient carrying YQ13530hy was hospitalized for 1 month from April 01, 2017 to April 19, 2022. Patient carrying YQ13422hy was treated with intravenous vancomycin, Imipenem and Cilastatin Sodium, as well as Cefoperazone Sodium and Sulbactam Sodium. Patient carrying YQ13530hy was treated with vancomycin, meropenem and levofloxacin. Both patients were hospitalized in the same ward. ANI analysis (Figure S2 and Table S2) and WGS showed that the two isolates were highly homologous, and the bla_{IMP-4}-bearing plasmids had 99.97% similarity, indicating the isolates' clonal spread. In fact, it is not clear how the clonal spread happened, but we suspect that it may have been through contact or through the air, because both strains were detected in sputum.

AST of *Enterobacter hormaechei* YQ13422hy and YQ13530hy

The isolates YQ13422hy and YQ13530hy both displayed resistance to aztreonam, ceftriaxone, cefotaxime, ceftazidime, levofloxacin, ciprofloxacin, gentamicin, piperacillin/tazobactam, chloromycin, amoxicillin-clavulanate, cefepime, with sensitivity to meropenem, amikacin, and polymyxin B. For imipenem, YQ13422hy and YQ13530hy were determined as intermediate. In the case of YQ13422hy, it exhibited intermediate resistance to fosfomycin, and susceptibility to trimethoprim/sulfamethoxazole and tigecycline. On the other hand, YQ13530hy showed resistance to trimethoprim/sulfamethoxazole and tigecycline, while it was susceptible to

fosfomycin. AST results revealed that both strains were MDR *E. hormaechei*. The results of AST of *E. hormaechei* YQ13422hy and YQ13530hy are shown in Table 1.

Location of bla_{IMP-4} and bla_{SFO-1} and the conjugation assays

S1-PFGE and hybridization experiments on YQ13422hy and YQ13530hy (Figure S1) showed that the plasmid harboring the *blaIMP-4* resistance gene was about 53 kb and it was named pYQ13422-IMP-4. The plasmid carrying bla_{SFO-1} resistance gene was designated as pYQ13422-SFO-1.

The transconjugant was identified as *E. coli* by MALDI-TOF/MS. Then PCR and Sanger sequencing were performed to determine that the transconjugant was carrying the bla_{IMP-4} resistance gene. The results of AST also indicated that the plasmid pYQ13422-IMP-4 was successfully transferred into recipient J53. A comparison of AST results between YQ13422hy and YQ13422-J53, YQ13530hy and YQ13530-J53 showed that the transconjugant was resistant to ceftriaxone, cefotaxime, ciprofloxacin, ceftazidime, amoxicillin-clavulanic acid and cefepime, sensitive to aztreonam, gentamicin, piperacillin/tazobactam, chloromycin and fosfomycin, and intermediate to levofloxacin and imipenem, but significantly increased the MIC value of the transconjugant to levofloxacin.

Through the analysis by the OriTFinder website, the complete conjugative modules on the plasmid pYQ13422-IMP-4, pYQ13530-IMP-4, pYQ13422-SFO-1, and pYQ13530-SFO-1 were identified, including the origin of transfer site (*oriT*), gene cluster for bacterial type IV secretion system (T4SS), gene encoding type IV coupling protein (T4CP), and relaxase gene (Table S4). Based on these results, it appears they are MDR plasmids that can be horizontal transferred (Figure 1). Because pYQ13422-IMP-4 and pYQ13530-IMP-4 are exactly the same, we only show pYQ13422-IMP-4 in Figure 1.

Characterization of the genome of *E. hormaechei* YQ13422hy and YQ13530hy

The result of S1-PFGE showed that YQ13422hy and YQ13530hy both carried three plasmids of different sizes, as mentioned above. WGS showed that YQ13422hy and YQ13530hy both carried four plasmids of different sizes. The plasmid pYQ13422hy-3 and Pyq13530hy-3 are not visible in the S1-PFGE result due to its small size; 4995bp.

According to the WGS results, YQ13422hy and YQ13530hy were shown by MLST to carry the genes *fusA* (4), *leuS* (6), *rplB* (4), *rpoB* (6), *dnaA* (4), *gyrB* (4), *pyrG* (37), confirming its typing as ST51. Specific genome information on plasmid sizes, Inc and MLST typing and resistance genes is displayed in Table 2.

TABLE 1 MIC values of antimicrobials for *E. hormaechei* YQ13422hy andYQ13530hy, recipient strain J53, transconjugants YQ13422hy-J53 and YQ13530hy-J53, and control strain *E. coli* 25922.

Antimicrobials	MIC values (mg/L)					
	YQ13422hy	YQ13422hy-J53	YQ13530hy	YQ13530hy-J53	J53	25922
Aztreonam	>128 (R)	0.5 (S)	128 (R)	0.5 (S)	0.5 (S)	0.5 (S)
Imipenem	2 (I)	2 (I)	2 (I)	2 (I)	0.5 (S)	0.25 (S)
Meropenem	1 (S)	1 (S)	1 (S)	1 (S)	0.03 (S)	0.03 (S)
Ceftriaxone	>128 (R)	128 (R)	>128 (R)	128 (R)	0.06 (S)	0.06 (S)
Cefotaxime	>128 (R)	128 (R)	>128 (R)	128 (R)	0.125 (S)	0.125 (S)
Ceftazidime	>128 (R)	>128 (R)	>128 (R)	>128 (R)	0.25 (S)	0.5 (S)
Levofloxacin	4 (R)	1 (I)	8 (R)	1 (I)	0.015 (S)	0.03 (S)
Ciprofloxacin	2 (R)	1 (R)	8 (R)	1 (R)	0.03 (S)	0.015 (S)
Amikacin	16 (S)	16 (S)	16 (S)	16 (S)	16 (S)	16 (S)
Gentamicin	>128 (R)	4 (S)	>128 (R)	4 (S)	4 (S)	4 (S)
Piperacillin/Tazobactam	>128/4 (R)	16/4 (S)	128/4 (R)	16/4 (S)	4/1 (S)	4/1 (S)
Fosfomycin	128 (I)	0.5 (S)	64 (S)	0.5 (S)	0.25 (S)	0.5 (S)
Chloromycin	>128 (R)	4 (S)	64 (R)	4 (S)	4 (S)	4 (S)
Trimethoprim/Sulfamethoxazole	0.5/9.5 (S)	0.125/2.375 (S)	4/76 (R)	0.125/2.375 (S)	0.125/2.375 (S)	0.125/2.375 (S)
Amoxicillin-Clavulanic acid	128/64 (R)	128/64 (R)	128/64 (R)	128/64 (R)	4/2 (S)	8/4 (S)
Cefepime	32 (R)	16 (R)	32 (R)	16 (R)	0.06 (S)	0.06 (S)
Tigecycline	0.5 (S)	0.25 (S)	8 (R)	0.25 (S)	0.5 (S)	0.25 (S)
Polymyxin B	1 (S)	1 (S)	1 (S)	0.5 (S)	1 (S)	1 (S)

R, resistant; S, susceptible; I, intermediate.

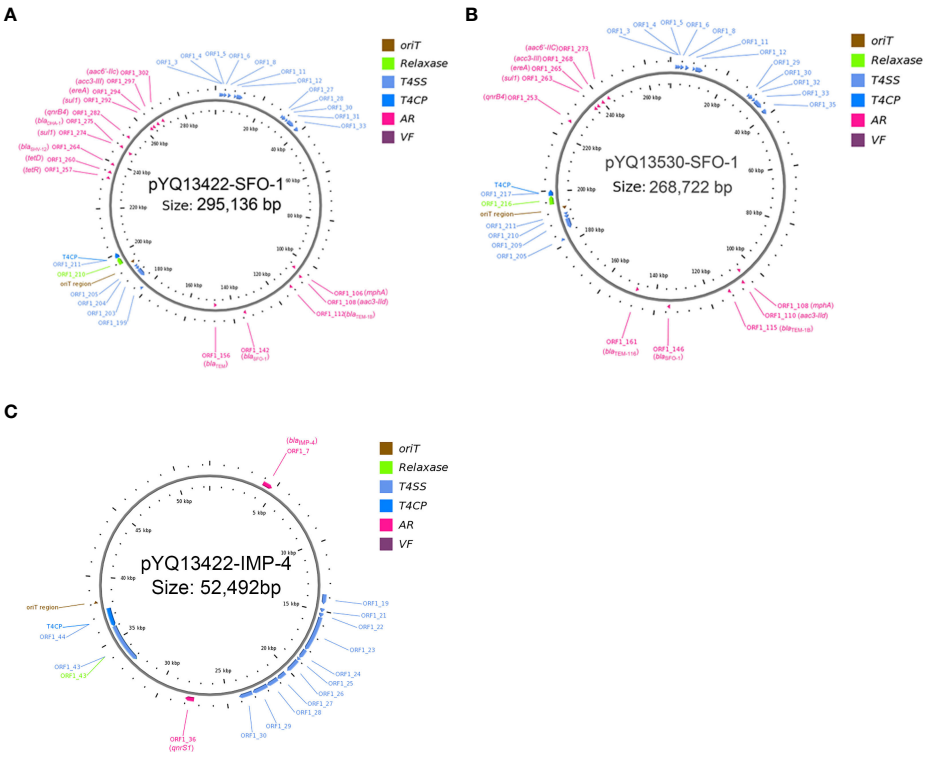

FIGURE 1
Three conjugative plasmids pYQ13422-SFO-1 **(A)** and pYQ13530-SFO-1 **(B)** and pYQ13422-IMP-4 **(C)**. AR (ARGs), acquired antibiotic resistance determinant genes; VF, virulence factors.

TABLE 2 Genome information and acquired antibiotic resistance genes of *E. hormaechei* YQ13422hy and YQ13530hy.

Genome	Size (bp)	G + C (%)	Typing	Resistance gene
YQ13422hy				
Chromosome	4,570,859	55.72%	ST51	*fosA*, bla_{ACT-7}
Plasmids				
pYQ13422hy-SFO-1	295,136	47.62%	IncHI2/2A	*aac(6')-IIc, aac(3)-IId, ere(A), mph(A), qnrB4,* bla_{SHV-12}, bla_{DHA-1}, bla_{TEM-1B}, bla_{SFO-1}, *sul1, tet(D), qacE, catA2*
pYQ13422hy-2	60,348	42.47%	undefined	
pYQ13422hy-IMP-4	52,492	50.85%	IncN	*qnrS1,* bla_{IMP-4}
pYQ13422-3	4,995bp	51.73%	undefined	/
YQ13530hy				
Chromosome	4,571,686	55.73%	ST51	*fosA*, bla_{ACT-7}
Plasmids				
pYQ13530hy-SFO-1	268,722	46.72%	IncHI2/2A	*aac(6')-IIc, aac(3)-IId, ere(A),mph(A), qnrB4, sul1,* bla_{SFO-1}, bla_{TEM-1B}, *qacE*
pYQ13530hy-2	60,311	42.45%	undefined	/
pYQ13530hy-IMP-4	52,492	50.85%	IncN	*qnrS1,* bla_{IMP-4}
pYQ13530hy-3	4,995bp	51.73%	undefined	/

Structural characterization of the transferable plasmid

The sequence length of plasmid pYQ13422-IMP-4 is 52,492bp, including 92 protein-encoding genes, and its G + C content is 50.85%. This plasmid carries the bla_{IMP-4} gene and the *qnrS1* gene, which is known from above. Its plasmid type is IncN by Plasmidfinder. The most similar plasmids (with 100% coverage and 99% identities) identified by NCBI blast are as follows: pIMP-GZ1517 (KT982618.1), pZHH-3 (CP059714), p128379-IMP (MF344559) and pIMP-GZ1058 (KU051709.1) from *E. coli*, and pIMP-HZ1 (KU886034) from *K. pneumoniae*. BLAST, Ring Image Generator (BRIG) generated the circular image of multiple plasmid comparisons, and the results were demonstrated in Figure 2. The plasmids carry multiple insertion sequences at different positions, such as IS*6100*, IS*1X2*, IS*26* and IS*Kpn19*. Further, we investigated the genetic environment of the IMP-4 resistance gene and found that it has an In*tI1* upstream and also carries a group II intron reverse transcriptase/maturase gene downstream of it. Comparison with pIMP-GZ1517 (KT982618.1) and pIMP-GZ1058 (KU051709.1) revealed that an insertion sequence IS*26* was missing on the YQ13422-IMP-4 plasmid (Figure S5). Integron In*823* was identified by INTEGRALL, whose array of gene cassettes is 5′CS-bla_{IMP-4}. YQ13422-SFO-1 is demonstrated in Figure 2B.

In addition to analyzing MDR plasmid characteristics, we also examined mobile elements flanking the resistant genes (Figure S5). The bla_{SFO-1} was detected on a Tn*3* unit (Tn*AS3*-IS*5075*-*traX*-*Δ*Tn*3*-*ampR*-bla_{SFO-1}-*Δ*IS*3*). According to the genetic mapping of bla_{SFO-1}, *ampR* was upstream of bla_{SFO-1}. Regulation of SFO-1 is carried out by the regulator *ampR*, which is inversely oriented upstream (Fernandez et al., 2011). Tn*3* and IS*5075* were located upstream of *ampR*, and genetic mapping also showed that the transposon Tn*3* was interrupted.

Phylogenetic analysis

We downloaded all genomic data of the bla_{IMP}-carrying ECC isolates (n = 167) from NCBI publicly available data and performed a phylogenetic analysis with YQ13422hy and YQ13530hy (Table S1). The data showed that the vast majority of bacteria carrying the bla_{IMP} resistance genes in the ECC are *E. hormaechei*, with 154 strains accounting for 91.12% of all strains. The results revealed that the bla_{IMP} resistance genes carried by the ECC were bla_{IMP-1} (n = 66), bla_{IMP-4} (n = 77), bla_{IMP-8} (n = 8), bla_{IMP-13} (n = 2), bla_{IMP-16} (n = 1), bla_{IMP-26} (n = 3), and bla_{IMP-70} (n = 12). Of these, 158 strains were isolated from humans, and only 11 strains had no host information. The majority of isolates were from Japan, China and Australia. The source of these strains is almost exclusively clinical, mainly blood, urine, sputum, and screening swab. YQ13422hy and YQ13530hy form a small cluster alone, and a larger cluster with GCA_015684015, GCA_021165665, GCA_015683815, but GCA_015684015 and GCA_015683815 are isolated from Australia, while GCA_021165665.1 is recovered from Ireland. They are both *E. hormaechei* and carry the drug resistance gene bla_{IMP-4}. More specific information is shown in Figure S6.

Discussion

ECC is increasingly being isolated from clinical specimens and is now one of the world's most critical nosocomial infectious pathogens (Bolourchi et al., 2022). The ECC carrying bla_{IMP} has emerged in six countries, including United Kingdom, the United States, Ireland, Japan, China, and Australia. Thus, the prevalence of the bla_{IMP} gene worldwide should be given sufficient attention.

According to our susceptibility results, strains carrying bla_{IMP-4} are intermediate to imipenem and sensitive to meropenem. There is evidence suggesting that IMP-4 enzyme has much stronger hydrolytic activity for imipenem than meropenem, which is consistent with previous findings (Chu et al., 2001). A considerable amount of literature now exists suggesting that multiple different species of bacteria carrying bla_{IMP-4} are intermediate or sensitive to imipenem and meropenem (Chu et al., 2001; Lee et al., 2017; Tarabai et al., 2021; Zhang et al., 2021b). However, the exact mechanism is still unclear. Intermediate susceptibility to imipenem and susceptibility to meropenem in strains carrying bla_{IMP-4} possible mechanism could be: i) related to the activity of efflux pumps (Zhang et al., 2021b), or (ii) It is possibly that the organisms had little or no expression of their bla_{IMP-4} gene (Chu et al., 2001), or (iii) It seems that IMP enzymes confer carbapenem resistance only in members of the family Enterobacteriaceae with concomitant permeability lesions (Chu et al., 2001).

Plasmids play a major role in the dissemination of antibiotic resistance genes among Enterobacteriaceae (Huang et al., 2013). Although there have been many studies on IncN-type plasmids, few studies have found that IncN-type plasmids carrying the IMP-4 resistance gene in *E. hormaechei*. IncN-type plasmids carrying genes such as bla_{KPC} (Gomez-Simmonds et al., 2022) and bla_{NDM} (Hirabayashi et al., 2021) have been found in *E. coli* (Dorr et al., 2022) and *Citrobacter* (Yao et al., 2021). Also, a lot of IncN bla_{IMP-4}-carrying plasmids were described in *Enterobacterales*, including one study showing the isolation of *Klebsiella pneumoniae* carrying an IncN-type plasmid with bla_{KPC-2} from dogs (Sellera et al., 2021). Wang and colleagues have already reported that an IncN ST7 plasmid carrying bla_{IMP-4} is disseminated in a variety of enterobacterial species originating from patients with epidemiological links in remote areas of China (Wang et al., 2017). The plasmids

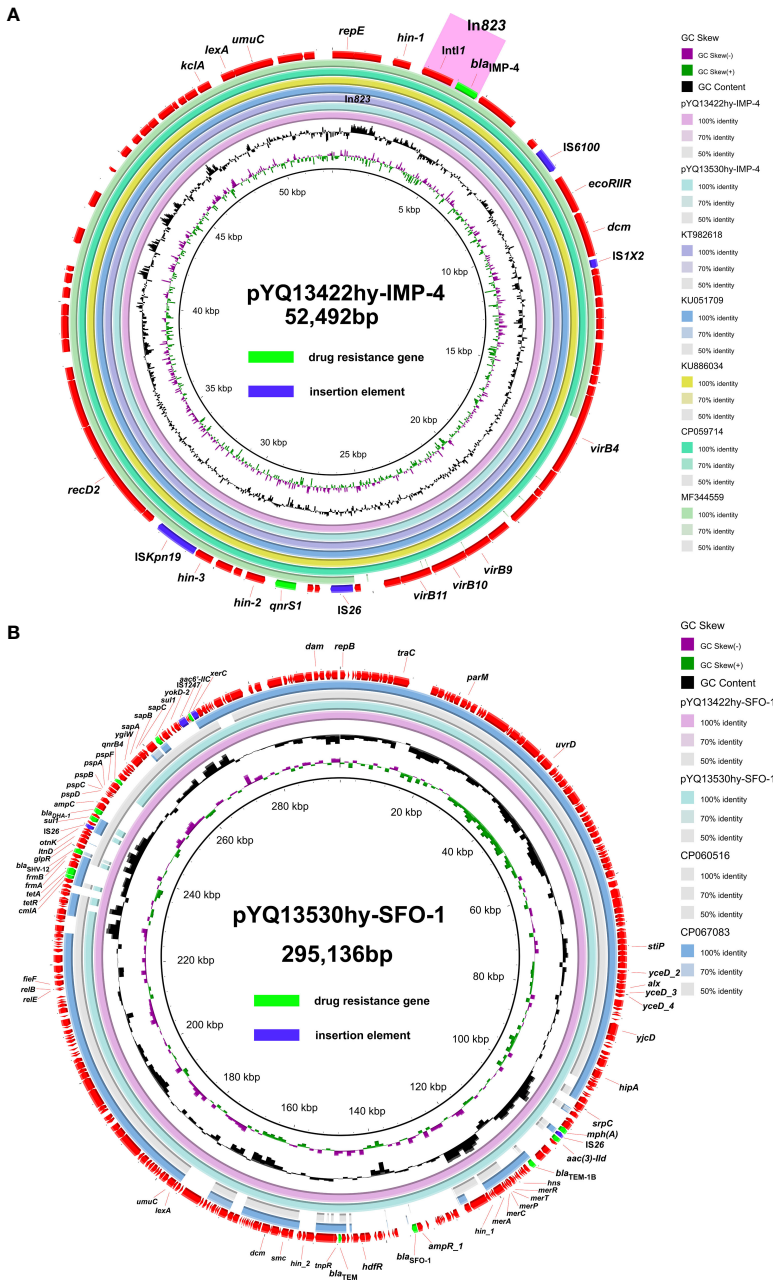

FIGURE 2
Genomic analyses of plasmid pYQ13422-IMP-4 **(A)** and pYQ13422-SFO-1 **(B)**. The comparative plasmid circular map of pYQ13422-IMP-4 and pYQ13422-SFO-1, generated using BLAST Ring Image Generator (BRIG), shows the genes and their locations.

carrying the bla_{IMP-4} gene of YQ13422hy and YQ13530hy are entirely identical. Besides, it's worth noting that we collected these two bacteria from different patients in the same ward at different times in the same hospital. In addition, based on the INTEGRALL database, bla_{IMP-4} is located on a class 1 integron In*823*, which is rare in *E. hormaechei*, with the array of gene cassettes 5′CS-bla_{IMP-4}. It has become a consensus that the proliferation of integrons has exacerbated the prevalence of drug-resistant genes, especially class 1 integrons (Souque et al., 2021). The 3′CS of most class I integrons include three open reading frames (ORFs): sulfa resistance gene (*sul1*), quaternary ammonium compound and ethidium bromide tolerance gene (*qacEΔ1*) and an ORF of unknown function. However, unlike the classical class 1 integron, the 3'CS of the class 1 integron of YQ13422-IMP-4, *sul1* and *qacEΔ1* was not found.

Meanwhile, we confirmed the presence of a transposon Tn*AS3* carrying the bla_{SFO-1} gene, which belongs to the transposon family Tn*3*. Studies on the Tn*3* family of transposons have been relatively extensive. Previous studies indicate that the most characteristic resolvases of the Tn*3* transposon family are members of the serine recombinase (S recombinase) family, but rarely are members of the tyrosine recombinase (Y recombinase) family (Nicolas et al., 2015). The plasmid YQ13422hy-SFO-1 carries tyrosine recombinase *xerC*. Meanwhile, through our study on the structure of the YQ13422-IMP-4 plasmid and comparative analysis with other plasmids, we found that the bla_{IMP-4} genes all contain a group II intron reverse transcriptase/maturase downstream, and speculated that this gene might be associated with the transfer and spread of bla_{IMP-4}. Compared with plasmids pIMP-GZ1517 (KT982618) and pIMP-GZ1517 (KU051709), pYQ13422-IMP-4 and pZHH-3 (CP059714) have no insert sequence IS*26*, which suggests that IntI*1* can transfer bla_{IMP-4} independently and IS*26* may not be the critical gene for bla_{IMP-4} gene transfer. In pIMP-GZ1517 (KT982618) and pIMP-GZ1517 (KU051709), the IntI*1* gene was interrupted by an IS*26* element, but bla_{IMP-4} could still be transferred. We believed that the truncated IntI*1* was out of its function, and the transfer was achieved by IS26. We also found that p128379-IMP does not have the integrase IntI*1*, but contains IS*26*. We discovered the entire complete conjugative modules on the plasmids pYQ13422-IMP-4, pYQ13422-SFO-1 and pYQ13530-SFO-1.

The studies on bla_{IMP-4} in *E. hormaechei* are rare worldwide, with significant differences between countries. A prospective cohort study (Roberts et al., 2020a) in Australia showed that the primary ST type of ECC carrying bla_{IMP-4} was ST90, and the plasmid carrying bla_{IMP-4} was IncHI2-type. Currently, bla_{IMP-4} is Australia's most common resistance gene (Sidjabat et al., 2015), and our phylogenetic analysis based on published data from NCBI confirmed this. Another study (Roberts et al., 2020b) also supported a similar view. Furthermore, we found that all the integrons of *E. hormaechei* carrying bla_{IMP-4} in the published studies rarely contain In*823*. This further indicates that the context of the bla_{IMP-4} gene may be different in China.

In China, few reports described the detection of bla_{IMP-4} gene in *E. hormaechei* (Chen et al., 2022). Kai Zhou et al. found a strain of *E. hormaechei* of ST418 carrying bla_{NDM-1}, *mcr-9.1*, and bla_{IMP-4} (Zhou et al., 2017). According to its research, the plasmid carrying bla_{IMP-4} was IncHI2-type, which is consistent with the global trend. The bla_{SFO-1} gene is not routinely monitored, but it could be an important weapon against antibiotics. So, the coexistence of bla_{SFO-1} and other antibiotic resistance genes should not be ignored. A previous study reported the co-producing of SFO-1 and IMP-4 in *Klebsiella pneumoniae* clinical isolate (Zhou et al., 2017). Moreover, in our work, we not only found the co-producing of SFO-1 and IMP-4 in *E. hormaechei*, but also found they are located at two different transferable plasmids. Antibiotic resistance may be increased by the presence of bla_{SFO-1}. The research of AST results on IMP-producing ECC (Hickey et al., 2021) also suggested that IMP metalloenzymes production in ECC infections is serious, and our work also validated the study. *E. hormaechei* carrying the bla_{IMP-4} gene spread rapidly, with enhanced drug resistance and changes in the genetic environment. Therefore, the coexistence of bla_{SFO-1} and bla_{IMP-4} undoubtedly complicates the treatment of *E. hormaechei* infections. The limitation of our work is that only two samples were studied, and there were no more samples to further elaborate on the prevalence of IncN-plasmid carrying IMP-4 in *E. hormaechei*.

Conclusion

Our study found the co-production of IMP-4 and SFO-1 in *E. hormaechei*. Besides, it revealed the IncN-type plasmid carrying bla_{IMP-4} in *E. hormaechei*, which indicated the potential horizontal transformation of ARGs. In conclusion, our work supplemented the studies of *E. hormaechei* carrying bla_{IMP-4} and bla_{SFO-1} in China, and also suggested that focusing on *E. hormaechei* will be important in future studies.

Data availabilitiy statement

The datasets presented in this study can be found in online repositories. The names of the repository/repositories and accession number(s) can be found in the article/Supplementary Material.

Ethics statement

Written informed consent was obtained from the individual(s) for the publication of any potentially identifiable images or data included in this article.

Author contributions

The experiments were conceived and designed by JG and BZ. The samples and experiments were collected and performed by JQ, HG, RL, CL and RC. The data was analyzed by HX and XG. The manuscript was written by JQ. All authors contributed to the article and approved the submitted version.

Funding

This work was supported by research grants from Henan Science and Technology Department (No. 192102310059), the National Natural Science Foundation of China (82072314), the Research Project of Jinan Microecological

Biomedicine Shandong Laboratory (JNL-2022011B), the Fundamental Research Funds for the Central Universities (2022ZFJH003), CAMS Innovation Fund for Medical Sciences (2019-I2M-5-045), and Henan Province Medical Science and Technology Research Project Joint Construction Project (No. LHGJ20190232).

Conflict of interest

The authors declare that the research was conducted in the absence of any commercial or financial relationships that could be construed as a potential conflict of interest.

Publisher's note

All claims expressed in this article are solely those of the authors and do not necessarily represent those of their affiliated organizations, or those of the publisher, the editors and the reviewers. Any product that may be evaluated in this article, or claim that may be made by its manufacturer, is not guaranteed or endorsed by the publisher.

Supplementary material

The Supplementary Material for this article can be found online at: https://www.frontiersin.org/articles/10.3389/fcimb.2022.998578/full#supplementary-material

SUPPLEMENTARY FIGURE 1
Plasmid profiles of **(E)** hormaechei YQ13422hyh and YQ13530hy. **(A)** Plasmid size determination by S1-PFGE, with Salmonella enterica serotype Braenderup H9812 as the size marker. **(B)** Southern blotting hybridization with an IMP-4-specific probe.

SUPPLEMENTARY FIGURE 2
The ANI analysis between YQ13422hy and YQ13530hy showed that there is a high level of similarity between the two genomes.

SUPPLEMENTARY FIGURE 3
Genomic analyses of plasmid pYQ13422-IMP-4. The comparative plasmid circular map of pYQ13422-IMP-4 generated using BLAST Ring Image Generator (BRIG), shows the genes and their locations.

SUPPLEMENTARY FIGURE 4
YQ13422hy and YQ13530hy 's genomes contain a wealth of information.

SUPPLEMENTARY FIGURE 5
Genetic context of blaIMP-4 on pYQ13422-IMP-4 and blaSFO-1 on pYQ13422-SFO-1. Genes are denoted by arrows. Genes, mobile elements, and other features are colored based on their functional classification.

SUPPLEMENTARY FIGURE 6
The phylogenetic tree of 167 strains ECC based on the blaIMP resistance genes, generated by kSNP3.0 plus *E. hormaechei* YQ13422hy (Biosample SAMN28918927) and YQ13530hy (Biosample SAMN28919657). The sources of strains are identified as clinical. We used different colors to represent different meanings. The seven circles around the phylogenetic tree indicate the species (inner circle), ST type, IMP-type, host, location, year, and source (outer circle) of these strains. We marked YQ13422hy and YQ13530hy in red.

References

Alikhan, N. F., Petty, N. K., Ben Zakour, N. L., and Beatson, S. A. (2011). BLAST ring image generator (BRIG): Simple prokaryote genome comparisons. *BMC Genomics* 12, 402. doi: 10.1186/1471-2164-12-402

Annavajhala, M. K., Gomez-Simmonds, A., and Uhlemann, A.-C. (2019). Multidrug-resistant enterobacter cloacae complex emerging as a global, diversifying threat. *Front. Microbiol.* 10. doi: 10.3389/fmicb.2019.00044

Aziz, R. K., Bartels, D., Best, A. A., Dejongh, M., Disz, T., Edwards, R. A., et al. (2008). The RAST server: Rapid annotations using subsystems technology. *BMC Genomics* 9, 75. doi: 10.1186/1471-2164-9-75

Bolourchi, N., Giske, C. G., Nematzadeh, S., Mirzaie, A., Abhari, S. S., Solgi, H., et al. (2022). Comparative resistome and virulome analysis of clinical NDM-1-producing carbapenem-resistant enterobacter cloacae complex. *J. Glob Antimicrob. Resist.* 28, 254–263. doi: 10.1016/j.jgar.2022.01.021

Chen, W., Hu, Z., Wang, S., Huang, D., Wang, W., Cao, X., et al. (2022). Letter to the Editor: Characterization of a clinical enterobacter hormaechei strain belonging to epidemic clone ST418 Co-carrying blaNDM-1, blaIMP-4, and mcr-9.1. *Microb. Drug Resist.* 28, 180–184. doi: 10.1089/mdr.2020.0568

Chu, Y. W., Afzal-Shah, M., Houang, E. T., Palepou, M. I., Lyon, D. J., Woodford, N., et al. (2001). IMP-4, a novel metallo-beta-lactamase from nosocomial acinetobacter spp. collected in Hong Kong between 1994 and 1998. *Antimicrob. Agents Chemother.* 45, 710–714. doi: 10.1128/AAC.45.3.710-714.2001

Dorr, M., Silver, A., Smurlick, D., Arukha, A., Kariyawasam, S., Oladeinde, A., et al. (2022). Transferability of ESBL-encoding IncN and IncI1 plasmids among field strains of different salmonella serovars and escherichia coli. *J. Glob Antimicrob. Resist.* 30, 88–95. doi: 10.1016/j.jgar.2022.04.015

Fernandez, A., Pereira, M. J., Suarez, J. M., Poza, M., Trevino, M., Villalon, P., et al. (2011). Emergence in Spain of a multidrug-resistant enterobacter cloacae clinical isolate producing SFO-1 extended-spectrum beta-lactamase. *J. Clin. Microbiol.* 49, 822–828. doi: 10.1128/JCM.01872-10

Gardner, S. N., Slezak, T., and Hall, B. G. (2015). kSNP3.0: SNP detection and phylogenetic analysis of genomes without genome alignment or reference genome. *Bioinformatics* 31, 2877–2878. doi: 10.1093/bioinformatics/btv271

Gomez-Simmonds, A., Annavajhala, M. K., Tang, N., Rozenberg, F. D., Ahmad, M., Park, H., et al. (2022). Population structure of blaKPC-harbouring IncN plasmids at a new York city medical centre and evidence for multi-species horizontal transmission. *J. Antimicrob. Chemother.* 77, 1873–1882. doi: 10.1093/jac/dkac114

Goncalves, D., Cecilio, P., Faustino, A., Iglesias, C., Branca, F., Estrada, A., et al. (2021). Intra- and extra-hospital dissemination of IMP-22-Producing klebsiella pneumoniae in northern Portugal: The breach of the hospital frontier toward the community. *Front. Microbiol.* 12, 777054. doi: 10.3389/fmicb.2021.777054

Gou, J. J., Liu, N., Guo, L. H., Xu, H., Lv, T., Yu, X., et al. (2020). Carbapenem-resistant enterobacter hormaechei ST1103 with IMP-26 carbapenemase and ESBL gene bla SHV-178. *Infect. Drug Resist.* 13, 597–605. doi: 10.2147/IDR.S232514

Hickey, C., Nguyen, S., Anes, J., Hurley, D., Donoghue, O., Fanning, S., et al. (2021). Differences in antimicrobial susceptibility testing complicating

management of IMP carbapenemase-producing enterobacterales infection. *J. Glob Antimicrob. Resist.* 27, 284–288. doi: 10.1016/j.jgar.2021.09.010

Hirabayashi, A., Yahara, K., Mitsuhashi, S., Nakagawa, S., Imanishi, T., Ha, V. T. T., et al. (2021). Plasmid analysis of NDM metallo-β-lactamase-producing enterobacterales isolated in Vietnam. *PLoS One* 16, e0231119. doi: 10.1371/journal.pone.0231119

Huang, T. W., Wang, J. T., Lauderdale, T. L., Liao, T. L., Lai, J. F., Tan, M. C., et al. (2013). Complete sequences of two plasmids in a blaNDM-1-positive klebsiella oxytoca isolate from Taiwan. *Antimicrob. Agents Chemother.* 57, 4072–4076. doi: 10.1128/AAC.02266-12

Hu, L., Zhong, Q., Shang, Y., Wang, H., Ning, C., Li, Y., et al. (2014). The prevalence of carbapenemase genes and plasmid-mediated quinolone resistance determinants in carbapenem-resistant enterobacteriaceae from five teaching hospitals in central China. *Epidemiol. Infect.* 142, 1972–1977. doi: 10.1017/S0950268813002975

Lee, J. H., Bae, I. K., Lee, C. H., and Jeong, S. (2017). Molecular characteristics of first IMP-4-Producing enterobacter cloacae sequence type 74 and 194 in Korea. *Front. Microbiol.* 8, 2343. doi: 10.3389/fmicb.2017.02343

Liew, S. M., Rajasekaram, G., Puthucheary, S. D., and Chua, K. H. (2018). Detection of VIM-2-, IMP-1- and NDM-1-producing multidrug-resistant pseudomonas aeruginosa in Malaysia. *J. Glob Antimicrob. Resist.* 13, 271–273. doi: 10.1016/j.jgar.2018.01.026

Matsumoto, Y., and Inoue, M. (1999). Characterization of SFO-1, a plasmid-mediated inducible class a beta-lactamase from enterobacter cloacae. *Antimicrob. Agents Chemother.* 43 (2), 307–313. doi: 10.1128/AAC.43.2.307

Matsumura, Y., Peirano, G., Motyl, M. R., Adams, M. D., Chen, L., Kreiswirth, B., et al. (2017). Global molecular epidemiology of IMP-producing enterobacteriaceae. *Antimicrob. Agents Chemother.* 72 (8), 2249–2258. doi: 10.1093/jac/dkx148

Mezzatesta, M. L., Gona, F., and Stefani, S. (2012). Enterobacter cloacae complex: clinical impact and emerging antibiotic resistance. *Future Microbiol.* 7, 887–902. doi: 10.2217/fmb.12.61

Nicolas, E., Lambin, M., Dandoy, D., Galloy, C., Nguyen, N., Oger, C. A., et al. (2015). The Tn3-family of replicative transposons. *Microbiol. Spectr.* 3, 693–726. doi: 10.1128/microbiolspec.MDNA3-0060-2014

Osei Sekyere, J., and Reta, M. A. (2021). Global evolutionary epidemiology and resistome dynamics of citrobacter species, enterobacter hormaechei, klebsiella variicola, and proteeae clones. *Environ. Microbiol.* 23, 7412–7431. doi: 10.1111/1462-2920.15387

Riccio, M. L., Franceschini, N., Boschi, L., Caravelli, B., Cornaglia, G., Fontana, R., et al. (2000). Characterization of the metallo-beta-lactamase determinant of acinetobacter baumannii AC-54/97 reveals the existence of bla(IMP) allelic variants carried by gene cassettes of different phylogeny. *Antimicrob. Agents Chemother.* 44, 1229–1235. doi: 10.1128/AAC.44.5.1229-1235.2000

Roberts, L. W., Catchpoole, E., Jennison, A. V., Bergh, H., Hume, A., Heney, C., et al. (2020a). Genomic analysis of carbapenemase-producing enterobacteriaceae in Queensland reveals widespread transmission of bla (IMP-4) on an IncHI2 plasmid. *Microb. Genom* 6 (1), e000321. doi: 10.1099/mgen.0.000321

Roberts, L. W., Harris, P. N. A., Forde, B. M., Ben Zakour, N. L., Catchpoole, E., Stanton-Cook, M., et al. (2020b). Integrating multiple genomic technologies to investigate an outbreak of carbapenemase-producing enterobacter hormaechei. *Nat. Commun.* 11, 466. doi: 10.1038/s41467-019-14139-5

Sellera, F. P., Fuga, B., Fontana, H., Esposito, F., Cardoso, B., Konno, S., et al. (2021). Detection of IncN-pST15 one-health plasmid harbouring bla(KPC-2) in a hypermucoviscous Klebsiella pneumoniae CG258 isolated from an infected dog, Brazil. *Transbound Emerg Dis* 68, 3083–3088. doi: 10.1111/tbed.14006.

Sidjabat, H. E., Townell, N., Nimmo, G. R., George, N. M., Robson, J., Vohra, R., et al. (2015). Dominance of IMP-4-producing enterobacter cloacae among carbapenemase-producing enterobacteriaceae in Australia. *Antimicrob. Agents Chemother.* 59, 4059–4066. doi: 10.1128/AAC.04378-14

Souque, C., Escudero, J. A., and Maclean, R. C. (2021). Integron activity accelerates the evolution of antibiotic resistance. *Elife*, 10. doi: 10.7554/eLife.62474.

Sullivan, M. J., Petty, N. K., and Beatson, S. A. (2011). Easyfig: A genome comparison visualizer. *Bioinformatics* 27, 1009–1010. doi: 10.1093/bioinformatics/btr039

Tarabai, H., Wyrsch, E. R., Bitar, I., Dolejska, M., and Djordjevic, S. P. (2021). Epidemic HI2 plasmids mobilising the carbapenemase gene bla(IMP-4) in Australian clinical samples identified in multiple sublineages of escherichia coli ST216 colonising silver gulls. *Microorganisms* 9 (3), 567. doi: 10.3390/microorganisms9030567

Wang, Y., Lo, W. U., Lai, R. W., Tse, C. W., Lee, R. A., Luk, W. K., et al. (2017). IncN ST7 epidemic plasmid carrying blaIMP-4 in enterobacteriaceae isolates with epidemiological links to multiple geographical areas in China. *J. Antimicrob. Chemother.* 72, 99–103. doi: 10.1093/jac/dkw353

Wang, S., Xu, L., Chi, X., Li, Y., Kou, Z., Hou, P., et al. (2019). Emergence of NDM-1- and CTX-M-3-Producing raoultella ornithinolytica in human gut microbiota. *Front. Microbiol.* 10, 2678. doi: 10.3389/fmicb.2019.02678

Watanabe, M., Iyobe, S., Inoue, M., and Mitsuhashi, S. (1991). Transferable imipenem resistance in pseudomonas aeruginosa. *Antimicrob. Agents Chemother.* 35, 147–151. doi: 10.1128/AAC.35.1.147

Xu, Y., Liu, Y., Liu, Y., Pei, J., Yao, S., and Cheng, C. (2015). Bacteriophage therapy against enterobacteriaceae. *Virol. Sin.* 30, 11–18. doi: 10.1007/s12250-014-3543-6

Xu, H., Wang, X., Yu, X., Zhang, J., Guo, L., Huang, C., et al. (2018). First detection and genomics analysis of KPC-2-producing citrobacter isolates from river sediments. *Environ. pollut.* 235, 931–937. doi: 10.1016/j.envpol.2017.12.084

Yan, J. J., Ko, W. C., and Wu, J. J. (2001). Identification of a plasmid encoding SHV-12, TEM-1, and a variant of IMP-2 metallo-beta-lactamase, IMP-8, from a clinical isolate of klebsiella pneumoniae. *Antimicrob. Agents Chemother.* 45, 2368–2371. doi: 10.1128/AAC.45.8.2368-2371.2001

Yao, Y., Falgenhauer, L., Falgenhauer, J., Hauri, A. M., Heinmüller, P., Domann, E., et al. (2021). Carbapenem-resistant citrobacter spp. as an emerging concern in the hospital-setting: Results from a genome-based regional surveillance study. *Front. Cell Infect. Microbiol.* 11, 744431. doi: 10.3389/fcimb.2021.744431

Zhang, Y., Gu, D., Yang, X., Wu, Y., Liu, C., Shen, Z., et al. (2021a). Emergence and genomic characterization of a KPC-2-, NDM-1-, and IMP-4-Producing klebsiella michiganensis isolate. *Front. Microbiol.* 12, 762509. doi: 10.3389/fmicb.2021.762509

Zhang, Y., Wang, X., Wang, Q., Chen, H., Li, H., Wang, S., et al. (2021b). Emergence of tigecycline nonsusceptible and IMP-4 carbapenemase-producing K2-ST65 hypervirulent klebsiella pneumoniae in China. *Microbiol. Spectr.* 9, e0130521. doi: 10.1128/Spectrum.01305-21

Zhou, K., Yu, W., Shen, P., Lu, H., Wang, B., Rossen, J. W. A., et al. (2017). A novel Tn1696-like composite transposon (Tn6404) harboring bla (IMP-4) in a klebsiella pneumoniae isolate carrying a rare ESBL gene bla (SFO-1). *Sci. Rep.* 7, 17321. doi: 10.1038/s41598-017-17641-2

Zhou, K., Zhou, Y., Zhang, C., Song, J., Cao, X., Yu, X., et al. (2020). Dissemination of a 'rare' extended-spectrum beta-lactamase gene blaSFO-1 mediated by epidemic clones of carbapenemase-producing enterobacter hormaechei in China. *Int. J. Antimicrob. Agents* 56, 106079. doi: 10.1016/j.ijantimicag.2020.106079

frontiers | Frontiers in Cellular and Infection Microbiology

TYPE Original Research
PUBLISHED 05 January 2023
DOI 10.3389/fcimb.2022.969117

OPEN ACCESS

EDITED BY
Ziad Daoud,
Central Michigan University,
United States

REVIEWED BY
Romain Martischang,
Hopitaux Universitaires de Genève,
Switzerland
Wei Sang,
The Affiliated Hospital of Xuzhou
Medical University, China

*CORRESPONDENCE
Junbin Hu
luckyjun@189.cn
Huafang Wang
whf2019@hust.edu.cn

†These authors have contributed
equally to this work and share
first authorship

SPECIALTY SECTION
This article was submitted to
Clinical Microbiology,
a section of the journal
Frontiers in Cellular and
Infection Microbiology

RECEIVED 14 June 2022
ACCEPTED 12 December 2022
PUBLISHED 05 January 2023

CITATION
Jian X, Du S, Zhou X, Xu Z, Wang K,
Dong X, Hu J and Wang H (2023)
Development and validation of
nomograms for predicting the risk
probability of carbapenem resistance
and 28-day all-cause mortality in
gram-negative bacteremia among
patients with hematological diseases.
Front. Cell. Infect. Microbiol. 12:969117.
doi: 10.3389/fcimb.2022.969117

Development and validation of nomograms for predicting the risk probability of carbapenem resistance and 28-day all-cause mortality in gram-negative bacteremia among patients with hematological diseases

Xing Jian[1†], Shuaixian Du[2†], Xi Zhou[1], Ziwei Xu[1], Kejing Wang[1], Xin Dong[1], Junbin Hu[1*] and Huafang Wang[1*]

[1]Institute of Hematology, Union Hospital, Tongji Medical College, Huazhong University of Science and Technology, Wuhan, China, [2]Department of Clinical Laboratory, Union Hospital, Tongji Medical College, Huazhong University of Science and Technology, Wuhan, China

Objectives: Gram-negative bacteria (GNB) bloodstream infections (BSIs) are the most widespread and serious complications in hospitalized patients with hematological diseases. The emergence and prevalence of carbapenem-resistant (CR) pathogens has developed into a considerable challenge in clinical practice. Currently, nomograms have been extensively applied in the field of medicine to facilitate clinical diagnosis and treatment. The purpose of this study was to explore risk indicators predicting mortality and carbapenem resistance in hematological (HM) patients with GNB BSI and to construct two nomograms to achieve personalized prediction.

Methods: A single-center retrospective case-control study enrolled 244 hospitalized HM patients with GNB-BSI from January 2015 to December 2019. The least absolute shrinkage and selection operator (LASSO) regression analysis and multivariate logistic regression analysis were conducted to select potential characteristic predictors of plotting nomograms. Subsequently, to evaluate the prediction performance of the models, the prediction models were internally validated using the bootstrap approach (resampling = 1000) and 10-fold cross validation.

Results: Of all 244 eligible patients with BSI attributed to GNB in this study, 77 (31.6%) were resistant to carbapenems. The rate of carbapenem resistance exhibited a growing tendency year by year, from 20.4% in 2015 to 42.6% in 2019 (p = 0.004). The carbapenem resistance nomogram constructed with the parameters of hypoproteinemia, duration of neutropenia ≥ 6 days, previous exposure to carbapenems, and previous exposure to cephalosporin/β-lactamase inhibitors indicated a favorable discrimination ability with a

modified concordance index (C-index) of 0.788 and 0.781 in both the bootstrapping and 10-fold cross validation procedures. The 28-day all-cause mortality was 28.3% (68/240). The prognosis nomogram plotted with the variables of hypoproteinemia, septic shock, isolation of CR-GNB, and the incomplete remission status of underlying diseases showed a superior discriminative ability of poorer clinical prognosis. The modified C-index of the prognosis nomogram was 0.873 with bootstrapping and 0.887 with 10-fold cross validation. The decision curve analysis (DCA) for two nomogram models both demonstrated better clinical practicality.

Conclusions: For clinicians, nomogram models were effective individualized risk prediction tools to facilitate the early identification of HM patients with GNB BSI at high risk of mortality and carbapenem resistance.

KEYWORDS

gram-negative bacteria, carbapenem resistance, mortality, prediction, nomogram, bloodstream infections

1 Introduction

Bloodstream infections (BSIs) are the most widespread and serious infectious complications in hospitalized patients with hematological diseases, characterized by significant high morbidity, mortality, and a heavy additional medical burden, primarily arising from the underlying diseases themselves and the cytotoxic chemotherapy-related immunosuppression (Feld, 2008; Misch and Andes, 2019). During recent years, there has been a pronounced trend reversal as regards the bacterial spectrum of bacteremia in patients with neutropenia and hematologic malignancies, with Gram-negative bacteria (GNB) being the most commonly reported pathogenic organisms nowadays (Trecarichi and Tumbarello, 2014; Trecarichi et al., 2015; Chen et al., 2021). In addition, owing to the high selection pressure of antimicrobial agents, a considerable increase has been observed in the infection of multiple antibiotic-resistant strains that are insusceptible to a wide variety of antibiotics. In this context, the progressively emergence and rapidly spread of multidrug-resistant bacteria has been emerging as a globally major challenge, particularly for carbapenem-resistant (CR) GNB (Lalaoui et al., 2020). Considering that it normally takes 2 to 3 days to obtain the results of blood cultures and antimicrobial susceptibility tests against the background of current clinical laboratory conditions, inappropriate empirical antibiotic therapy is life-threatening for patients infected with these strains. Therefore, early identification of risk factors associated with carbapenem resistance and exploration of prognosis-related indicators is essential to purposefully improving clinical outcomes for hematological (HM) patients infected with GNB BSI.

Currently, nomograms have been diffusely applied in medical research as an effective complementary tool to implement clinical decisions for clinicians (Balachandran et al., 2015; Wu et al., 2020; Lin et al., 2020; Song et al., 2021; Dong et al., 2021; He et al., 2022). As a graphical tool, compared with traditional predictive scoring systems based on regression analysis, the nomogram can provide a visual representation of the complex statistical model and accurately estimate the individual probability of a clinical event by integrating multiple predictive variables that can diagnose diseases or predict clinical outcomes (Park, 2018; Jiang et al., 2022). However, nomograms predicting the risk factors of mortality and carbapenem resistance in HM patients with GNB BSI have rarely received attention. Consequently, the primary objective of this study was to develop and validate two clinical predictive models for the early individualized and accurate prediction of carbapenem resistance risk and 28-day all-cause mortality in HM patients suffering from GNB BSI, respectively.

2 Methods

2.1 Study setting and patient population

The retrospective case-control study was performed between January 2015 and December 2019 at the Institute of Hematology, Union Hospital, Tongji Medical College, Huazhong University of Science and Technology, a 5000-bed tertiary care teaching hospital in central China. Episodes of BSI were identified from the clinical microbiology laboratory

database in accordance with the US Centers for Disease Control and Prevention (CDC) criteria (Horan et al., 2008). The first episodes of BSI caused by GNB that occurred in hospitalized hematological patients older than 16 years were included in this study. Meanwhile, patients who had been treated with hematopoietic stem cell transplantation before BSI were excluded, as well as those with polymicrobial bacteremia. Ultimately, 244 patients with GNB BSI met the inclusion and exclusion criteria were enrolled in the retrospective cohort.

2.2 Data collection and study design

Date extracted from the hospital microbiology laboratory database and the medical electronic medical record systems included demographics (age and sex), microbiological data, underlying diseases and the stage of disease at the time of GNB BSI, comorbidities (diabetes mellitus, cardiovascular disease, hepatic disease, pulmonary infection at the time of GNB BSI), the use of immunosuppressants and corticosteroids, invasive procedures and/or devices, antibiotic therapy, the presence and duration of neutropenia, clinical outcomes, and so on. The flowchart of study design was shown in Figure 1. For the purposes of developing a predictive model for carbapenem-resistant bacteremia in this study, patients were divided into the carbapenem-resistant (CR-GNB) groups (77 cases) and the carbapenem-sensitive (CS-GNB) groups (167 cases) based on the reports of antimicrobial susceptibility testing (AST). Simultaneously, we also analyzed the potential risk factors affecting mortality within 28 days following the onset of GNB BSI.

2.3 Definition

Hospital-acquired BSI was considered as the isolation of pathogens from at least one blood culture specimen after 48 hours of admission to hospital. The onset of BSI was defined as the collection date of a positive blood culture sample. Neutropenia was defined as an absolute neutrophil count (ANC) < 500 neutrophils/μl at the time of BSI onset. Corticosteroid therapy was defined as the administration of prednisone (dose ≥ 20mg/day, duration ≥ 5 days) or its equivalent. Immunosuppressive therapy referred to the use of at least one of cyclosporine, tacrolimus, rituximab, and ATG/ALG. Hypoproteinemia was defined as a serum albumin value of less than 30 g/L on the day (or within 24 hours) of the collection of a positive blood culture specimen. Mucosal barrier damage was defined as gastrointestinal mucositis or oropharyngeal mucositis. Antimicrobial agent exposure was defined as the use of antibiotics for more than 72 hours within 30 days before BSI. Typical antimicrobial agents administered within 30 days prior to BSI in this study included carbapenems (imipenem and meropenem), aminoglycosides (etimicin, amikacin and kanamycin), quinolones (levofloxacin and moxifloxacin), tigecyclines, penicillins/β-lactamase inhibitor combinations (piperacillin-tazobactam) and cephalosporins/β-lactamase inhibitor combinations (cefoperazone-tazobactam, cefoperazone-sulbactam, ceftazidime-tazobactam and ceftriaxone-tazobactam). The diagnosis of septic shock followed the Third International Consensus Definitions for Sepsis and Septic Shock (Sepsis-3) clinical criteria (Singer et al., 2016). Carbapenem resistance was defined as resistance to one or more of meropenem, imipenem, and ertapenem.

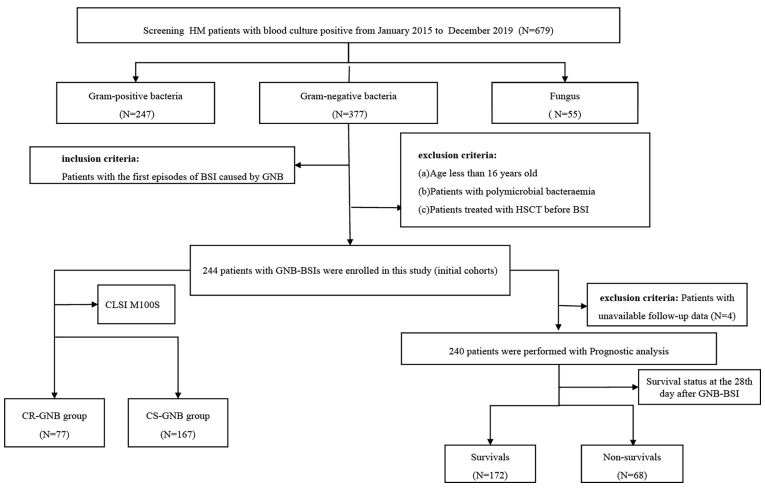

FIGURE 1
Flowchart of the study design. HM, hematological; CLSI,clinical and laboratory standards institute; GNB, gram-negative bacteria; BSI, bloodstream infection; CR, carbapenem-resistant; CS, carbapenem-sensitive.

Empirical antimicrobial therapy was considered appropriate when receiving at least one antimicrobial agent with *in vitro* activity within 48 hours after the episode of BSI. The final clinical outcome was determined by the survival status on the 28th day after the onset of GNB BSI. If a patient was discharged from a hospital within 28 days of the onset of BSI, the clinical outcome was determined by telephone follow-up.

2.4 Microbiological method

Microbial identification and antibiotic susceptibility testing were conducted in the clinical microbiology laboratory of hospital using a fully automated microbiology system (BD phoenix™-100). Antibiotic susceptibilities were interpreted according to the guidelines of the Clinical and Laboratory Standards Institute M100S (CLSI M100S), except for colistin and tigecycline, which were determined in accordance with the European Committee on Antimicrobial Susceptibility Testing (EUCAST) clinical breakpoints.

2.5 Derivation and performance evaluation of the nomogram

The least absolute shrinkage and selection operator (LASSO) regression model with ten-fold cross validation could avoid the multicollinearity of variables and minimize the possibility of model overfitting or underfitting (Iasonos et al., 2008; Friedman et al., 2010; Collins et al., 2015). Given the large number of predictors, the LASSO regression analysis and multivariate logistic regression analysis were performed to select potential characteristic predictors. Afterward, the clinical nomogram were formulated based on the potential characteristic predictors screened above and the significant predictors that had an essential impact on clinical outcomes. In the nomogram, each predictor was visually assigned a corresponding score. The accumulated total points for a clinical event could be calculated by adding the scores of each predictor, corresponding to the predicted probability of the clinical event.

The prediction performance of the nomogram model was evaluated with internal validation, which were primarily conducted using the bootstrap method (resampling = 1000) and 10-fold cross validation. In addition, to minimize the risk of bias of single-center studies, we further evaluate the stability of the prediction model using other cross validation methods such as hold-out cross validation (7:3), leave-one-out cross validation, and bootstrapping with 10-fold cross validation (resampling = 1000). The Concordance index (C-index) or area under the receiver operating characteristic (ROC) curve (AUC) was used to assess the discrimination ability of a predictive model. The C-index of a nomogram was equal to the AUC values of a logistic regression model since the ROC for the logistic regression model was drawn based on the predicted probability. Ordinarily, the C-index and AUC values >0.7 are considered to have relatively good discriminative accuracy. The calibration curves were used to evaluate the calibration ability of a predictive model-that is, the ability of the predicted probabilities of clinical outcomes to be consistent with the actual probabilities. Besides this, decision curve analysis (DCA) was also performed to estimate the clinical application value of the model.

2.6 Statistical analysis

Data analysis was performed using SPSS 25.0 statistical software (SPSS, Chicago, IL, USA) and R software version 4.1.3. The R packages used for statistical analysis in the R project (version 4.1.3) mainly consisted of glmnet, rms, caret, pROC, and rmda. All statistical analyses were two-tailed, with P-values < 0.05 considered statistically significant. The Kolmogorov-Smirnov normality test was utilized to assess the normality distribution of continuous variables. Continuous variables were expressed as median (M) or interquartile range (IQR) and compared using the Mann-Whitney U test. Categorical variables were represented as numbers or percentages (%) of cases and analyzed using the Chi-squared test or the Fisher's exact test. Survival curves were plotted based on the Kaplan-Meier method and compared using the log-rank test.

3 Results

3.1 Distributions of GNB isolates in the original study cohorts

According to the inclusion and exclusion criteria, a total of 244 patients with GNB BSI were included in the study from January 2015 to December 2019. Of all the 244 isolates of GNB, 173 (70.9%) were of *Enterobacteriaceae*, 62 (25.4%) were *glucose non-fermenting* (GNF) GNB, and 9 (3.7%) were of *Vibrionaceae*. *Klebsiella pneumoniae* (KP) (n = 79) and *Escherichia coli* (EC) (n = 66) were the main members of the *Enterobacteriaceae*, while *Pseudomonas aeruginosa* (PA) (n = 30) and *Acinetobacter baumannii* (AB) (n = 23) were the most common GNF GNB; only *Aeromonas* spp. (n = 9) were observed in the *Vibrionaceae*. Bacterial species and numbers of CR-GNB and CS-GNB were described in Table 1. There were 77 of 244 GNB isolates (31.6%) resistant to carbapenems, and the rate of carbapenem resistance appeared to be increasing year on year, from 20.4% in 2015 to 42.6% in 2019 ($p = 0.004$) (Figure 2A). In the CR-GNB cohort, *Klebsiella pneumoniae* (n = 30; 39.0%) was the most frequently encountered strain, followed by *Acinetobacter baumannii* (n = 21; 27.3%) and *Escherichia coli* (n = 13; 16.9%) (Table 1).

TABLE 1 Distribution of bacterial species and numbers of CR-GNB and CS- GNB.

Bacterial species	CR-GN B(n=77,%)	CS-GNB (n=167,%)	Totals (n=244,%)
Enterobacteriaceae	45 (58.4)	128 (76.6)	173 (70.9)
Escherichia coli	13 (16.9)	53 (31.7)	66 (27.0)
enterobacter cloacae	2 (2.6)	13 (7.8)	15 (6.1)
Klebsiella pneumoniae	30 (39.0)	49 (29.3)	79 (32.4)
Klebsiella oxytoca	0	3 (1.8)	3 (1.2)
Prpteus spp.	0	3 (1.8)	3 (1.2)
Serratia marcescens	0	3 (1.8)	3 (1.2)
others	0	4 (2.4)	4 (1.6)
Glucose non-fermenting GNB	30 (38.9)	32 (19.1)	62 (25.4)
Pseudomonas aeruginosa	0	30 (18.0)	30 (12.3)
Acinetobacter baumannii	21 (27.3)	2 (1.2)	23 (9.4)
Acinetobacter junii	1 (1.3)	0	1 (0.4)
Stenotrophomonas maltophilia	8 (10.4)	0	8 (3.3)
Vibrionaceae	2 (2.6)	7 (4.2)	9 (3.7)
Aeromonas spp.	2 (2.6)	7 (4.2)	9 (3.7)

CR-GNB, carbapenem-resistant gram-negative bacteria; CS-GNB, carbapenem-sensitive gram-negative bacteria.

3.2 Demographic and clinical characteristics of patients with GNB BSI

The demographic and clinical characteristics of these patients are summarized in Table 2. Among these 244 patients with GNB, 226 (92.6%) were recognized as hospital-acquired bacteremia, which included all patients (n = 77; 100%) with CR-GNB and the majority (n = 149; 89.2%) with CS-GNB. In the study, the median age of the patients was 44 years (IQR, 29.25-53) and the majority were male (n = 136; 55.7%). At the same time, we observed that AML, ALL, and lymphoma were the predominant underlying diseases (110 cases, 64 cases, and 30 cases, respectively), accounting for 45.1%, 26.2%, and 12.3% of the total number of cases.

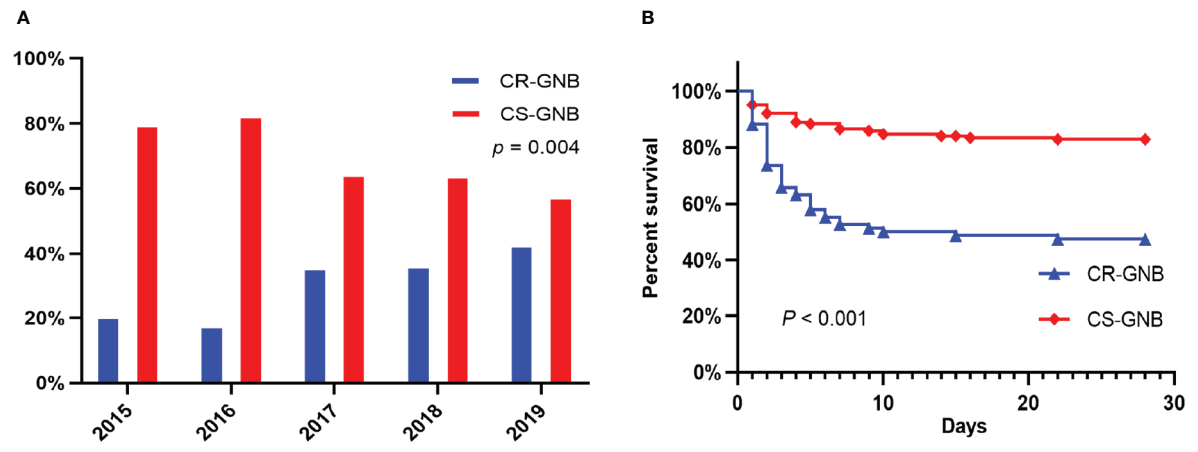

FIGURE 2
Percentages of Resistance to Carbapenems among Gram-negative bacteria during the Study Period **(A)**; Kaplan-Meier Survival Analysis among Hematological Patients with BSI caused by Carbapenem resistant (CR) and carbapenem susceptible (CS) Gram-negative bacteria **(B)**.

TABLE 2 Clinica and demographic characteristics of hematological patients with bloodstream infection caused by gram-negative bacteria based on the carbapenem resistance of strains.

Variables	Total (n=244)	CR-GNB (n=77)	CS-GNB (n=167)	*P* values
Demographics				
Gender,male	136 (55.7)	50 (64.9)	86 (51.5)	0.050
Age,Years,median (IQR)	44 (29.25-53)	44 (29-52)	44 (30-53)	0.637
Underlying disease				0.947
Acute lymphatic leukemia	64 (26.2)	22 (28.6)	42 (25.1)	
Acute myeloid leukemia	110 (45.1)	33 (42.9)	77 (46.1)	
lymphoma	30 (12.3)	9 (11.7)	21 (12.6)	
Myelodysplastic syndrome	7 (2.9)	3 (3.9)	4 (2.4)	
Multiple Myeloma	6 (2.5)	1 (1.3)	5 (3.0)	
Aplastic anemia	16 (6.6)	6 (7.8)	10 (6.0)	
others	11 (4.5)	3 (3.9)	8 (4.8)	
incomplete remission status of underlying disease	178 (73.0)	62 (80.5)	116 (69.5)	0.071
Hypoproteinemia [b]	100 (41.0)	47 (61.0)	53 (31.7)	<0.001
Comorbidities				
Diabetes mellitus	19 (7.8)	6 (7.8)	13 (7.8)	0.998
Hepatobiliary disease	28 (11.5)	7 (9.1)	21 (12.6)	0.427
Cardiovascular diseases	29 (11.9)	8 (10.4)	21 (12.6)	0.624
pulmonary infection at the time of BSI	121 (49.6)	47 (61.0)	74 (44.3)	0.015
Corticosteroid therapy before BSI [a]	86 (35.2)	34 (44.2)	52 (31.1)	0.048
immunosuppressive therapy before BSI [a]	18 (7.4)	5 (6.5)	13 (7.8)	0.720
Duration of neutropenia, Days,median (IQR)	5 (3-9.75)	8 (5-17)	4 (2-7)	<0.001
Duration of neutropenia ≥ 6 days [a]	111 (45.5)	55 (71.4)	56 (33.5)	<0.001
Mucosal barrier damage [b]	94 (38.5)	42 (54.5)	52 (31.1)	<0.001
Hospital-acquired BSI	226 (92.6)	77 (100)	149 (89.2)	0.003
Antifungal agents use within 30 days before BSI	137 (56.1)	62 (80.5)	75 (44.9)	<0.001
Antibiotics use within 30 days before BSI				
Carbapenems	96 (39.5)	52 (67.5)	44 (26.5)	<0.001
Aminoglycosides	23 (9.4)	11 (14.3)	12 (7.2)	0.078
Quinolones	41 (16.8)	15 (19.5)	26 (15.6)	0.448
Cephalosporin/β-lactamase inhibitor combinations	81 (33.2)	41 (53.2)	40 (24.0)	<0.001
Piperacillin-tazobactam	46 (18.9)	20 (26.0)	26 (15.6)	0.053
Tigecyclines	41 (16.8)	22 (28.6)	19 (11.4)	0.001
Indwelling central venous catheter [a]				0.460
PICC	164 (67.2)	56 (72.7)	108 (64.7)	
PORT	34 (13.9)	9 (11.7)	25 (15.0)	

(Continued)

TABLE 2 Continued

Variables	Total (n=244)	CR-GNB (n=77)	CS-GNB (n=167)	*P* values
Indwelling urinary catheter [a]	11 (4.5)	7 (9.1)	4 (2.4)	0.019
28-Day mortality (n=240)	68 (28.3)	40 (52.6)	28 (17.1)	<0.001
Inappropriate empirical therapy (n=243)	51 (21.4)	49 (63.6)	3 (1.8)	<0.001
Appropriate empirical therapy (n=243)	191 (78.6)	28 (36.4)	163 (98.2)	<0.001
Septic shock [c]	53 (21.7)	27 (35.1)	26 (15.6)	0.001

[a]Before bloodstream infection within 30 days.
[b]At the time of bloodstream infection.
[c]Before the result of Antibiotic susceptibility testing.
PICC, peripherally inserted central catheter; PORT, implantable venous access port; BSI, bloodstream infection; CR-GNB, carbapenem-resistant gram-negative bacteria; CS-GNB, carbapenem-sensitive gram-negative bacteria; IQR, interquartile range.

3.3 Establishment and validation of the nomogram for early predicting the risk probability of carbapenem resistance in HM patients with GNB BSI

3.3.1 Risk factors for carbapenem resistance in patients with GNB BSI

To minimize the risk of multicollinearity of variables in the prediction model of this study, LASSO regression analysis was performed to filter potential risk factors for carbapenem resistance among hematological patients with GNB BSI. Figure 3 illustrated the selection process of potential risk factors for carbapenem resistance using the LASSO regression model. As demonstrated in Figure 3B, lambda.lse (λ = 0.07182097) (right dotted line) was identified as the optimal lambda for five variables with non-zero coefficients. These variables with potential risk of carbapenem resistance included duration of neutropenia ≥ 6 days before BSI, previous exposure to cephalosporin/β-lactamase inhibitor combinations, previous exposure to carbapenems, antifungal agents use within 30 days before BSI, and hypoproteinemia. To further analyze independent risk factors for CR-GNB BSI, five variables selected from the LASSO regression model were incorporated into the multivariate logistic regression model. Ultimately, multivariate logistic analysis (Table 3 Model-A) demonstrated that duration of neutropenia ≥ 6 days before BSI (OR 2.764, 95% CI: 1.437-5.317; p = 0.002), hypoproteinemia (OR 2.249, 95% CI: 1.196-4.227; p = 0.012), previous exposure to carbapenems (OR 3.460, 95% CI: 1.822-6.571; p < 0.001) and previous exposure to cephalosporin/β-lactamase inhibitors (OR 2.162, 95% CI: 1.134-4.120; p = 0.019) were independent risk factors of CR-GNB BSI.

3.3.2 Establishment and validation of the nomogram

Combining clinical knowledge and the results of previous studies (Lalaoui et al., 2020), we finally constructed a nomogram containing four variables (hypoproteinemia, duration of neutropenia ≥ 6 days, previous exposure to carbapenems, and previous exposure to cephalosporins/β-lactamase inhibitors, respectively) to personalize the prediction of the probability of carbapenem resistance in HM patients with GNB BSI, which was abbreviated as the carbapenem resistance nomogram (Figure 4A). In the nomogram, each variable was represented visually with a corresponding score. The total points of a patient with GNB BSI could be calculated by adding the scores of each predictive variable, which was corresponded to the predicted probability of carbapenem resistance.

The internal validation results of this nomogram were depicted graphically in Figure 5. As shown in Figure 5A, the AUC values of the carbapenem resistance nomogram was 0.799 (0.739-0.859), and the sensitivity and specificity were 68.3% and 83.1%, respectively. Subsequently, overfitting or underfitting was assessed by bootstrapping and 10-fold cross validation method, and the model was found to be well-fitting. The modified C-index for the nomogram were 0.788 and 0.781 according to bootstrapping and 10-fold cross validation, respectively, indicating that the predictive model possessed a favorable capacity for discrimination of carbapenem resiatance. In addition, the accuracy or C-index of this model based on other cross validation was summarized in Table SII. Similarly, it was worth noting that the calibration plots of the prediction model were all extremely approximated to the corresponding actual observed curves for both the bootstrapping and 10-fold cross validation (Figures 5C, D), suggesting that the nomogram provided a satisfactory prediction accuracy. Meanwhile, we also assessed the clinical applicability of the prediction model using DCA, as displayed in Figure 5B, and found that the model had excellent clinical utility.

3.4 Treatments and outcomes

To evaluate the risk factors for 28-day mortality following the onset of GNB BSI, we eliminated cases with unavailable

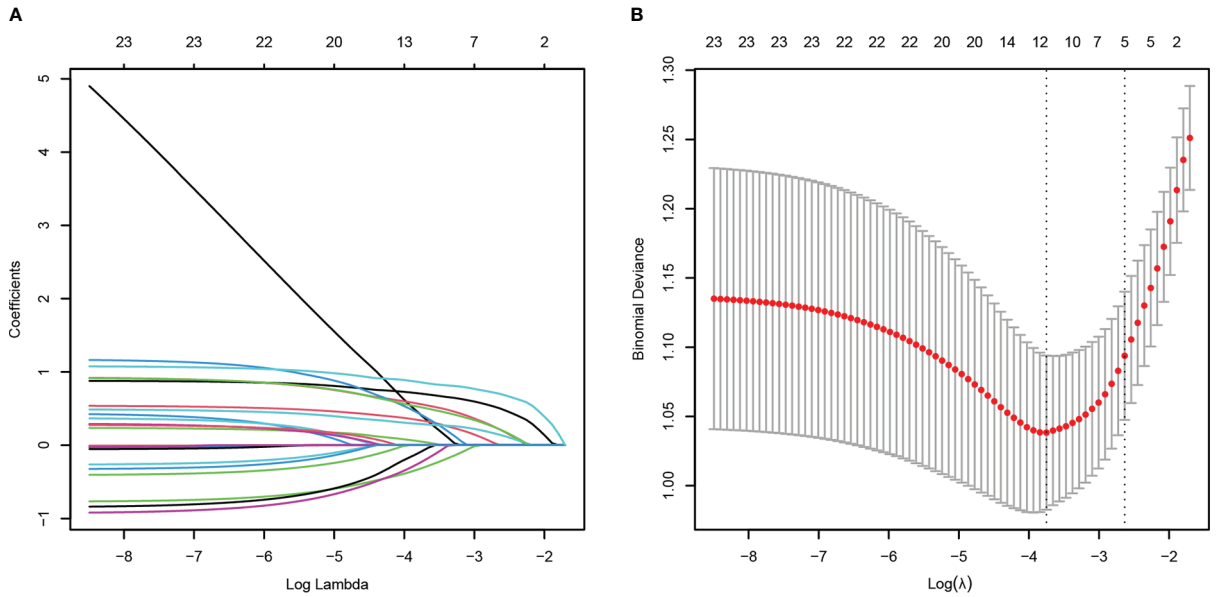

FIGURE 3
Potential risk factors selection for carbapenem resistance using the least absolute shrinkage and selection operator (LASSO) regression model with 10-fold cross validation. LASSO coefficient profiles of 23 variables **(A)**. A coefficient profile plot was constructed from the log (lambda) sequence **(B)**. The number of characteristic variables was filtered by drawing dotted vertical lines at lambda.min (left dotted line) and lambda.1se (right dotted line) respectively according to the minimum criterion. LASSO, least absolute shrinkage and selection operator; SE, standard error.

TABLE 3 Multivariate analysis of risk Factors for carbapenem resistance (Model A) and 28-day all-cause mortality (Model B) in patients with hematological diseases suffering from bloodstream infections caused by gram-negative bacteria.

Variables	*B*	*P*	*OR*	*95%CI*
Model(A)				
Duration of neutropenia ≥ 6 days [a]	1.017	0.002	2.764	(1.437-5.317)
Hypoproteinemia [b]	0.810	0.012	2.249	(1.196-4.227)
Previous exposure to carbapenems [a]	1.241	<0.001	3.460	(1.822-6.571)
Previous exposure to Cephalosporin/β-lactamase inhibitor combinations [a]	0.771	0.019	2.162	(1.134-4.120)
Model(B)				
Hypoproteinemia [b]	0.783	0.049	2.189	(1.002-4.781)
Incomplete remission status of underlying disease [b]	2.290	0.001	9.880	(2.569-37.989)
Isolation of CR-GNB	1.459	<0.001	4.304	(1.921-9.644)
Septic shock [c]	2.830	<0.001	16.950	(6.846-41.967)

[a]Before bloodstream infection within 30 days.
[b]At the time of bloodstream infection.
[c]Before the result of Antibiotic susceptibility testing.
CR-GNB, carbapenem-resistant gram-negative bacteri.

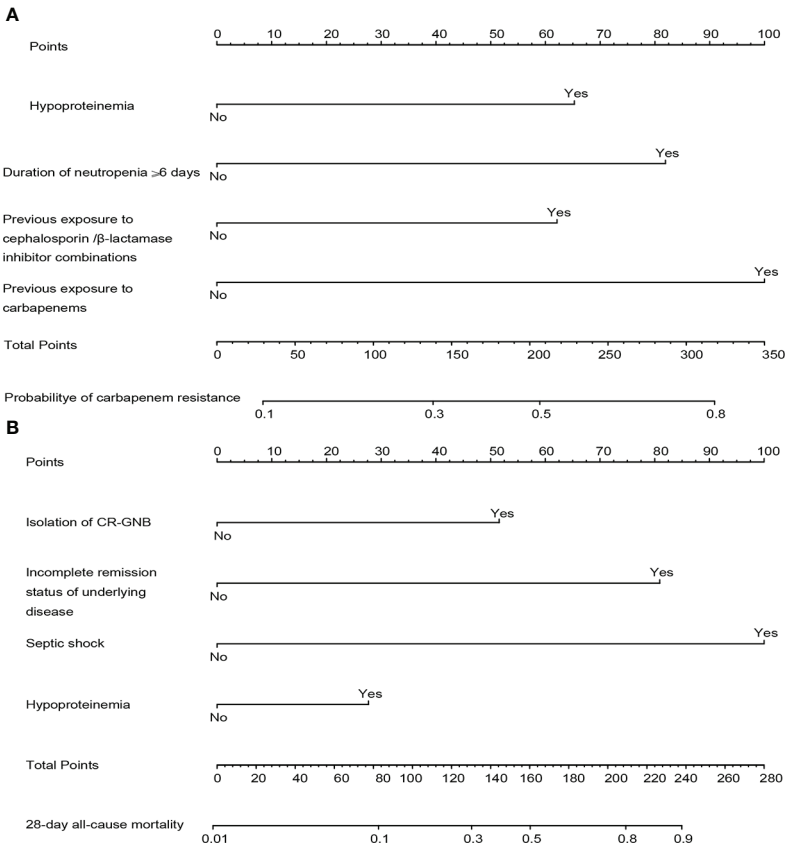

FIGURE 4
The constructed nomograms for predicting risk probability of carbapenem resistance and 28-day all-cause mortality in gram-negative bacteremia among patients with hematological diseases, abbreviated as the carbapenem resistance nomogram **(A)** and the prognosis nomogram **(B)**. Each predictor has corresponding points, and the total score for an individual patient could be obtained by summing up all scores. CR-GNB, carbapenem-resistant gram-negative bacteria.

follow-up data (4 cases). Eventually, a total of 240 episodes of GNB BSI were analyzed. Following the collection of blood culture specimens, an empirical antimicrobial regimen was implemented for all febrile patients immediately in accordance with Clinical Practice Guidelines for the management of patients with febrile neutropenia in the USA and Europe, with 77.9% (187/240) of patients receiving appropriate empirical therapy. The 28-day all-cause mortality in HM patients with GNB BSI was 28.3% (68/240) and 44.1% (30/68) of non-survivors suffered from insufficient empirical antimicrobial therapy (Table SI). Moreover, there was a significantly higher mortality in CR-GNB BSI patients than that in CS-GNB BSI patients (40/77, 52.6% vs 28/167, 17.1%; $P < 0.001$). Meanwhile, in our cohorts, a considerably greater proportion of the CR-GNB patients received inappropriate empirical treatment than CS-GNB patients (48/76, 63.2% vs 3/155, 1.9%; $P < 0.001$). A Kaplan-Meier survival analysis also demonstrated the higher possibility of mortality among patients infected with CR strains ($P < 0.001$) (Figure 2B).

3.5 Establishment and validation of the nomogram for early predicting the risk probability of 28-day mortality in HM patients with GNB BSI

3.5.1 Risk factors for 28-day all-cause mortality in patients with GNB BSI

The HM patients with GNB BSI were classified into survivor and non-survivor groups according to the clinical outcomes of the 28th day. As with the approach for screening the most appropriate variables of carbapenem resistance, we identified possible prognostic predictors through lasso regression and multivariate logistic regression analysis. As presented in Figure 6, isolation of CR-GNB, hypoproteinemia, previous exposure to carbapenems, incomplete remission status of underlying disease, septic shock, and appropriate empirical therapy were potential variables screened to predict clinical prognosis with the LASSO regression analysis. Multivariate logistic regression

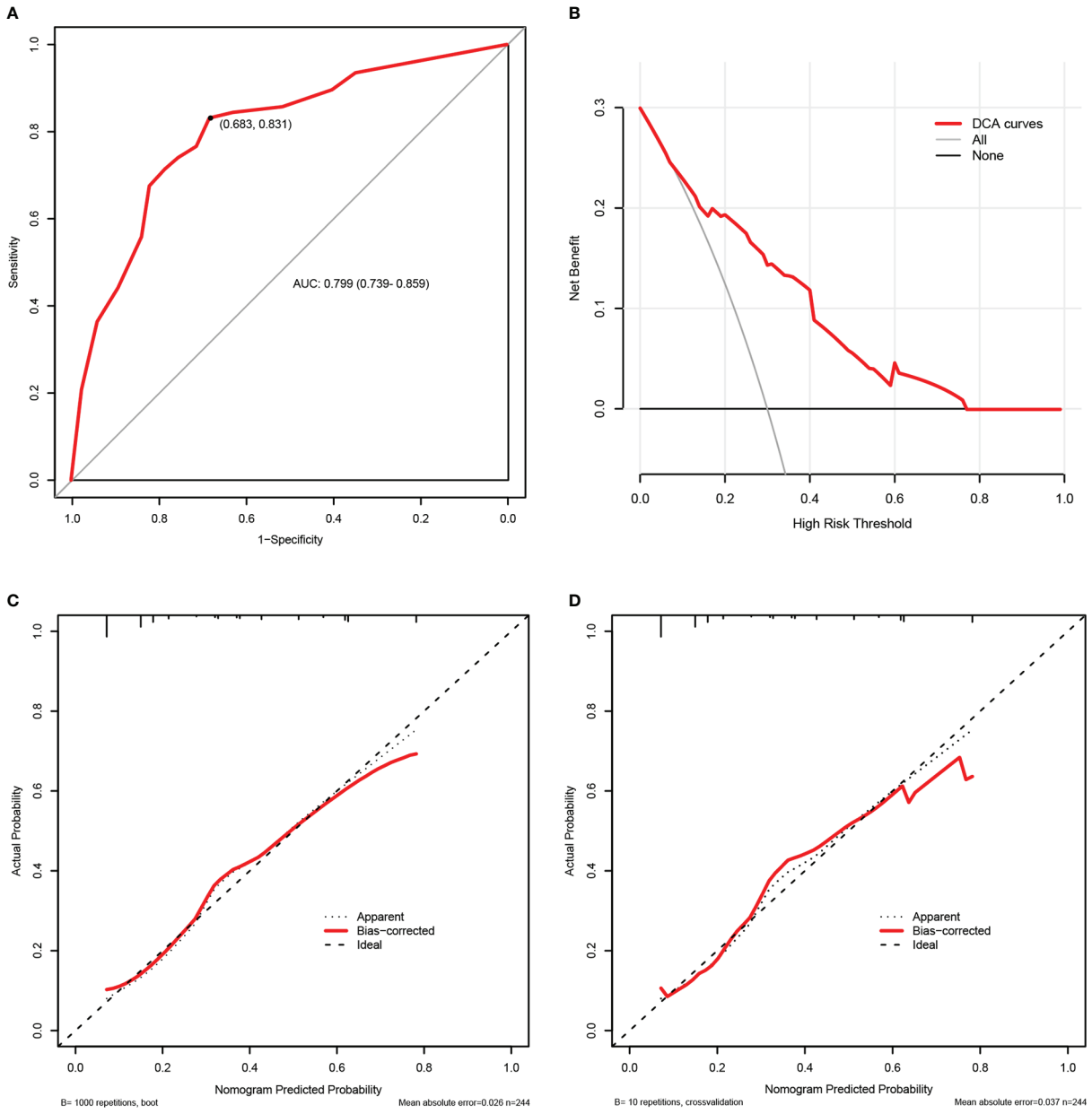

FIGURE 5
The internal validation of the carbapenem resistance nomogram according to bootstrap method and 10-fold cross validation. Receiver operating characteristic (ROC) curves of the carbapenem resistance nomogram **(A)**. Decision curve analysis (DCA) of the carbapenem resistance nomogram **(B)**. Calibration plots of the carbapenem resistance nomogram based on bootstrap method **(C)** and 10-fold cross validation **(D)**.

analysis (Table 3 Model-B) further indicated that the following factors were independently associated with a higher risk of mortality for GNB BSI: hypoproteinemia (OR 2.189, 95%CI: 1.002-4.781; P = 0.049), septic shock (OR 16.950, 95%CI: 6.846-41.967; P < 0.001), incomplete remission status of underlying diseases (OR 9.880, 95%CI: 2.569-37.989; P = 0.010), and isolation of CR-GNB (OR 4.304, 95%CI: 1.921-9.644; P < 0.001).

3.5.2 Establishment and validation of the nomogram

The four independent prognostic predictors (hypoproteinemia, septic shock, incomplete remission status of underlying diseases, and isolation of CR-GNB) were incorporated to generate a predictive nomogram for early individualized prediction of 28-day all-cause mortality in patients with GNB BSI, which was abbreviated as the prognosis nomogram (Figure 4B).

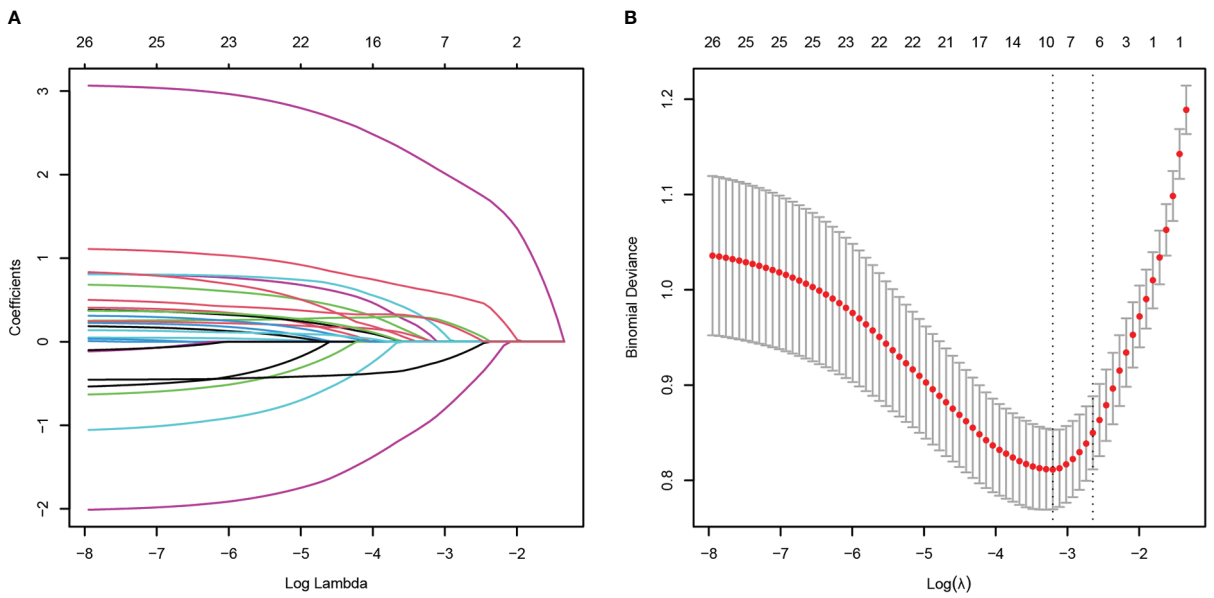

FIGURE 6
Potential risk factors selection for 28-day all-cause mortality using the least absolute shrinkage and selection operator (LASSO) regression model with 10-fold cross validation. LASSO coefficient profiles of 26 variables **(A)**. A coefficient profile plot was constructed from the log (lambda) sequence **(B)**. The number of characteristic variables was filtered by drawing dotted vertical lines at lambda.min (left dotted line) and lambda.1se (right dotted line) respectively according to the minimum criterion. LASSO, least absolute shrinkage and selection operator; SE, standard error.

Figure 7 exhibited the performance evaluation findings of the nomogram using bootstrapping and 10-fold cross validation, respectively. According to Figure 7A, the AUC of the prognosis nomogram was 0.881 (0.833-0.929), with a sensitivity of 82.0% and a specificity of 76.5%. When validated internally by bootstrapping and 10-fold cross validation method, the modified C-indexes of the nomogram were 0.873 and 0.887, respectively, revealing that the predictive model had a superior discriminative ability for the identification of poorer clinical prognosis. In addition, Table SII summarized the accuracy or C-index of this model based on additional cross validation. The calibration curves for both the bootstrapping and 10-fold cross validation demonstrated a relatively high agreement between prediction and actual observation (Figures 7C, D). Likewise, the decision curve analysis (DCA) demonstrated that the prognostic nomogram model had greater net benefits for identifying clinical outcomes with worse prognoses (Figure 7B).

4 Discussion

The clinical management of bloodstream infection (BSI) is crucial to the overall prognosis of patients with hematological disorders. In the present research, we systematically summarized the clinical characteristics of Gram-negative bacteremia in patients with hematological diseases at our hospital and screened the potential high risk factors of 28-day all-cause mortality and carbapenem resistance using LASSO regression analysis and multivariate logistic regression analysis. On the basis of the aforementioned predictive indicators, we established two nomograms to earlier identify the probability of carbapenem resistance at the time of the isolation of GNB and the 28-day mortality risk for each patient encountering Gram-negative bacteremia in the hematology department. Our nomograms exhibited relatively excellent performance in terms of discrimination, calibration, and clinical practicality, as measured by the C-index or AUC values, calibration plots, and DCA curves. Therefore, they might be straightforward and practical pictorial prediction tools that provide beneficial information for clinicians in the prevention and control of BSI. This appears to be, to our knowledge, a first report focusing on the development and validation of nomograms for early personalized prediction of the possibility of carbapenem resistance and mortality risk in patients with hematological disorders suffering from BSI caused by GNB.

In accordance with earlier research findings (Trecarichi and Tumbarello, 2014; Di Domenico et al., 2021), GNB remained the most prevalent microorganism species (377/679, 55.5%) causing BSI in our cohort of patients by far (Figure 1). However, the variety of pathogenic microorganisms varies according to

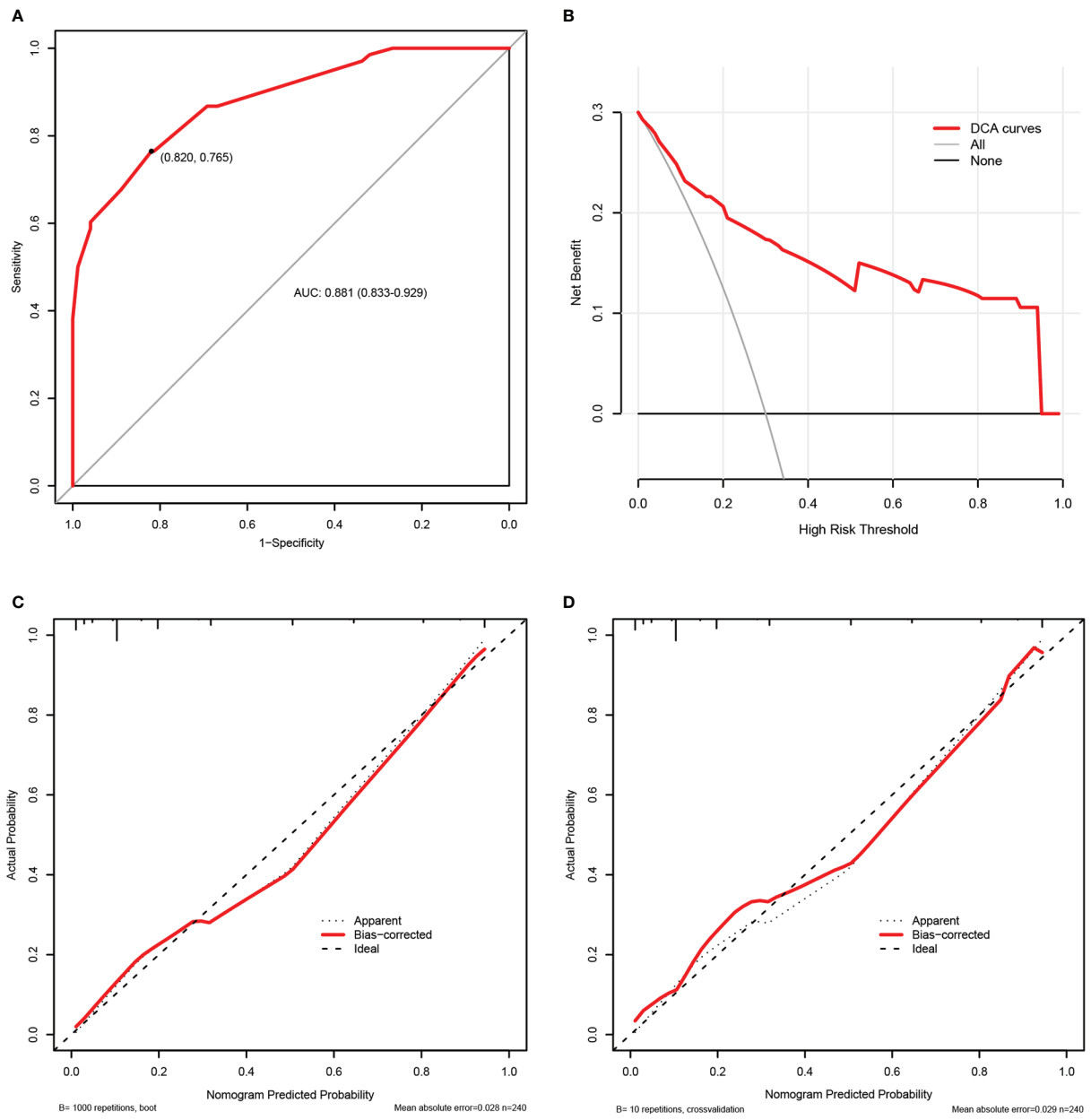

FIGURE 7
The internal validation of the prognosis nomogram according to bootstrap method and 10-fold cross validation. Receiver operating characteristic (ROC) curves of the prognosis nomogram **(A)**. Decision curve analysis (DCA) of the prognosis nomogram **(B)**. Calibration plots of the prognosis nomogram based on bootstrap method **(C)** and 10-fold cross validation **(D)**.

geographic areas, years, and other factors. Our data indicated that KP was the predominantly isolated pathogen, followed by EC, and PA during the study period (2015-2019). These data differed slightly from what has been reported in association with epidemiological studies performed on HM patients in other countries and in other cities of our country, in which EC represented the most frequently isolated bacteria, followed by PA or KP (Trecarichi and Tumbarello, 2014; Andria et al., 2015; Chen et al., 2017; Islas-Muñoz et al., 2018; Di Domenico et al., 2021). Previous researches have shown that carbapenem resistance in GNB has become a significant problem worldwide and a new public health threat in view of limited antimicrobial treatment options and high mortality (Righi et al., 2017; Nordmann and Poirel, 2019). Notably, the overall trend of

carbapenem resistance in our research has increased from 20.4% in 2015 to 42.6% in 2019, which is consistent with the finding of the national bloodstream infection surveillance program conducted in China from 2014 to 2019 (Chen et al., 2022). In agreement with previous published studies conducted in HM patients (Andria et al., 2015; Trecarichi et al., 2016; Lalaoui et al., 2020), the overall mortality of CR-GNB BSI patients was significantly higher than that of CS-GNB BSI patients in our study(52.6% vs 17.1%; $P < 0.001$), and isolation of CR-GNB was independently correlated with 28-day all-cause mortality. These results highlight the necessity of regular surveillance to comprehend the clinical epidemiological characteristics of BSI among hematological patients in the local hospital.

In this study, the 28-day all-cause mortality of GNB BSI was 28.3%, and the majority of non-survivors (58.8%) suffered from BSI caused by CR-GNB (Table SI). Until now, a variety of risk factors have been demonstrated to be associated with carbapenem resistance in gram-negative bacteria, of which exposure to carbapenems before infections represented the most frequently observed risk factor across the different pathogens and types of infection (Satlin et al., 2016; Righi et al., 2017; Ting et al., 2018; Xiao et al., 2020; Zhao et al., 2020; Palacios-Baena et al., 2021). The use of carbapenems prior to BSI was also recognized as an independent risk factor for CR-GNB BSI in our analysis. Furthermore, a multi-center study conducted in China concerning the correlation between antibiotics consumption and carbapenem resistance equally revealed that carbapenem resistance in GNB was positively and significantly correlated with increased consumption of carbapenem antibiotics (Yang et al., 2018). Such a correlation may be attributed to the high selective pressure of carbapenems exposure. Notably, Laurence et al (Armand-Lefevre et al., 2013) found that even short-duration exposure to carbapenems may increase the risk of colonization or infection with carbapenem-resistant pathogens. Our study also suggested that previous use of cephalosporins/β-lactamase inhibitor combinations was associated with CR-GNB BSI. As with our research findings, there was an analogous positive correlation between prior cephalosporins/β-lactamase inhibitor combinations usage and carbapenem resistance in several other studies (Satlin et al., 2016; Liang et al., 2021). A plausible interpretation for this may be that broad-spectrum antibiotics have the potential to cause alteration of intestinal flora and may select for and promote the growth of carbapenem-resistant organisms in intestinal microbiota. Therefore, antimicrobial stewardship programs are essential to alleviate the emergence of resistance owing to the selective pressure of antibacterial usage. Zou et al (Zou et al., 2014) indicated that reduced use of antimicrobials was parallel with the amelioration of bacterial resistance without deteriorating medical quality indicators, which underlines the importance and feasibility of antimicrobial stewardship.

Previous retrospective clinical studies (Murthy et al., 2018; Omiya et al., 2021) found that, in addition to previous antibacterial usage, neutropenia was an another significant independent risk factor for carbapenem resistance. However, the relationship between the duration of neutropenia and carbapenem resistance has received limited consideration. Our study found that the duration of neutropenia ≥ 6 days was associated with a higher risk of carbapenem resistance in HM patients with BSI. Meanwhile, hypoproteinemia was a statistically screened independent risk factor associated with carbapenem resistance in our study, and yet has rarely been observed to be related to carbapenem resistance in previous studies. Given that hypoproteinemia has been linked to disease progression and clinical prognosis in different clinical settings (Murthy et al., 2018; Aziz et al., 2020; Omiya et al., 2021; Jiang et al., 2022), it was also incorporated into the plotting of the carbapenem resistance nomogram.

According to our findings, the isolation of CR-GNB, hypoproteinemia, the incomplete remission status of underlying diseases, and septic shock were strongly associated with a high risk of clinical worsening prognosis. Carbapenem-resistant GNB tended to be multi-drug resistant or even pan-resistant and had a limited choice of available antibiotic types. Trecarichi et al. (2016) and Andria et al., (2015) proved that inappropriate empirical antimicrobial regimens were strongly associated with high mortality and the majority of patients with CR-GNB BSI failed to obtain appropriate empirical antibiotic treatment. In our study, 44.1% (30/68) of non-survivors underwent inadequate empirical antimicrobial therapy, with a significantly higher proportion of inappropriate empirical therapy in the CR-GNB group than that in the CS-GNB group (63.6% vs 1.8%; $P < 0.001$). At the same time, we found that 15.6% of patients with BSI in the CS-GNB group progressed to sepsis shock and even clinical death. This could not be ruled out in connection with the increasing emergence of strains with high virulence and pathogenicity, which are active against most antibiotics *in vitro* but possess a high mortality risk (Zhang et al 2016; Russo and Marr 2019). It has been documented that infections caused by highly virulent Klebsiella pneumoniae (hvKP) most frequently occurred in the Asia-Pacific region (Russo and Marr 2019). Additionally, a systematic multi-center study of hvKP infection performed in China reported that the percentage of hvKP infection varied from 8.33% to 73.9%, with the highest prevalence in Wuhan (Zhang et al. 2016). Of course, it is essential to carry out more studies in the future to confirm the presence of highly virulent GNB in our hematology.

In addition, we also found that septic shock was the predominant and significant predictor for 28-day mortality in our nomogram. Not surprisingly, septic shock, as a clinical manifestation of the severity of infections and organ dysfunction, has been detected to be associated with high mortality in several previous studies involving patients with HM and the general populations (Andria et al., 2015; Chumbita et al.,2022; Xiao et al., 2020; Zhang et al 2020). In the current study, we could understand that 60.3% (41/68) of non-survivors underwent septic shock, of which 50.9% (27/53) of patients were categorized as CR-GNB BSI. Therefore, in clinical practice, the severity of the infection plays a crucial role in the prognosis. As demonstrated by Chumbita et al., (2022), when administered with inappropriate experimental antibiotic therapy, septic shock was associated with extremely high mortality in febrile neutropenic patients with BSI. Apparently, this conclusion further highlights the importance of epidemiological surveillance in different hospitals. Furthermore, the stage of hematological disease was a non-negligible variable in our study as well, where 95.6% (65/68) of non-survivors failed to attain complete remission status. It might be that when patients were in the status of incomplete remission, the tumor load was high and a more effective high-dose chemotherapy regimen was required.

In recent years, nomograms have become increasingly important in the clinical management of infectious diseases (Dong et al., 2021; He et al., 2022), while are rarely implemented in patients with hematological diseases. In hematological patients with BSI, the majority of studies have focused on the description of outcomes for regression models or the development of predictive scoring systems (Satlin et al., 2016; Xiao et al., 2020), which are not as simple and intuitive as nomograms. In this study, we improved the accuracy of predictor selection using LASSO analysis and built quantitative nomograms to provide a quick and easy evaluation of the probability of carbapenem resistance and mortality risk. In accordance with the TRIPOD statement (Collins et al., 2015), our nomograms were internally validated using the original study sample based on bootstrapping and 10-fold cross validation method, and exhibited relatively good predictive performance. Because of this, the findings emphasize the importance of antibiotic stewardship and the identification of patients at high risk of carbapenem resistance.

However, we have to acknowledge the existence of several shortcomings in the study. First, this is a single-center retrospective study, and the lack of an independent external validation cohort is a drawback of nomogram models, despite the relatively excellent predictive performance of nomogram models demonstrated with internal validation based on both the bootstrap method and 10-fold cross validation. Furthermore, other variables in this study that could not be identified from the electronic medical record system, such as the intestinal colonization of carbapenem-resistant organisms and the source of BSI, which are relatively associated with the development of carbapenem resistance and the clinical prognosis separately, may interfere with the ultimate results of predictive models. Thus, a more comprehensive multi-center prospective study in the future is required to demonstrate the reproducibility of nomograms and further revise our models, which also indicates the necessity of cyclic evaluations for similar clinical events. Secondly, the detection performance of microbiological methods and the use of antimicrobials prior to specimen collection may underestimate the amount of microbial growth in clinical cultures and influence the final results to some extent. In spite of these limitations, our study still provides a certain reference value to adjust management strategies for the prevention and control of Gram-negative bacteremia in patients with hematological diseases.

In summary, Gram-negative bacteria remain the leading pathogens of bloodstream infections in the department of hematology. Carbapenem resistance is associated with a worse prognosis in patients with GNB BSI. Meanwhile, individualized risk prediction models were established and validated in this study for predicting the risk of 28-day all-cause mortality and carbapenem resistance in gram-negative bacteremia among patients with hematological diseases. These models could serve as simple, reliable tools to make individualized risk predictions of clinical events and to provide useful information for clinicians in the management of infection control measures.

Data availability statement

The raw data supporting the conclusions of this article will be made available by the authors, without undue reservation.

Ethics statement

The studies involving human participants were reviewed and approved by the Ethics Committee of Union Hospital, Tongji Medical College, Huazhong University of Science and Technology. Written informed consent from the participants' legal guardian/next of kin was not required to participate in this study in accordance with the national legislation and the institutional requirements.

Author contributions

JH and HW designed the study. XJ, SD, XZ, ZX, KW, and XD collected data. XJ and SD analyzed the data and wrote the article. JH and HW critically reviewed the manuscript. All authors contributed to the article and approved the submitted version.

Funding

This project was supported by the National Natural Science Foundation of China (No.81770134) and Beijing Medical Award Foundation of China (YXJL-2019-0163-0114).

Acknowledgments

The authors would like to acknowledge the contributions of the researchers and all the patients who participated in the present study.

Conflict of interest

The authors declare that the research was conducted in the absence of any commercial or financial relationships that could be construed as a potential conflict of interest.

Publisher's note

Supplementary material

The Supplementary Material for this article can be found online at: https://www.frontiersin.org/articles/10.3389/fcimb.2022.969117/full#supplementary-material

References

Andria, N., Henig, O., Kotler, O., Domchenko, A., Oren, I., Zuckerman, T., et al. (2015). Mortality burden related to infection with carbapenem-resistant gram-negative bacteria among haematological cancer patients: A retrospective cohort study. *J. Antimicrob. Chemother.* 70, 3146–3153. doi: 10.1093/jac/dkv218

Armand-Lefevre, L., Angebault, C., Barbier, F., Hamelet, E., Defrance, G., Ruppe, E., et al. (2013). Emergence of imipenem-resistant gram-negative bacilli in intestinal flora of intensive care patients. *Antimicrob. Agents Chemother.* 57, 1488–1495. doi: 10.1128/AAC.01823-12

Aziz, M., Fatima, R., Lee-Smith, W., and Assaly, R. (2020). The association of low serum albumin level with severe COVID-19: A systematic review and meta-analysis. *Crit. Care (London England)* 24, 255. doi: 10.1186/s13054-020-02995-3

Balachandran, V. P., Gonen, M., Smith, J. J., and DeMatteo, R. P. (2015). Nomograms in oncology: More than meets the eye. *Lancet Oncol.* 16, e173–e180. doi: 10.1016/S1470-2045<(>14<)>71116-7

Chen, Y., Ji, J., Ying, C., Liu, Z., Yang, Q., Kong, H., et al. (2022). Blood bacterial resistant investigation collaborative system (BRICS) report: A national surveillance in China from 2014 to 2019. *Antimicrob. Resist. Infect. Control* 11, 17. doi: 10.1186/s13756-022-01055-5

Chen, S., Lin, K., Li, Q., Luo, X., Xiao, M., Chen, M., et al. (2021). A practical update on the epidemiology and risk factors for the emergence and mortality of bloodstream infections from real-world data of 3014 hematological malignancy patients receiving chemotherapy. *J. Cancer* 12, 5494–5505. doi: 10.7150/jca.50802

Chen, C., Tien, F., Sheng, W., Huang, S., Yao, M., Tang, J., et al. (2017). Clinical and microbiological characteristics of bloodstream infections among patients with haematological malignancies with and without neutropenia at a medical centre in northern taiwan, 2008–2013. *Int. J. Antimicrob. Ag.* 49, 272–281. doi: 10.1016/j.ijantimicag.2016.11.009

Chumbita, M., Puerta-Alcalde, P., Gudiol, C., Garcia-Pouton, N., Laporte-Amargos, J., Ladino, A., et al. (2022). Impact of empirical antibiotic regimens on mortality in neutropenic patients with bloodstream infection presenting with septic shock. *Antimicrob. Agents Chemother.* 66, e174421. doi: 10.1128/AAC.01744-21

Collins, G. S., Reitsma, J. B., Altman, D. G., and Moons, K. G. M. (2015). Transparent reporting of a multivariable prediction model for individual prognosis or diagnosis (TRIPOD): The TRIPOD statement. *BMJ* 350, g7594. doi: 10.1136/bmj.g7594

Di Domenico, E. G., Marchesi, F., Cavallo, I., Toma, L., Sivori, F., Papa, E., et al. (2021). The impact of bacterial biofilms on end-organ disease and mortality in patients with hematologic malignancies developing a bloodstream infection. *Microbiol. Spectr.* 9, e55021. doi: 10.1128/Spectrum.00550-21

Dong, Y., Sun, J., Li, Y., Chen, Q., Liu, Q., Sun, Z., et al. (2021). Development and validation of a nomogram for assessing survival in patients with COVID-19 pneumonia. *Clin. Infect. Dis.* 72, 652–660. doi: 10.1093/cid/ciaa963

Feld, R. (2008). Bloodstream infections in cancer patients with febrile neutropenia. *Int. J. Antimicrob. Ag.* 32, S30–S33. doi: 10.1016/j.ijantimicag.2008.06.017

Friedman, J., Hastie, T., and Tibshirani, R. (2010). Regularization paths for generalized linear models *via* coordinate descent. *J. Stat. Softw.* 33, 1–22. doi: 10.18637/jss.v033.i01

He, Y., Xu, J., Shang, X., Fang, X., Gao, C., Sun, D., et al. (2022). Clinical characteristics and risk factors associated with ICU-acquired infections in sepsis: A retrospective cohort study. *Front. Cell Infect. Mi.* 12. doi: 10.3389/fcimb.2022.962470

Horan, T. C., Andrus, M., and Dudeck, M. A. (2008). CDC/NHSN surveillance definition of health care-associated infection and criteria for specific types of infections in the acute care setting. *Am. J. Infect. Control* 36, 309–332. doi: 10.1016/j.ajic.2008.03.002

Iasonos, A., Schrag, D., Raj, G. V., and Panageas, K. S. (2008). How to build and interpret a nomogram for cancer prognosis. *J. Clin. Oncol.* 26, 1364–1370. doi: 10.1200/JCO.2007.12.9791

Islas-Muñoz, B., Volkow-Fernández, P., Ibanes-Gutiérrez, C., Villamar-Ramírez, A., Vilar-Compte, D., and Cornejo-Juárez, P. (2018). Bloodstream infections in cancer patients. risk factors associated with mortality. *Int. J. Infect. Dis.* 71, 59–64. doi: 10.1016/j.ijid.2018.03.022

Jiang, A., Shi, X., Zheng, H., Liu, N., Chen, S., Gao, H., et al. (2022). Establishment and validation of a nomogram to predict the in-hospital death risk of nosocomial infections in cancer patients. *Antimicrob. Resist. Infect. Control* 11, 29. doi: 10.1186/s13756-022-01073-3

Lalaoui, R., Javelle, E., Bakour, S., Ubeda, C., and Rolain, J. (2020). Infections due to carbapenem-resistant bacteria in patients with hematologic malignancies. *Front. Microbiol.* 11. doi: 10.3389/fmicb.2020.01422

Liang, C., Zhang, X., Zhou, L., Meng, G., Zhong, L., and Peng, P. (2021). Trends and correlation between antibacterial consumption and carbapenem resistance in gram-negative bacteria in a tertiary hospital in China from 2012 to 2019. *BMC Infect. Dis.* 21, 444. doi: 10.1186/s12879-021-06140-5

Lin, Y., Wang, M., Jia, J., Wan, W., Wang, T., Yang, W., et al. (2020). Development and validation of a prognostic nomogram to predict recurrence in high-risk gastrointestinal stromal tumour: A retrospective analysis of two independent cohorts. *Ebiomedicine* 60, 103016. doi: 10.1016/j.ebiom.2020.103016

Misch, E. A. M., and Andes, D. R. M. (2019). Bacterial infections in the stem cell transplant recipient and hematologic malignancy patient. *Infect. Dis. Clin. N. Am.* 33, 399–445. doi: 10.1016/j.idc.2019.02.011

Murthy, H. S., Sheets, K., Kumar, A., Nishihori, T., Mina, A., Chavez, J. C., et al. (2018). Hypoalbuminemia at day +90 is associated with inferior nonrelapse mortality and overall survival in allogeneic hematopoietic cell transplantation recipients: A confirmatory study. *Biol. Blood Marrow Transplant.* 24, 400–405. doi: 10.1016/j.bbmt.2017.09.022

Nordmann, P., and Poirel, L. (2019). Epidemiology and diagnostics of carbapenem resistance in gram-negative bacteria. *Clin. Infect. Dis.* 69, S521–S528. doi: 10.1093/cid/ciz824

Omiya, K., Sato, H., Sato, T., Wykes, L., Hong, M., Hatzakorzian, R., et al. (2021). Albumin and fibrinogen kinetics in sepsis: A prospective observational study. *Crit. Care* 25, 436. doi: 10.1186/s13054-021-03860-7

Palacios-Baena, Z. R., Giannella, M., Manissero, D., Rodríguez-Baño, J., Viale, P., Lopes, S., et al. (2021). Risk factors for carbapenem-resistant gram-negative bacterial infections: A systematic review. *Clin. Microbiol. Infect.* 27, 228–235. doi: 10.1016/j.cmi.2020.10.016

Park, S. Y. (2018). Nomogram: An analogue tool to deliver digital knowledge. *J. Thorac. Cardiovasc. Surg.* 155, 1793. doi: 10.1016/j.jtcvs.2017.12.107

Righi, E., Peri, A. M., Harris, P. N. A., Wailan, A. M., Liborio, M., Lane, S. W., et al. (2017). Global prevalence of carbapenem resistance in neutropenic patients and association with mortality and carbapenem use: Systematic review and meta-analysis. *J. Antimicrob. Chemoth.* 72, w459. doi: 10.1093/jac/dkw459

Russo, T. A., and Marr, C. M. (2019). Hypervirulent klebsiella pneumoniae. *Clin. Microbiol. Rev.* 32, e00001–19. doi: 10.1128/CMR.00001-19

Satlin, M. J., Cohen, N., Ma, K. C., Gedrimaite, Z., Soave, R., Askin, G., et al. (2016). Bacteremia due to carbapenem-resistant enterobacteriaceae in neutropenic patients with hematologic malignancies. *J. Infect.* 73, 336–345. doi: 10.1016/j.jinf.2016.07.002

Singer, M., Deutschman, C. S., Seymour, C. W., Shankar-Hari, M., Annane, D., Bauer, M., et al. (2016). The third international consensus definitions for sepsis and septic shock (Sepsis-3). *JAMA* 315, 801–810. doi: 10.1001/jama.2016.0287

Song, L., Zhu, Z., Wu, H., Han, W., Cheng, X., Li, J., et al. (2021). Individualized nomogram for predicting ALK rearrangement status in lung adenocarcinoma patients. *Eur. Radiol.* 31, 2034–2047. doi: 10.1007/s00330-020-07331-5

Ting, S. W., Lee, C. H., and Liu, J. W. (2018). Risk factors and outcomes for the acquisition of carbapenem-resistant gram-negative bacillus bacteremia: A retrospective propensity-matched case control study. *J. Microbiol. Immunol. Infect.* 51, 621–628. doi: 10.1016/j.jmii.2016.08.022

Trecarichi, E. M., Pagano, L., Candoni, A., Pastore, D., Cattaneo, C., Fanci, R., et al. (2015). Current epidemiology and antimicrobial resistance data for bacterial bloodstream infections in patients with hematologic malignancies: An Italian multicentre prospective survey. *Clin. Microbiol. Infect.* 21, 337–343. doi: 10.1016/j.cmi.2014.11.022

Trecarichi, EM, Pagano, L, Martino, B, Candoni, A, Di Blasi, R, Nadali, G, et al. (2016) Bloodstream infections caused by Klebsiella pneumoniae in oncohematological patients: clinical impact of carbapenem resistance in a multicentre prospective survey. *Am J. Hematol.* 91, 1076–1081. doi: 10.1002/ajh.24489

Trecarichi, E. M., and Tumbarello, M. (2014). Antimicrobial-resistant gram-negative bacteria in febrile neutropenic patients with cancer: Current epidemiology and clinical impact. *Curr. Opin. Infect. Dis.* 27, 200–210. doi: 10.1097/QCO.0000000000000038

Wu, J., Zhang, H., Li, L., Hu, M., Chen, L., Xu, B., et al. (2020). A nomogram for predicting overall survival in patients with low-grade endometrial stromal sarcoma: A population-based analysis. *Cancer Commun.* 40, 301–312. doi: 10.1002/cac2.12067

Xiao, T., Zhu, Y., Zhang, S., Wang, Y., Shen, P., Zhou, Y., et al. (2020). A retrospective analysis of risk factors and outcomes of carbapenem-resistant klebsiella pneumoniae bacteremia in nontransplant patients. *J. Infect. Dis.* 221, S174–S183. doi: 10.1093/infdis/jiz559

Yang, P., Chen, Y., Jiang, S., Shen, P., Lu, X., and Xiao, Y. (2018). Association between antibiotic consumption and the rate of carbapenem-resistant gram-negative bacteria from China based on 153 tertiary hospitals data in 2014. *Antimicrob. Resist. Infect. Control* 7, 137. doi: 10.1186/s13756-018-0430-1

Zhang, G, Zhang, M, Sun, F, Zhou, J, Wang, Y, Zhu, D, et al (2020). Epidemiology, mortality and risk factors for patients with K. Pneumoniae bloodstream infections: Clinical impact of carbapenem resistance in a tertiary university teaching hospital of Beijing. *J. Infect. Public Health*. 13.1710–1714. doi: 10.1016/j.jiph.2020.09.012

Zhang, Y., Zhao, C., Wang, Q., Wang, X., Chen, H., Li, H., et al. (2016). High prevalence of hypervirulent klebsiella pneumoniae infection in china: Geographic distribution, clinical characteristics, and antimicrobial resistance. *Antimicrob. Agents Ch.* 60, 6115–6120. doi: 10.1128/AAC.01127-16

Zhao, Y., Lin, Q., Liu, L., Ma, R., Chen, J., Shen, Y., et al. (2020). Risk factors and outcomes of antibiotic-resistantPseudomonas aeruginosa bloodstream infection in adult patients with acute leukemia. *Clin. Infect. Dis.* 71, S386–S393. doi: 10.1093/cid/ciaa1522

Zou, Y. M., Ma, Y., Liu, J. H., Shi, J., Fan, T., Shan, Y. Y., et al. (2014). Trends and correlation of antibacterial usage and bacterial resistance: Time series analysis for antibacterial stewardship in a Chinese teaching hospital <(>2009–2013<)>. *Eur. J. Clin. Microbiol.* 34, 795–803. doi: 10.1007/s10096-014-2293-6

frontiers | Frontiers in Cellular and Infection Microbiology

TYPE Original Research
PUBLISHED 30 January 2023
DOI 10.3389/fcimb.2023.1109418

OPEN ACCESS

EDITED BY
Milena Dropa,
Faculty of Public Health, University of São Paulo, Brazil

REVIEWED BY
Aristine Cheng,
National Taiwan University, Taiwan
Wang Ke,
Guangxi Medical University, China

*CORRESPONDENCE
Xiaoli Chen
chenxiaoli202211@163.com

†These authors have contributed equally to this work and share first authorship

SPECIALTY SECTION
This article was submitted to Clinical Microbiology, a section of the journal Frontiers in Cellular and Infection Microbiology

RECEIVED 27 November 2022
ACCEPTED 16 January 2023
PUBLISHED 30 January 2023

CITATION
Liao Q, Feng Z, Lin H, Zhou Y, Lin J, Zhuo H and Chen X (2023) Carbapenem-resistant gram-negative bacterial infection in intensive care unit patients: Antibiotic resistance analysis and predictive model development.
Front. Cell. Infect. Microbiol. 13:1109418.
doi: 10.3389/fcimb.2023.1109418

Carbapenem-resistant gram-negative bacterial infection in intensive care unit patients: Antibiotic resistance analysis and predictive model development

Qiuxia Liao[1†], Zhi Feng[2†], Hairong Lin[1], Ye Zhou[1], Jiandong Lin[1], Huichang Zhuo[1] and Xiaoli Chen[1,3*]

[1]Department of Intensive Care Unit, First Affiliated Hospital of Fujian Medical University, Fuzhou, Fujian, China, [2]Department of Thoracic Surgery, First Affiliated Hospital of Fujian Medical University, Fuzhou, Fujian, China, [3]Department of Intensive Care Unit, National Regional Medical Center, Binhai Campus of the First Affiliated Hospital, Fujian Medical University, Fuzhou, China

In this study, we analyzed the antibiotic resistance of carbapenem-resistant gram-negative bacteria (CR-GNB) in intensive care unit (ICU) patients and developed a predictive model. We retrospectively collected the data of patients with GNB infection admitted to the ICU of the First Affiliated Hospital of Fujian Medical University, who were then divided into a CR and a carbapenem-susceptible (CS) group for CR-GNB infection analysis. Patients admitted between December 1, 2017, and July 31, 2019, were assigned to the experimental cohort (n = 205), and their data were subjected to multivariate logistic regression analysis to identify independent risk factors for constructing the nomogram-based predictive model. Patients admitted between August 1, 2019, and September 1, 2020, were assigned to the validation cohort for validating the predictive model (n = 104). The Hosmer–Lemeshow test and receiver operating characteristic (ROC) curve analysis were used to validate the model's performance. Overall, 309 patients with GNB infection were recruited. Of them, 97 and 212 were infected with CS-GNB and CR-GNB, respectively. Carbapenem-resistant *Klebsiella pneumoniae* (CRKP), carbapenem-resistant *Acinetobacter baumannii* (CRAB) and carbapenem-resistant *Pseudomonas aeruginosa* (CRPA) were the most prevalent CR-GNB. The multivariate logistic regression analysis results of the experimental cohort revealed that a history of combination antibiotic treatments (OR: 3.197, 95% CI: 1.561–6.549), hospital-acquired infection (OR: 3.563, 95% CI: 1.062–11.959) and mechanical ventilation ≥ 7 days (OR: 5.096, 95% CI: 1.865–13.923) were independent risk factors for CR-GNB infection, which were then used for nomogram construction. The model demonstrated a good fit of observed data (p = 0.999), with an area under the ROC curve (AUC) of 0.753 (95% CI: 0.685–0.820) and 0.718 (95% CI: 0.619–0.816) for the experimental and validation cohort, respectively. The decision curve analysis results suggested that the model has a high practical value for clinical practice. The Hosmer–Lemeshow test indicated a good fit of the model in the validation cohort (p-value, 0.278). Overall, our proposed predictive model exhibited a good predictive value in identifying patients at high risk of developing CR-GNB infection in the ICU and could be used to guide preventive and treatment measures.

KEYWORDS

carbapenem-resistant gram-negative bacteria, risk factor, predictive model, logistic regression, area under the receiver operating characteristic curve

1 Introduction

The widespread application and irrational use of carbapenem antibiotics have led to a steady rise in the incidence of carbapenem-resistant gram-negative bacterial (CR-GNB) infections (Nordmann and Poire, 2019) due to the presence of β-lactamase genes on mobile genetic elements (Logan and Weinstein, 2017). Thus, CR-GNB infections remain a major global public health concern requiring urgent prevention and control measures (Jean et al., 2022).

Carbapenem antibiotics are extensively used in patients admitted to the intensive care unit (ICU) because of the illness severity, low immunity and numerous invasive procedures performed. Consequently, the ICU has become a high-prevalence area of multi-antibiotic-resistant GNB infections in hospitals (Aleidan et al., 2021; Sader et al., 2022).

Klebsiella pneumoniae, *Acinetobacter baumannii* and *Pseudomonas aeruginosa* are the main organisms that may invade the respiratory tract, urinary tract, peritoneal cavity and bloodstream of patients to cause pneumonia, and urinary tract, peritoneal and bloodstream infections. These infections can considerably increase treatment costs and patients' mortality risks (Brink, 2019; Wilke et al., 2022). In the absence of new and effective antibiotics, the strong antibiotic resistance of CR-GNB limits pharmacological options and exacerbates treatment difficulty (Garg et al., 2019).

Presently, inconsistent results have been reported in the few existing studies on predictive models of CR-GNB infections in ICU patients (Liang et al., 2022; Montrucchio et al., 2022). Therefore, to improve therapeutic outcomes, we believe it is essential to analyze CR-GNB antibiotic resistance to determine relevant risk factors and construct a reliable predictive model that could help identify high-risk patients and formulate individualized treatments. To this end, in this study, we retrospectively analyzed the data of patients with GNB infection in an ICU setting to provide a scientific basis for their clinical treatment, which could be used to strategize prevention and control measures for CR-GNB infection.

2 Patients and methods

2.1 Participants

This was a retrospective study on patients diagnosed with GNB infection and admitted to the ICU ward between December 1, 2017, and September 1, 2020, at the First Affiliated Hospital of Fujian Medical University (Fuzhou, China). The study inclusion criteria were: (1) age ≥18 years and (2) specimens had been collected after ICU admission for culture, from which a confirmed diagnosis of GNB infection and antibiotic susceptibility test results were obtained. Only the first positive culture result was selected in the case of multiple culture results. The exclusion criteria were as follows: (1) duration of ICU stay ≤ 24 h and (2) specimens sent for testing had been contaminated. The observation endpoint was patient discharge or in-hospital death.

The eligible patients were then classified into an experimental cohort and a validation cohort. The experimental cohort comprised patients admitted to the ICU between December 1, 2017, and July 31, 2019. They were divided into a CR-GNB group and a carbapenem susceptible (CS)-GNB group, and their data were subjected to multivariate logistic regression analysis for nomogram-based predictive model construction. Using the same selection and exclusion criteria, the validation cohort comprised patients admitted between 1 August 1, 2019, and September 1, 2020.

2.2 Definitions

CR-GNB: GNB identified from specimen culture that was resistant to imipenem, meropenem and ertapenem according to the antibiotic susceptibility test results (Ma et al., 2020).

Sepsis-related Organ Failure Assessment (SOFA) score: a six-organ dysfunction score of 0–24 points (Singer et al., 2016). Daily evaluations were performed based on the lowest score (Singer et al., 2016).

APACHE II score: the score comprised three components, namely the acute physiology score, age points, and chronic health points. It was used as a predictor of mortality rate in ICU patients (Naved et al., 2011).

Combination antibiotic treatment: the combined use of two or more types of antibiotics for anti-infective treatment.

Hospital-acquired infection: infection acquired after 48 h of hospital admission by a patient who had no infection and had not been in the incubation stage of infection at the time of hospital admission (Ministry of Health of the People's Republic of China, 2001).

2.3 Pathogenic bacteria and antibiotic susceptibility testing

Identification and routine antibiotic susceptibility testing of pathogenic bacteria were performed using the Vitek 2 Compact automated identification or antibiotic susceptibility testing system from bioMerieux (Lyon, France). Antibiotic susceptibility test results were interpreted using the 2017 edition of the Performance Standards for Antimicrobial Susceptibility Testing published by the Clinical and Laboratory Standards Institute (CLSI, 2017).

2.4 Data collection

The data retrieved from the patient's medical records included sex, age, underlying diseases (such as hypertension, chronic obstructive pulmonary disease (COPD), malignancy, diabetes mellitus and cerebral infarction), hypoalbuminemia, history of recent hospitalization, glucocorticoid therapy, central venous catheterization, tracheal intubation, mechanical ventilation, hemodialysis, septic shock, history of antibiotic use within 1 month before the first positive culture test result, types of antibiotics used (including β-lactams, carbapenems, macrolides, tetracyclines, aminoglycosides, clindamycin, polypeptides, polymyxins, sulphonamides and quinolones), SOFA and Acute Physiology and Chronic Health Evaluation (APACHE II) scores on the day of admission, white blood cell (WBC) count, procalcitonin level, site of infection, pathogenic bacteria, and antibiotic susceptibility of bacteria.

2.5 Statistical analysis

Statistical analyses were performed using Stata SE15 from StataCorp LLC (Texas, United States of America). The normality of continuous variables was assessed using Shapiro–Wilk test. Non-normally distributed continuous variables are expressed as median (interquartile range) and compared using Mann–Whitney *U* test. Categorical data are expressed as count (frequency) and compared using the χ^2 test. Fisher's exact test was adopted when the expected frequency in the fourfold table was <5. All significant factors (p <0.05) in univariate analysis were used for multivariate analysis. Independent risk factors for CR-GNB infection were determined using multivariate logistic regression analysis, with variables selected using the stepwise forward selection method. Subsequently, a nomogram-based predictive model was constructed based on the independent risk factors. The model's scoring criteria were established based on the magnitude of the regression coefficient of all independent variables to visualize the predictive model results. The model stability was assessed using the Hosmer–Lemeshow goodness-of-fit test, and the predictive ability of the model was evaluated using the area under the receiver operating characteristic (ROC) curve (AUC). The model's practical value in clinical practice was determined using decision curve analysis (DCA). Differences were considered statistically significant when p was < 0.05.

2.6 Ethics approval and consent to participate

The study was approved by the Ethics Review Form for Medical Research and Clinical Technology Application and Ethics committee of the First Affiliated Hospital of Fujian Medical University (ID: [2015]084-1).

3 Results

3.1 Distribution of pathogenic bacteria and sites of infection

A total of 908 patients were admitted to the ICU ward of the First Affiliated Hospital of Fujian Medical University between December 1, 2017, and September 1, 2020. Based on the study criteria, 309 (experimental cohort, n=205; validation cohort, n=104) patients with GNB infection were eligible for this study. They comprised 244 men and 65 women, aged between 18 and 96 years. Of them, 97 had CS-GNB infection, and 212 had CR-GNB infection. Carbapenem-resistant *K. pneumoniae* (CRKP), carbapenem-resistant *A. baumannii* (CRAB) and carbapenem-resistant *P. aeruginosa* (CRPA) accounted for 131 (61.80%), 60 (28.30%) and 16 (7.55%) of the 212 detected strains in the patients, respectively, and were the most common GNB (Table 1). Overall, 96.70% of the pathogenic bacteria originated from the patients' sputum (Table 2).

3.2 Antibiotic susceptibility test results of CR-GNB main types

One hundred and thirty-one CRKP strains had low resistance to tigecycline and polymyxin but exhibited a resistance rate of ≥80% to all other antibiotics commonly used in clinical practice (Table 3). Sixty CRAB strains demonstrated a resistance rate of 65%, 70% and 80% to amikacin, trimethoprim-sulfamethoxazole and tobramycin, respectively. In addition, CRAB exhibited high susceptibility to tigecycline and polymyxin and a resistance rate of ≥90% to ticarcillin-clavulanic acid, cefoperazone-tazobactam, piperacillin-tazobactam, ceftazidime, ceftriaxone, cefepime, aztreonam, ciprofloxacin and levofloxacin. Piperacillin-tazobactam, ceftazidime, cefepime, amikacin, and polymyxin showed good *in vitro* antibacterial activity against the 16 CRPA strains. The resistance rate of the CRPA strains to tobramycin, ciprofloxacin, levofloxacin, aztreonam and trimethoprim-sulfamethoxazole was 50.00%, 56.25%, 56.25%, 81.25% and 100%, respectively (Table 3).

3.3 Comparison between the groups of patients in the experimental cohort

The experimental cohort consisted of 205 patients with GNB infection admitted to the ICU between December 1, 2017, and July 31, 2019. Of them, 62 had CS-GNB infection, and 143 had CR-GNB infection. Compared to patients with CS-GNB infection, those with CR-GNB infection had a significantly greater number of recent hospitalization, carbapenem use, central venous catheterization, and combination antibiotic treatment; number of types of antibiotics used; duration of antibiotic use and mechanical ventilation before the

TABLE 1 Distribution of pathogenic bacteria associated with CR-GNB infection.

Pathogenic bacterium	No. of strains (n = 212)	Percentage (%)
Klebsiella pneumoniae	131	61.80
Acinetobacter baumannii	60	28.30
Pseudomonas aeruginosa	16	7.55
Escherichia coli	2	0.94
Stenotrophomonas Maltophilia	2	0.94
Citrobacter freundii	1	0.47

CR-GNB, carbapenem-resistant gram-negative bacteria.

TABLE 2 Sources of specimens in which pathogenic CR-GNB were detected.

Source of specimens	No. of strains (n = 212)	Percentage (%)
Sputum	205	96.70
Blood	3	1.42
Urine	0	0.00
Peritoneal cavity	2	0.94
Wound exudate	2	0.94

CR-GNB, carbapenem-resistant gram-negative bacteria.

occurrence of infective bacteria; hospital-acquired infection; and mechanical ventilation ≥ 7 days ($p < 0.05$). In addition, patients with CR-GNB infection presented a significantly higher incidence of septic shock and in-hospital mortality than patients with CS-GNB infection ($p < 0.05$). No significant difference was observed in sex, age, history of hypertension, COPD, malignancy, diabetes mellitus, cerebral infarction, hypoalbuminemia, SOFA and APACHE II scores on the day of ICU admission, history of β-lactam use, tracheal intubation, hemodialysis, WBC count, neutrophil count, and procalcitonin level ($p \geq 0.05$) between the two groups (Table 4).

3.4 Risk factors for CR-GNB infection

The occurrence or non-occurrence of CR-GNB infection in ICU patients was set as the dependent variable. The variables with $p < 0.05$ in the univariate analysis (including history of recent hospitalization, combination antibiotic treatment, duration of antibiotic use, number of types of antibiotics used, hospital-acquired infection, history of glucocorticoid use, history of carbapenem use, history of central venous catheterization, duration of mechanical ventilation before the occurrence of infective bacteria, and mechanical ventilation ≥ 7 days) were used as independent variables. The multivariate logistic regression analysis was performed using the stepwise forward selection method to include single factors with $p < 0.05$ into the formula. The derived results indicated that combination antibiotic treatment (OR: 3.197, 95% CI: 1.561–6.549), hospital-acquired infection (OR: 3.563, 95% CI: 1.062–11.959) and duration of mechanical ventilation ≥ 7 days (OR: 5.096, 95% CI: 1.865–13.923) were independent risk factors for CR-GNB infection occurrence in ICU patients (Table 5).

TABLE 3 Antibiotic susceptibility test results of the main types of CR-GNB.

Anti-bacterial agent	CRKP (n = 131)		CRAB (n = 60)		CRPA (n = 16)	
	No. of strains	Rate of resistance (%)	No. of strains	Rate of resistance (%)	No. of strains	Rate of resistance (%)
Ticarcillin/clavulanic acid	129	98.47	60	100	-	-
Cefoperazone-tazobactam	128	97.71	55	91.67	-	-
Piperacillin-tazobactam	128	97.71	59	98.33	4	25.00
Ceftazidime	130	99.24	59	98.33	5	31.25
Ceftriaxone	131	100.00	60	100.00	-	-
Cefepime	131	100.00	60	100.00	4	25.00
Aztreonam	130	99.24	60	100.00	13	81.25
Imipenem	131	100.00	60	100.00	16	100.00
Meropenem	131	100.00	60	100.00	16	100.00
Amikacin	105	80.15	39	65.00	2	12.50
Tobramycin	112	85.50	48	80.00	8	50.00
Ciprofloxacin	128	97.71	59	98.33	9	56.25
Levofloxacin	126	96.18	56	93.33	9	56.25
Trimethoprim-sulfamethoxazole	121	92.37	42	70.00	16	100.00
Tigecycline	11	8.40	1	1.67	-	-
Polymyxin	0	0.00	0	0.00	0	0.00

CR-GNB, carbapenem-resistant gram-negative bacteria; CRKP, carbapenem-resistant Klebsiella pneumoniae; CRAB, carbapenem-resistant Acinetobacter baumannii; CRPA, carbapenem-resistant Pseudomonas aeruginosa; -: susceptibility testing was not performed.

3.5 Nomogram-based predictive model of CR-GNB infection in ICU patients

Independent risk factors screened from the multivariate logistic regression analysis were used to construct a nomogram-based predictive model of CR-GNB infection for ICU patients. The predictive model formula was $P = 1/[1+\exp[-(-1.090 + 1.162X_1 + 1.271X_2 + 1.628X_3)]]$. The scores of various independent variables were calculated using the corresponding regression coefficients and were as follows: combination antibiotic treatment: 7.1 points, hospital-acquired infection: 7.8 points, duration of mechanical ventilation ≥ 7 days: 10.0 points, and overall model score: 0–24.9 points. The scores of the independent variables were summed to obtain the overall score, which was used to predict the probability of CR-GNB infection of

TABLE 4 Comparison of baseline characteristics between the CS-GNB and CR-GNB groups of the experimental cohort.

Variable	CS-GNB(n = 62)	CR-GNB(n = 143)	*p*-value
Sex (male)	47 (75.8%)	110 (76.9%)	0.862
Age (years)	62.50 (54.00, 74.00)	62.00 (51.00, 74.00)	0.674
COPD	58 (93.5%)	129 (90.2%)	0.440
Hypertension	34 (54.8%)	77 (53.8%)	0.896
Malignancy	7 (11.3%)	20 (14.0%)	0.600
Diabetes mellitus	15 (24.2%)	38 (26.6%)	0.721
Cerebral infarction	16 (25.8%)	30 (21.0%)	0.447
Hypoalbuminaemia	16 (25.8%)	54 (37.8%)	0.097
History of recent hospitalization	40 (64.5%)	116 (81.1%)	0.010
History of carbapenem use	16 (25.8%)	77 (53.8%)	<0.001
History of β-lactam use	34 (54.8%)	94 (65.7%)	0.139
Combination antibiotic treatment	17 (27.4%)	86 (60.1%)	<0.001
Multi-site infection	13 (21.0%)	35 (24.5%)	0.586
Hospital-acquired infection	51(82.3%)	138(96.5%)	<0.001
History of glucocorticoid use	10 (16.1%)	47 (32.9%)	0.014
History of central venous catheterization	19 (30.6%)	83 (58.0%)	<0.001
Tracheal intubation	42 (67.7%)	94 (65.7%)	0.780
Haemodialysis	4 (6.5%)	14 (9.8%)	0.438
Mechanical ventilation ≥7 days	5 (8.2%)	53 (37.1%)	<0.001
Duration of mechanical ventilation before the occurrence of infective bacteria (days)	1.00 (0.00, 2.00)	3.00 (1.00, 8.00)	<0.001
SOFA score	5.00 (4.00, 6.00)	5.00 (4.00, 8.00)	0.119
APACHE II score	17.00 (13.00, 20.00)	17.00 (13.00, 21.00)	0.609
Duration of antibiotic use (days)	4.00 (1.00, 16.00)	12.00 (6.00, 22.00)	<0.001
No. of types of antibiotics used	1.00 (1.00, 3.00)	3.00 (1.00, 3.00)	<0.001
WBC count (10^9/L)	11.51 (8.35, 15.45)	9.87 (7.44, 14.96)	0.213
Neutrophil count (10^9/L)	9.79 (7.32, 13.39)	8.19 (5.68, 13.73)	0.190
PCT (ng/mL)*	0.39 (0.16, 2.62)	0.44 (0.15, 2.80)	0.949
Duration of hospital stay (days)	20.50 (17.00, 27.00)	19.00 (12.00, 26.00)	0.050
Duration of ICU stay (days)	19.50 (14.00, 24.00)	17.00 (11.00, 23.00)	0.033
Septic shock	12 (19.4%)	52 (36.4%)	0.016
In-hospital death	4 (6.5%)	24 (16.8%)	0.048

CS-GNB, carbapenem-susceptible gram-negative bacteria; CR-GNB, carbapenem-resistant gram-negative bacteria; COPD, chronic obstructive pulmonary disease; SOFA, sepsis-related organ failure assessment; APACHE II, acute physiology and chronic health evaluation; WBC, white blood cell; PCT, procalcitonin; ICU, intensive care unit. Continuous variables that did not follow a normal distribution are expressed as [M (P25, P75)]; categorical variables are expressed as [n (%)]. *Normal range for PCT was 0-0.06 ng/mL.

TABLE 5 Univariate and multivariate analysis for factors associated with CR-GNB infection in ICU patients.

Variable	Univariate analysis			Multivariate analysis		
	OR	95% CI	*p*-value	OR	95% CI	*p*-value
History of recent hospitalization	2.363	1.212–4.608	0.012	-	-	-
Combination antibiotic treatment (X_1)	3.994	2.084–7.656	<0.001	3.197	1.561–6.549	0.001
Duration of mechanical ventilation before the occurrence of infective bacteria (days)	1.050	1.018–1.083	0.002	-	-	-
No. of types of antibiotics used	1.544	1.222–1.950	<0.001	-	-	-
Hospital-acquired infection (X_2)	5.953	1.972–17.970	0.002	3.563	1.062–11.959	0.040
History of glucocorticoid use	2.546	1.189–5.451	0.016	-	-	-
History of carbapenem use	3.354	1.739–6.470	<0.001	-	-	-
History of central venous catheterization	3.131	1.661–5.901	<0.001	-	-	-
Duration of mechanical ventilation (days)	1.165	1.067– 1.272	0.001	-	-	-
Duration of mechanical ventilation ≥7 days (X_3)	6.471	2.437–17.181	<0.001	5.096	1.865–13.923	0.001

CR-GNB, carbapenem-resistant gram-negative bacteria; OR, odds ratio; CI, confidence interval; -: variables that were excluded through the stepwise forward regression method.

ICU patients. The plotted nomogram indicated that the predicted probability of the occurrence of CR-GNB in ICU patients was >80% when the total score was >16 points (Figure 1).

3.6 Internal validation of the predictive model

The assessment of the goodness of fit of the model using the Hosmer–Lemeshow test showed an χ^2 value of 0.07 and a *p*-value of 0.999, suggesting that the predicted probability of occurrence was consistent with actual probability and that the model presented a good fit of the observed data (Figure 2). The AUC of the predictive model was 0.753 (95% CI: 0.685–0.820), indicative of a good predictive performance (Figure 3). The AUC obtained using 1000 bootstrap replications was 0.753 (95% CI: 0.687–0.818), indicating that the model had good discriminatory power and repeatability. The DCA curve showed that the maximum clinical benefit could be obtained with the model when the predicted probability was >0.7, suggesting that the model could provide high practical value in clinical practice (Figure 4).

3.7 Validation of the proposed predictive model

The validation cohort consisted of 104 GNB infection patients admitted to the ICU between August 1, 2019, and September 1, 2020. Of them, 35 had CS-GNB infection, and 69 had CR-GNB infection. The assessment of the goodness of fit using the Hosmer–Lemeshow test showed an χ^2 value of 5.09 and a *p*-value of 0.278 (Figure 5),

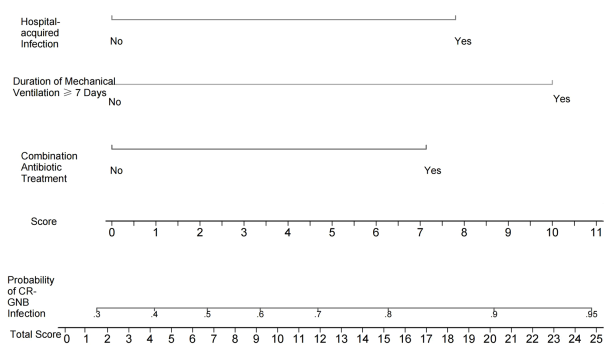

FIGURE 1
Nomogram for estimating the probability of CR-GNB infection in ICU patients. The scores of various independent variables were as follows: combination antibiotic treatment: 7.1 points, hospital-acquired infection: 7.8 points, and duration of mechanical ventilation ≥7 days: 10.0 points. The scores of the independent variables were summed to obtain the overall score, which can be used to predict the probability of CR-GNB infection in ICU patients. For instance, the predicted probability of CR-GNB infection occurrence in ICU patients was >80% when the total score was >16 points.

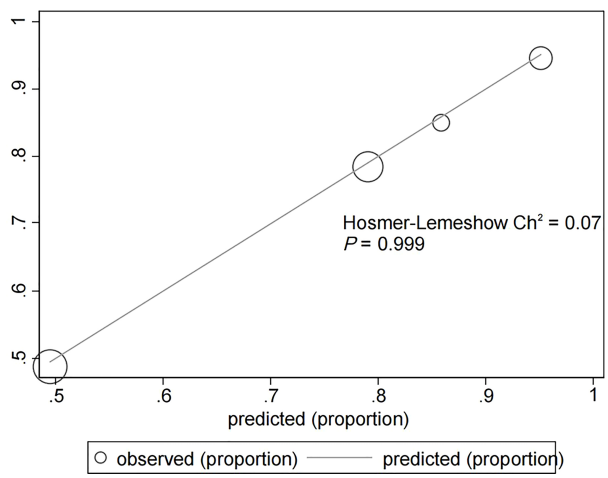

FIGURE 2
Hosmer–Lemeshow test provided a χ^2 value of 0.07 (p = 0.999) for the predictive model in the experimental cohort, suggesting that the model presented a good fit for the observed data.

suggesting that the model presented a good fit in the validation cohort. The AUC was 0.718 (95% CI: 0.619–0.816), indicating a good prediction performance of the model in the validation cohort (Figure 6). The DCA curve indicated that the model showed a high practical value in clinical practice when the predicted probability was >0.75 in the validation cohort (Figure 7).

4 Discussion

The reported incidence rate of CR-GNB infection in the ICU is reported to range between 25.2% and 47% (Kiddee et al., 2018; Siwakoti et al., 2018). In addition, a substantial increase in the mortality of patients with CR-GNB infection has been observed in clinical practice (Dantas et al., 2019). In this study, we found that the probability of septic shock or in-hospital death was significantly higher in patients with CR-GNB infection than in patients with CS-GNB infection. Therefore, the early identification of patients with CR-GNB infection is an urgent need in clinical practice to improve their survival outcomes. This study retrospectively analyzed the antibiotic resistance of CR-GNB in infected ICU patients and successfully constructed and validated a clinical predictive model to assess the probability of CR-GNB infection occurrence in ICU patients. Altogether, our results could serve as a scientific basis to guide the clinical use of antibiotics and reduce irrational antibiotic use, which might contribute to improving patient outcomes and reducing hospitalization costs.

Our results indicated that *K. pneumoniae*, *A. baumannii* and *P. aeruginosa* were the three most prevalent CR-GNB in ICU patients, which is largely consistent with the findings of Ma et al. (Ma et al., 2020). In this study, *K. pneumoniae* had the highest proportion (61.80%) among all CR-GNB species detected. In addition, the 2021 results of the China Antimicrobial Surveillance Network (CHINET) surveillance of bacterial resistance across China revealed that the rate of *K. pneumoniae* resistance to imipenem and meropenem significantly increased from 3.0% and 2.9% in 2005 to 25.0% and 26.3% in 2018, respectively (Hu et al., 2022). In this study, we observed that CRKP in the specimens of our ICU patients had low resistance to tigecycline and polymyxin; however, it exhibited a resistance rate of ≥80% to all other antibiotics commonly used in clinical practice. This result indicates that the multi-antibiotic resistance of CRKP remains severe and poses major difficulties for clinical treatment, consistent with the findings of Zeng et al. (Zeng et al., 2021). A possible reason for this could be associated with the unique ability of *K. pneumoniae* to acquire exogenous resistance-encoding and hypervirulence-encoding genetic elements (Yang et al., 2021). The main mechanism by which *K. pneumoniae* develops carbapenem resistance involves the plasmid-mediated carbapenemase *K. pneumoniae* carbapenemase (KPC) (Qin et al., 2020), with bla_{KPC-2} being the most common genotype in China (Li et al., 2019). Our results showed that CRKP, CRAB and CRPA had high susceptibility to polymyxin, suggesting that polymyxin combined with other antibiotics could achieve good therapeutic effects in treating CR-GNB infections.

We found that combination antibiotic treatment was an independent risk factor for CR-GNB infection in ICU patients. Previous research has also demonstrated a relationship between the history of antibiotic use and CR-GNB infection (Li et al., 2019; Qin et al., 2020), which might be attributed to the fact that combination antibiotic treatment causes dysbiosis in the microbiota, whereby the majority of susceptible bacteria are eradicated, while the antibiotic-resistant strains survive. In this regard, using comparative genomics to investigate the population dynamics of *Acinetobacter baumannii* during host colonization, Wen et al. found that antibiotic usage and host environment could selectively drive the rapid adaptive evolution to enhance their colonization (Wen et al., 2014). Additionally, Wang et al. found a novel *Pseudomonas aeruginosa* strain that underwent rapid adaptive evolution during ventilator-associated pneumonia to become resistant to β-lactams due to the selective pressure imposed by intensive β-lactam treatments (Wang et al., 2017). Thus, antibiotic resistance of bacteria changes with time and the excessive use of antibiotics may accelerate this process (Raman et al., 2018), thereby increasing the risks of CR-GNB infection. Therefore, the occurrence of CR-GNB infection could be effectively reduced through the minimization of irrational antibiotic use and timely identification of

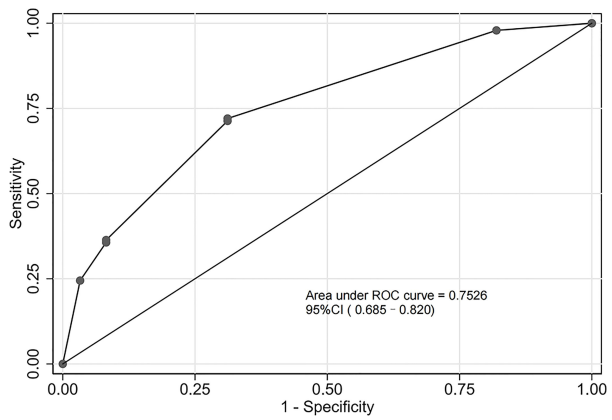

FIGURE 3
Receiver operating characteristic (ROC) curve of the predictive model in the experimental cohort. The predictive model had a good discriminative power with an area under the ROC curve of 0.753 (95% confidence interval: 0.685–0.820).

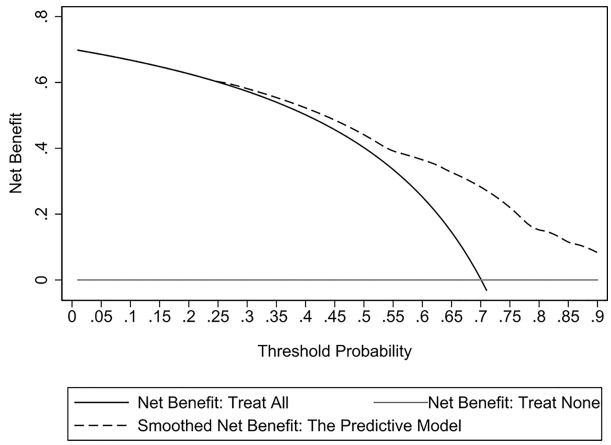

FIGURE 4
Decision curve analysis (DCA) curves of the predictive model in the experimental cohort. The DCA curve showed that the maximum clinical benefit could be obtained with the model when the predicted probability was >0.7.

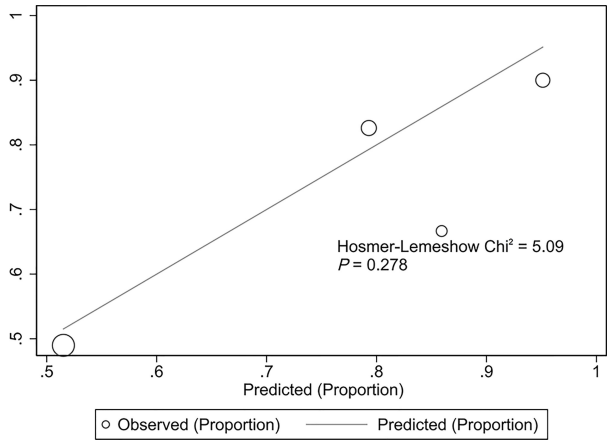

FIGURE 5
Hosmer–Lemeshow plot of the predictive model for the validation cohort. Assessment of the goodness of fit using the Hosmer–Lemeshow test showed an χ^2 value of 5.09 and a p-value of 0.278, suggesting that the model presented a good fit in the validation cohort.

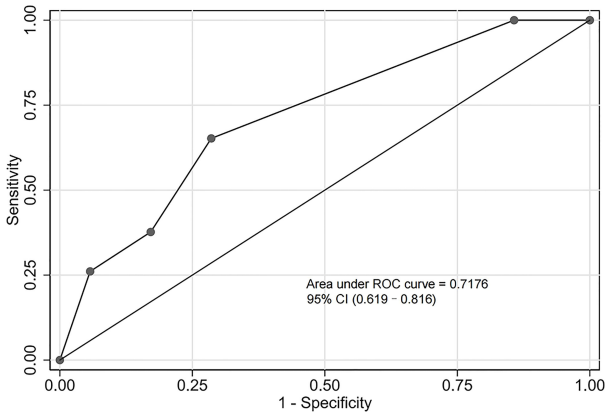

FIGURE 6
Receiver operating characteristic (ROC) curve of the predictive model for the validation cohort. The area under the ROC curve was 0.718 (95% confidence interval: 0.619–0.816), indicating a good prediction performance of the model in the validation cohort.

pathogenic bacteria for targeted anti-infective treatment. Our results suggest that hospital-acquired infection may also increase the risk of CR-GNB infection in ICU patients. Given that multiantibiotic-resistant bacteria survive for long periods in hospital environments and the low immunity of inpatients, inadequate or inappropriate prevention and control measures by a hospital may lead to a high tendency of cross-infection or even an outbreak among healthcare workers and patients. O'Hara et al. reported that the gloves and gowns of healthcare workers were prone to contamination by carbapenem-resistant Enterobacterales members and are considered to play an important role in the transmission of antibiotic-resistant bacteria among inpatients (O'Hara et al., 2021). This finding suggests that improvements in hand hygiene and environmental disinfection for reducing the occurrence of hospital-acquired infection have effectively prevented CR-GNB infection. Our results also indicated that the duration of mechanical ventilation ≥7 days was associated with CR-GNB infection in ICU patients, which was similar to the results of previous studies (Liu et al., 2018; Palacios-Baena et al., 2021). These findings suggest that for patients receiving mechanical ventilation, the possibility of weaning should be evaluated daily, and timely measures should be implemented to reduce CR-GNB infection.

Recently, several predictive models have been proposed for subsequent infections after CR-GNB colonization in different types of diseases. In the study of Wu et al. (Wu et al., 2022), after reviewing the data of patients with hematological malignancy (n = 437), they constructed a scoring model based on mucositis, duration of agranulocytosis, hypoalbuminemia and remission induction chemotherapy, which could stratify high-risk from low-risk patients with an OR (95%CI) of 3.347 (2.218-5.094) and AUC of 0.708. However, they did not investigate the different strains of CR-GNB nor validate their findings. Yan et al. constructed a model for the early prediction of death risk in severe acute pancreatitis patients infected with GNB (Yan et al., 2022). They found that platelets, hemoglobin, septic shock and carbapenem resistance were independent risk factors for mortality in these patients, based on which they proposed a nomogram for predicting the risk of mortality. Their model demonstrated good reliability based on an AUC of 0.942 and 0.911 in their training and validation cohort. However, despite these promising findings, most existing models either lacked validation or focused on only one disease. Comparatively, our proposed model was based on different strains of CR-GNB infection (Table 1), assessed the different specimens (Table 2), performed antibiotic susceptibility tests for a wide range of commonly used anti-bacterial agents (Table 3), and involved severely diseased patients with different ailments (Table 4). Our multivariate logistic regression analysis revealed that a history of combination antibiotic treatment, hospital-acquired infection and duration of mechanical ventilation ≥7 days were independent risk factors for CR-GNB infection in ICU patients. Subsequently, a nomogram-based predictive model was constructed based on these three risk factors, successfully validated (AUC, 0.718), and demonstrated good repeatability of the model. Model scores can be used to predict the probability of CR-GNB infection occurrence in ICU patients, whereby patients at high risk of CR-GNB infection could be subjected to early intervention, and excessive intervention

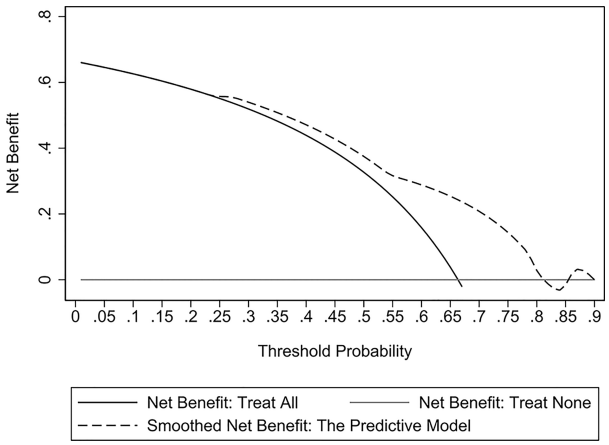

FIGURE 7
Decision curve analysis (DCA) curves of the predictive model for the validation cohort. The DCA curve showed that the model provided a high practical value in clinical practice when the predicted probability was > 0.75 in the validation cohort.

could be avoided for those at low risk of CR-GNB infection. Our proposed model has a certain level of novelty, possesses promising practical implications, and its use might improve the clinical decision-making process of clinicians to increase the net benefits of treatments and positively improve patient outcomes.

Despite the interesting findings reported here, there were some limitations that should be mentioned. First, since this was a single-center retrospective study with a small number of patients and considering the smaller number of cases in the validation cohort, further prospective large-sample studies are needed to validate the effects of the predictive model on a wider range of patients and the clinical decisions of clinicians. Second, we only selected the first positive culture and did not account for cases such as second episodes of ventilator-associated pneumonia caused by CR-PsA or CRAB, multiple culture results, etc., which should be considered in future studies to improve the proposed nomogram. Third, we did not completely exclude the effects of collinearity in the effects of carbapenem for combination use of antibiotics because there were patients who did not use carbapenem either as single or combination therapy, thereby portraying real-world clinical scenarios to a certain extent. Fourth, since all carbapenem-resistant gram-negative bacteria were resistant to imipenem and meropenem, no analysis for resistance to imipenem and sensitivity to meropenem was performed. Lastly, the inclusion of pan-carbapenem-resistant bacteria could be an improvement for future studies to formulate a more widely applicable nomogram.

5 Conclusion

In conclusion, this study analyzed the antibiotic resistance of CR-GNB. Our findings revealed that CRKP, CRAB, and CRPA were the three most prevalent CR-GNB in ICU patients. Based on independent factors associated with CR-GNB infection, we constructed and successfully validated a nomogram for CR-GNB infection risk prediction of ICU patients. Altogether, these findings could be used to formulate individualized treatments for these patients, based on which effective control and preventive measures could be taken to reduce the risk of CR-GNB infection, especially in ICU settings.

Data availability statement

The raw data supporting the conclusions of this article will be made available by the authors, without undue reservation.

Ethics statement

The studies involving human participants were reviewed and approved by the Ethics Review Form for Medical Research and Clinical Technology Application and Ethics Committee of the First Affiliated Hospital of Fujian Medical University. The patients/participants provided their written informed consent to participate in this study.

Author contributions

QL, XC, and ZF conceived and designed the study. QL, ZF, YZ, and HL collected the data. XC, HZ, QL, and ZF performed the analysis and interpreted the results. QL, HZ, XC, and ZF drafted the manuscript. QL, ZF, HZ, JL, and XC revised the manuscript. HZ and XC supervised the study and manuscript submission. All authors contributed to the article and approved the submitted version.

Funding

This study was funded by Fujian Medical University Foundation (2021QH1082).

Acknowledgments

This study was supported by the staff of the Department of Intensive Care Unit at the First Affiliated Hospital of Fujian Medical University.

Conflict of interest

The authors declare that the research was conducted in the absence of any commercial or financial relationships that could be construed as a potential conflict of interest.

Publisher's note

All claims expressed in this article are solely those of the authors and do not necessarily represent those of their affiliated organizations, or those of the publisher, the editors and the reviewers. Any product that may be evaluated in this article, or claim that may be made by its manufacturer, is not guaranteed or endorsed by the publisher.

References

Aleidan, F. A. S., Alkhelaifi, H., Alsenaid, A., Alromaizan, H., Alsalham, F., Almutairi, A., et al. (2021). Incidence and risk factors of carbapenem-resistant enterobacteriaceae infection in intensive care units: A matched case-control study. *Expert Rev. Anti Infect. Ther.* 19, 393–398. doi: 10.1080/14787210.2020.1822736

Brink, A. J. (2019). Epidemiology of carbapenem-resistant gram-negative infections globally. *Curr. Opin. Infect. Dis.* 32, 609–616. doi: 10.1097/QCO.0000000000000608

CLSI (2017). *Performance standards for antimicrobial susceptibility testing* (Wayne PA: Clinical and Laboratory Standards Institute), M100–MS27.

Dantas, L. F., Dalmas, B., Andrade, R. M., Hamacher, S., and Bozza, F. A. (2019). Predicting acquisition of carbapenem-resistant gram-negative pathogens in intensive care units. *J. Hosp. Infect.* 103, 121–127. doi: 10.1016/j.jhin.2019.04.013

Garg, A., Garg, J., Kumar, S., Bhattacharya, A., Agarwal, S., and Upadhyay, G. C. (2019). Molecular epidemiology & therapeutic options of carbapenem-resistant gram-negative bacteria. *Indian J. Med. Res.* 149, 285–289. doi: 10.4103/ijmr.IJMR_36_18

Hu, F., Guo, Y., Zhu, D., Wang, F., Jiang, X., Xu, Y., et al. (2022). CHINET surveillance of antimicrobial resistance among the bacterial isolates in 2021. *Chin. J. Infect. Chemother.* 22, 521–530. doi: 10.16718/j.1009-7708.2022.05.001

Jean, S. S., Harnod, D., and Hsueh, P. R. (2022). Global threat of carbapenem-resistant gram-negative bacteria. *Front. Cell Infect. Microbiol.* 12. doi: 10.3389/fcimb.2022.823684

Kiddee, A., Assawatheptawee, K., Na-Udom, A., Treebupachatsakul, P., Wangteeraprasert, A., Walsh, T. R., et al. (2018). Risk factors for gastrointestinal colonization and acquisition of carbapenem-resistant gram-negative bacteria among patients in intensive care units in Thailand. *Antimicrob. Agents Chemother.* 62, e00341–18. doi: 10.1128/AAC.00341-18

Liang, Q., Zhao, Q., Xu, X., Zhou, Y., and Huang, M. (2022). Early prediction of carbapenem-resistant gram-negative bacterial carriage in intensive care units using machine learning. *J. Glob Antimicrob. Resist.* 29, 225–231. doi: 10.1016/j.jgar.2022.03.019

Li, Y., Shen, H., Zhu, C., and Yu, Y. (2019). Carbapenem-resistant klebsiella pneumoniae infections among ICU admission patients in central China: Prevalence and prediction model. *BioMed. Res. Int.* 2019, 9767313. doi: 10.1155/2019/9767313

Liu, P., Li, X., Luo, M., Xu, X., Su, K., Chen, S., et al. (2018). Risk factors for carbapenem-resistant klebsiella pneumoniae infection: A meta-analysis. *Microb. Drug Resist.* 24, 190–198. doi: 10.1089/mdr.2017.0061

Logan, L. K., and Weinstein, R. A. (2017). The epidemiology of carbapenem-resistant enterobacteriaceae: The impact and evolution of a global menace. *J. Infect. Dis.* 215, S28–S36. doi: 10.1093/infdis/jiw282

Ma, C. F., Li, X. P., and Zhao, Q. (2020). Risk factors for carbapenem-resistant gram-negative bacteria infections in ICU patients and drug resistance. *Chin. J. Nosocomiol.* 30, 1335–1339. doi: 10.11816/cn.ni.2020-191528

Ministry of Health of the People's Republic of China (2001). Diagnostic criteria for nosocomial infection (Trial implementation). *Natl. Med. J. China* 81, 314–319. doi: 10.3760/j:issn:0376-2491.2001.05.027

Montrucchio, G., Costamagna, A., Pierani, T., Petitti, A., Sales, G., Pivetta, E., et al. (2022). Bloodstream infections caused by carbapenem-resistant pathogens in intensive care units: Risk factors analysis and proposal of a prognostic score. *Pathogens* 11, 718. doi: 10.3390/pathogens11070718

Naved, S. A., Siddiqui, S., and Khan, F. H. (2011). APACHE-II score correlation with mortality and length of stay in an intensive care unit. *J. Coll. Physicians. Surg. Pak.* 21, 4–8.

Nordmann, P., and Poire, L. (2019). Epidemiology and diagnostics of carbapenem resistance in gram-negative bacteria. *Clin. Infect. Dis.* 69, S521–S528. doi: 10.1093/cid/ciz824

O'Hara, L. M., Nguyen, M. H., Calfee, D. P., Miller, L. G., Pineles, L., Magder, L. S., et al. (2021). Risk factors for transmission of carbapenem-resistant enterobacterales to healthcare personnel gloves and gowns in the USA. *J. Hosp. Infect.* 109, 58–64. doi: 10.1016/j.jhin.2020.12.012

Palacios-Baena, Z. R., Giannella, M., Manissero, D., Rodriguez-Bano, J., Viale, P., Lopes, S., et al. (2021). Risk factors for carbapenem-resistant gram-negative bacterial infections: a systematic review. *Clin. Microbiol. Infect.* 27, 228–235. doi: 10.1016/j.cmi.2020.10.016

Qin, X., Wu, S., Hao, M., Zhu, J., Ding, B., Yang, Y., et al. (2020). The colonization of carbapenem-resistant klebsiella pneumoniae: Epidemiology, resistance mechanisms, and risk factors in patients admitted to intensive care units in China. *J. Infect. Dis.* 221, S206–S214. doi: 10.1093/infdis/jiz622

Raman, G., Avendano, E. E., Chan, J., Merchant, S., and Puzniak, L. (2018). Risk factors for hospitalized patients with resistant or multidrug-resistant pseudomonas aeruginosa infections: A systematic review and meta-analysis. *Antimicrob. Resist. Infect. Control.* 7, 79. doi: 10.1186/s13756-018-0370-9

Sader, H. S., Mendes, R. E., Streit, J. M., Carvalhaes, C. G., and Castanheira, M. (2022). Antimicrobial susceptibility of gram-negative bacteria from intensive care unit and non-intensive care unit patients from united states hospitals, (2018-2020). *Diagn. Microbiol. Infect. Dis.* 102, 115557. doi: 10.1016/j.diagmicrobio.2021.115557

Singer, M., Deutschman, C. S., Seymour, C. W., Shankar-Hari, M., Annane, D., Bauer, M., et al. (2016). The third international consensus definitions for sepsis and septic shock (Sepsis-3). *JAMA* 315, 801–810. doi: 10.1001/jama.2016.0287

Siwakoti, S., Subedi, A., Sharma, A., Baral, R., Bhattarai, N. R., and Khanal, B. (2018). Incidence and outcomes of multidrug-resistant gram-negative bacteria infections in intensive care unit from Nepal- a prospective cohort study. *Antimicrob. Resist. Infect. Control.* 7, 114. doi: 10.1186/s13756-018-0404-3

Wang, K., Chen, Y. Q., Salido, M. M., Kohli, G. S., Kong, J. L., Liang, H. J., et al. (2017). The rapid in vivo evolution of pseudomonas aeruginosa in ventilator-associated pneumonia patients leads to attenuated virulence. *Open Biol.* 7, 170029. doi: 10.1098/rsob.170029

Wen, H., Wang, K., Liu, Y., Tay, M., Lauro, F. M., Huang, H., et al. (2014). Population dynamics of an acinetobacter baumannii clonal complex during colonization of patients. *J. Clin. Microbiol.* 52, 3200–3208. doi: 10.1128/JCM.00921-14

Wilke, M. H., Preisendörfer, B., Seiffert, A., Kleppisch, M., Schweizer, C., and Rauchensteiner, S. (2022). Carbapenem-resistant gram-negative bacteria in Germany: incidence and distribution among specific infections and mortality: An epidemiological analysis using real-world data. *Infection* 50, 1535–1542. doi: 10.1007/s15010-022-01843-6

Wu, Q., Qian, C., Yin, H., Liu, F., Wu, Y., Li, W., et al. (2022). A novel risk predictive scoring model for predicting subsequent infection after carbapenem-resistant gram-negative bacteria colonization in hematological malignancy patients. *Front. Oncol.* 12. doi: 10.3389/fonc.2022.897479

Yang, X., Dong, N., Chan, E. W., Zhang, R., and Chen, S. (2021). Carbapenem resistance-encoding and virulence-encoding conjugative plasmids in klebsiella pneumoniae. *Trends Microbiol.* 29, 65–83. doi: 10.1016/j.tim.2020.04.012

Yan, J., Yilin, H., Di, W., Jie, W., Hanyue, W., Ya, L., et al. (2022). A nomogram for predicting the risk of mortality in patients with acute pancreatitis and gram-negative bacilli infection. *Front. Cell Infect. Microbiol.* 12. doi: 10.3389/fcimb.2022.1032375

Zeng, L., Yang, C., Zhang, J., Hu, K., Zou, J., Li, J., et al. (2021). An outbreak of carbapenem-resistant klebsiella pneumoniae in an intensive care unit of a major teaching hospital in chongqing, China. *Front. Cell Infect. Microbiol.* 11. doi: 10.3389/fcimb.2021.656070

frontiers | Frontiers in Cellular and Infection Microbiology

TYPE Brief Research Report
PUBLISHED 01 February 2023
DOI 10.3389/fcimb.2023.1051020

OPEN ACCESS

EDITED BY
Milena Dropa,
Faculty of Public Health, University of São Paulo, Brazil

REVIEWED BY
Maria Fernanda Mojica,
Case Western Reserve University, United States
Leena Al-Hassan,
Brighton and Sussex Medical School, United Kingdom

*CORRESPONDENCE
Chinmoy Sahu
sahu.chinmoy@gmail.com

†These authors have contributed equally to this work

SPECIALTY SECTION
This article was submitted to Clinical Microbiology, a section of the journal Frontiers in Cellular and Infection Microbiology

RECEIVED 22 September 2022
ACCEPTED 18 January 2023
PUBLISHED 01 February 2023

CITATION
Pathak A, Tejan N, Dubey A, Chauhan R, Fatima N, Jyoti, Singh S, Bhayana S and Sahu C (2023) Outbreak of colistin resistant, carbapenemase (*bla*$_{NDM}$, *bla*$_{OXA-232}$) producing *Klebsiella pneumoniae* causing blood stream infection among neonates at a tertiary care hospital in India. *Front. Cell. Infect. Microbiol.* 13:1051020. doi: 10.3389/fcimb.2023.1051020

Outbreak of colistin resistant, carbapenemase (*bla*$_{NDM}$, *bla*$_{OXA-232}$) producing *Klebsiella pneumoniae* causing blood stream infection among neonates at a tertiary care hospital in India

Ashutosh Pathak[1†], Nidhi Tejan[1†], Akanksha Dubey[1], Radha Chauhan[1], Nida Fatima[1], Jyoti[1], Sushma Singh[2], Sahil Bhayana[3] and Chinmoy Sahu[1*]

[1]Department of Microbiology, Sanjay Gandhi Post Graduate Institute of Medical Sciences, Lucknow, India, [2]Department of Cardiology, Sanjay Gandhi Post Graduate Institute of Medical Sciences, Lucknow, India, [3]Amity Institute of Microbial Technology, Amity University, Noida, India

Infections caused by multi-drug resistant *Klebsiella pneumoniae* are a leading cause of mortality and morbidity among hospitalized patients. In neonatal intensive care units (NICU), blood stream infections by *K. pneumoniae* are one of the most common nosocomial infections leading to poor clinical outcomes and prolonged hospital stays. Here, we describe an outbreak of multi-drug resistant *K. pneumoniae* among neonates admitted at the NICU of a large tertiary care hospital in India. The outbreak involved 5 out of 7 neonates admitted in the NICU. The antibiotic sensitivity profiles revealed that all *K. pneumoniae* isolates were multi-drug resistant including carbapenems and colistin. The isolates belonged to three different sequence types namely, ST-11, ST-16 and ST-101. The isolates harboured carbapenemase genes, mainly *bla*$_{NDM-1}$, *bla*$_{NDM-5}$ and *bla*$_{OXA-232}$ besides extended-spectrum β-lactamases however the colistin resistance gene *mcr-1, mcr-2 and mcr-3* could not be detected. Extensive environmental screening of the ward and healthcare personnel led to the isolation of *K. pneumoniae* ST101 from filtered incubator water, harboring *bla*$_{NDM-5}$, *bla*$_{OXA-232}$ and ESBL genes (*bla*$_{CTX-M}$) but was negative for the *mcr* genes. Strict infection control measures were applied and the outbreak was contained. This study emphasizes that early detection of such high-risk clones of multi-drug resistant isolates, surveillance and proper infection control practices are crucial to prevent outbreaks and further spread into the community.

KEYWORDS

outbreak, multi-drug resistant, *K. pneumoniae*, antimicrobial stewardship, hospital infection control

Introduction

Klebsiella pneumoniae, a Gram negative bacterium, is a member of the order *Enterobacterales*. It is a dreaded pathogen owing to its potential for carbapenemase production and harbouring multiple resistance genes. The evolution and rapid dissemination of carbapenem resistant *K. pneumoniae* is a significant problem worldwide as it is responsible for high mortality and morbidity in hospitalized and immuno-compromised patients (Couto et al., 2007; Gorrie et al., 2017). These characteristics make it a 'difficult to treat' pathogen. Outbreaks in hospitals due to resistant isolates of *Klebsiella pneumoniae* have been described across the world. Emergence of nosocomial multi-drug resistant *K. pneumoniae* infections can be attributed to acquisition and evolution of new resistance genes, use of invasive devices, immuno-compromised state, inappropriate use of antibiotics and inadequate surveillance system (Ayukekbong et al., 2017). The transmission may occur from patient to patient or through the hands of healthcare staff. Neonatal sepsis is one the leading cause of mortality and morbidity in hospitalized neonates (Shah et al., 2015). In neonatal intensive care unit (NICUs), bloodstream infections are one of the most common nosocomial infections and neonatal sepsis accounts for 28% to 50% of all such cases with high prevalence of *K. pneumoniae* (Hassuna et al., 2020). A recent study has reported the emergence of colistin resistant carbapenemase producing *K. pneumoniae* belonging to diverse sequence types in 14 neonates admitted in NICU of tertiary care hospital in India (Sharma et al., 2022). There is paucity of reports on blood stream infections among neonates attributed to multi-drug resistant *K. pneumoniae* in India. The aim of the present study was to characterize the *Klebsiella pneumoniae* isolates from an outbreak in NICU at a tertiary care hospital in India. The pathogen was isolated from 5 neonates over a period of 2 weeks. We also investigated for the possible sources of dissemination and isolated *Klebsiella pneumoniae* from environment of the same ward. The study also reports about the infection control measures enforced to contain the outbreak.

Materials and methods

We conducted an outbreak investigation which was suspected to have involved 5 out of 7 neonates admitted in a 7 bedded Neonatal Intensive Care Unit (NICU) at Sanjay Gandhi Post Graduate Institute of Medical Sciences, a 900 bed tertiary care referral hospital in North India, during the last week of June till second week of July, 2021.

Bacterial strains

The blood samples from the neonates were received at our laboratory for routine bacterial culture and sensitivity testing. A total of 5 multi-drug resistant *K. pneumoniae* isolates were recovered. All the isolates were identified by conventional biochemical tests and later confirmed by automated MALDI-TOF-MS system (BioMérieux, Marcy l'Étoile, France).

Demographic and clinical data collection

All the demographic and clinical data of the patients were collected from the hospital information system of the institute.

Antimicrobial susceptibility testing

The antibiotic susceptibility pattern and minimum inhibitory concentration (MIC) was determined by liquid broth microdilution method. The results were interpreted according to Clinical and Laboratory Standards Institute (CLSI) guidelines (CLSI, 2021) except for colistin for which European Committee on Antimicrobial Susceptibility Testing (EUCAST) breakpoints were followed (EUCAST, 2021).

Investigation of resistance mechanism

The resistance mechanisms in the 5 *K. pneumoniae* isolates were analyzed using polymerase chain reaction to detect the genes encoding carbapenemases (bla_{NDM}, bla_{KPC}, bla_{OXA-48}, bla_{IMP}, bla_{VIM}), ESBLs (bla_{CTX-M}), other class A β-lactamases (bla_{SHV}, bla_{TEM}) and colistin resistance genes *mcr-1*, *mcr-2* and *mcr-3* using previously described methods and primers (Singh et al., 2018; Singh et al., 2021). Following isolates from our previous studies were used as positive controls: *K. pneumoniae* CR*kp*21 and CR*kp*22 for bla_{NDM}, bla_{OXA-48}, bla_{IMP}, bla_{VIM}, bla_{CTX-M}, bla_{SHV}, bla_{TEM} (Singh et al., 2021) while *K. pneumoniae* CRL3 for *mcr* gene (Singh et al., 2018). Positive control for bla_{KPC} gene was not available. *E. coli* DH5α was used as a negative control. The details of the primers used in the study are provided in the Table S1.

Clonal diversity and multi-locus sequence typing

Clonal diversity was examined by pulse field gel electrophoresis (PFGE) using *XbaI* (Invitrogen Inc., USA) digested DNA of 5 clinical isolates and one environmental isolate of *K. pneumoniae* according to a previously described method (Qin et al., 2014). The results were analyzed using the criteria laid down by Tenover et al. (1995). Banding patterns were analyzed and dendrogram was generated using BioNumerics software version 7.6 (Applied-Maths, Sint-Martens-Latem, Belgium).

Multi-locus sequence typing (MLST) of 5 *K. pneumoniae* isolates was performed as described previously (Diancourt et al., 2005). The seven housekeeping genes were amplified and sequenced. The sequence type (ST) was assigned by determining the allele number for each of the housekeeping genes using the database maintained by Pasteur Institute at http://bigsdb.pasteur.fr/klebsiella/klebsiella.html/.

Environmental screening

Screening cultures (swabs) were obtained from different sites in NICU like entrance of room, incubator, oxygen connectors, IV stand,

10% dextrose, normal saline, reverse osmosis water, ringer lactate. The samples were inoculated onto Blood agar and MacConkey agar and incubated for 16-18 hours aerobically. Samples were also inoculated in the Robertson cooked meat broth for 16-18 hours. Sub-cultures were done on blood agar and MacConkey agar after 48 hours. Air samples were also taken by the air sampler for air bio-load monitoring.

Infection control measures

In order to control outbreaks and hospital acquired infections, we have a hospital infection control committee comprising of hospital administrators, microbiologists, physicians, nurses, technical staff and sanitation workers. During the outbreak we applied strict infection control measures including a) temporary evacuation of the infected ICU with transfer of all patient to the alternative ICU area; b) the empty infected ICU was cleaned by fogging and sodium hypochlorite; c) use of shared medical equipment were stopped; d) sanitation workers were educated about cleaning processes, cleaning protocol were established which included use of disposable cloths for each area using sodium hypochlorite solution kept in closed container to prevent evaporation and replacing it in every 24 hours; e) hand hygiene inspection and observation of infection control nurses and resident doctors were increased, educational sessions of standard precautions and hand hygiene practices were carried out by infection control physicians and nurses; f) environmental screening of bacterial cultures from different sites and hands of hospital personnel were continued;

Besides the NICU and its staff, the infection control measures were implemented in other areas of the hospital especially other ICUs and critical care units. The adherence to infection control measures in the NICU was approximately 70% before the outbreak but it was enhanced to 100% to contain the outbreak and was continued for the next one month, to prevent any further outbreaks.

NCBI data submission

The nucleotide sequences of the bla_{NDM} and $bla_{OXA-232}$ genes were submitted in the NCBI GenBank database under accession numbers OL544134-OL544138 and OK351259-OK351263 respectively.

Results

Out of 5 neonates with blood stream infections, 3 were preterm and 2 were term babies. The demographic details of the patients are given in Table 1. All the 5 samples were positive for *Klebsiella pneumoniae* isolates (KPNIC1, KPNIC3, KPNIC4, KPNIC5 and KPNIC6) as confirmed by MALDI-TOF-MS. Among the environmental samples, filtered incubator water was positive for multi-drug resistant *K. pneumoniae* (KPNIC2). Antibiotic sensitivity testing revealed that all the isolates, including the environmental isolate, were resistant to first generation cephalosporins, carbapenems, aminoglycosides and colistin except KPNIC6 which was sensitive to ciprofloxacin (Table 2).

Molecular screening of carbapenemase genes revealed that bla_{NDM-5} was present in 2 isolates (KPNIC1 and KPNIC3) while bla_{NDM-1} was present in 2 isolates (KPNIC4 and KPNIC5). The gene $bla_{OXA-232}$ (bla_{OXA-48} like variant) co-existed with bla_{NDM-1} and bla_{NDM-5} in all these 4 isolates. Among other carbapenemases, bla_{IMP} gene was absent in all while bla_{VIM} was present in one isolate (KPNIC5). Screening of other β-lactamases revealed that bla_{SHV} gene was present in all isolates which is intrinsic to *K. pneumoniae* while bla_{TEM} was present in 3 isolates (KPNIC1, 3, 4). Among ESBLs, $bla_{CTX\text{-}M}$ co-existed with bla_{NDM-1} in 2 isolates (KPNIC4 and KPNIC5) and was absent in others. Colistin resistance genes *mcr*-1,-2 and-3 were absent in all isolates. Other variants of the *mcr* gene and the chromosomal mutations were not

TABLE 1 Patient demographics and; details of *K. pneumoniae* isolates, sequence types and antibiotic resistance genes.

Patient S. No.	Age at the time of admission	Gender	Co-morbidities	Days before onset of symptoms	Isolate ID	Source	Antibiotic resistance genes	MLST Sequence type (ST)	Duration of hospital stay	Clinical Outcomes
1.	1 day	Female	Preterm birth	26 days	KPNIC4	Blood	bla_{NDM-1}, $bla_{OXA-232}$, bla_{SHV}, bla_{TEM}, bla_{CTX-M}	ST16	47days	Dead
2.	16 days	Female	Portosystemic shunts	7 days	KPNIC6	Blood	bla_{SHV}	ST101	63 days	Normal discharge
3.	6 days	Male	Acute Respiratory Distress Syndrome (ARDS)	7 days	KPNIC3	Blood	bla_{NDM-5}, $bla_{OXA-232}$, bla_{SHV}, bla_{TEM}	ST101	25 days	Normal discharge
4.	1day	Female	Preterm birth	2 days	KPNIC5	Blood	bla_{NDM-1}, $bla_{OXA-232}$, bla_{VIM}, bla_{SHV}, bla_{CTX-M}	ST11	50 days	Normal discharge
5.	15 days	Male	Preterm birth	2 days	KPNIC1	Blood	bla_{NDM-5}, $bla_{OXA-232}$, bla_{SHV}, bla_{TEM}	ST16	62 days	Normal discharge

10.3389/fcimb.2023.1051020

TABLE 2 Antimicrobial susceptibility and minimum inhibitory concentration (MIC) table of *K. pneumoniae* isolates.

Organism/No. of Isolates	Antibiotics (Range tested, µg/ml)	CLSI (2021) MIC breakpoint ≤S/≥R	Isolates with MIC (µg/ml)					
			KPNIC1	KPNIC2	KPNIC3	KPNIC4	KPNIC5	KPNIC6
Klebsiella pneumoniae (n= 6)	Imipenem (1-512)	≤1/≥4	128	128	128	128	256	64
	Meropenem (1-512)	≤1/≥4	128	128	128	128	128	128
	Tobramycin (1-512)	≤2/>4	≥512	256	≥512	256	256	16
	Aztreonam (1-512)	≤4/≥16	128	256	128	128	128	128
	Colistin (1-512)	≤1/≥4	≥512	≥512	≥512	≥512	≥512	≥512
	Ciprofloxacin (1-512)	≤4/≥16	32	≥512	32	≥512	128	8
	Ceftazidime (1-512)	≤4/≥16	≥512	≥512	≥512	≥512	≥512	256
	Cefotaxime (1-512)	≤0.25/≥1	≥512	512	512	512	256	128

investigated. The environmental isolate of *K. pneumoniae* was positive for bla_{NDM-5}, $bla_{OXA-232}$, bla_{SHV}, bla_{TEM}, and bla_{CTX-M} but negative for *mcr*. Clonal lineage profiling by MLST revealed that out of 5 clinical isolates 2 each belonged to ST101 and ST16 respectively while 1 isolate belonged to ST11. The environmental isolate belonged to ST101 (Table 1). Clonal diversity analysis using PFGE revealed that the two ST101 clinical isolates (KPNIC3 and KPNIC6), the ST101 environmental isolate (KPNIC2) and the two ST16 clinical isolates (KPNIC1 and KPNIC4) were closely related to each other while the ST11 clinical isolate (KPNIC5) belonged to a different pulsotype. The two clinical isolates and the environmental isolate belonging to ST101 clustered together with >90% similarity while the ST16 isolates displayed >83% similarity with the ST101 cluster (Figure 1).

In order to evaluate the effects of infection control measures and decrease in prevalence of *K. pneumoniae* in the NICU, environmental screening was repeated from different sites in the ward, and from the hospital personnel; and it was observed that after 48 hours of aerobic incubation all the samples were sterile.

Discussion

Hospital acquired infections are one of the leading cause of prolonged hospital stays and mortality among admitted patients. Studies have revealed that multidrug resistant *Klebsiella pneumoniae* is responsible for 18% to 31% of all nosocomial infections. Mortality due to *K. pneumoniae* is reported to be 30% to 54% in ICUs (Couto et al., 2007; Tao et al., 2014; Stefaniuk et al., 2016). We report the investigation of an outbreak due to *K. pneumoniae* in an NICU of a tertiary care hospital in the most populated state of north India. The outbreak involved 5 out of 7 neonates admitted in the NICU. Among the 5 neonates, 3 were preterm babies while the other 2 had portosystemic shunt and ARDS respectively at the time of admission. It is likely that the patients obtained *K. pneumoniae* isolates in the hospital as all of them tested positive 48 hours post admission. Hospital acquired infections are those infections acquired in hospital that first appear 48 hour or more after admission (Revelas, 2012). In Europe and US, there are several reports of outbreaks with carbapenem resistant *K. pneumoniae* and majority of them are associated with bla_{KPC}. In Asian countries, such outbreaks have been found to be associated with MBLs (Ballot et al., 2019). In India, bla_{NDM} and bla_{OXA-48} and its variants have often been found to be vehicles of swift dissemination of such isolates (Bakthavatchalam et al., 2016; Sharma et al., 2022). In our study, bla_{NDM-1} and bla_{NDM-5} co-existed with $bla_{OXA-232}$ along with bla_{SHV}, bla_{TEM} and bla_{CTX-M} in majority of the isolates. The isolates were resistant to colistin but we could not detect *mcr* gene in any of the isolates possibly because the

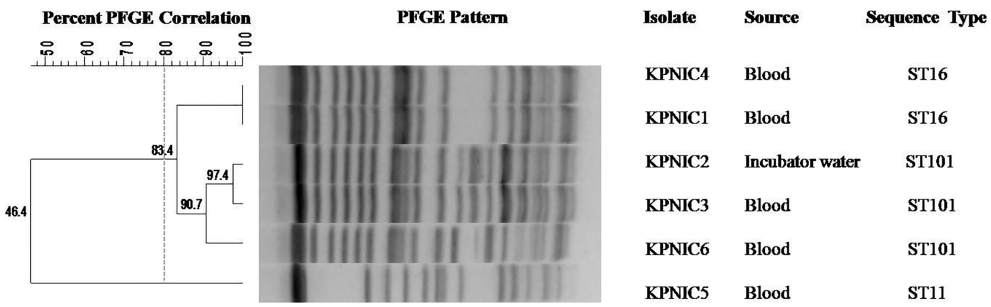

FIGURE 1
Dendrogram generated by Bionumerics software, showing results of the cluster analysis on the basis of PFGE fingerprinting of five clinical and one environmental isolate of *Klebsiella pneumoniae*. Similarity analysis was performed using Dice coefficient (optimization 1.5%, tolerance 1%) and clustering was done by the unweighted-pair group method (UPGMA). A similarity coefficient of 80% was chosen for cluster definition and grey dotted line shows the delineation line. The degree of similarity is shown in the scale.

isolates harboured the chromosomal mutations leading to colistin resistance which we did not analyze. In a recent study from our centre we have reported *K. pneumoniae* ST16 harboring mutations in chromosomal gene *mgrB* (Singh et al., 2021). Multi-locus sequence typing results revealed that the 5 *K. pneumoniae* isolates belonged to 3 different sequence types, ST101, ST16 and ST11. The isolate obtained from the incubator water belonged to ST101. PFGE is considered to be an important tool for molecular epidemiology of bacterial isolates. PFGE data indicated that both clinical and environmental isolates belonging to ST101 and the clinical isolates belonging to ST16 were closely related to each other according to the criteria laid down by Tenover et al. (1995). The ST16 belongs to clonal group CG17/20, ST101 to CG43 while ST11 belongs to CG258 (Wyres et al., 2020). The CG258 consisting of ST11, ST258 and ST512 is a global problem clonal group and is responsible for approximately 60% of all global outbreaks (Navon-Venezia et al., 2017). ST11 is a paraphyletic group of CG258 while ST258 arose from ST11-like ancestor following genomic recombination events (Wyres and Holt, 2016). Studies have reported that ST16 and ST101 belong to the sub-lineages of ST258 believed to have evolved because of large genomic recombination events (Wyres and Holt, 2016; Cherak et al., 2021). Recent reports suggest that ST101 is an international clone and is a potential candidate for becoming high risk multi-drug resistant *K. pneumoniae* in future (Loconsole et al., 2020). In India, a study from south India has reported *K. pneumoniae* ST101 carrying bla_{KPC-2} in bloodstream infection (Shankar et al., 2018). In case of our study the gene bla_{KPC} was not detected indicating that the plasmid carrying the gene was not present in any of the isolates. The *K. pneumoniae* ST16 is an internationally spread clone but studies have reported that it shows high variability in terms of antimicrobial resistome content thereby indicating that different variants of the clone are circulating in different countries (Espinal et al., 2019). A study performed on 344 *K. pneumoniae* isolates collected from 8 different centers in India has reported 3% prevalence of ST16 with variable genomic profile (Nagaraj et al., 2021). In our study also, 2 isolates KPNIC1 and KPNIC4 belonging to ST16 had different resistome profiles which is similar to the pattern observed in other studies. To the best of our knowledge, this is the second report describing presence of ST11from India. Initially, reported from China, a recent retrospective study which included 8 centers from India reported ST11 in 1.3% of *Klebsiella pneumoniae* clinical isolates. These strains are hypervirulent and have been described in association with spread of KPC, especially in China and Taiwan (Nagaraj et al., 2021).

Hospital acquired infections are a major cause of morbidity and mortality in admitted patients. Overcrowded healthcare facilities especially in low and low-middle income countries are hot-spots for dissemination of multi-drug resistant bacteria. Infections due to colistin resistant carbapenemase producing Gram negative bacterial pathogens are a menace as there are limited options available to treat such infections. Transmission of such multi-drug resistant organisms can be controlled by strict infection control measures and proper hand-hygiene practices. In the current outbreak, we tracked the source of environmental isolate to the jars used for storing incubator water in the NICU. The staffs responsible for autoclaving of jars were informed and corrective measures taken which led to the containment of outbreak.

Conclusion

This study investigates an outbreak of colistin resistant carbapenemase (bla_{NDM} and $bla_{OXA-232}$) producing *K. pneumoniae* involving neonates admitted in NICU at a large tertiary care hospital in north India. The outbreak had a serious bearing on the clinical outcomes leading to mortality and prolonged hospital stays of the neonates. Molecular epidemiology of the clinical isolates revealed presence of sequence types ST16, ST101 and ST11 but the PFGE pattern indicated that the ST16 and ST101 isolates were closely related. While carbapenemase associated ST16 and ST101 are internationally spread clones and have been associated with outbreaks of *K. pneumoniae* in various countries including India, ST11 is not a prevalent sequence type in India. One major limitation of our study was lack of whole genome sequencing of the isolates that provides detailed information about the resistome profiles and also helps to understand the dissemination pattern of the high-risk clones. In addition to the transmissible *mcr* gene, chromosomal mutations in *mgrB*, *phoP*/*phoQ*, *pmrA* and *pmrB* genes are responsible for colistin resistance but we did not analyze the alternative mechanisms and it was a limitation of our study. Further, we could track the source of the isolates belonging to ST101 to the incubator water but the source of ST11 could not be traced. Furthermore, we could not isolate ST16 from the environmental samples and after surveillance of the healthcare personnel although it was found to be closely related to the ST101 obtained from the incubator water in our study, indicating that more rigorous surveillance and environmental screening should have been performed. However, owing to the close relatedness of five out six isolates in the current outbreak we believe that the incubator water was the source of infection. Further, after taking corrective measures for proper autoclaving of the jar by the concerned staff the outbreak was contained. Though infection control measures were not robust in our set up but our surveillance actions spread more awareness among the staff. Early detection of such high-risk clones of multi-drug resistant isolates, surveillance and proper infection control practices are crucial to prevent outbreaks and further spread into the community.

Data availability statement

The datasets presented in this study can be found in online repositories. The names of the repository/repositories and accession number(s) can be found below: The nucleotide sequences of the bla_{NDM} and $bla_{OXA-232}$ genes were submitted in the NCBI GenBank database under accession numbers OL544134-OL544138 and OK351259-OK351263 respectively.

Ethics statement

The studies involving human participants were reviewed and approved by Institutional Ethics Committee, Sanjay Gandhi Post Graduate Institute of Medical Sciences, Lucknow, India. Written informed consent for participation was not required for this study in accordance with the national legislation and the institutional requirements.

Author contributions

CS, AP and NT conceived and designed the study. AP and NT wrote the manuscript. CS critically revised the manuscript. All authors carried out the experiments and collected the data. All authors contributed to the article and approved the submitted version.

Conflict of interest

The authors declare that the research was conducted in the absence of any commercial or financial relationships that could be construed as a potential conflict of interest.

Publisher's note

Supplementary material

The Supplementary Material for this article can be found online at: https://www.frontiersin.org/articles/10.3389/fcimb.2023.1051020/full#supplementary-material

References

Ayukekbong, J. A., Ntemgwa, M., and Atabe, A. N. (2017). The threat of antimicrobial resistance in developing countries: causes and control strategies. *Antimicrob. Resist. Infect. Control* 6, 47. doi: 10.1186/s13756-017-0208-x

Bakthavatchalam, Y. D., Anandan, S., and Veeraraghavan, B. (2016). Laboratory detection and clinical implication of oxacillinase-48 like carbapenemase: The hidden threat. *J. Glob Infect. Dis.* 8 (1), 41–50. doi: 10.4103/0974-777X.176149

Ballot, D. E., Bandini, R., Nana, T., Bosman, N., Thomas, T., Davies, V. A., et al. (2019). A review of -multidrug-resistant enterobacteriaceae in a neonatal unit in Johannesburg, south Africa. *BMC Pediatr.* 19 (1), 320. doi: 10.1186/s12887-019-1709-y

Cherak, Z., Loucif, L., Moussi, A., and Rolain, J. M. (2021). Carbapenemase-producing gram-negative bacteria in aquatic environments: a review. *J. Glob Antimicrob. Resist.* 25, 287–309. doi: 10.1016/j.jgar.2021.03.024

CLSI (2021). *Performance standards for antimicrobial susceptibility testing. 31st ed* (Wayne, PA: Clinical and Laboratory Standards Institute). CLSI supplement M100.

Couto, R. C., Carvalho, E. A., Pedrosa, T. M., Pedroso, E. R., Neto, M. C., and Biscione, F. M. (2007). A 10-year prospective surveillance of nosocomial infections in neonatal intensive care units. *Am. J. Infect. Control* 35 (3), 183–189. doi: 10.1016/j.ajic.2006.06.013

Diancourt, L., Passet, V., Verhoef, J., Grimont, P. A., and Brisse, S. (2005). Multilocus sequence typing of *Klebsiella pneumoniae* nosocomial isolates. *J. Clin. Microbiol.* 43 (8), 4178–4182. doi: 10.1128/JCM.43.8.4178-4182.2005

Espinal, P., Nucleo, E., Caltagirone, M., Mattioni Marchetti, V., Fernandes, M. R., Biscaro, V., et al. (2019). Genomics of *Klebsiella pneumoniae* ST16 producing NDM-1, CTX-M-15, and OXA-232. *Clin. Microbiol. Infect.* 25 (3), 385.e1–385.e5. doi: 10.1016/j.cmi.2018.11.004

Gorrie, C. L., Mirceta, M., Wick, R. R., Edwards, D. J., Thomson, N. R., Strugnell, R. A., et al. (2017). Gastrointestinal carriage is a major reservoir of *Klebsiella pneumoniae* infection in intensive care patients. *Clin. Infect. Dis.* 65 (2), 208–215. doi: 10.1093/cid/cix270

Hassuna, N. A., AbdelAziz, R. A., Zakaria, A., and Abdelhakeem, M. (2020). Extensively-drug resistant *Klebsiella pneumoniae* recovered from neonatal sepsis cases from a major NICU in Egypt. *Front. Microbiol.* 11. doi: 10.3389/fmicb.2020.01375

Loconsole, D., Accogli, M., De Robertis, A. L., Capozzi, L., Bianco, A., Morea, A., et al. (2020). Emerging high-risk ST101 and ST307 carbapenem-resistant *Klebsiella pneumoniae* clones from bloodstream infections in southern Italy. *Ann. Clin. Microbiol. Antimicrob.* 19 (1), 24. doi: 10.1186/s12941-020-00366-y

Nagaraj, G., Shamanna, V., Govindan, V., Rose, S., Sravani, D., Akshata, K. P., et al. (2021). High-resolution genomic profiling of carbapenem-resistant *Klebsiella pneumoniae* isolates: A multicentric retrospective Indian study. *Clin. Infect. Dis.* 73 (Suppl_4), S300–S307. doi: 10.1093/cid/ciab767

Navon-Venezia, S., Kondratyeva, K., and Carattoli, A. (2017). Klebsiella pneumoniae: a major worldwide source and shuttle for antibiotic resistance. *FEMS Microbiol. Rev.* 41 (3), 252–275. doi: 10.1093/femsre/fux013

Qin, S., Fu, Y., Zhang, Q., Qi, H., Wen, J. G., Xu, H., et al. (2014). High incidence and endemic spread of NDM-1-positive enterobacteriaceae in henan province, China. *Antimicrob. Agents Chemother.* 58 (8), 4275–4282. doi: 10.1128/AAC.02813-13

Revelas, A. (2012). Healthcare - associated infections: A public health problem. *Niger Med. J.* 53 (2), 59–64. doi: 10.4103/0300-1652.103543

Shah, J., Jefferies, A. L., Yoon, E. W., Lee, S. K., and Shah, P. S. (2015). Canadian Neonatal network. risk factors and outcomes of late-onset bacterial sepsis in preterm neonates born at < 32 weeks' gestation. *Am. J. Perinatol* 32 (7), 675–682. doi: 10.1055/s-0034-1393936

Shankar, C., Shankar, B. A., Manesh, A., and Veeraraghavan, B. (2018). KPC-2 producing ST101 *Klebsiella pneumoniae* from bloodstream infection in India. *J. Med. Microbiol.* 67 (7), 927–930. doi: 10.1099/jmm.0.000767

Sharma, S., Banerjee, T., Kumar, A., Yadav, G., and Basu, S. (2022). Extensive outbreak of colistin resistant, carbapenemase (bla_{OXA-48}, bla_{NDM}) producing *Klebsiella pneumoniae* in a large tertiary care hospital, India. *Antimicrob. Resist. Infect. Control* 11 (1), 1. doi: 10.1186/s13756-021-01048-w

Singh, S., Pathak, A., Kumar, A., Rahman, M., Singh, A., Gonzalez-Zorn, B., et al. (2018). Emergence of chromosome-borne colistin resistance gene *mcr-1* in clinical isolates of *Klebsiella pneumoniae* from India. *Antimicrob. Agents Chemother.* 62 (2), e01885–e01817. doi: 10.1128/AAC.01885-17

Singh, S., Pathak, A., Rahman, M., Singh, A., Nag, S., Sahu, C., et al. (2021). Genetic characterisation of colistin resistant *Klebsiella pneumoniae* clinical isolates from north India. *Front. Cell Infect. Microbiol.* 11. doi: 10.3389/fcimb.2021.666030

Stefaniuk, E., Suchocka, U., Bosacka, K., and Hryniewicz, W. (2016). Etiology and antibiotic susceptibility of bacterial pathogens responsible for community-acquired urinary tract infections in Poland. *Eur. J. Clin. Microbiol. Infect. Dis.* 35 (8), 1363–1369. doi: 10.1007/s10096-016-2673-1

Tao, X. B., Qian, L. H., Li, Y., Wu, Q., Ruan, J. J., Cai, D. Z., et al. (2014). Hospital-acquired infection rate in a tertiary care teaching hospital in China: a cross-sectional survey involving 2434 inpatients. *Int. J. Infect. Dis.* 27, 7–9. doi: 10.1016/j.ijid.2014.05.011

Tenover, F. C., Arbeit, R. D., Goering, R. V., Mickelsen, P. A., Murray, B. E., Persing, D. H., et al. (1995). Interpreting chromosomal DNA restriction patterns produced by pulsed-field gel electrophoresis: criteria for bacterial strain typing. *J. Clin. Microbiol.* 33 (9), 2233–2239. doi: 10.1128/jcm.33.9.2233-2239.1995

The European Committee on Antimicrobial Susceptibility Testing (2021) *Breakpoint tables for interpretation of MICs and zone diameters. version 11.0.* Available at: http://www.eucast.org.

Wyres, K. L., and Holt, K. E. (2016). Klebsiella pneumoniae population genomics and antimicrobial-resistant clones. *Trends Microbiol.* 24 (12), 944–956. doi: 10.1016/j.tim.2016.09.007

Wyres, K. L., Lam, M. M. C., and Holt, K. E. (2020). Population genomics of klebsiella pneumoniae. *Nat. Rev. Microbiol.* 18 (6), 344–359. doi: 10.1038/s41579-019-0315-1

Frontiers in
Cellular and Infection Microbiology

Investigates how microorganisms interact with their hosts

Explores bacteria, fungi, parasites, viruses, endosymbionts, prions and all microbial pathogens as well as the microbiota and its effect on health and disease in various hosts.

Discover the latest Research Topics

See more →

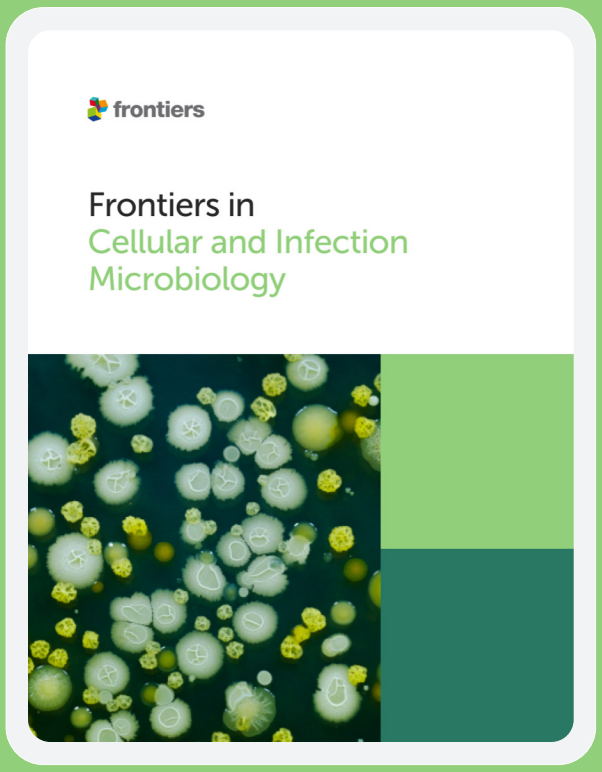

Frontiers

Avenue du Tribunal-Fédéral 34
1005 Lausanne, Switzerland
frontiersin.org

Contact us

+41 (0)21 510 17 00
frontiersin.org/about/contact